Voorwoord

Zoals wel meer dingen in het leven is ook het maken van een doctoraatsthesis niet het werk van slechts één persoon. Vooraleer over te gaan naar het wetenschappelijk werk is het dus zeker op zijn plaats een aantal mensen te bedanken die hebben bijgedragen tot dit werk en deze thesis hebben gemaakt tot wat ze uiteindelijk geworden is.

In de eerste plaats zou ik mij promotoren Prof. Dr. Dirk Vanderzande en Prof. Dr. Jan Gelan willen bedanken om mij de mogelijkheid te geven een doctoraat aan te vangen in hun onderzoeksgroep. Zonder hun professionele begeleiding en steun zou dit werk zeker niet gelukt zijn.

Prof. Dr. Peter Adriaensens verdient hier ook een vermelding voor het helpen verklaren van dikwijls ingewikkelde NMR spectra. Ook al de andere mensen binnen de NMR sectie van ons labo, Anne, Liesbet, Robby, Hilde en ja zelfs Roel hebben allemaal wel eens ooit een spectrum voor mij opgenomen (de een al meer dan de ander) en verdienen een bedankje. Anne, ik vond het immer keitof om aan uw zijde de biologen een beetje chemische kennis bij te brengen al was dit meestal een bijzonder moeilijke bevalling. De avondjes uit met Gène moeten in de toekomst zeker blijven bestaan. Eugène, ik wou dat mijn labo tafel altijd zo proper was als uw labo's.

Fil (alias Filip en door zijn broers nog dikwijls anders genoemd…), gij met uwe (meestal) flauwe zever zorgde voor wat leven in de labo en ons discussies gingen meestal over een of ander ferm studente en al het fraais daarrond maar slechts zelden over scheikunde. Ook de Orléans kampioenen kwamen dikwijls ter sprake en veel werd verbloemd met menige eeuwenoude en slechts door weinigen gekende Georgische spreekwoorden. Niettegenstaande dit alles waren uw chemische inzichten en commentaren dikwijls van goudwaarde. Muchas gracias para todo.

Dr. Laurence Lutsen dank ik omdat ze meestal onze resultaten presenteerde op externe meetings en voor de menige activiteiten die ze organiseerde in het labo, niet in het minse dan de labokuis. Ook alle anderen van het labo moet ik hier met naam vernoemen want ook zij zorgden elke dag voor de aangename werksfeer. Anja omdat gij zonder twijfel de meest behulpzame persoon zijt in ons labo, Els omdat we samen doodsangsten (vooral gij dan) uitstonden op weg naar het IWT. Iris omdat ge altijd de meest nette labotafel hebt en Jos gij de meest slordige (al moest die van mij meestal zeker niet onder doen). Huguette

omdat gij het gezondste eet van ons allemaal en Veerle omdat gij voor de LUC-kat zorgt (mijn bescheiden bijdrage is in ieder geval nuttig besteed geweest). Lieve, tegen u heb ik altijd al eens een matchke willen spelen maar het is er nooit van gekomen… . Tom, ik wil altijd wel proefkonijn zijn voor een nieuw recept. Bart, het jaar dat ge bij ons zat was de moeite, ook nog eens merci voor het adres van Inge Godts, wie weet waar ik anders nu zat?
Ook mag niet vergeten worden dat Dr. Mic Van der Borgth een deel van dit werk heeft geïnitieerd, ik hoop dat het vervolg u een beetje aanstaat.
Zarina en Wauter waren mijn twee thesis studenten die een paar weken zijn komen proeven van het laboleven en een positieve inbreng hebben gehad in dit werk.
Het nemen alsook het interpreteren van de massa spectra was onmogelijk geweest zonder de inzet en verhelderende kijk van Jan Czech.
Jos Kaelen dank ik voor het maken van de meest gekke stukken glaswerk die een mens zich kan voorstellen. Bij Koen kon ik altijd terecht als een apparaat er de brui aan had gegeven en Christel bestelde desnoods onmiddellijk een nieuw. Sali, Turkije zal nooit wereldkampioen worden. Ook dank aan al de dames van het SBG secretariaat en aan Danny Smets op het studentensecretariaat.
I should also acknowledge my Swedish friends Maria Jonforsen en Mats Anderson for given me the opportunity to come and work in Sweden. My Swedish did not improve a lot during my stay (the only thing I can remember is öl) but we had some nice scientific results in a relative short time. I'll definitely come back some day…

Ma en pa, merci voor me de kans te geven om verder te studeren. Zonder jullie liefde en steun zou het niet gelukt zijn. Eva, Jeroen en tegenwoordig ook Kobe, het peterschap ligt mij wel.
Poepie, als er een iemand is die mij heeft gesteund de afgelopen jaren dan zijt gij het wel. 11 mei was een van de mooiste dagen uit mijn leven. Ik hou ongelofelijk veel van u.
Ook bij Frans en Magda is het altijd gezellig om te vertoeven. Frans, ooit mix ik voor u de ideale verf en dan kunt ge nog een meesterwerk maken.
Al mijn ander vrienden en vriendinnen die ik hier niet allen bij naam kan noemen hebben zich altijd afgevraagd wat ik nu juist deed op het LUC. Eiegenlijk is daar maar één antwoord op: doctoreren is gewoon genieten.

Table of contents

Chapter 1

Introduction.

1.1 Introduction

Since the beginning of mankind, polymers have been exploited wherever they could be useful. Over the last decades the synthetic polymer business boomed and nowadays it is impossible to imagine a world without polymers. These "common" polymers are known for their elasticity, their good insulation properties, their good mechanical properties, their low specific weight, etc. More recently (1977), three brilliant scientists (Heeger, MacDiarmid and Shirakawa) discovered that the conductivity of polyacetylene could be increased by seven orders of magnitude by exposing it to iodine vapour.[1] For this discovery they were rewarded the Nobel Price in Chemistry in 2000. This initial breakthrough triggered an extensive worldwide research which resulted in a new polymer family, conjugated polymers. Over the years many different conjugated polymers have been synthesised. (Scheme 1)

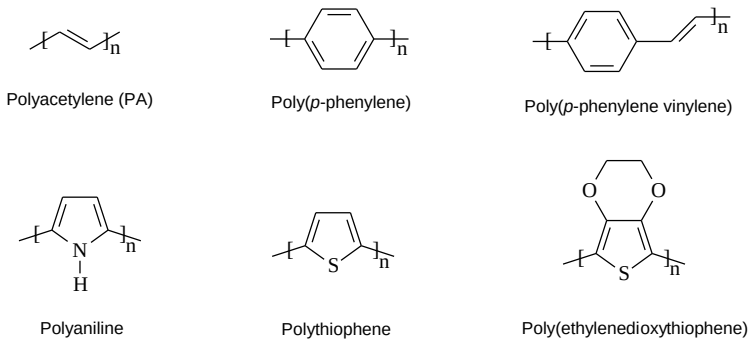

Scheme 1: Chemical structure of some conjugated polymers.

Ultimately, conjugated polymers should combine the physical properties of polymers with those of semiconductors to obtain unique and novel materials with enormous potential. In becoming electrically conductive, a polymer has to imitate a metal, that is, its electrons need to be free to move and not bound to the atoms. A key feature which makes these polymers conductive is the alternation of single and double bonds along the polymer backbone. However, pristine conjugated polymers normally have very low conductivity and they are only semiconductive. Fortunately the electrical conductivity can be increased significantly by several orders of magnitude by disturbing the polymer structure.[1] Oxidation (p-doping) or reduction (n-doping) introduces positive or negative charges on the polymer chain and the conjugated system allows the charges to move along the chain. This process can also be viewed as a movement of the double bonds to the empty positions, which in the end results in electrical conductivity.

1.2 Conjugated polymers: Organic Semiconductors

The electronic conductivity behaviour of conjugated polymers is best explained by the band model. This model is based on extending the simple model of a bond between two atoms over a complete polymer matrix. These bands stem from the splitting of interacting molecular orbitals of the constituent repeating units throughout the polymer chain. So with respect to electronic energy levels, conjugated polymers hardly differ from inorganic semiconductors. Both have their electrons organised in bands rather than in discrete levels and both have their ground state energy bands either completely filled or completely empty. What differs conjugated polymers from metals is the gap between the two bands which only makes them semiconductors. The highest occupied band (which originates from the HOMO of the repeating unit) is called the valence band (VB) and the lowest unoccupied band (which originates from the LUMO of the repeating unit) is called the conduction band (CB). The difference between these energy levels is called the band gap and is determined by the nature of the polymer structure. For comparison, in metals this band gap is zero whether it varies between approximately 1 and 4 eV for conjugated polymers. Since conjugated polymers virtually allow an endless manipulation of their chemical structure, control of the band gap can be achieved by varying the chemical structure. Tuning the band gap may lead to conjugated polymers with desired electrical and optical properties. Because

of this band gap, which causes conjugated polymers to be semiconductors, conversion to a conductor can only be accomplished by the introduction of charges onto the polymer chain (doping). Several ways exist to create charges in the polymer, either by electron-removal (oxidation or p-doping) or by electron-injection (reduction or n-doping).[2] (Figure 1)

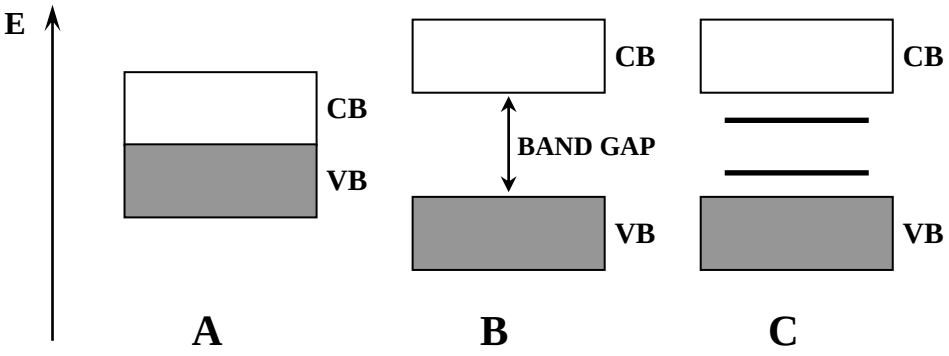

Figure 1: Schematic overview of the band model. ***A****: Band structure for metals;* ***B****: Band structure for conjugated polymers;* ***C****: Band structure for a n-doped conjugated polymer.*

The band gap, and thus the energy levels for the conduction and valence band can be manipulated by the implementation of electron donating or electron accepting groups on the polymer backbone. As will be shown further on, electron withdrawing groups such as a cyano group will lower both the energy levels of the conduction and valence band. In this way electron accepting conjugated polymers result which are less liable to oxidation than compared to non substituted polymer.[3,4,5,6,7] On the other hand, electron donating groups will increase both the energy levels of the conduction and valence band which makes these materials even more susceptible to oxidation.

1.3 Synthesis

The interesting semiconducting properties of conjugated polymers have intrigued scientists for many years now and a lot of different classes of conjugated polymers have resulted. (Scheme 1) Within this broad gamma of conjugated polymers we will only focus on the conjugated polymer poly(*p*-phenylene vinylene), PPV and some of its derivatives. (Scheme 1) Ever since the initial report of Burroughes *et al*. on electroluminescence of PPV,[8] this

conjugated polymer and its derivatives have emerged as one of the most important families within the domain of conjugated polymers. PPV shows the single-double bond alternation through phenylene rings that are connected in *para* by vinylene bonds. Like in all conjugated polymers, the conjugated structure results in very rigid polymers that are insoluble, nor are they meltable. In order to obtain soluble, processable conjugated polymers two options are at hand. First, solubility can be introduced by implanting flexible side-chains on the conjugated structure. Such solubilising spacers are often long alkyl or alkoxy chains and MEH-PPV[9,10] and OC_1C_{10}[11] are examples of PPV derivatives that are soluble in the conjugated form and can be processed. (Scheme 2) Largely because of their good solubility properties, which opens the possibility to efficient processing, these two materials have emerged as the workhorses in the field and nowadays they are commercially available.[9,10,11] These two derivatives differ from each other by the length of the spacer.

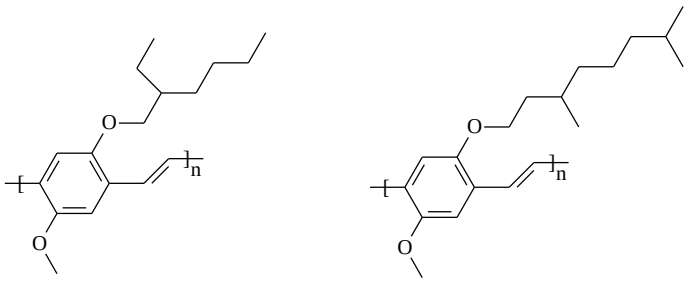

MEH-PPV **OC_1C_{10}**

Scheme 2: Chemical structures of MEH-PPV [poly(2-methoxy-5,2'-ethylhexyloxy)-1,4-phenylene vinylene] and OC_1C_{10} [poly(2-methoxy-5-(3,7-dimethyloctyloxy)-1,4-phenylene vinylene].

Over the years many different synthetic pathways, using a variety of chemical reactions, have been employed in the synthesis of PPV and its derivatives. Two different approaches can be distinguished. First, a battery of reactions exist in organic synthesis that create a vinylene double bond. Wittig[12]- and Knoevenagel[13,14]-type reactions are among the most commonly used reactions and consequently these reactions have been applied in the synthesis of conjugated polymers.[12,13,14] (Scheme 3) In this approach the double bond is formed *in situ* which means the conjugated structure is generated during the condensation reaction. This makes the incorporation of long alkoxy side-chains a necessity to keep the conjugated polymers soluble both during the reaction but also afterwards during the processing step. Apart from the obliged alkoxy chains that guarantee good solubility, the

major drawbacks of these reactions are the relative low molecular weight of the conjugated polymers that result. Another reaction that generates the double bond *in situ* is the Heck coupling reaction.[15] In this reaction a palladium catalyst is used to couple the reaction products. (Scheme 3) Main disadvantage of this approach is the relative strict conditions needed to perform the Heck reaction in good yield.

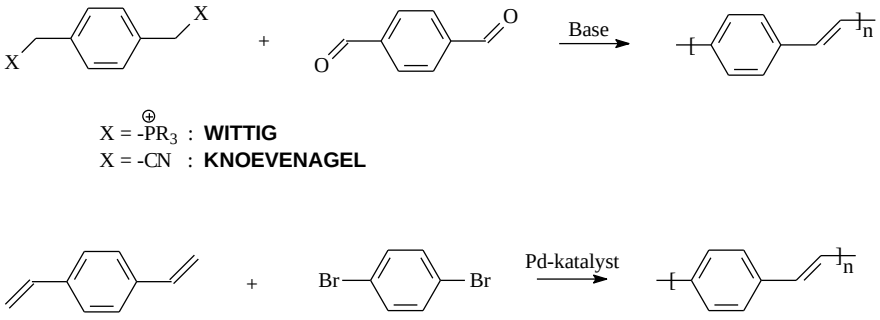

Scheme 3: Direct synthesis of PPV. Wittig- and Knoevenagel-type reaction (upper) and Heck coupling reaction (lower).

A second way to come to processable conjugated polymers is the synthesis of soluble, non-conjugated precursor polymers. Once these precursor polymers are processed conjugation is achieved by thermally eliminating a small molecule from the polymer in the solid state. Different precursor routes exist towards PPV and its derivatives which differ by the eliminable group used. (Scheme 4)

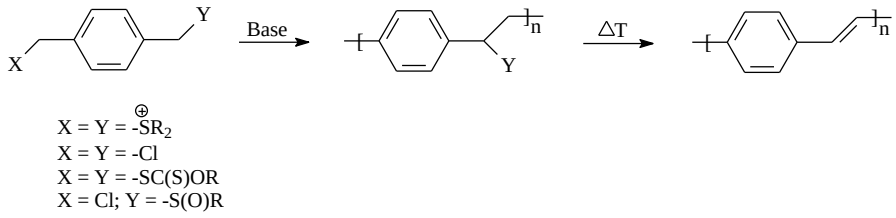

Scheme 4: Precursor routes towards PPV.

One of the main disadvantages of these precursor routes at the present moment is the lack of understanding concerning the elimination reaction. A controlled elimination process is crucial in the device preparation and incomplete elimination and/or removal of the elimination products can cause significant problems. Moreover, in some precursor routes

very reactive elimination products are liberated. A more detailed study on the elimination behaviour of sulphinyl precursor polymers is presented in the dissertation of Els Kesters.[16] Obviously, the soluble PPV derivatives shown in Scheme 2 can also be synthesised by most of these precursor routes. However the interesting feature of the precursor approach is that it allows the synthesis of PPV and some of its derivatives without solubilising side chains. On the precursor stage these polymers are soluble and can be processed.
There are four different precursor routes towards PPV, each of them has its advantages and disadvantages as will be explained in the following sections.

1.3.1 The sulfonium precursor route

This precursor route towards PPV was discovered by Wessling and Zimmerman in 1968 and is also often referred to as the Wessling precursor route.[17,18] Since then the Wessling route became the most studied precursor route towards PPV and currently still is an important method for the synthesis of PPV and some of its derivatives. The synthetic procedure was optimised several times and is shown in Scheme 5.[19,20,21] The symmetrical bissulfonium salt **1** is best treated with slightly less than one equivalent of base at 0°C in order to prevent partial base-induced elimination. Both linear and cyclic thioethers can be used, although the latter are preferred because of fewer side-reactions during the thermal elimination to the conjugated structure.[19] Aqueous media, or more in general, polar protic solvents are often used to perform the polymerisation reaction in and polymerisation yields vary between 20 and 90 percent depending on the exact experimental conditions.[18,19,20]

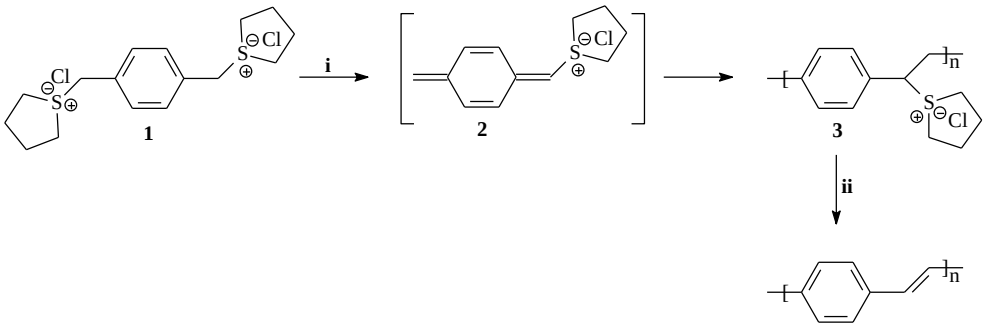

Scheme 5: The sulphonium precursor route. Reaction conditions: ***i****: NaOH, MeOH/H_2O or Bu_4NOH, MeOH, 0°C, 1h, 20-90%;* ***ii****: 160-300°C, vacuum, 12h.*

An important feature of this polymerisation is the initial monomer concentration. When this concentration is high (0.2 M) high polymerisation yields are obtained but also an insoluble gel-like polymer is obtained. Reduction of the initial monomer concentration proved crucial and a decrease to 0.05 M results in the formation of a soluble precursor polymer. Unfortunately the polymerisation yield simultaneously drops to about 55 percent.

Due to the irreversible interactions between the ionic precursor polymer **3** and the chromatography columns, SEC measurements are difficult and often give irreproducible results.[22] Therefore, the sulphonium groups in precursor polymer **3** are mostly substituted by phenylthiolate[22] or methoxide ions[23]. The resulting polymers can be analysed since they are soluble in chloroform and THF.

The polymerisation mechanism has been studied by different groups and it is accepted that the polymerisation is a multi-step process.[18,24] The first step involves a proton abstraction followed by an 1,6-elimination of one thioether group to yield the actual monomer in the polymerisation – the *p*-quinodimethane system (**2**).[24b] This very reactive intermediate polymerises spontaneously either by an anionic or a radical mechanism.[24] The exact polymerisation mechanism has been a topic of intense discussion for several years now and some experiments have been in favour of a radical polymerisation mechanism and some of an anionic mechanism. It is possible that radical and anionic mechanism are both possible and compete with each other. The outcome of the polymerisation may well depend on both the monomer and solvent used. It is beyond the scope of this thesis to give a full explanation for the exact polymerisation mechanism. For a more detailed picture on the polymerisation behaviour of *p*-quinodimethane systems we refer to the dissertation of Lieve Hontis.[25]

A variety of PPV derivatives have been polymerised via this precursor route, including monomers with substituents on the aromatic ring.[26,27] However, when electron poor aromatic systems (nitro or cyano substituent) or monomers with extended aromatic systems are used, Wessling polymerisation becomes extremely difficult and is even impossible in some cases.[28,29] This restriction seriously limits the scope of monomers that can be polymerised via this precursor route. Furthermore, sulfonium precursor polymers are not very stable. Due to the good leaving group capacities and its sensitivity for nucleofiles, the sulfonium group can undergo all kinds of side reactions during polymerisation and storage.[30] In the end this results in for example gel formation, premature elimination and

irreversible sp^3 defects in the polymer backbone or a combination of all. Sulfonium precursor polymers are only soluble in polar solvents like methanol or water but these solvents are poor solvents for efficient processing techniques as for example spin coating.
The sulphonium precursor polymers **3** can be converted to the conjugated structure by a thermal treatment between 160 and 300°C for a sufficient long time.[31] More importantly, during elimination hydrogen chloride is formed as one of the elimination products. This harmful elimination product is best removed from the polymer matrix since it has been shown to react with the electrode materials used in device structures.[32]
Although the synthesis of some PPV derivatives is impossible via this route, the Wessling precursor route is a fairly versatile route which allows the synthesis of many PPV derivatives. However, the symmetrical build up of the bissulfonium monomers and the high reactivity of the sulfonium group lead to undesired defects in the conjugated structure.

1.3.2 Dehalogenation precursor route

Gilch and Wheelwright first performed this type of polymerisation on the symmetrical α,α'-dichloro-*p*-xylene monomer **4** which they treated with a tenfold excess of base (KO*t*BuO) in benzene.[33] (Scheme 6) Due to premature basic elimination insoluble PPV fragments were obtained which could not be analysed. In order to obtain a soluble precursor polymer (**5**) one equivalent of base has to be used.[34] Conversion to the conjugated structure is accomplished by a thermal treatment at 300°C for 1 hour. Like in the Wessling precursor route hydrogen chloride is produced during the elimination process which may hamper efficient device performance.[32]

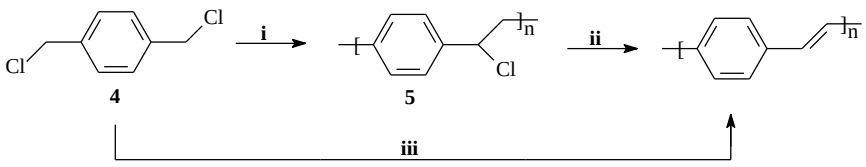

Scheme 6: The Gilch Route. Reaction conditions: ***i****: 1 equiv. KtBuO, THF or 1,4-dioxane, RT;* ***ii****: ΔT;* ***iii****: 10 equiv. KtBuO, THF or 1,4-dioxane, reflux.*

This synthetic approach is also often referred to as the Gilch route. In the real sense of the word the Gilch route can only be called a "precursor" route if no more than one equivalent of base is used during the polymerisation. If more than one equivalent is used, premature

elimination will occur and the precursor polymer **5** can no longer be isolated and processed. In literature no real distinction is made between these two routes, it is always referred to as the Gilch route. At present, this method is mostly used to synthesise soluble conjugated polymers and the elimination reaction is performed *in situ*, in solution by using an excess of base. In industry the Gilch route is the most widely used route to synthesise soluble conjugated polymers such as MEH-PPV and OC_1C_{10}. (Scheme 2) If other, intrinsic insoluble PPV derivatives are desired, the Gilch precursor route is less suited since very high molecular weight and largely insoluble precursor polymers are obtained. Furthermore, from our experience the polymerisation reaction is difficult to reproduce.[25]

1.3.3 The xanthate precursor route

This precursor route was discovered by Son *et al*. and it uses a symmetrical bisxanthate monomer **6** which is polymerised in dry THF at 0°C using K*t*BuO as a base.[35] The polymerisation is proposed to proceed via a *p*-quinodimethane intermediate, although no evidence was presented. The precursor polymers **7** are stable at room temperature and are soluble in common organic solvents.

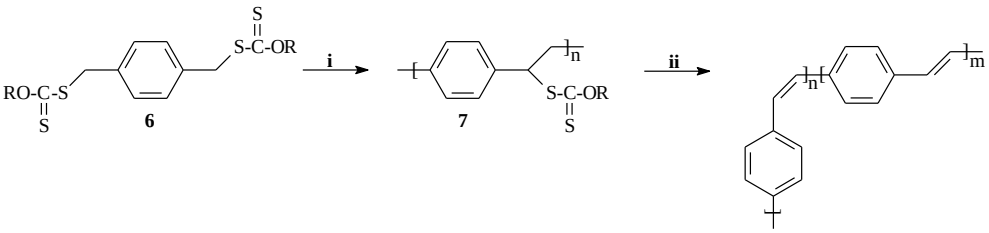

Scheme 7: The xanthate precursor route. Reaction conditions: ***i****: KtBuO, THF, 0°C;* ***ii****: 160-250°C, Ar.*

Polymerisation yields for this precursor route are not often reported but from our experience (Chapter 5) moderate polymerisation yields can only be obtained if the polymerisation temperature is sufficiently low. The conversion to the conjugated structure is performed between 160 and 250°C. The authors claim an internal EL efficiency of 0.22% for a single layer device (ITO-PPV-Al), which is much higher than the 0.01% reported by Burroughes *et al*.[8] This phenomenon is explained by the presence of *cis*-linkages in the conjugated structure which reduces the effective conjugation length and makes the PPV

more amorphous.[35] Apparently, the conversion to the conjugated structure yields both *cis*- and *trans*-double bonds as was concluded from the IR signals at 862 and 956 cm^{-1} respectively. However, a recent publication by Burn *et al*. proves the higher EL efficiencies are a result of the absence of the harmful hydrogen chloride which is produced during elimination of a Wessling precursor polymer and reacts with the ITO electrode thus lowering EL efficiency.[32] In the xanthate precursor route no hydrogen chloride is formed during the elimination reaction and thus higher EL efficiencies can be achieved.

Compared to the sulphonium route, the xanthate precursor route offers certain advantages. The non-ionic precursor polymers are stable at room temperature and soluble in common organic solvents. Recently some publications have appeared that use the xanthate precursor route in the synthesis of some PPV derivatives.[36]

Also in this work the xanthate precursor route is used in the synthesis of poly(thienylene vinylene) (PTV) because specific problems prevent the use of the sulphinyl precursor route in this synthesis. (Chapter 3) In chapter 5 a detailed study on the synthesis and elimination behaviour of some xanthate containing precursor polymers and oligomers will be described.

1.3.4 The sulphinyl precursor route

The precursor route used in this work is the sulphinyl precursor route. This precursor route to PPV and its derivatives was designed to overcome the problems that are attached to the precursor routes mentioned before. All the synthetic routes described above make use of symmetrical monomers where the same group acts as both a leaving group and a polariser. Ideally, the leaving group needs to be an atom or a functional group with good leaving group capacities so the actual monomer in the polymerisation – the *p*-quinodimethane system – is formed very efficiently upon elimination of this moiety. The polariser is an atom or a functional group that should polarise the *p*-quinodimethane system in such a way that propagation occurs via consecutive head to tail additions and the undesired head to head and tail to tail additions are kept to an absolute minimum. Such additions will undoubtedly lead to defects in the final conjugated structure and must be avoided. A second task of the polariser is that it should generate solubility on the precursor stage and this preferably in solvents that are well suited for processing techniques such as spin coating. A third important task of the polariser is its ability to be eliminated thermally from the precursor polymer to generate the final conjugated structure. The temperature at which this

conversion is performed should not be to high since than degradation may already occur for some conjugated polymers. However the elimination temperature should not be to low either because then the precursor polymer will be unstable and elimination may already (partially) occur during the synthesis or storage. Another important requirement of the polariser is that upon elimination, the formation of harmful elimination products should be avoided since these may hamper an efficient device performance. Since it is impossible to combine all these requirements into one atom or functional group a non-symmetrical monomer **8** is used in the sulphinyl precursor route.[37] In this way the specifications just described are met in the closest way possible. We should admit that synthesis of such a non-symmetrical monomer **8** is more difficult than that of a symmetrical one but over the years we have come up with very efficient ways to introduce this non-symmetry.[38] A general overview of the sulphinyl precursor route is shown in Scheme 8. The non-symmetrical monomer **8** is build up of a *para*-xylene moiety with a halogen atom attached on one side and a sulphinyl (-S(O)R) functionality on the other. Halogen atoms were chosen because they posses good leaving group capacities. The sulphinyl group is an ideal polarising group and has little or no leaving group capacities. This functional group provides good solubility on both the monomer and the precursor polymer stage if a long aliphatic chain is used. Secondly, the sulphinyl group polarises the *p*-quinodimethane system in such a way that nearly only head to tail addition occurs during the propagation. Indeed, ^{13}C-NMR experiments on labelled sulphinyl precursor polymers proved that the amount of defects in conjugated polymers synthesised via this route is much smaller than that of the same polymers prepared via the Gilch route.[39] Furthermore, the sulphinyl group functionality can be eliminated at relatively low temperatures from the precursor polymer to yield an all *trans* conjugated polymer.[40]

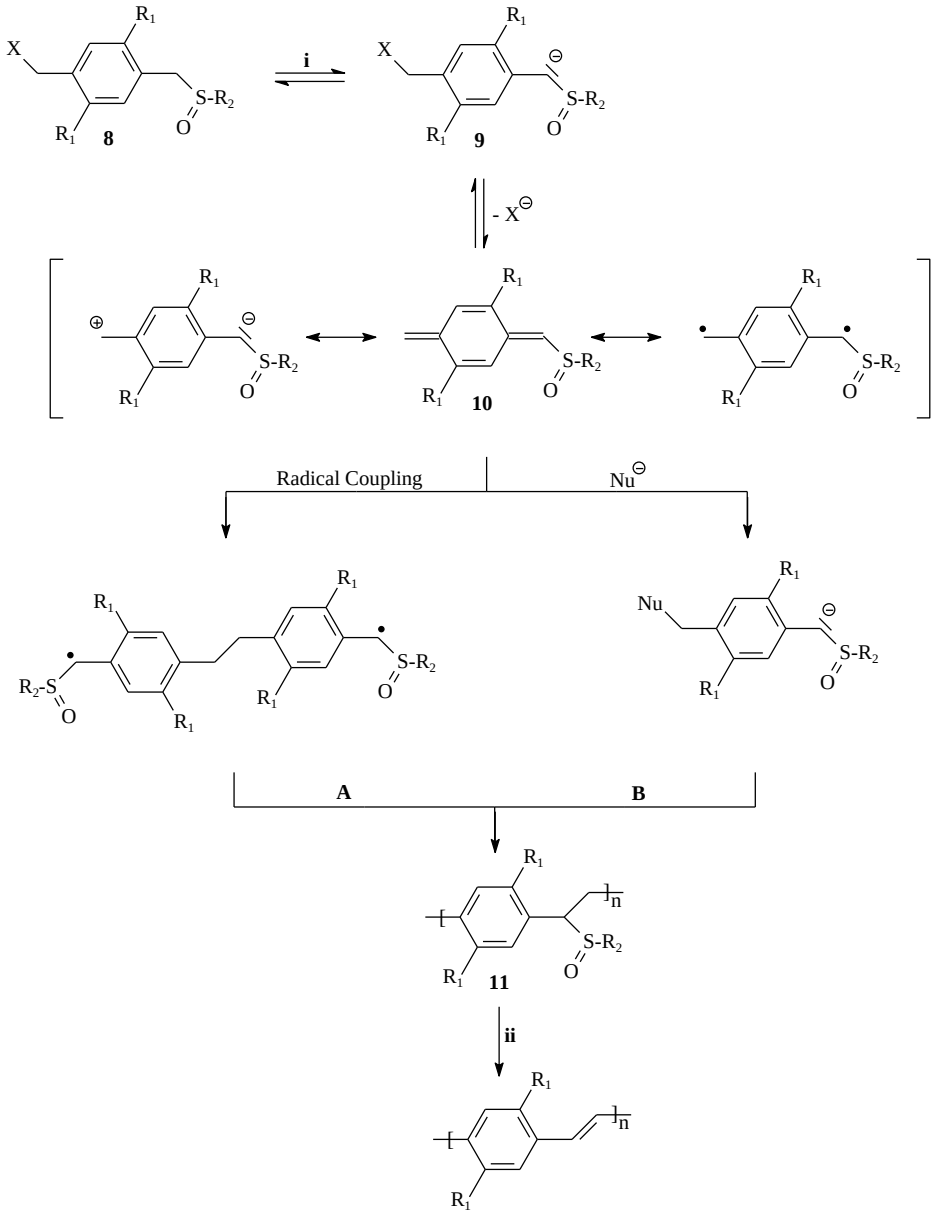

*Scheme 8: The sulphinyl precursor route. R_1= H, alkyl, alkoxy, Cl, CN; R_2= alkyl, aryl. **A**: Radical chain polymerisation; **B**: Anionic chain polymerisation. Reaction conditions: **i**: NatBuO, solvent; **ii**: 100-150°C, vacuum.*

When monomer **8** is allowed to react with a base (usually Na*t*BuO), deprotonation occurs selectively alpha to the sulphinyl group as this position bears the most acid proton. In this

way anion **9** is created and by subsequent 1,6-elimination of the leaving group the actual monomer – the *p*-quinodimethane system (**10**) – is generated. Depending on the exact chemical structure of the monomer and the solvent the polymerisation is performed in, polymerisation can either occur by a radical chain polymerisation or by a anionic chain polymerisation. Both polymerisation mechanisms have been proven possible and compete with each other depending on the monomer and the experimental conditions used.[37c,41] Generally, the radical polymerisation pathway has the upper hand but when more electron poor monomers (containing electron withdrawing functionalities on the phenylene ring such as chlorine atoms or nitro- or cyano-functionalities) or dipolar non-protic solvents (NMP, DMF) are used, the anionic polymerisation process becomes increasingly important.[42] This is probably due to the increased stability of the anion formed in the first step of the polymerisation process. This aspect will be handled more into detail in the following chapters.

Once the non-ionic sulphinyl precursor polymers (**11**) are isolated by precipitation they remain stable at room temperature and stay soluble in common organic solvents which allows efficient device engineering. Conversion to the final conjugated polymer can be accomplished by a thermal treatment at a temperature as low as 100°C, which is relatively low compared to the temperatures used in the other precursor routes. A detailed study on the elimination behaviour of sulphinyl precursor polymers also revealed this elimination is a relatively fast process.[16,40]

1.3.4.1 Monomer synthesis

In literature many different methods exist to synthesise sulphoxides.[43] The most widely spread manner is the oxidation of the corresponding thioether. In this approach the first step to the sulphoxides is the synthesis of the thioether. In addition, this synthesis has to be carried out in such a way that the mono substituted thioether is generated is high selectivity. The creation of non-symmetry is one of the more difficult points in the sulphinyl monomer synthesis. Over the years our research group has come up with very efficient synthetic pathways to introduce this non-symmetry in the monomer.[38] In the beginning the monothioether (**13**) was synthesised by reacting the α,α'-dihalide-*p*-xylene (**12**) with a nucleofile sulphur anion.[44] (Scheme 9) Because the disubstituted product **13** always is an unwanted side-product, a large excess (3 equivalents) of dihalide **12** was used and a

chromatographique separation was necessary to isolate the different reaction products. Anyhow, even if this side reaction could be reduced to an absolute minimum, the maximum conversion to the monothioether would only be about 30 percent. The selectivity towards monosubstitution can be improved by performing this reaction in a two phase system (water/toluene) in the presence of a phase transfer catalyst (Aliquat 336).[45] In this way a 1:1 ratio between compound **12** and the sulphur anion can react which results in about 60 percent selectivity towards monothioether **13**.

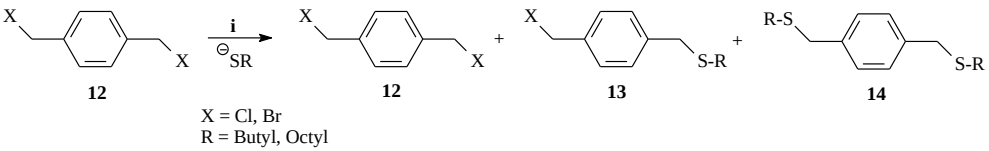

*Scheme 9: Synthesis of the mono substituted thioethers (**13**). Reaction conditions: **i**: **12**, HSR/NaH, THF or **12**, H_2O/toluene, Aliquat 336, HSR, NaOH.*

More recently van Breemen *et al*. found another way to introduce this non-symmetry much more selectively.[38] (Scheme 10) This approach is somewhat similar to a Wessling polymerisation and starts from the bissulfonium salt **1**. The salt is dissolved in methanol and a solution of the thiolate anion is added in one portion. The thiolate anion will abstract a proton to create anion **1a**. Subsequent 1,6-elimination of one sulfonium group yields the non-symmetric intermediate **2**. In a Wessling polymerisation this highly reactive quinoid intermediate would normally polymerise. Here however, the presence of the thiol together with the dilute conditions prevent polymerisation and all quinoid compounds will immediately react with a thiol molecule to yield compound **15**. The key feature in this synthesis is the creation of a non-symmetric intermediate (**2**). Once this non-symmetric quinoid structure is quenched by a thiol molecule the non-symmetry is introduced irreversibly and subsequent substitution of the sulfonium group by a chloride atom yields the mono substituted thioether **13**. Stoichiometry of the reactants used is critical to assure the typical high selectivity (90 percent) and to prevent side reactions from taking place.

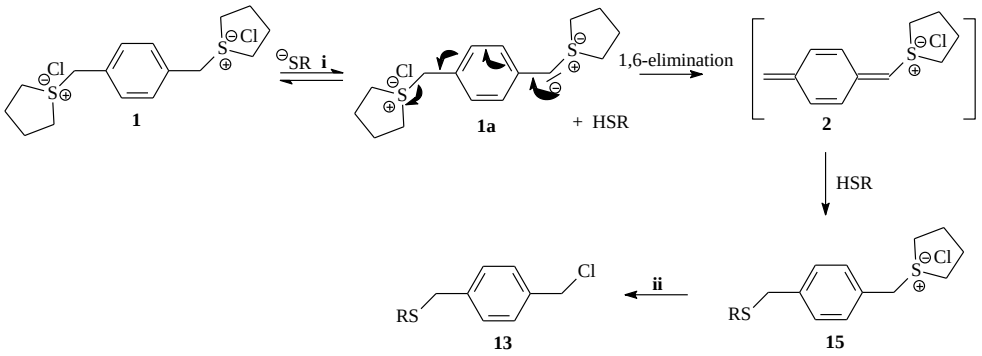

*Scheme 10: Mechanism for the very selective thioether synthesis. Reaction conditions: **i: 1**, MeOH, HSR/NatBuO, MeOH, **ii**: n-octane.*

The oxidation of the mono substituted thioether can yield the corresponding sulphoxides or the corresponding sulphone or a mixture of both.[43,46] The exact product distribution depends on the method used for oxidation. Note that sulphones are less desirable since, on the precursor polymer stage, these groups eliminate at much higher temperatures compared to their sulphoxides counterparts. Selective oxidation to the sulphoxides is desired. Overoxidation to sulphones can be avoided by using a tellurium dioxide (TeO_2) catalyst selective oxidation with H_2O_2 as the oxidant.[47] Using this oxidising systems generally yields the corresponding sulphoxides in 90 percent yield.

1.3.4.2 Polymerisation

Over the years a more or less "standard" procedure was developed to perform the polymerisation of sulphinyl monomers. The polymerisation is generally performed in a specially designed set-up as depicted in Figure 2. After degassing both the base and the monomer solution by passing nitrogen for one hour, the base solution is added to the monomer solution in one shot. Usually sodium-*tert*-butoxide (Na*t*BuO) is used as a base in 1 to 1.3 equivalents. The monomer concentration is set at 0.1M. Note that this concentration is calculated on the total volume of solvent used. Polymerisation is allowed to proceed for one hour and the passing of nitrogen is continued. The polymerisation reaction is terminated by pouring the reaction mixture into ice water whereupon the precursor polymer precipitates. The aqueous solution is neutralised using dilute hydrogen chloride (1M). After extraction (chloroform) the combined organic layers are concentrated

in vacuo. The crude polymer is dissolved in an organic solvent and precipitated in a non-solvent, collected and dried. The residual fraction is also concentrated *in vacuo* and analysed.

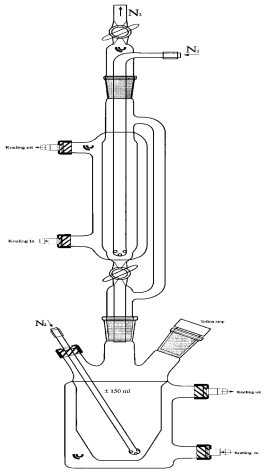

Figure 2: Polymerisation set-up used in the sulphinyl precursor route.

This polymerisation can be performed for many different monomers in a wide range of solvents (2-BuOH has proven to be particularly suitable). As will be shown repeatedly throughout this thesis the polymerisation results can be tuned by varying one or more polymerisation parameter(s) as for example the solvent, the temperature, the base, etc. In this way a virtually endless chemical toolbox is available that can be used in the polymerisation of a specific PPV derivative. In the precursor routes mentioned earlier the polymerisation conditions are more strict which seriously limits the polymerisation capabilities of some monomers. To date the sulphinyl precursor route is the most versatile precursor route towards PPV and its derivatives.

1.3.4.3 Conversion to the conjugated structure

The final step in the sulphinyl precursor route is the thermal elimination of the sulphinyl group to yield the double bond an thus create the desired conjugated structure. Such an elimination reaction is often used in organic chemistry for the synthesis of double bonds.[48] The elimination mechanism is considered to proceed via a *syn*-elimination in which the intermediate has a planar structure.[49] Two transition states are possible for this

intermediate, a first one leads to a *cis*-double bond where the second will lead to a *trans*-double bond. Due to the steric hindrance of the eclipsed polymer chain the *trans*-vinylene double bond is selectively formed. By expulsion of a sulphenic acid the vinylene bond is generated.[50] The sulphenic acid molecules are unstable and spontaneously dimerise with the formation of a thiosulphinate and water. This thiosulphinate disproportionates to a thiosulphonate and a disulphide.[51] (Scheme 11)

The efficiency of the elimination reaction is one of the factors that determines the performance of the final conjugated polymer. The elimination reaction should be as complete as possible and the elimination products are best removed from the polymer matrix. For a more detailed study on the elimination behaviour of sulphinyl precursor polymers we refer to the dissertation of Els Kesters.[16]

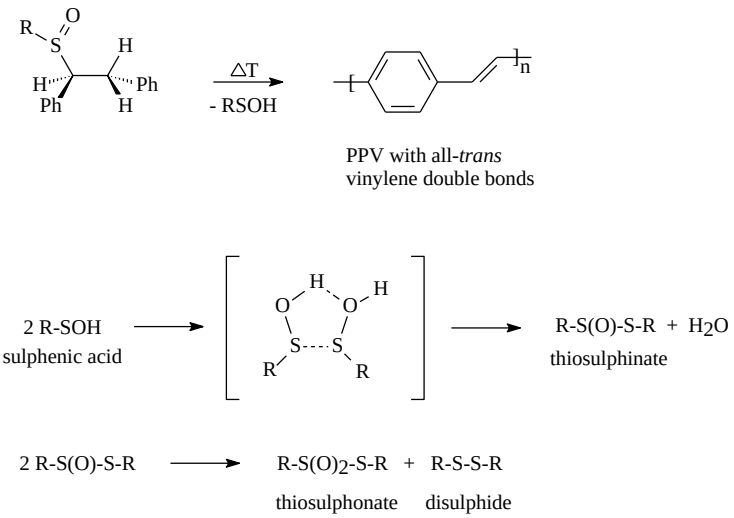

Scheme 11: Elimination reaction of sulphinyl precursor polymers and formation of the elimination products.

1.4 Applications

Not surprisingly conjugated polymers have considerable commercial potential and, over the years, they have been demonstrated to be useful as active material in many successful prototypes of applications, including lasers,[52] non-linear optics,[53] sensors,[54] light-emitting

diodes,[8,55] field-effect transistors[56] and photovoltaic devices[57]. Nowadays, the three last ones have emerged as the most important.

1.4.1 Light Emitting devices

Over the years, electroluminescence – the generation of light by electrical excitation – has been observed in a wide range of organic semiconductors.[8,55] The first organic light-emitting diode was fabricated with anthracene crystals in 1963[58] and ever since a large number of other molecular materials have been used. Electroluminescence from conjugated polymers was first reported in 1990, using poly(*p*-phenylene vinylene), PPV, as a single semiconductor layer between metallic electrodes.[8] In a typical device the polymer layer is sandwiched between two metal electrodes, one of which must be transparent. (Figure 3) Intrinsically, the active organic material has no free charges. Hence the charges that run through the polymer LED during operation are injected into the organic layer from the electrode contacts.

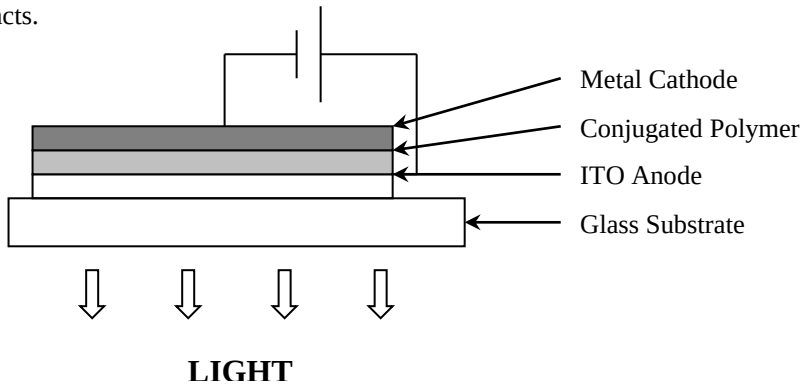

Figure 3: Device structure of a single-layer polymer electroluminescent device.

In this structure, the ITO (indium tin oxide) layer functions as transparent electrode, and allows the light generated within the diode to leave the device. The top electrode (Ca, Mg or Al) is normally formed by thermal evaporation of the metal. Electroluminescence is achieved when the diode is biased sufficiently to achieve injection of positive and negative charge carriers from opposite electrodes. Combination of oppositely charged carriers creates an excited state in the polymer matrix, which can then return to the ground state by sending out a photon. However, not all excited states return to the ground state by emitting light. An estimate of the theoretical limit on the efficiency achievable with PPV devices can

be made from considerations of spin statistics. The recombination of charge carriers produces both triplet and singlet excited states in the ratio 3:1 and only singlet excited states decay by emitting visible light. So 75 percent of the total amount of electron-hole pairs formed do not decay radiatively.[55] Furthermore, also other sources of losses exist which further lower the maximal achievable percentage of radiative decay. The relaxation to the ground state can be non-radiative, for example due to migration to quenching sites such as carbonyl groups,[59] or by interchain interactions that produce lower excited states which are not strongly radiatively coupled with the ground state.[59] Taking in account all these factors a realistic target for the EL efficiency would be 6 percent, a figure that would make PPV highly attractive for commercial applications. To date the highest efficiencies reported reach 5 percent and this led to strong efforts towards commercialisation of polymer LEDs by Philips, CDT, Dupont (Uniax), etc.[60]

One of the most important factors that determines the device performance of polymer LEDs is the nature of the interfaces, between the polymer and metal electrode, or between the polymer and ITO anode. For most conjugated polymers incorporated in LEDs electron injection has been found to be more difficult than the injection of holes from the anode. It is known that balanced charge injection from both electrodes and comparable mobility of both charge carrier types inside the polymer matrix are crucial for high device efficiencies.[61] The facility of charge injection depends on the barriers between the molecular frontier orbitals of the polymer and the work function of the contact metal electrodes. Although electron injection can be facilitated by using low work function metals such as calcium or magnesium as cathodes, the instability of such metals toward air and moisture makes hermetical encapsulation a necessity. However, when polymers with increased electron affinity are incorporated in a LED the barrier to electron injection is reduced which allows electron injection from more stable cathodes like aluminium. (Figure 4) In conjugated polymers with high electron affinity, both the energy levels for the lowest unoccupied molecular orbitals (LUMO) and the highest occupied molecular orbitals (HOMO) lie at lower energies than those of typical conjugated polymer like PPV. This seriously improves electron injection from more stable cathodes like aluminium which on its turn causes the recombination zone of electron and hole to shift to the anode side. This lowers the quenching by the cathode metal and therefore results in higher efficiency devices. Note that at the same time the barrier for hole injection is increased but this can be circumvented

relatively easy by incorporation of an additional PEDOT/PPS [poly(3,4-ethylenedioxythiophene)/poly(styrenesulphonic acid)] layer.[62] Other strategies to obtain a good match between electrons and holes include the fabrication of double- or multi-layered devices.[14] Here materials with different electron affinities are used to improve the matching of energy levels and hence the efficiency. In this way a broader scope of electrode materials becomes accessible. Polymers with cyano-substituents in the backbone have been used in a two-layer LED in which PPV was the hole-transporting layer.[14]

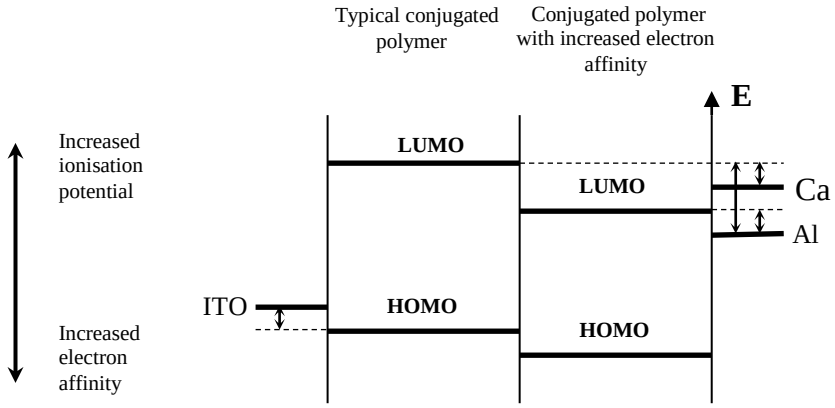

Figure 4: Schematic overview of a two layered LED using an additional layer of a conjugated polymer with increased electron affinity.

Other requirements that have to be met before polymer LEDs can be produced in mass are an appropriate turn-on voltage, a high device stability and a relative simple method for device fabrication (ink-jet process has been introduced for the pixelisation of LEDs[63]). Moreover the colour blue still remains a problem and stable and efficient blue emitting conjugated polymers still have to be found in order to come to full colour displays. Once these needs have been adjusted the commercialisation is imminent in the fields of automobile navigation systems, mobile phones and backlights for LCDs. At the point where an active matrix display is accessible, an all polymer, flexible, full colour television screen is within reach.

1.4.2 Photovoltaic devices

In the next decades renewable energy sources will become increasingly important since the supply of today's main energy sources (oil, gas, coal, uranium) is limited and inevitably

will get scarce at some point in the (near) future. Converting sunlight into electric energy is an appealing feature in this context. Inorganic solar cells have been around for a long time but only recently it was discovered that conjugated polymers could also be used in these device structures.[57] A polymeric solar cell will combine the opto-electronic properties of conventional semiconductors with the excellent mechanical and processing properties of polymers. Devices can be processed relatively easy from solution onto e.g. flexible substrates using simple and therefore cheaper deposition methods like spin coating. The photophysics of such photoactive devices is based on the photo-induced charge transfer from donor-type semiconducting conjugated polymers (MEH-PPV or OC_1C_{10}) to acceptor-type conjugated polymers (CN-PPV) or acceptor molecules such as fullerene, C_{60}. Solar cells of this donor/acceptor type can be constructed either as double-layer devices or by blending the donor and acceptor components.[57] The device construction is basically the same as for LEDs (Figure 2), only other active materials have to be used. The conversion of solar light into an electric current requires the generation of both negative and positive charges as well as a driving force that can push these charges through the external electric circuit. In general two different processes have to be distinguished in organic photovoltaic devices. First, a photoinduced charge generation (electron transfer efficiency) and secondly, the transport of the created charges to the electrodes (charge carrier mobility). In an organic solar cell an electron-hole pair is created upon interaction of the donor-type polymer (MEH-PPV) with a photon of sufficient energy. The polymer is promoted to an excited state that is initially neutral, the electron and hole are still bound by their Coulomb attraction. This state is called an exciton and these excitons can move along the polymer chain. These excitons are normally bound and would not break up. If however, a semiconductor with high electron affinity (CN-PPV or C_{60}) is placed in close contact with the polymer, it can be energetically favourable for the electron to leave the exciton and jump to the acceptor with high electron affinity. In this way hole and electron are separated, subsequently transported to the respective electrodes and a current is generated. The exciton can only break up if its binding energy is smaller than the difference ΔE_a in electron affinity between the donor-type polymer and the acceptor. (Figure 5) Recently, relatively good functioning double layer solar cells have been fabricated using a cyano-substituted MEH-PPV (CN-MEH-PPV) polymer as electron accepting material together with the photon absorbing MEH-PPV.[64]

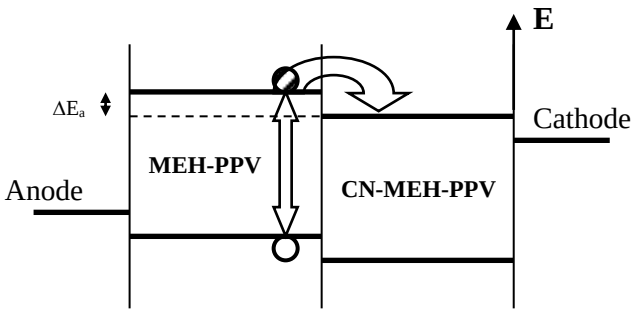

Figure 5: Schematic overview of the MEH-PPV/CN-MEH-PPV heterojunction.

In this process MEH-PPV acts as an electron donor and CN-PPV as an electron acceptor, in what can be seen as a molecular heterojunction. Such an exciton splitting system has an efficiency close to 100%, but can only work if the accepting polymer is spatially close enough to allow the donor exciton to migrate to the interface before it relaxes back to the ground state. The active region of these photovoltaic devices extends only up to approximately ten nanometers from the heterojunction. Consequently a high ratio between device volume and donor-accepting interface area, together with a long exciton lifetime, is required to maximise efficiency. Organic photovoltaic devices are interesting for their linear response to light as well as for their potential to be up-scaled to large area light detectors and solar cells for power production.

Nowadays the highest efficiencies (3%) reached in conjugated polymer photovoltaic devices use OC_1C_{10} as a donor material blended with PCBM, a fullerene derivative, as an acceptor in a 1:3 ratio.[65] This efficiency is still far from the 25-30% efficiencies reached by crystalline inorganic solar cells but the polymeric solar cells are constantly improving. Because of the large amounts of C_{60} needed in these devices the search for other electron accepting materials is on. So far only a handful of conjugated polymers with high electron affinities have been used in photovoltaic devices largely because the lack of such materials.[64] There is a large demand for conjugated polymers with high electron affinity and some of the polymers synthesised in the next chapters may be suitable candidates. Unfortunately, the quest for new materials that can compete with C_{60} is a difficult task because C_{60} and its derivatives posses properties that are ideally fit for solar cells and will be hard to match for other organic materials. For example, the electron transfer from the conjugated donor-type polymer to C_{60} occurs in less than 45 fsec, while the back-transfer is

much slower. Moreover, the electron mobility is also relatively high and C_{60} is also easier reduced than most acceptor-type conjugated polymers reported to date.

Other strategies to achieve higher efficiencies currently explore the optimalisation of the morphology[66] of the device and the use of so called low band gap materials[67]. Undoubtedly, the intensive research in this field will lead to further improvements of this technology. With 3% power conversion already demonstrated, with still large potential for improvement, this approach represents a viable route to realizing large-area "plastic solar power conversion technology".

1.4.3 Organic field effect transistors

Organic semiconductors can also be used as active material in thin-film field effect transistors (TFT).[56,68] (Figure 6) This application is mentioned here because poly(thienylene vinylene), PTV, synthesised in chapter 3, was tested in such a device structure.

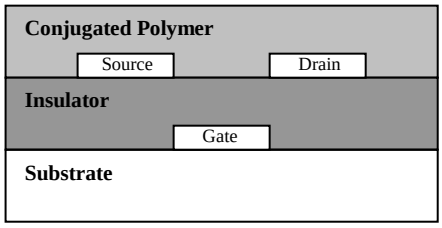

Figure 6: Schematic cross section of an organic TFT with bottom-contacts. The organic semiconductor is deposited onto the prefabricated source and drain electrodes.

Other materials used in this application are poly(3-hexylthiophene)[56c] and pentacene[69]. A significant current can flow between source and drain in the accumulation regime, when a negative voltage is applied to the gate. This means that the holes are the dominant charge carriers and these semiconductors are all p-type materials. This is in contrast with the electron accepting conjugated polymers which preferably transport electrons (n-type). Source and drain are built using high work function metals (Al, Au) or heavily doped p-type conjugated polymers (polyaniline)[70] to ease the injection process. Because of the relatively low mobility of the organic semiconductors, organic TFTs cannot rival the performance of field-effect transistors based on single-crystalline inorganic semiconductors, such as Si and Ge, which have charge carrier mobilities about three orders of magnitude higher. Consequently, organic TFTs are not suitable for use in applications

that require very high switching speeds. However, the processing characteristics and demonstrated performance of organic TFTs suggest that they can be competitive for existing or novel thin-film-transistors applications. The intrinsic properties of polymers allow the low cost fabrication of large-area, flexible TFT devices at low temperature. Current applications of organic TFTs include "electronic paper" displays,[71] low-end smart cards and electronic identification tags. In the future the application range may broaden and switching devices for active-matrix flat-panel displays based on liquid crystal pixels or organic LEDs may be within the possibilities. For the time being, amorphous silicon is most commonly used as active layer in TFT backplanes since the higher performance of polycrystalline silicon is required for well-performing devices. However, this field is still in a development stage and improvements in the efficiency of both organic LEDs and TFTs could change this requirement.

1.5 Aim and outline of the thesis

The aim of the research presented in this work is the synthesis and characterisation of new PPV derivatives via the sulphinyl precursor route. Mainly PPV derivatives with increased electron affinity will be handled since these derivatives are not easily accessible via the other precursor routes. Moreover, such high electron affinity PPV derivatives may be very useful in several applications. Due to specific synthetic problems at some points, small adaptations had to be made to the sulphinyl precursor route in order to polymerise certain monomers. This work will show repeatedly that the sulphinyl route is the most versatile precursor route towards PPV and its derivatives.

In chapter two some PPV derivatives containing electron withdrawing side groups will be presented. Both synthesis and characterisation will be addressed.

Chapter three deals with the synthesis and characterisation of some hetero-aromatic PPV derivatives and in chapter four the copolymerisation behaviour of several monomers is studied.

Finally, the polymerisation behaviour of some xanthate containing monomers towards PPV precursor polymers as well as their thermal elimination behaviour will be discussed in chapter five.

Note that in the remainder of this thesis, the nomenclature of chemical compounds, schemes, figures and tables starts over in each chapter.

1.6 References

[1] Shirakawa, H.; Louis, E. J.; MacDiarmid, A. G.; Chiang, C. K.; Heeger, A. H. *J. Chem. Soc. Chem. Comm.* **1977**, 578.

[2] Brédas, J.-L.; Street, G. B. *Acc. Chem. Rev*. 18, **1985**, 309.

[3] Papdimitrakopoulos, F.; Yan, M.; Rothberg, L. J.; Katz, H. E.; Chandross, E. A.; Galvin, M. E. *Mol. Cryst. Liq. Cryst*. 256, **1994**, 663.

[4] Cumpston, B. H.; Jensen, K. F. *Synth. Met*. 73, **1995**, 195.

[5] Scurlock, R. D.; Wang, B.; Ogilby, P. R.; Sheats, J. R.; Clough, R. L. *J. Am.Chem.Soc*. 117, **1995**, 10194.

[6] Koch, A. T. H.; Harrison, N. T.; Haylett, N.; Daik, R.; Feast, W. J.; Friend, R. H. *Synth. Met*. 100, **1999**, 113.

[7] Rio, G.; Berthelot, J. *Bull. Soc. Chim. Fr*. 10, **1969**, 3609.

[8] Burroughes, J. H.; Bradley, D. D. C.; Brown, A. R.; Marks, R. N.; Mackay, K.; Friend, R. H.; Burns, P. L.; Holmes, A. B. *Nature* 347, **1990**, 539.

[9] Braun, D.; Heeger, A. J. *Appl. Phys. Lett*. 58, **1991**, 1982.

[10] Wudl, F.; Sardanov, G. *US Patent* 5, 189, 136, **1993**.

[11] Becker, H.; Spreitzer, H.; Kreuder, W.; Kluge, E.; Schenk, H.; Parker, I.; Cao Y. *Adv. Mater.* 12(1), **2000**, 42.

[12] Hörhold, H.-H.; Opfermann, J. *Makromol. Chem*. 131, **1970**, 105.

[13] Lenz, R. W.; Handlovits, C. E. *J. Org. Chem*. 25, **1960**, 813.

[14] Greenham, N. C.; Moratti, S. C.; Bradley, D. D. C.; Friend, R. H.; Holmes, A. B. *Nature* 365, **1993**, 628.

[15] Heck, R. F. *Accounts Chem. Res*. 12, **1979**, 146.

[16] Kesters, E. *Ph.D. Dissertation*, **2002**, Limburgs Universitair Centrum, Diepenbeek, Belgium.

[17] Wessling, R. A.; Zimmerman, R. G. *US Patent* **1969**, 3401152.

[18] Wessling, R. A. *J.Polym. Sci., Polym. Symp*. 72, **1985**, 55.

[19] Lenz, R. W.; Han, C.-C.; Stenger-Smith, J.; Karasz, F. E. *J. Polym. Sci. Polym. Chem*. 26, **1988**, 3241.

[20] Garay, R.; Lenz, R. W. *Makromol. Chem. Suppl*. 15, **1989**, 1.

[21] Burn, P. L.; Bradley, D. D. C.; Friend, R. H.; Halliday, D. A.; Holmes, A. B.; Jackson, R. W.; Kraft, A. *J. Chem. Soc. Perkin Trans. 1*, **1992**, 3225.

[22] Machado, J. M.; Denton, F. R. III; Schlenoff, J. B.; Karasz, F. E.; Lahti, P. M. *J. Polym. Sci. Part B: Polym. Phys*. 27, **1989**, 199.

[23] Halliday, D. R.; Burn, P. L.; Friend, R. H.; Bradley, D. D. C.; Holmes, A. B. *Synth. Met*. 55, **1993**,902.

[24] a) Denton, F. R. III; Lahti, P. M.; Karasz, F. E. *J. Polym. Sci. Part A: Polym. Chem*. 30, **1992**, 2223. b) Cho, B. R.; Kim, Y. K.; Han, M. S. *Macromolecules* 31, **1998**, 2098.

[25] Hontis, L. *Ph.D. Dissertation*, **2002**, Limburgs Universitair Centrum, Diepenbeek, Belgium.

[26] Garay, R.; Karasz, F. E.; Lenz, R. W. *J. Macromol. Sci.-Pure Appl. Chem. A* 32, **1995**, 905.

[27] McCoy, R. K.; Karasz, F. E. *Chem. Mater*. 3, **1991**, 941.

[28] Denton, F.R.; Sarker, A.; Lahti, P. M.; Garay, R. O.; Karasz, F. E. *J. Polym. Sci. Part A: Polym. Chem*. 30, **1992**, 2233.

[29] Sarker, A.; Lahti, P. M. *Polym. Prep*. 35(1), **1994**, 790.

[30] a) Gmeiner, J.; Karg, S.; Meier, M.; Riess, W.; Strhriegl, P.; Schwoerer, M. *Acta Polym*. 44, **1993**, 201. b) Hsieh, B. R.; Antoniadis, H.; Abkowitz, M. A.; Stolka, H. *Polym. Prep*. 33, **1992**, 414.

[31] a) Garay, R. O.; Baier, U.; Bubeck, C.; Mullen, K. *Adv. Mater*. 5, **1993**, 561. b) Zhang, C.; Braun, D.; Heeger, A. J. *J. Appl. Phys*. 76, **1993**, 5177.

[32] Lo S-C.; Palsson L-O.; Kilitziraki M.; Burn P. L.; Samuel I. D. W. *J. Mat. Chem*. 11, **2001**, 2228.

[33] Gilch, H. G.; Wheelwright, W. L. *J. Polym. Sci*. 4, **1966**, 1337.

[34] Swatos, W. J.; Gordon, B. *Polym. Prep*. 31(1), **1990**, 505.

[35] Son S.; Dodabalapur A.; Lovinger A. J.; Galvin M. E. *Science* 269, **1995,** 376.

[36] a) Lo S-C.; Sheridan, A. K.; Samuel I. D. W.; Burn P. L. *J. Mat. Chem*. 10, **2000**, 275. b) Lo S-C.; Sheridan, A. K.; Samuel I. D. W.; Burn P. L. *J. Mat. Chem*. 9, **1999**, 2165.

[37] a) Louwet, F.; Vanderzande, D.; Gelan, J.; *Synth. Met.* 52, **1992**, 125. b) Louwet, F.; Vanderzande, D.; Gelan, J.; Mullens, J. *Macromolecules* 28, **1995**, 1330. c) Vanderzande, D.; Issaris, A.; Van Der Borght, M.; van Breemen, A.; de Kok, M.; Gelan, J. *Macromol. Symp.* 125, **1997**, 189.

[38] a) van Breemen, A.; Vanderzande, D.; Adriaensens, P.; Gelan, J. *J. Org. Chem.* 64, **1999**, 3106. b) van Breemen, A. *Ph.D. Dissertation*, **1999**, Limburgs Universitair Centrum, Diepenbeek, Belgium.

[39] Roux, H. *et al*, to be published.

[40] Kesters E.; Lutsen L.; Vanderzande D.; Gelan J.; Nguyen T. P.; Molinié P. *Thin Solid Films* 403-404, **2002**, 120.

[41] a) Issaris, A.; Vanderzande, D.; Gelan, J. *Polymer* 38(1), **1997**, 2571. b) Issaris, A. *Ph.D. Dissertation*, **1997**, Limburgs Universitair Centrum, Diepenbeek, Belgium. c) Hontis, L.; Van Der Borght, M.; Vanderzande, D.; Gelan, J. *Polymer* 40, **1999**, 6615.

[42] a) Van Der Borght, M.; Vanderzande, D.; Gelan, J. *Polymer* 39, **1998**, 4171. b) Van Der Borght, M. *Ph.D. Dissertation*, **1998**, Limburgs Universitair Centrum, Diepenbeek, Belgium.

[43] a) Drabowicz, J.; Kielbasinski, P.; Mikolajczyk, M. in: *The Chemistry of Sulfones and Sulfoxides* Patai, S; Rappoport, Z.; Stirling, C. John Wiley & Sons Ltd., Chichester, UK, **1988**, 233-378. b) Drabowicz, J.; Kielbasinski, P.; Mikolajczyk, M. in: *The Chemistry of Sulfones, Sulfoxides and Cyclic Sulphides* Patai, S; Rappoport, Z. John Wiley & Sons Ltd., Chichester, UK, **1994**, 255-388.

[44] Tagaki, W. in: *Organic Chemistry of Sulphur* Oae, S. Ed., Plenum Press, London, **1977**, 231-302.

[45] Herriot, A. W. *Synthesis* **1975**, 447.

[46] Madesclaire, M. *Tetrahedron* 42, **1986**, 5459.

[47] Kim, K. S.; Hwang, H. J.; Cheong, C. S.; Hahn, C. S. *Tetrahedron Lett.* 31, **1990**, 2893.

[48] a) Durst, T. *Comprehensive Organic Chemistry volume 3* Jones, D. N., Oxford Pergamon **1979**, 121. b) Trost, B. M.; Salzmann, T. N.; Hiroi, K. J. *J. Am. Chem. Soc.* 98, **1976**, 4887. c) Trost, B. M. Acc. Chem. Res. 11, 1978, 453. d) Paptai, S. *The chemistry of Sulphones and Sulphoxides*, John Wiley & Sons Ltd., Chichester, UK, **1988.**

[49] a) Kwart, H.; George, T. J.; Louwe, R.; Ultee, W. *J. Am. Chem. Soc.* **1978**, 3927. b) Janssen, J. W. A. M.; Kwart, H. *J. Org. Chem.* 42, **1977**, 1530.

[50] a) Kingsbury, C. A.; Cram, D. J. *J. Am. Chem. Soc.* 82, **1960**, 1810. b) Shelton, J. R.; Davis, K. E. *Int. J. Sulphur Chem.* 8, **1973**, 205. c) Yoshimure, T.; Tsukurimichi, E.; Iizuka, Y.; Mizuno, H.; Isaji, H.; Shimasaki, C. *Bull. Chem. Soc. Jpn.* 62, **1989**, 1891.

[51] a) Koch, P.; Ciuffarin, E.; Fava, A. *J. Am. Chem. Soc.* 92, **1970**, 5971. b) Kice, J. L.; Cleveland, J. P. *J. Am. Chem. Soc.* 95, **1973**, 109. c) Davis, F. A.; Jankins, L. A.; Billmers, R. L. *J. Org. Chem.* 51, **1986**, 1033.

[52] a) Hide, F.; Diaz-Garcia, M. A.; Schwartz, B. J.; Andersson, M. R.; Pei, Q.; Heeger, A. *Science* 273, **1996**, 1833. b) Tessler, N.; Denton, F. R.; Friend, R. H. *Nature* 382, **1996**, 695.

[53] Nalwa, H. S. In *Handbook of Organic Conductive Molecules and Polymers*, Nalwa, H. S., Ed.; John Wiley & Sons Ltd, New York, **1997**, vol. 4, 261-363.

[54] McQuade, D. T.; Pullen, A. E.; Swager, T. *Chem. Rev.* 100, **2000**, 2537.

[55] a) Bradley, D. D. C. *Synth. Met.* 54, **1993**, 401. b) Friend, R. H.; Gymer, R. W.; Holmes, A. B.; Burroughes, J. H.; Marks, R. N.; Taliani, C.; Bradley, D. D. C.; Dos Santos, D. A.; Brédas, J. L.; Lögdlund, M.; Salaneck, W. R. *Nature* 397, **1999**, 121.

[56] a) Tsumura, A.; Koezuka, H.; Ando, T. *Appl. Phys. Lett.* 49, **1986**, 1210. b) Burroughes, J. H.; Jones, C. A.; Friend, R. H. *Nature* 355, **1988**, 137. c) Bao, Z.; Dodabalapur, A.; Lovinger A. J. *Appl. Phys. Lett.* 69, **1996**, 4108.

[57] a) Brabec, C. J.; Sariciftci, N. S.; Hummelen, J. C. *Adv. Funct. Mater.* 11, **2001**, 15. b) Brabec, C. J.; Sariciftci, N. S. *Monatshefte für Chemie* 132, **2001**, 421. c) Yu, G.; Gao, J.; Hummelen, J. C.;

Wudl, F.; Heeger, A. J. *Science* 270, **1995**, 1789. d) Halls, J. J. M.; Walsh, C. A.; Greenham, N. C.; Marseglia, E. A.; Friend, R. H.; Moratti, S. C.; Holmes, A. B. *Nature* 376, **1995**, 498.

[58] Pope, M.; Kallmann, H. P.; Magnante, P. *J. Chem. Phys.* 38, **1963**, 2042.

[59] Rothberg, L. J.; Yan, M.; Papadimitrakopoulos, F.; Galvin, M. E.; Kwock, E. W.; Miller, T. M. *Synth. Met.* 80, **1996**, 41.

[60] *European Plastics News* march, **1998**, 21.

[61] a) Brown, A. R.; Bradley, D. D. C.; Burn, P. L.; Burroughes, J. H.; Friend, R. H.; Greenham, N.; Kraft, A. *Appl. Phys. Lett.* 61, **1992**, 2793. b) Parker, I. D.; Pei, Q.; Marrocco, M. *Appl. Phys. Lett.* 65, **1994**, 1272.

[62] Groenendaal, L.; Jonas, F.; Freitag, D.; Pielartzik, H.; Reynolds, J. R. *Adv. Mater.* 12, **2000**, 481.

[63] Toshiba America Electronic Components Inc.; *Toshiba Develops World's First 260,000-Color Polymer LED*, **2001**, www.toshiba.com.

[64] Yu, G.; Heeger, A. J. *J. Appl. Phys.* 78, **1995**, 4510.

[65] Munters T.; Martens T.; Goris L.; Vrindts V.; Manca J.; Lutsen L.; De Ceuninck P.; Vanderzande D.; De Schepper L.; Gelan J.; Sariciftci S.; Brabec C. *Thin Solid Films* 403-404, **2002**, 247.

[66] Chen, L. C.; Godovsky, D.; Inganäs, O.; Hummelen, J. C.; Janssen, R. A. J.; Svensson, M; Andersson, M. R. *Adv. Mater.* 12, **2000**, 1367.

[67] a) Dhanabalan, A.; van Duren, J. K. J.; van Hal, P. A.; van Dongen, J. L. J.; Janssen, R. A. J. *Adv. Funct. Mater.* 11, **2001**, 255. b) Shaheen, S. E.; Vangeneugden, D.; Kiebooms, R.; Vanderzande, D.; Fromhertz, T.; Padinger, F.; Brabec, C. J.; Sariciftci, N. S. *Synth. Met.* 121, **2001**, 1583.

[68] Dimitrakopoulos, C. D.; Mascaro, D. J. *IBM J. Res. & Dev*. 45(1), **2001**, 11.

[69] Lin, Y.-Y.; Gundlach, D. J.; Nelson, S.; Jackson, T. N. *IEEE Electron Device Lett.* 18, **1997**, 606.

[70] Gelink, G. H.; Geuns, T. C. T.; de Leeuw, D. M. Appl. Phys. Lett. 77(10), 2000, 1487.

[71] Wisnieff, R. *Nature* 394, **1998**, 225.

Chapter 2

PPV derivatives with increased electron affinity.

2.1 Introduction

In chapter two the synthesis and characterisation of some conjugated polymers with an increased electron affinity will be discussed. As already mentioned in chapter one, the reasons for synthesising these polymers are manifold. Most of the conjugated polymers, synthesised to date, have low electron affinity (p-type) which makes them highly susceptible to oxidation. Conjugated polymers with high electron affinity (n-type) are less sensitive to oxidation and are desired in certain applications.

In general, several ways exist to create electron accepting conjugated polymers. In this work only some PPV derivatives with increased electron affinity will be discussed.

The first and most obvious choice for the design of high electron affinity PPV derivatives would be the attachment of one or more electron withdrawing side-group to the aromatic moiety or the vinylene double bond. A halogen atom, a cyano- or nitro-group are common examples of such groups since these are among the most widespread electron withdrawing groups in organic chemistry. PPV derivatives with electron accepting groups on the aromatic ring are not often synthesised, largely because the most commonly used polymerisation routes (for example the Wessling precursor route) are less suited for the polymerisation of electron deficient monomers. The Wessling polymerisation of halogen substituted monomers was reported in the early days and resulted in very low molecular

weight polymers (**1**-**3**).[1,2] (Scheme 1) Moreover, the conversion to the conjugated structure was less effective when compared to the unsubstituted PPV. When more electron deficient groups (cyano or nitro) were implanted on the monomers Wessling polymerisation completely failed and only some oligomeric fragments could be isolated.[1,2]

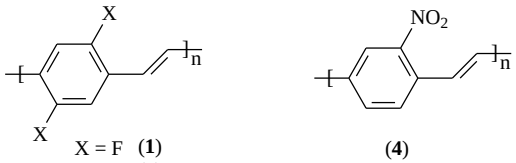

X = F (**1**)
X = Cl (**2**)
X = Br (**3**)

(**4**)

Scheme 1: Chemical structures of some PPV derivatives with electron withdrawing substituents on the aromatic ring.

More recently, Van der Borght in our research group synthesised and characterised the dichloro- and nitro-substituted PPV derivatives (**2** and **4**) via the sulphinyl precursor route.[3] In the appropriate solvent these derivatives could be polymerised in relatively good yields.[3] The majority of the electron accepting PPV polymers reported to date are those with cyano side-groups. Ever since Holmes *et al*. reported on the synthesis of a cyano-MEH-PPV polymer (**5**)[4] several publications have appeared that address this issue, mainly because these polymers are interesting candidates to increase both stability and efficiency of polymer LEDs.[5] Cyano groups were placed on the vinylene double bond (**5**) and on the aromatic moiety (**6**). In fact, the polymers synthesised were all copolymers between the cyano containing monomer and an alkoxy substituted monomer. The long alkoxy chains were necessary to guarantee good solubility of the conjugated polymer which allows efficient device fabrication. Moreover, these copolymers were not synthesised via a precursor route but via a Wittig/Knoevenagel- or Heck type reaction which *in situ* generates the double bond.[4,5] Due to the intrinsic nature of the Wittig and Knoevenagel type reaction only relative low molecular weight polymers (M_w~10^3) were obtained. Using a Heck coupling reaction allows the synthesis of polymers **5** and **6** with higher molecular weight (M_w~10^4).

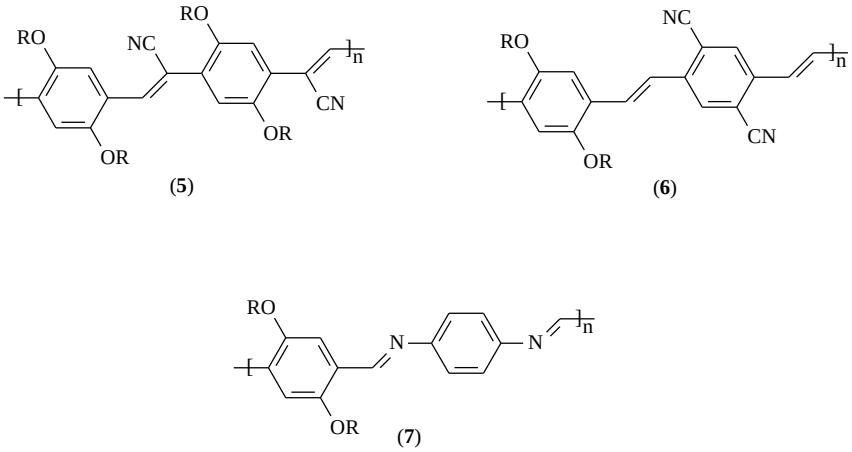

Scheme 2: Chemical structures of some electron accepting copolymers.

A second way to obtain PPV derivatives with increased electron affinity is to introduce more electronegative atoms, such as an imine nitrogen, in the polymeric backbone. The imine nitrogen atom can be introduced between the aromatic rings, like in polyazomethines (**7**)[6,7] or in the aromatic ring. Examples of such electron deficient aromatic rings are pyridine,[8,9] bipyridine,[10,11] pyrimidine,[12] quinoline[13] and others. Poly(pyridylene vinylene) and poly(bipyridylene vinylene) will be discussed in chapter 3. An additional feature of these nitrogen containing conjugated polymers is the possibility to protonate or alkylate the polymers that result thus generating a completely new set of conjugated polymers.[11,14] In the case of the bipyridine derivatives complexation with a large number of different metal ions is possible.[10]

In this chapter the synthesis and characterisation of three different electron accepting PPV derivatives via the sulphinyl precursor route is discussed. The electron withdrawing groups used here are a chlorine atom and a cyano group. These groups are introduced on the double bond (**8** and **9**) or on the aromatic ring (**10**). (Scheme 3)

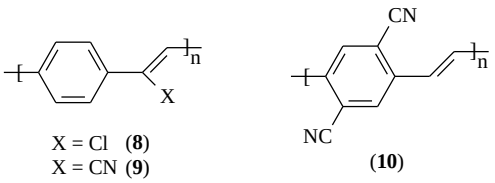

Scheme 3: Chemical structure of the electron accepting PPV derivatives discussed in this chapter.

As will be shown, the presence of these atoms or groups effects the polymerisation capabilities of the different monomers. The polymerisation conducted were all homopolymerisations of the respective monomers. The copolymerisation between OC_1C_{10} and an electron accepting monomer will be discussed in Chapter 4.

2.2 Electron withdrawing groups on the vinylene double bond

The first electron deficient PPV derivatives discussed in this chapter are the ones with an electron withdrawing group on the double bond (**8** and **9**). (Scheme 3) We chose the relatively weak electron withdrawing chlorine atom on the one hand and a much stronger electron withdrawing cyano group on the other hand.

2.2.1 Monomer synthesis

Synthesis of both monomers **A** and **B** is similar and is shown in Scheme 4.

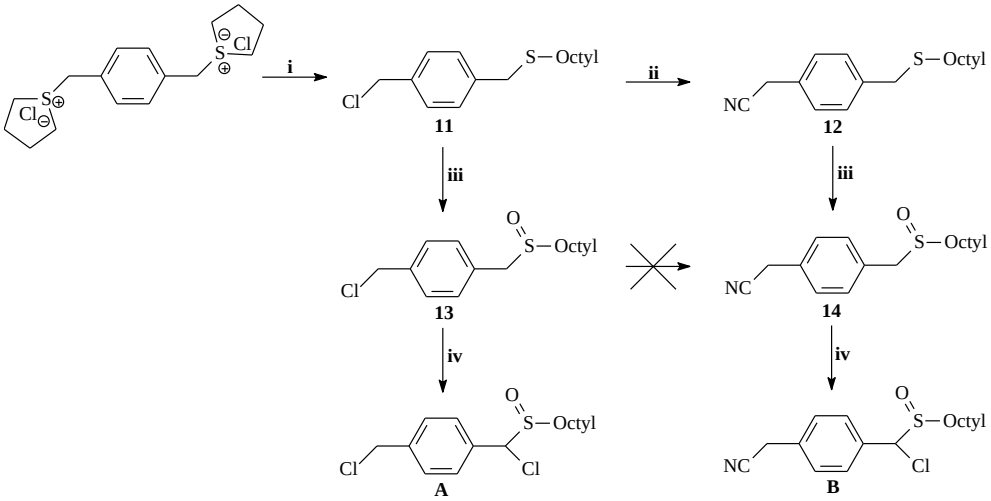

*Scheme 4: Synthesis of monomer **A** and **B**. Reaction conditions: **i**: HSOctyl, NatBuO, MeOH; **ii**: NaCN, H_2O/MeOH, ΔT; **iii**: H_2O_2/TeO_2, 1,4-dioxane; **iv**: NCS, CH_2Cl_2, pyridine.*

Monomer **A** was synthesised via a classical sulphinyl monomer synthesis[15] followed by a chlorination alpha to the sulphoxide. Selective halogenation of a sulphoxide leading to the corresponding alpha-halogen derivative can be performed using a variety of reagents and many mechanism have been presented on the basis of kinetic and stereochemical studies.[16,17] In this work, this reaction is performed very selectively in high yield when

mixing sulphoxides **13** or **14** together with NCS in dichloromethane and pyridine. The pyridine plays an important role in this reaction and acts as a base.[17]

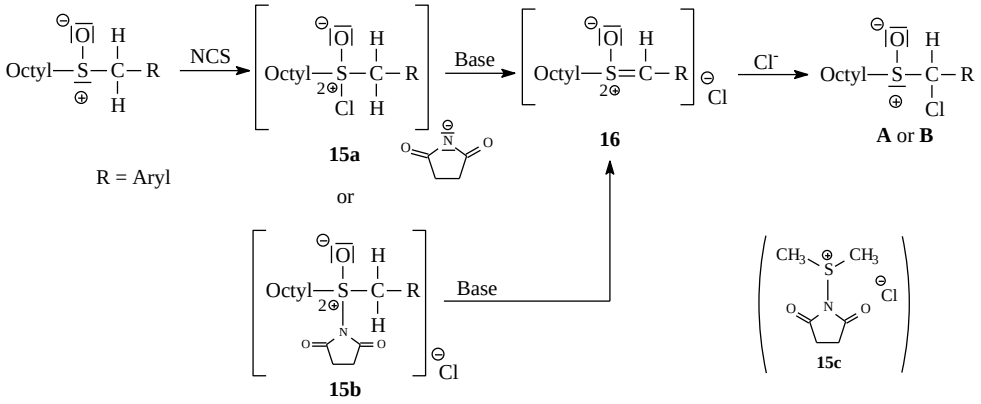

Scheme 5: Selective formation of alpha-chlorosulphoxides.

Once the oxosulphonium salt **15a** or **15b** is formed a base-assisted (pyridine) elimination of the succinimide group takes place to form intermediate **16**. The intermediary formation of **15b** also has to be considered based on the fact that S-(N-succinimido)dimethylsulphonium chloride **15c** was isolated in the reaction of dimethyl sulphide with NCS. However the possibility that a chloro-oxosulphonium salt **15a** is produced as an intermediate and that **15a** is in equilibrium with **15b** cannot be excluded.[17] Consecutive attack of the halide anion in intermediate **16** yields the desired alpha-chlorosulphoxides **A** and **B**.[17] (Scheme 5) The chloride substitution selectively occurs at the benzylic position alpha to the sulphoxide because these benzylic protons have the lowest Pk_a. This reaction results in the formation of 2 diastereomers which are inseparable using simple chromatographic techniques. Consequently, the mixture of products is used in all polymerisation reactions. Typical yields for this reaction are situated around 70 percent. According to this procedure monomer **A** could be synthesised in 46 percent overall yield starting from the bissulfonium salt.

The synthesis of monomer **B** was similar but slightly more complicated. Substitution of the benzylic chlorine atom by a cyano group on the sulphinyl monomer stage (**13)** proved impossible since the sodium cyanide used in this reaction may also act as a base and cause polymerisation. Moreover, the conditions in which this reaction has to be carried out in order to come to acceptable yields are rather harsh which made the co-occurring

polymerisation the dominating process. In order to circumvent this problem the cyano group had to be introduced at an earlier stage. On the thioether-stage (**11**) the cyanide group could be introduced in high yield without causing polymerisation. Consecutive oxidation followed by selective chlorination alpha to the sulphoxide yielded monomer **B** in good yield (35 percent overall yield starting from the bissulfonium salt).

Monomers **A** and **B** were characterised with NMR spectroscopy. The ^{1}H-NMR spectrum clearly shows the selective chlorination alpha to the sulphoxide. Before chlorination compound **13** (classical sulphinyl monomer) shows signals that can be assigned to protons H1-H3. Due to the sulphoxide functionality the protons H2 split up to yield a doublet of doublets with a large coupling constant of 12.9 Hz. Due to the asymmetry the sulfoxide group introduces, the protons H3 also yield a multiplet. (Figure 1a) After the selective chlorination (performed as just described) the proton spectrum has changed significantly and the spectrum obtained corresponds to that of monomer **A**. (Figure 1b) The protons H1' remain unchanged as can be concluded from their identical chemical shift. The chlorination does not occur at this benzylic position. Proton H2' has shifted downfield considerably (5.5 ppm) and the multiplicity has disappeared which suggests only one proton remains thus yielding a singulet. The multiplicity of the protons H3' has also increased due to the presence of two racemic centres in the immediate neighbourhood. These spectra clearly demonstrate the chlorination occurs selectively at the benzylic position alpha to the sulphinyl group. A similar observation is seen for the alpha chlorination towards monomer **B**.

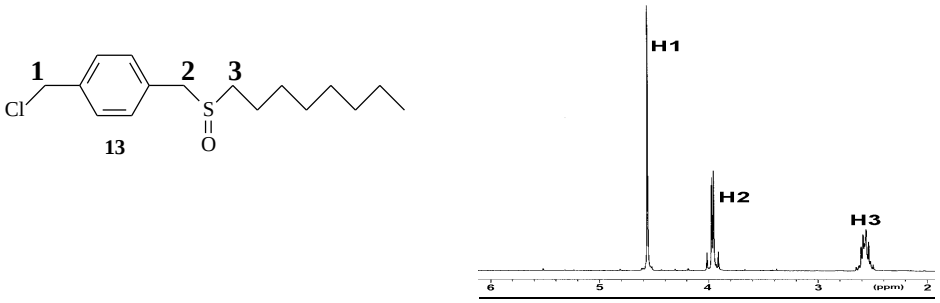

*Figure 1a: Enlarged part of the ^{1}H-NMR spectrum of compound **13**.*

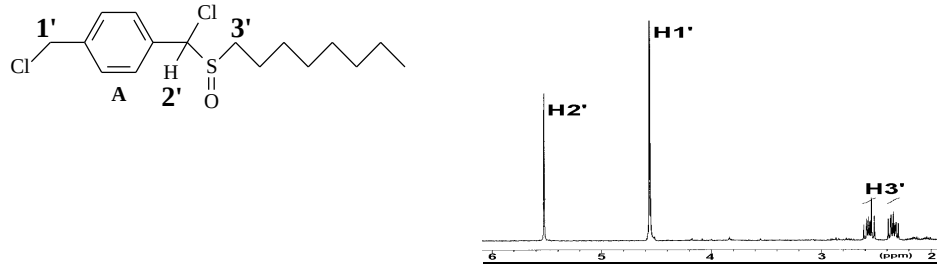

*Figure 1b: Enlarged part of the [1]H-NMR spectrum of monomer **A**.*

2.2.2 UV-Vis measurements on monomers A and B

Once these monomers were synthesised, the formation of the actual monomer in the polymerisation – the *p*-quinodimethane system (**17** or **18**) - was investigated with UV-Vis measurements. (Scheme 6) It is well known that quinoid compounds show very characteristic and distinct absorption signals around 300 nm.[18] By continuously following the intensity of this absorbance versus time a clear idea about the formation and the reacting away of the quinoid compound is obtained. A stop-flow apparatus was used to allow very fast measurements and the concentrations used were to low to initiate polymerisation. During these measurements monomer and base (Na*t*BuO) solutions (10^{-4}M in 2-BuOH) were brought together in the measuring cell of the spectrometer and the absorption at the maximum wavelength for the respective quinoid compound was followed versus time. As already explained in chapter one, the first step in the polymerisation process is the abstraction of the most acidic proton in the monomer. After this acid-base reaction a 1,6-elimination will then yield the *p*-quinodimethane system which is the actual monomer in the polymerisation. (Scheme 6) In general, evaluation of this process by UV-Vis measurements is a relatively simple way to learn about the polymerisation capabilities of a specific monomer.

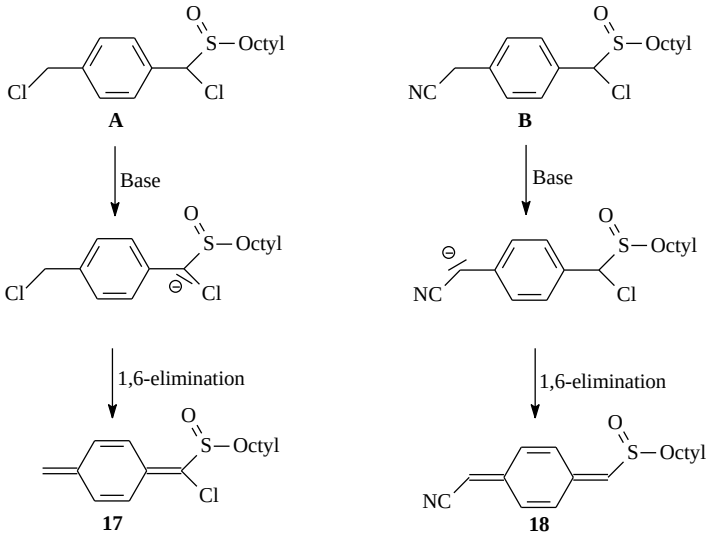

*Scheme 6: Schematic overview of the formation of the p-quinodimethane systems **17** and **18** from monomers **A** and **B**.*

In monomer **A** the base abstracts the proton alpha to the sulphoxide group and via a subsequent 1,6-elimination the quinoid **17** is formed. Figure 2 shows the absorption spectrum of monomer **A** when brought together with a base solution. A new absorption quickly arises at 330 nm and then declines again. This decline, which corresponds to the consecutive reaction of the *p*-quinodimethane system with the solvent (2-BuOH) yields compounds **19**. (Scheme 7) Mass spectroscopy proved the presence of these compound. At 270 nm a clear isosbestic point is observed.

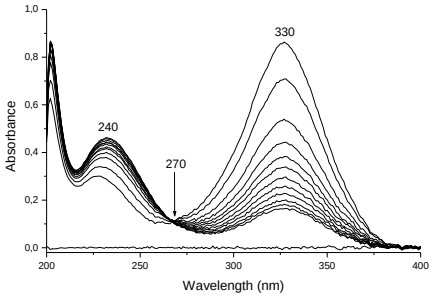

*Figure 2: UV-Vis spectra showing formation and consumption of quinoid **17**.*

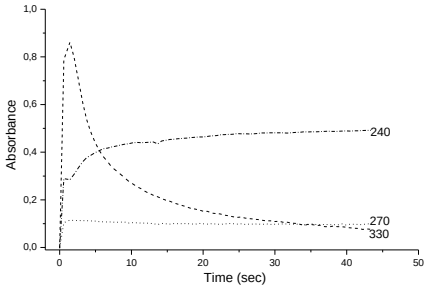

Figure 3: Absorption at 330, 270 and 240 nm versus time.

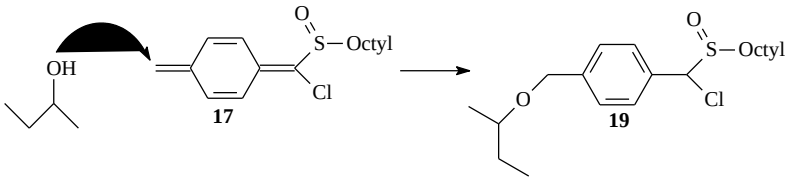

*Scheme 7: Formation of the solvent substituted products **19**.*

Figure 3 shows the absorbance at three characteristic wavelengths (330, 270 and 240 nm) versus time. In this way the relative trends of the processes that occur become clear. The quinoid absorption at 330 nm reaches its maximum absorbance after a 2.4 seconds and then declines again. The absorption at 240 nm corresponds to the absorption of the solvent substituted product (**19**) and continuously increases during the measurement. The absorption at the isosbestic point (270 nm) remains constant.

Exactly the same measurements were conducted on monomer **B** and a similar conclusion can be drawn for this monomer. In this case, the base abstracts the proton alpha to the cyano group because quinoid formation can only occur by abstraction of this proton followed by a 1,6-elimination of the chloride atom. (Scheme 6) Here, although exact the same concentrations were used, the quinoid absorption at 350 nm reaches it maximum absorption faster than compared to that of monomer **A**. The decline in quinoid absorption also is much faster. Since identical conditions were used in both measurements, these differences can only be caused by the differences in chemical structure of the different monomers. The maximum absorbance for the quinoid structures **17** and **18** versus time are plotted in Figure 4.

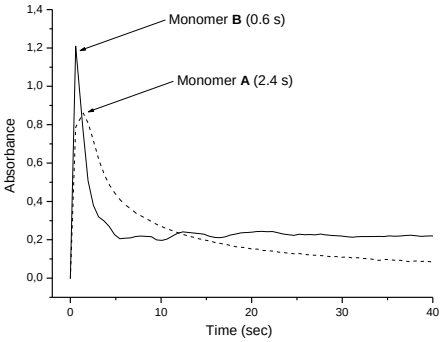

*Figure 4: Absorption at the maximum wavelength for the quinoid compounds of monomer **A** and monomer **B**.*

For comparison, the quinoid compound formed from the classical sulphinyl PPV monomer (**13)** (as obtained from an identical measurement) only reaches it maximal absorption after 650 seconds so quinoid structures **17** and **18** reach their maximum absorbance much faster (2.4 and 0.6 seconds respectively). These dissimilarities may be brought back to the differences in acidity of the proton that has to be abstracted in the first step of the process. In total, quinoid formation is a very complicated process which is influenced by a lot of parameters and a lot of further research is required to obtain a better understanding of this process. Nevertheless, these UV-Vis measurements have shown that quinoid formation is relatively easy for monomers **A** and **B**. Consequently, we expect these monomers can be polymerised in 2-BuOH.

2.2.3 Polymerisation of monomer A

Monomer **A** was polymerised in different solvents according to the "standard" procedure. (Experimental Section) Before bringing them together, the base (Na*t*BuO, 1.05 eqv) and monomer solutions were degassed by a continuous flow of nitrogen. The base solution was added to the monomer solution in one shot and the reaction time was one hour during which the passing of nitrogen was continued. The polymerisation temperature was 30°C. The reaction was terminated by pouring the polymerisation mixture in ice-water. Extraction and precipitation in a cold ether/*n*-hexane mixture yielded the precursor polymer **20**. The

filtrate was evaporated to yield the restfraction. Both the precursor polymer and the restfraction were analysed.

Polymerisations were performed in 2-BuOH, THF or a 50/50 (vol%) mixture of both. GPC on the precursor polymers was performed versus PS standards using THF as the eluent. Molecular weights and polydispersities are summarised in Table 1. Each restfraction was analysed with ^{1}H-NMR spectroscopy and consisted of pure solvent substituted product (**19**) when 2-BuOH was present in the solvent mixture. (Scheme 7) In THF no solvent substitution can occur and consequently, the restfraction of this polymerisation consisted purely of unreacted monomer.

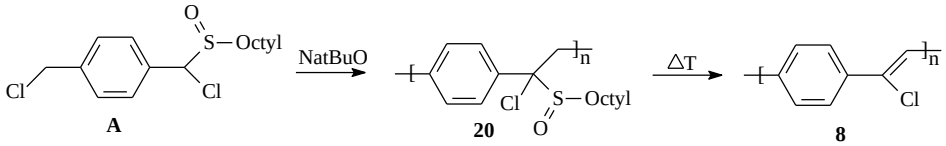

A **20** **8**

*Scheme 8: Synthesis of the precursor polymer **20** and consecutive conversion to the conjugated structure (**8**).*

Polymerisation		**Copolymer**		**Restfraction**	
Solvent	Yield (%)	M_w (x 10^{-3})	PD	Mon **A**[a]	Comp **19**[a]
2-BuOH	59	912	4.41	0	100
2-BuOH/THF (50/50)	46	364	3.05	0	100
THF	36	71	2.25	100	0

*Table 1: Polymerisation results for monomer **A**. GPC was performed versus PS standards using THF as eluent. [a]: Composition of the restfraction as determined with ^{1}H-NMR spectroscopy.*

The polymerisation of monomer **A** in 2-BuOH results in very high molecular weight precursor polymers. When the polymerisation is performed in THF the molecular weight of the precursor polymer obtained has dropped significantly and when a 50/50 mixture of these solvents is used an intermediate molecular weight is obtained. For the polymerisation yield a similar trend can be observed. The highest yields are obtained in 2-BuOH, when

THF is added as a co-solvent the polymerisation yield drops. These observations suggests that the molecular weight can be tuned depending on the amount of THF that is added as a co-solvent.

Like in all ^{1}H-NMR spectra for sulphinyl precursor polymers, the ^{1}H-NMR spectrum of the precursor polymer **20** shows broad signals because the relatively short T_2 (spin-spin relaxation time). (Figure 5) In this spectrum, protons H3 do not give rise to two separate signals as in the spectrum of a non-substituted sulphinyl precursor polymer. All resonances can be assigned to the respective hydrogen atoms.

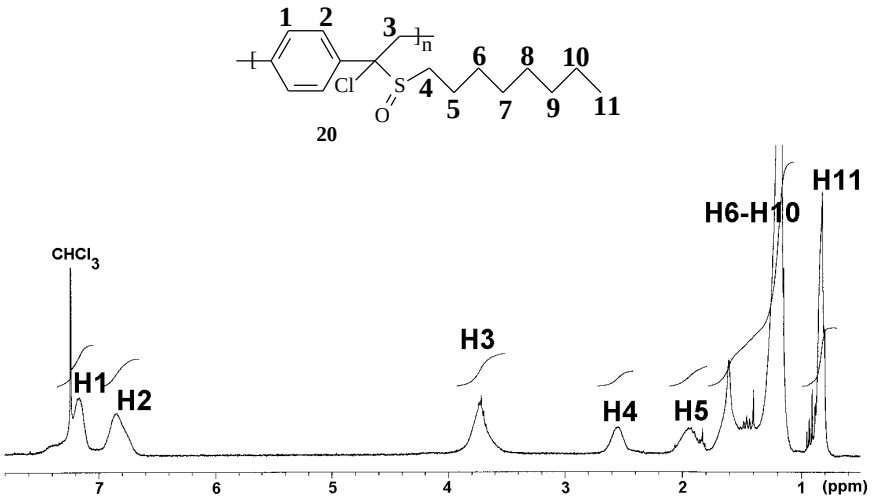

*Figure 5: ^{1}H-NMR spectrum of the precursor polymer **20**.*

2.2.4 Thermal conversion of precursor polymer 20 to the conjugated structure

The final step in the sulphinyl precursor route is the thermal elimination of the sulphinyl group to yield the double bond. As explained in chapter one this elimination is an expulsion of sulphenic acid and the formation of a double bond on the polymer backbone.[19] The double bonds formed are all *trans* due to steric hindrance in the transition state which leads to *cis* double bonds. Numerous techniques can be applied to monitor the elimination process. The ones used here are *in situ* UV-Vis spectroscopy, *in situ* FT-IR spectroscopy and direct insertion probe mass spectroscopy (DIP-MS).

UV-Vis spectroscopy measurements were carried out on film, spin-coated on quartz windows. An experimental set-up was used which allowed *in situ* monitoring of the elimination process. For this purpose a specially designed oven which contained the precursor polymer spincoated on the quarts window was placed in the beam of the spectrometer. A dynamic heating program of 2°C/min up to 275°C, under a continuous flow of nitrogen, was used. Before heating, the precursor polymer shows strong absorptions below 250 nm. (Figure 6) As the heating program progresses, new absorption bands appear that gradually red shift with increasing temperature. When higher temperatures are reached the fine structure disappears and the absorption band broadens to cover the various oligomer bands. Finally the maximal conjugated polymer with an absorption maximum around 354 nm is obtained. This maximum is blue shifted compared to the absorption maximum of PVV prepared via the sulphinyl route (420 nm). Apparently the chlorine substitution on the vinylene double bond disrupts the "effective conjugation length" which causes the absorption maximum to blue shift. Similar blue shifts have been observed when other substituents were placed on the vinylene double bond, e.g. a methyl or phenyl group.[20] The gradual formation of the conjugated structure is shown in Figure 6. When the absorption at this maximum wavelength (354 nm) is plotted versus temperature, the elimination and stability behaviour of the polymer becomes clear. (Figure 7) Formation of the first stilbene like conjugated units commences around 60°C and the maximal absorption at 354 nm is reached when the temperature has reached 100°C at a temperature ramp of 2°C/min. During this short temperature interval the maximal conjugated structure is formed. Between 100 and 200°C the conjugated system is stable since there is no decline in the maximal absorption. Starting from 200°C, the absorption at 354 starts to decrease. This observation probably corresponds to a slow degradation of the conjugated structure at these temperatures. Together with this decline in maximum absorption a small blue shift of the absorption maximum is observed which may be explained by a shortening of the conjugated segments in the polymer backbone.

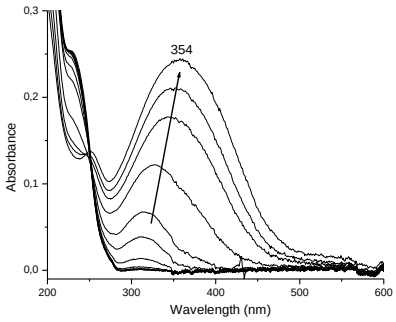

Figure 6: Gradual formation of the conjugated structure.

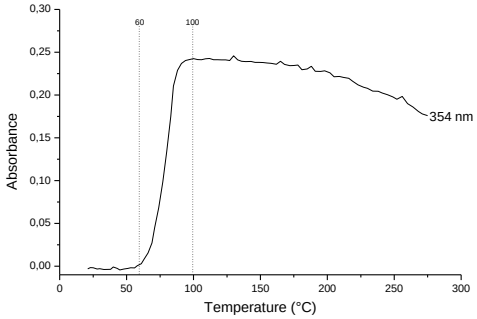

Figure 7: Absorption at 354 nm versus temperature.

A second technique that was used to study the thermal elimination and stability of the sulphinyl precursor polymer **20** was *in situ* FT-IR. In this technique an identical experimental set-up was used as in the *in situ* UV-Vis measurements. Because of the identical experimental set-up the results derived from both techniques complement each other and a very detailed picture of the elimination process is obtained. *In situ* FT-IR measurements were performed on film, spincoated on KBr disks and a dynamic heating program of 2°C/min up to 200°C, under a continuous flow of nitrogen, was used. The most important and distinct absorption bands in the IR spectrum, which are changed during the elimination process, are those of the sulphoxide group at 1068 cm^{-1} and that of the vinylene double bond at 990 cm^{-1}. (Figure 8) The absorption bands at 1686 and 1598 cm^{-1} probably also originate from the double bond as their thermal behaviour is similar to that of the vinylene double bond. The relative trends in both elimination and stability behaviour of the precursor polymer **20** become clear when the intensity of the most important absorption bands is plotted versus temperature. (Figure 9) From these IR data we conclude that the fully conjugated system is formed in the temperature domain between 60 and 80°C. At 140°C the absorption bands that originate from the double bond start to decline again which suggests that this conjugated polymer **8** is not very stable at elevated temperatures. The results obtained from the FT-IR measurements are in accordance with the UV-Vis data.

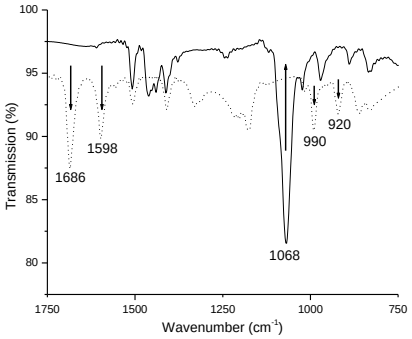

Figure 8: Enlarged part of the IR spectrum during conversion.

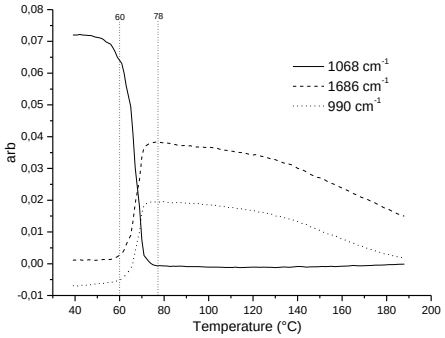

Figure 9: Absorption at 1686, 1068 and 990 cm^{-1} versus temperature.

The elimination and stability behaviour was also studied with DIP-MS, to allow the analysis of the elimination products. In this technique the precursor polymer is placed directly on the heating element of the probe and measurements are performed under high *vacuum*. The heating rate used in this technique was 10°C/min and the sample was heated till 650°C. By plotting the total ion current versus temperature, the thermal stability of both precursor and conjugated polymer can be visualised. (Figure 10) As expected two signals can be observed in the thermogram, the first one (between 80 and 160°C), based on the fragments detected, corresponds to the elimination of the sulphinyl groups to yield the double bonds. These temperatures are higher than those obtained from the UV-Vis and IR measurements because of the different heating rates used. The second signal (between 400 and 500°C) corresponds to the degradation of the conjugated structure.

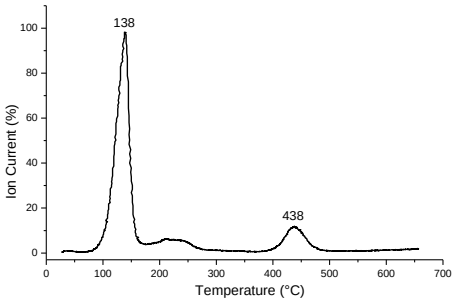

*Figure 10: Thermogram of the sulphinyl precursor polymer **20**.*

DIP-MS (138°C)	
Fragment	**m/z**
$C_8H_{17}SSC_8H_{17}$	290
$SS(O)C_8H_{17}$	194
$S(O)C_8H_{17}$	161
SC_8H_{17}	145

Table 2: Mass fragments of the elimination products.

In conclusion, the data obtained from these different techniques indicate that the elimination for this precursor polymer is a very fast process and can be performed starting from a temperature around 60°C. Furthermore, from the FT-IR and UV-Vis data it is assumed that temperatures above 150°C can already give rise to the thermal degradation of the conjugated structure.

2.2.5 Polymerisation of monomer B

Monomer **B** was polymerised in the same "standard" conditions as were used for the polymerisation of monomer **A**. (Scheme 9) As mentioned before, UV-Vis measurements had shown that the quinoid structure of monomer **B** is formed very quickly which suggests polymerisation is possible in 2-BuOH. Unfortunately, polymerisation of monomer **B** towards high molecular weight sulphinyl precursor polymers proved impossible and only very low molecular weight fragments were obtained. The nature of this behaviour largely results from the presence of the cyano group as will be explained later on.

Polymerisations were conducted in 2-BuOH or THF and Na*t*BuO was always used as the base. Both the precursor polymer and the restfraction were analysed. GPC was performed versus PS standards with DMF as the eluent. The polymerisation results are summarised in Table 3.

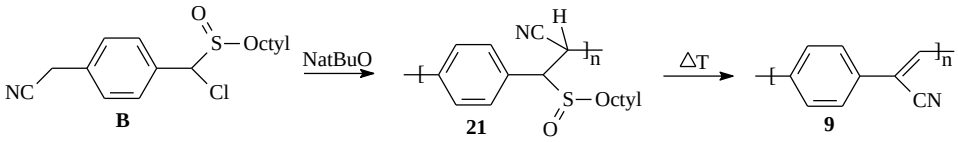

*Scheme 9: Synthesis of the precursor polymer **21** and consecutive conversion to the conjugated structure (**9**).*

Polymerisation			Polymer		Restfraction	
Solvent	Temp. (°C)	Yield (%)	M_w	PD	Mon **B**[a]	Comp **22**[a]
2-BuOH	32	36	7800	1.54	0	100
$THF_{(dry)}$	30	37	6200	1.35	100	0

*Table 3: Polymerisation results for monomer **B** under "standard conditions" in 2-BuOH and dry THF. [a]: Composition of the restfraction as determined with ^{1}H-NMR spectroscopy.*

In both solvents tested, polymers with similar molecular weight distributions were obtained in comparable yields. The restfraction of each polymerisation was analysed with ^{1}H-NMR spectroscopy and showed it consisted completely of solvent substituted monomer **22** when the polymerisation was performed in 2-BuOH. Note that this solvent substitution only occurs at the less sterically hindered side of the quinoid system which results in the selective formation of compound **22**. (Scheme 10) In THF, this side-reaction is impossible and only unreacted monomer remained.

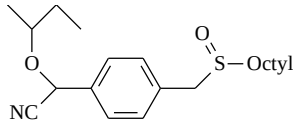

22

*Scheme 10: Chemical structure of the solvent-substituted monomer (**22**) when the polymerisation is performed in 2-BuOH.*

Worth mentioning is the fact that upon addition of the base, the solution immediately changed colour from colourless to dark blue-black. The precursor polymers obtained were also deep orange-red coloured which suggests elimination of the sulphinyl groups already (partially) occurred. When looking for an explanation for the low molecular weights we have to evaluate the polymerisation process more in detail. As already mentioned, once the actual monomer in the polymerisation – the quinoid compound – is formed, it self-initiates its own radical chain polymerisation. Because the quinoid structure (**18**), formed from monomer **B**, is substituted at both sides, sterical hindrance can possibly block this self-initiation and thus prevent polymerisation. It is known that quinoid compounds with electron withdrawing substituents on both sides of the *p*-xylylene unit are relatively stable and polymerisation can only occur when an external initiator is applied.[21,22] In order to test this feature additional polymerisations were performed in 2-BuOH. In a first instance the radical initiator AIBN was added to the polymerisation mixture and consequently the polymerisation temperature had to be raised to 60°C to allow thermal decomposition of the AIBN and the generation of radicals. The temperature could not be raised any further because than elimination of the sulphinyl groups can be initiated. A second polymerisation performed in 2-BuOH was a 50/50 copolymerisation between monomer **B** and the classical sulphinyl PPV monomer **13**. By adding an amount of the classical PPV monomer we were

hoping that this monomer would perform the self-initiation and that monomer **B** could be incorporated once the polymerisation had been initiated. Still, low molecular weight polymers were obtained in both polymerisation reactions and similar results were obtained as for the polymerisations without the external initiator. (Table 4) To our surprise, also in the 50/50 copolymerisation no higher molecular weight polymers could be isolated. In this copolymerisation the classical sulphinyl PPV monomer does not homo-polymerise towards high molecular weight precursor polymers. For some reason homo-polymerisation of either monomer or a copolymerisation between the two is impossible in this case. Based on the ^{1}H-NMR spectrum, the restfraction for this copolymerisation (performed in 2-BuOH) consisted out of three compounds, the solvent substituted monomer **22** (57 percent), the unchanged classical sulphinyl monomer (11 percent) and the solvent substituted product of this compound (32 percent). As already shown with the UV-Vis measurements in solution, this composition again indicates the different reactivity towards solvent substitution for monomer **B** and the classical sulphinyl monomer.

Both experiments demonstrate that external initiation of these polymerisations is not evident.

Raising the concentration from the standard used 0.1M to a ten times as concentrated solution (1M) did not yield higher molecular weight precursor polymers either although the polymerisation yield increased slightly. (Table 4)

Polymerisation			**Polymer**		**Remarks**
Solvent	Temp. (°C)	Yield (%)	Mw	PD	
2-BuOH	30	52	5900	1.39	50/50 copolymeristion with PPV
2-BuOH	60	30	6700	1.37	10% AIBN was added
$THF_{(dry)}$	30	46	6400	1.44	Concentration raised to 1M

*Table 4: Polymerisation results for monomer **B** under slightly altered "standard conditions". Molecular weights were determined relative to PS standards with DMF as the eluent.*

Characterisation of the precursor polymers with NMR spectroscopy proved very difficult, the limited solubility of the polymers strongly hindered these measurements and only very diffuse spectra could be obtained from which it is hard to draw any conclusions.

In conclusion, the polymerisation of monomer **B** only yields low molecular weight precursor polymers. The reason for this behaviour is caused by the intrinsic chemical nature of the precursor polymers synthesised and the electron withdrawing cyano group plays an important role in this aspect. A general overview of the processes that can occur during polymerisation is depicted in Scheme 11.

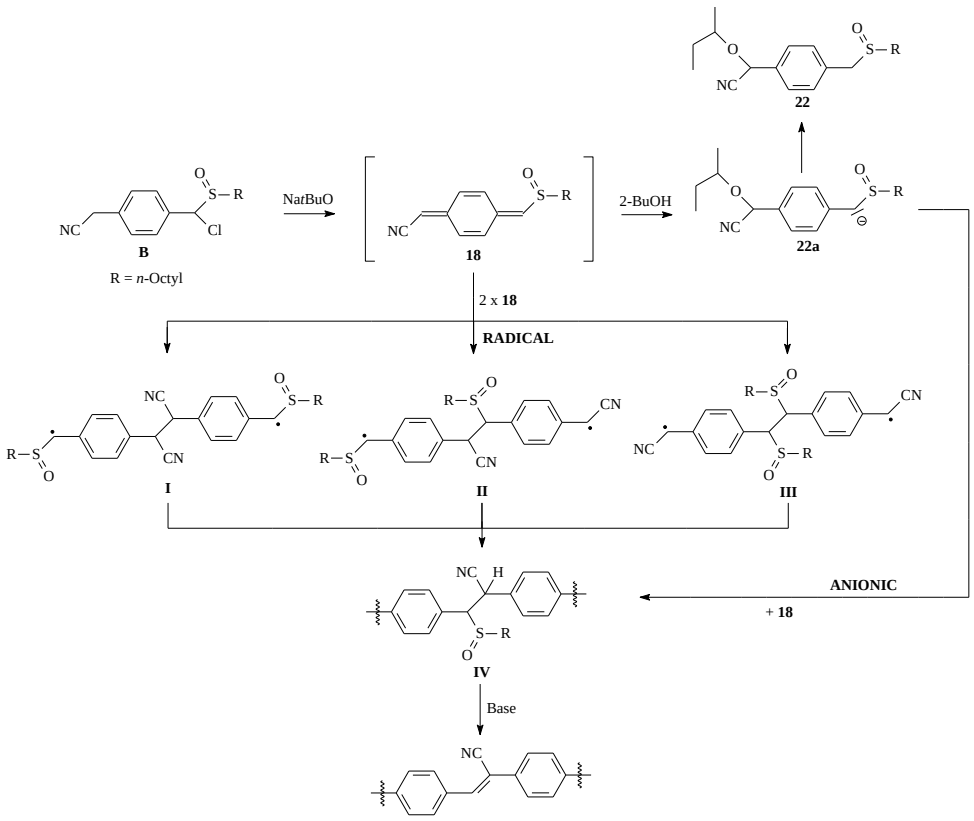

*Scheme 11: Schematic overview of the processes that can occur during the polymerisation of monomer **B**.*

Once the quinoid structure **18** is formed (the actual formation was confirmed by UV-Vis measurements in solution) it can react via several pathways. When 2-BuOH is present a side-reaction that is likely to occur is the reaction between the quinoid compound **18** and 2-BuOH to yield the anion **22a**. This anion can be quenched to form the solvent substituted

monomer **22** or it can further propagate with a quinoid compound **18**. This last process is referred to as the anionic polymerisation process and eventually yields a precursor polymer **IV**. The amount of solvent substituted product **22** is largely determined by the reactivity of the quinoid as was proven by the UV-Vis measurements in solution and from the composition of the restfraction of the 50/50 copolymerisation. The reactivity of this quinoid structure towards solvent substitution is very high, this systems proved to be much more reactive towards solvent substitution than the classical sulphinyl PPV monomer. This side-reaction can probably account for the relatively low polymerisation yields in 2-BuOH.

On the other hand, two quinoid systems may also couple to form a diradical (**I**, **II** or **III**). This step is also referred to as the self-initiation step in the polymerisation reaction. As explained in chapter one, self-initiation in a classical sulphinyl polymerisation proceeds via coupling of the two less sterically hindered sides of the quinoid system. For this quinoid compound (**18**) different diradicals (**I**, **II** or **III**) are possible but diradicals **I** and **II** are probably favoured due to the reduced sterical hindrance upon coupling. However, the formation of diradical **III** can not be ruled out, a cyano group is a very efficient stabiliser for radicals (e.g. AIBN).

Anyhow, independent of the exact nature of the polymerisation mechanism, consecutive propagation reactions will inevitably lead to precursor polymers that contain the repeating unit **IV**. (Scheme 11) The presence of the acid proton alpha to the cyano group may contribute to the formation of the low molecular weight precursor polymers. Due to the presence of the sulphinyl group in the beta-position, the pK_a of this proton is lower than that of the proton alpha to the cyano group in monomer **B**. Furthermore, the pK_a of this proton is further reduced because a basic 1,2-elimination of the sulphinyl group will lead to the formation of the double bond. In this way a conjugated system is formed which results in an insoluble polymer that precipitates from the reaction mixture. This formation of double bonds also causes the bright orange-red colour of the “precursor” polymers and in the end will probably prevent propagation towards high molecular weight polymers.

This assumption of premature elimination was also confirmed by UV-Vis and IR measurements on films of spincoated “precursor” polymer. Even before the heating program started the conjugated structure was already (partially) present. As can be seen

from the UV-Vis measurement, (Figure 11) the "precursor" polymer **21** already has an absorption maximum at 362 nm at room temperature (dashed line). This indicates that already a lot of sulphinyl groups have been eliminated to yield double bonds. When higher temperatures (165°C) are reached the maximum absorption further shifts to 374 nm (solid line). For comparison, the UV-Vis spectrum of any other sulphinyl precursor polymer at room temperature hardly ever shows absorption bands above 300 nm.

The IR spectrum of the same "precursor" polymer already shows an absorption at 914 cm^{-1} at room temperature (dashed line) which again indicates the vinylene double bond has already been formed partially. (Figure 12) During the heating up the sulphinyl absorption at 1048 cm^{-1} further declines and the absorption at 914 cm^{-1} still slightly increases. At 165°C the sulphinyl absorption has declined completely (solid line).

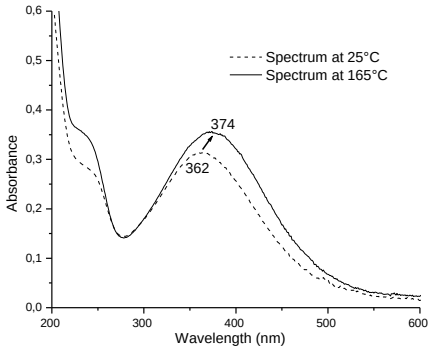

*Figure 11: UV-Vis spectra of the "precursor polymer" **21**.*

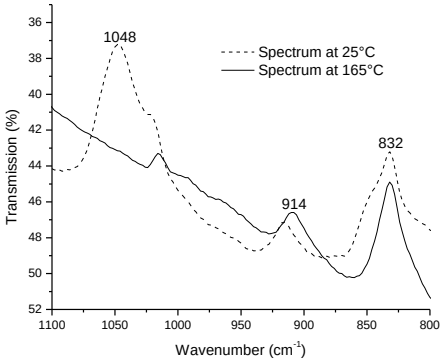

*Figure 12: IR spectra of the "precursor polymer" **21**.*

In conclusion, due to the chemical structure of the monomer **B** and largely because of the presence of the strong electron withdrawing cyano group, polymerisation of this monomer only yields very low molecular weight polymers.

2.3 Poly(2,5-dicyano-1,4-phenylene vinylene)

A third electron deficient PPV derivative discussed in this chapter is the poly(2,5-dicyano-1,4-phenylene vinylene) or dicyano-PPV. (Scheme 12) Addition of two cyano-groups to the phenyl ring leads to PPV derivatives with enhanced electron affinity and electrochemical stability. Others already reported on the incorporation of a cyano containing conjugated polymer in a double-layered LED (ITO/PPV/CN-PPV/Al) which resulted in very high internal quantum efficiencies (up to 4%).[4,23] This improved device efficiency was attributed to an enhanced electron injection facilitated by the electron withdrawing cyano groups. Ever since this report, numerous papers have appeared which address the interesting properties of cyano containing conjugated polymers.[5,24] The references sited all make use of different copolymers between a cyano containing monomer and an alkoxy substituted monomer. The latter is a necessity to guarantee solubility in common organic solvents and to allow efficient device fabrication.

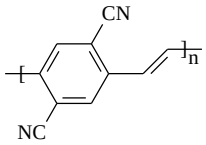

Scheme 12: Chemical structure of poly(2,5-dicyano-1,4-phenylene vinylene)

In the past several attempts have been made to synthesise the homo poly(2,5-dicyano-1,4-phenylene vinylene). However, the existing precursor routes (Wessling and Gilch) do not allow an efficient synthesis of this PPV derivative towards sufficiently high molecular weight polymers. When a direct synthetic approach (Wittig condensation or Heck coupling reaction) is used, insoluble very low molecular weight oligomeric fragments are obtained and careful control over the reaction conditions is required. As mentioned above, copolymerisation with an alkoxy-substituted PPV derivative (MEH-PPV) is necessary to enhance the solubility (also in the conjugated form) and allow efficient device preparation.[5] Even than, relatively low amounts of the dicyano-monomer could be incorporated because of solubility limitations. The synthesis of a copolymer between the dicyano-monomer and OC_1C_{10} via the sulphinyl precursor route will be discussed in chapter 4.

Here we will evaluate the possibilities the sulphinyl precursor route offers in the synthesis of the homo poly(2,5-dicyano-1,4-phenylene vinylene). At present, this polymer has again been placed in the spotlight because of its good electron accepting properties. In this context the cyano-PPV derivatives may well prove to be challenging candidates that could replace the bucky balls, nowadays used in organic solar cells, thus allowing the production of an all polymer solar cell. Here, we will demonstrate that the sulphinyl precursor route allows the synthesis of this derivative, better and more efficiently than any other synthetic pathway reported to date. This again demonstrates the versatile character of our precursor route.

2.3.1 Monomer synthesis

Monomer synthesis started from the commercially available 2,5-dibromodimethylbenzene (**23**) which was transformed to the 2,5-dicyanodimethylbenzene (**24**) using CuCN in DMF at reflux temperature.[25] This displacement can be performed in excellent yield (80-90%) and proceeds via the formation of an intermediate complex (**23a**). (Scheme 13)

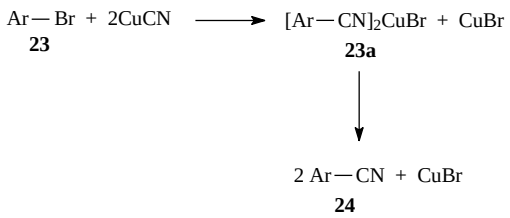

Scheme 13: Synthesis of arylnitriles.

As the reaction progresses the mixture becomes dark brown. The complex formed (**23a**) between the nitrile and the cuprous bromide is soluble in DMF while the cupper, the uncomplexed cupperbromide and the excess cuprous cyanide remain as precipitates. A very important step in this reaction process is the decomposition of the complex (**23a**) formed during reaction. Aqueous ferric chloride proved a very efficient reagent for destroying the reaction complexes. After extraction the dicyanide **24** was purified by crystallisation from ethanol. A key intermediate, like in all synthesises towards sulphinyl monomers, is played by the dihalogenide. In this case the dibromide **25** was synthesised from compound **24** via a radical halogenation reaction with NBS.[26] (Scheme 14) The reaction is performed in CCl_4 and dibenzoylperoxide is used as an initiator. This methodology is well documented in

literature and such radical halogenation reactions are used frequently in organic synthesis.[27] However, a drawback of this reaction is its low selectivity towards the desired dibromo compound **25**. Monohalogenation can be achieved in good to excellent yields but when dihalogenation is desired a complicated reaction mixture usually results. Here, the reaction mixture proved to consist for only 25 percent of dibromo **25** as was concluded from GC-mass spectroscopic measurements on the crude reaction mixture. Unreacted starting product **24** and monobromide **26** were present for approximately 30 and 38 percent respectively. In the remaining 7 percent there are a few unidentified reaction products and about 3 percent of tribromo products. The formation of a small fraction trihalogenated products always is an undesired side reaction that occurs during a radical halogenation. Fortunately, the dibromo compound **25** could be partially isolated in a nearly pure form by simple crystallisation from the reaction mixture. Apparently, the solubility behaviour of the dibromo compound **25** is very different to that of compounds **24** and **26**. A chromatographic separation further separated the reaction products and compounds **24** and **26** could be recycled in the reaction sequence which in the end (after 3 repetitions) increased the overall yield for this reaction to 51 percent. (Scheme 14)

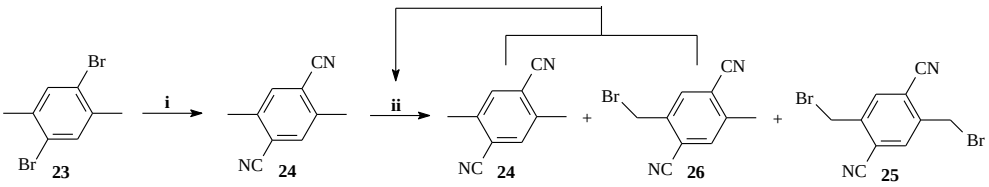

Scheme 14: Synthesis of the dibromide 27. Reaction conditions: ***i****: CuCN, DMF, ΔT;* ***ii****: NBS, DBP, ΔT*

The next step in a classical sulphinyl monomer synthesis would be the synthesis of bissulfonium salt **27** which can then be converted to the monosulphide in a highly selective way.[15] This approach could not be used in this synthesis because the bissulfonium salt (**27**) could only be formed in about 30 percent from the dibromide **25**. Probably, the strong electron withdrawing cyano groups lower the leaving capacities of the benzylic bromine atoms thus preventing an efficient formation of bissulfonium salt **27**. Furthermore, the consecutive reaction towards the monosulphide **28** did not prove to be selective towards the

desired product, largely because of the low solubility of the bissulfonium salt **27**. These drawbacks made an alternative synthetic approach necessary. (Scheme 15)

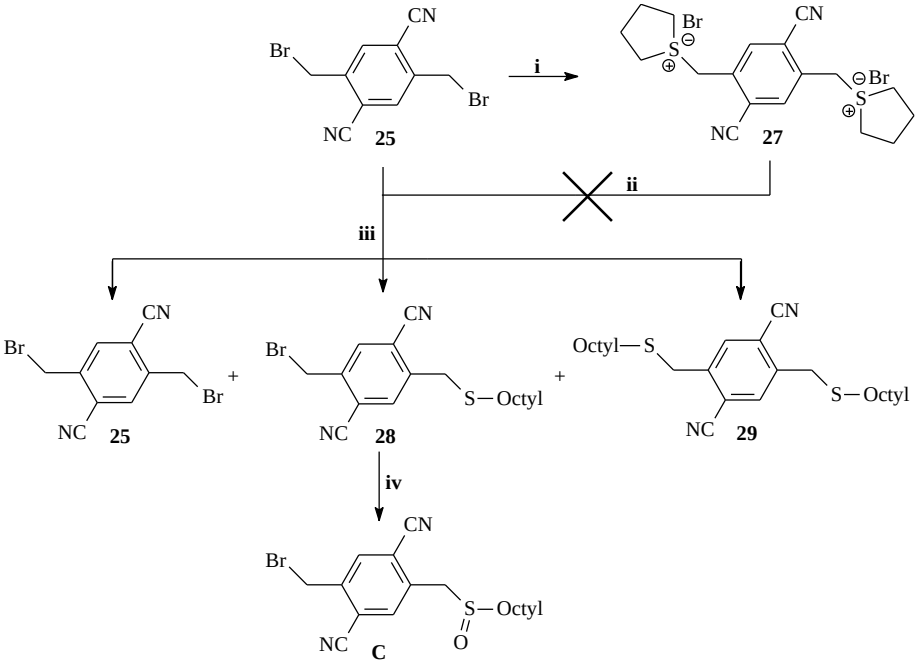

*Scheme 15: Synthesis of the dicyano sulphinyl monomer **C**. Reaction conditions: **i**: THT, MeOH; **ii**: HSOctyl/NatBuO, MeOH; **iii**: HSOctyl/NaH, $THF_{(dry)}$; **iv**: H_2O_2/TeO_2, 1,4-dioxane.*

As already mentioned in the introduction (Chapter 1) other ways exist to synthesise the monosulphide compounds. These methods are less selective and an excess of the dihalogenide (**25**) has to be used to prevent large amounts of disubstituted product (**29**) of being formed. After oxidation the excess dihalogenide (**25**) can be recuperated from the reaction mixture by a chromatographic separation. Here, a threefold excess of dibromide **25** was used. To a solution of compound **25** was added the octyl thiolate anion and reaction was allowed to proceed for 3 hours. The *n*-octyl chain was used to enhance the solubility on both the monomer and the precursor polymer stage. GC-MS measurements revealed the composition of the reaction mixture. (Table 4)

Product	Dibromide **25**	Monosulphide **28**	Disulphide **29**
Amount (%)	71	26	3

Table 4: Relative amounts of the different reaction products when a 3:1 ratio dibromide:octylthiolate anion is used. Percentages were determined by GC-MS measurements.

As expected, 71 percent of the reaction mixture proved to be starting product **25**. The desired monosulphide **28** was present for 26 percent and the quantity of the undesired disubstituted product **29** could be minimized to 3 percent. The oxidation to the sulphoxide was performed on the crude reaction mixture by using the H_2O_2/TeO_2 system in 1,4-dioxane. A chromatographic separation finally yielded the pure dicyano sulphinyl monomer **C** while the large excess of starting dibromide **25** could be recycled in the reaction process.
Monomer **C** was analysed by different techniques such as mass- and NMR-spectroscopy which all confirmed the chemical structure. The ^{1}H-NMR spectrum of monomer **C** is shown in Figure 13. The aromatic proton H6 lays down field compared to the other aromatic proton H3 because it is closest to the sulphinyl group. Protons H1 yield a singulet around 4.6 ppm. Due to the adjacent sulphoxide group, which introduces asymmetry, the protons H10 split up to yield a doublet of doublets with a large coupling constant of 13,2 Hz. The rest of the resonances in the ^{1}H-NMR spectrum can be assigned to the protons H11 to H18 which belong to the aliphatic tale of the sulphinyl group. Again because of the neighbouring sulphoxide group, the signal for H11 splits up to yield a multiplet.

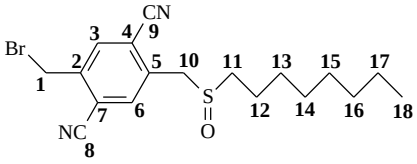

Monomer **C**

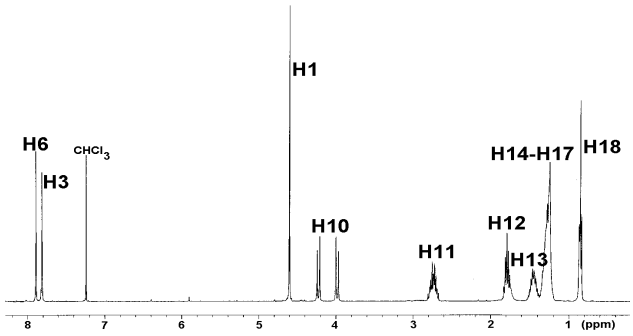

*Figure 13: [1]H- NMR spectrum of monomer **C**.*

Another thing worth mentioning is the assignment of the different carbon atoms in the ^{13}C-NMR spectrum, in particular those of the aromatic region. Full assignment of these carbon atoms was possible by combination of different NMR spectroscopic techniques. An APT (Attached Proton Test) enables a reliable determination of the carbon multiplicity. (Figure 14) In monomer **C** the aromatic carbon signals can be divided into the protonated aromatic carbons C3 and C6 (negative signals) and the quaternary carbons C2, C4, C5 and C7 (positive signals). Moreover the quaternary signals for the carbon atoms of the nitrile group C8 and C9 also appear in this domain (positive signals). By combining these data with those obtained from the ^{13}C-NMR spectrum of dibromide **25** complete assignment of all carbon atoms was possible. (Table 5) For example, in compound **25** C2 absorbs at 135.75 ppm, so consequently in monomer **C**, C2 will also be situated around this value and not more down field towards the resonance of C5. In this way C2 and C5 can be assigned. This reasoning can be extrapolated towards all other aromatic carbon atoms and complete assignment is possible by comparison of the different spectra.

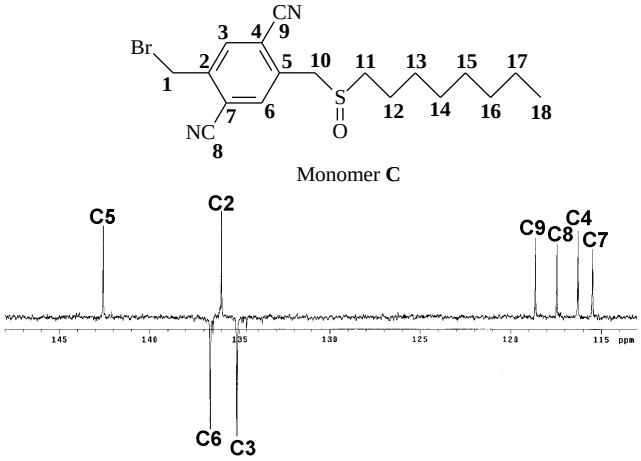

*Figure 14: Aromatic Part of the APT spectrum of monomer **C**.*

Carbon	Monomer **C** δ (ppm)	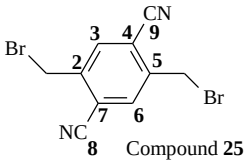 Compound **25** δ (ppm)
C2	136.02	135.75
C3	135.15	132.86
C4	116.29	115.04
C5	142.57	135.75
C6	136.63	132.86
C7	115.49	115.04
C8	117.44	116.92
C9	118.63	116.92

*Table 5: ^{13}C-NMR chemical shifts of monomer **C** and compound **27**.*

Once the monomer **C** was synthesised it was polymerised to the precursor polymer in different solvents. The polymerisation results will be discussed in the next paragraph. In the last sections of this paragraph we will focus on some small chemical modifications that were made on the monomer level. Such modifications were made in order to enhance the polymerisation process and come to precursor polymers with higher molecular weights.

Recently, a UV-Vis study on the classical sulphinyl PPV monomer revealed some new features.[28] During these measurements the formation of the actual monomer in the polymerisation – the *p*-quinodimethane system – is monitored as a function of time. The results obtained suggest that quinoid formation, for the classical sulphinyl PPV monomer, can be enhanced by improving the leaving group or by increasing the acidity of the proton alpha to the sulphinyl group. Indeed, when the leaving group was gradually improved in the series Cl, Br to I the quinoid compound was formed faster. The same holds true when the sulphinyl group (S(O)) is further oxidised to a sulphonyl group ($S(O)_2$). We should stress that a sulphonyl group is less interesting on the precursor polymer stage as it eliminates at much higher temperatures (250-300°C) compared to a sulphinyl group (65-110°C). These observations suggest that quinoid formation is the rate determining step in the overall polymerisation process. As just shown, within the boarders of the sulphinyl precursor route several options are at hand to improve quinoid formation. Both methods have also been applied here on the dicyano monomer. In this context, the bromine atom in monomer **C** was replaced by a iodine atom (better leaving group, monomer **D**) on the one hand and the sulphinyl group in monomer **C** was further oxidised to a sulphonyl group (increased acidity, monomer **E**) on the other hand. In monomer **F** both these chemical modifications were made. The transformations were performed by simple reactions in excellent yield. (Scheme 16)

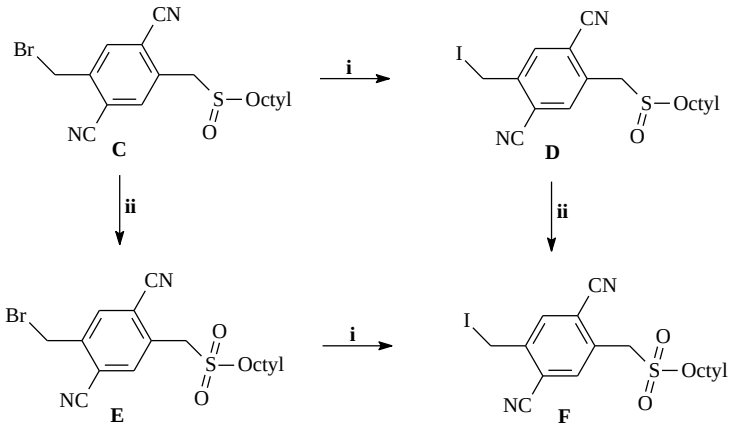

Scheme 16: Chemical modifications on the monomer stage. Reaction conditions: ***i****: NaI, acetone , ΔT (87%);* ***ii****: m-CPBA, CH_2Cl_2, 0°C (89%).*

2.3.2 Polymerisation of monomers C, D, E and F

Monomers **C** to **F** were polymerised to the respective precursor polymers in a range of solvents according to the "standard" procedure. (Experimental Section) (Scheme 17)

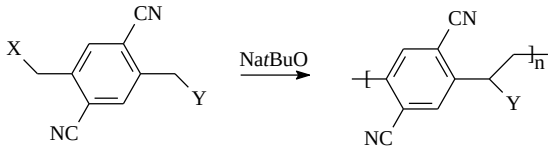

Scheme 17: Precursor polymer synthesis. (X= Br or I; Y= S(O)Octyl or S(O)$_2$Octyl)

All polymerisation reactions were conducted at 30°C (except for the polymerisation in 2-BuOH which was performed at 60°C) and Na*t*BuO was always used as a base in a slight excess of 1.05 equivalents. Worth mentioning is the fact that upon addition of the base the colour of the polymerisation mixture immediately turned dark blue. This sharp colour change may indicate the formation of anions. The polymerisation results obtained vary depending on the solvent that was used for the polymerisation. The highest molecular weights were obtained when dried solvents were used.

2.3.2.1 Polymerisation in dry THF and dry 1,4-dioxane

When the polymerisation of monomers **C** and **D** was performed in solvents like dry THF or dry 1,4-dioxane the molecular weight distribution of the precursor polymers obtained was rather broad and several peak maxima could be observed in the GPC chromatogram. (Figure 15) This behaviour had also been observed in former work within our research group where the polymerisation of the 2,5-xylene dichlorosulphinyl monomer was studied.[29] (Scheme 18) Depending on the solvent this monomer was polymerised in, the molecular weight distribution shifted. This alteration proved to be caused by two competitive polymerisation mechanisms which proceed simultaneously. A radical chain polymerisation leads to the high molecular weight fraction whereas the moderate molecular weight fraction was formed by an anionic chain polymerisation process. Owing to the intrinsic nature of these different processes, the former could be suppressed completely by addition of 0,5 equivalents of radical trap. TEMPO (2,2,6,6-tetramethyl-1-piperidiniloxy) (Scheme 18), which is a stable radical, was used for this purpose. It immediately reacts with

radicals formed and thus inhibits radical polymerisation. The anionic chain polymerisation could be blocked completely by simple addition of 5 vol% of water.

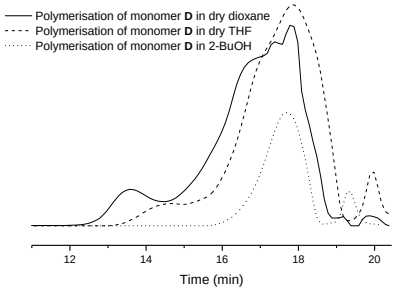

Figure 15: GPC curves of the precursor polymers synthesised in different solvents.

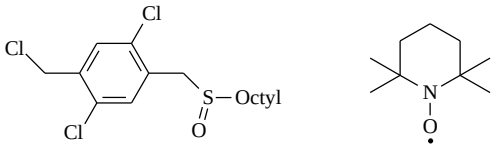

Scheme 18: Chemical structures of the dichloro-sulphinyl monomer (left) and TEMPO (right).

In the case of the polymerisation of monomers **C** and **D** different signals could also be observed in the GPC chromatogram. (Figure 15) As can be seen, the high molecular weight fraction only represents a minor part of the total molecular weight distribution. The major signal in the GPC chromatogram results from precursor polymers with moderate molecular weights. Analogous with the interpretation for the 2,5-xylene dichlorosulphinyl monomer this behaviour can be interpreted as caused by two different competitive polymerisation mechanism. Compared to the 2,5-xylene dichlorosulphinyl monomer, monomers **C** and **D** are much more electron accepting due to the presence of the much stronger electron withdrawing cyano groups. This probably causes the competition between the two polymerisation mechanisms to shift strongly to the anionic side and the precursor polymers formed will mainly have moderate molecular weights because they are formed by the anionic chain polymerisation process. An additional feature that can be observed from the GPC chromatogram is the presence of a third signal. This signal results from precursor oligomers with very low molecular weights and was not present in the precursor polymers synthesised from the 2,5-xylene dichlorosulphinyl monomer.[29] A more detailed explanation for this phenomenon as well as an explanation for the competitive polymerisation processes will be presented later on, after all the polymerisation results have been discussed. The hypothesis of the radical and anionic mechanism was further confirmed by an additional experiment. Here 0.5 equivalents of TEMPO (Scheme 19) was added to the polymerisation

mixture thus preventing radical chain polymerisation. Indeed, when TEMPO was added to the polymerisation mixture only the moderate molecular weight fraction remained. (Table 6) This result again suggests the high molecular weight polymer, which is absent in this case, is formed via a radical polymerisation process whereas the moderate molecular fraction remains and consequently must be formed by an anionic polymerisation process. The molecular weight of the precursor polymers was determined with GPC versus PS standards and DMF was used as the eluent. (Table 6) In order to get a clear overview, the molecular weight of the different fractions in the GPC chromatogram are given separately. When the polymerisation is performed in dry 1,4-dioxane the very low molecular weight oligomeric fraction is absent. The molecular weight of the high molecular weight fraction varies between 400,000 and 500,000. These molecular weights are comparable with the molecular weight of classical sulphinyl PPV precursor polymers synthesised in these solvents.[30] As the leaving group (on the monomer stage) is improved from a bromine atom to a iodine atom both the polymerisation yield and the molecular weight increase.

X	**Y**	**Solvent**	**Yield (%)**	**M_w ($x10^{-3}$) High**	**M_w ($x10^{-3}$) Moderate**	**M_w ($x10^{-3}$) Low**
Br	S(O)Octyl	THF	44	365	18	2.2
Br	S(O)Octyl	1,4-dioxane	29	433	17	-
I	S(O)Octyl	1,4-dioxane	49	498	19	-
I	S(O)Octyl	1,4-dioxane	68*	-	11	-

*Table 6: Polymerisation results for monomers **C** and **D** in dry THF and dry 1,4-dioxane at 30°C. *: 0.5eqv TEMPO were added to the polymerisation mixture.*

In order to obtain results that could be compared with those acquired for the polymerisation of monomers **C** and **D**, the polymerisation of the sulphonyl monomers **E** and **F** was performed in dry 1,4-dioxane at 30°C under identical "standard" conditions. One thing that immediately catches the eye when analysing the sulphonyl precursor polymers is the strange shape of the curves in the GPC chromatograms. (Figure 16)

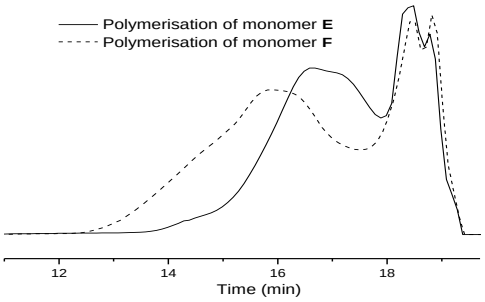

*Figure 16: GPC chromatogram of sulphonyl precursor polymers synthesised in dry 1,4-dioxane at 30°C from monomer **E** (solid line) and from monomer **F** (dashed line).*

In these sulphonyl precursor polymers the high molecular weight polymers are absent while the very low molecular weight oligomeric fraction became increasingly important compared to the earlier results for the sulphinyl precursor polymers. The molecular weight of the sulphonyl precursor polymers was determined using GPC versus PS standards with DMF as eluent. (Table 7)

X	Y	Solvent	Yield (%)	M_w ($x10^{-3}$) High	M_w ($x10^{-3}$) Moderate	M_w ($x10^{-3}$) Low
Br	$S(O)_2$Octyl	1,4-dioxane	71	-	25	4
I	$S(O)_2$Octyl	1,4-dioxane	81	-	84	4

*Table 7: Polymerisation results for monomers **E** and **F** in 1,4-dioxane at 30°C.*

The sulphonyl precursor polymers are formed in excellent yields and the molecular weight of the moderate weight fraction is significantly higher that the results obtained before. This higher molecular weight can be explained by the presence of a shoulder in the GPC chromatogram towards high molecular weights. Similar to the high molecular weight fraction in the precursor polymer synthesised from monomer **D** in 1,4-dioxane (Table 6), the higher molecular weight fraction in this case probably also originates from a radical polymerisation process. The higher molecular weight of the moderate weight fraction is probably a result of the calculation method used, the high molecular weight shoulder is

included in the calculation for M_w. Although the molecular weights of the moderate weight fractions are very different, the molecular weights obtained for the very low molecular fractions are identical. Moreover, the process by which these very low molecular weight sulphonyl precursor oligomers are formed becomes much more important during the polymerisation of monomers **E** and **F** than compared for monomers **C** and **D**. These observations must be related to the chemical structure of the different monomers as will be explained further on.

2.3.2.2 Polymerisation in 2-BuOH and DMSO

The polymerisation of monomer **C** was also tested in solvents like 2-BuOH and DMSO. In these solvents the high molecular weight precursor polymers were not formed at all as could be concluded from the GPC chromatograms. (Figure 16) Only the moderate and low molecular weight precursor polymers were present here. Molecular weights were determined using GPC versus PS standards with DMF as eluent. (Table 8)

X	Y	Solvent	Yield (%)	M_w ($x10^{-3}$) High	M_w ($x10^{-3}$) Moderate	M_w ($x10^{-3}$) Low
Br	S(O)Octyl	2-BuOH*	53	-	9	2.1
Br	S(O)Octyl	DMSO	31	-	16.5	2.2

*Table 8: Polymerisation results for monomer **C** in 2-BuOH and DMSO. *:Polymerisation temperature = 60°C.*

Both the polymerisation yield and the molecular weight of these respective precursor polymers fractions are similar to those obtained when the polymerisation is performed in dried solvents. The only thing that changes is the absence of the high molecular weight polymer fraction. Probably the radical chain polymerisation process is largely suppressed in these solvents and the precursor polymers will mainly be formed by an anion polymerisation process. Compared to THF or 1,4-dioxane, the anion formed in the first step of the polymerisation process is stabilised more efficiently in 2-BuOH and consequently the further conversion to the quinoid compound is expected to be less effective. This could mean that a critical amount of quinoid compounds, needed to self-initiate a radical chain

polymerisation, can probably only be formed in relatively non-polar and non-protic solvents as THF or 1,4-dioxane. Even in these solvents the high molecular weight precursor polymers, formed via the radical pathway only represents a minor percentage. When the polymerisation is performed in DMSO, which selectively solvatates cations, similar results are obtained. In this solvent the nucleofilicity of the anion formed in the first step of the polymerisation process is enhanced greatly and it is expected that only anionic polymerisation processes will occur.

2.3.2.3 Interpretation and explanation of the different results

Before formulating a hypothesis that can rationalise the observations mentioned above we should first comment on some UV-Vis experiments. In these experiments the formation of the actual monomer in the polymerisation (the quinoid structures **31b** and **31c**) was examined in different solvents. From these measurements we could conclude that the quinoid formation for these monomers **C**-**F** is an extremely slow process. Independent of the solvent and the exact base concentration used, the quinoid formation could hardly be observed. This observation suggests a high stability of the anion (**30b** and **30c**) formed in the first step of the polymerisation process. As already explained, the base (Na*t*BuO) abstracts the proton alpha to the sulphinyl or sulphonyl group to create the anion **30a-c**. (Figure 17) This proton is much more acid in monomers **C** to **F** than compared to that in the plain sulphinyl PPV monomer because of the presence of the two strong electron withdrawing cyano groups on the aromatic moiety and thus a much lower energy (enhanced stabilisation by electron withdrawing groups) for anions **30b** and **30c** is envisaged in the energy diagram. (Figure 17) Consequently the energy barriers (E_2 and E_3) that have to be overcome in order to form the *p*-quinodimethane structures (**31b** and **31c**) may be much higher for anions **30b** and **30c** than that for the plain sulphinyl PPV anion **30a**. This big energy leap that has to be overcome can than explain the very slow quinoid formation suggested by the UV-Vis experiments in solution. This assumes a strongly reduced stabilisation effect stabilisation effect by the cyano groups in the transition state towards the *p*-quinodimethane system. Such an supposition may not be unreasonable in view of the expected localisation of negative charge on the leaving group in the transition state.

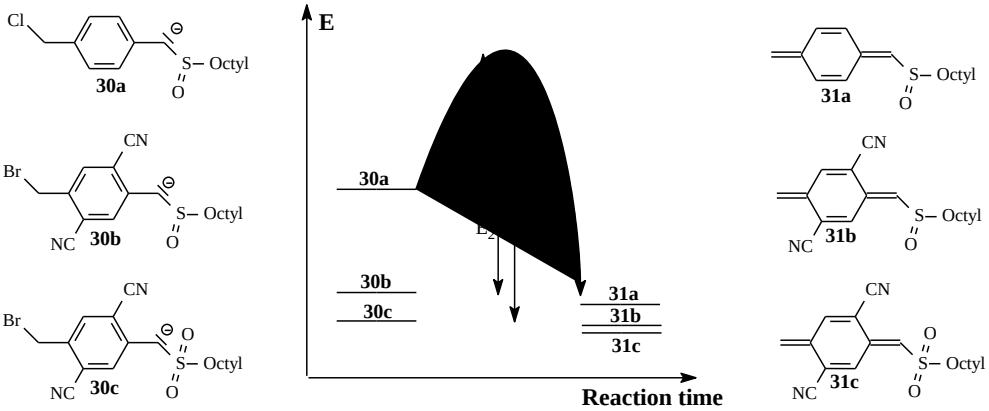

Figure 17: Energy diagram showing the different energies needed to form the respective quinoid structures.

Once on the quinoid level (**31**) the cyano groups will stabilise the structure. It is well known that electron withdrawing groups stabilise *p*-quinodimethane systems. TCNQ (7,7,8,8-tetracyanoquinodimethane) is an example of a stable quinoid structure that can only be polymerised when an external initiator is applied.[21a] (Scheme 19)

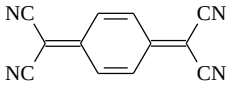

Scheme 19: Chemical structure of 7,7,8,8-tetracyanoquinodimethane (TCNQ).

Because of this stabilisation effect, the quinoid structures **31b** and **31c** lay at lower energy compared to their plain PPV analogue **31a**. In total, the limiting step in the complete polymerisation process of these cyano substituted monomers probably is the formation of the quinoid structure. The energy barrier that has to be overcome in order to form the quinoid structure is to high to get a very efficient formation. As shown from the UV-Vis measurements in solution, the actual formation of the quinoid compounds is very slow. As a consequence, the concentration of quinoid compounds (**31b**) is relatively low at any time during the polymerisation which probably results in little self-initiation and thus very little radical chain polymerisation. For these monomers, the majority of the precursor polymers are probably formed by an anionic polymerisation process. As can be seen from the results described above, this process can be influenced in a minor way by varying the solvent the polymerisation is performed in. Only in non-polar and non-protic solvents (THF and 1,4-

dioxane) the quinoid formation will probably be efficiently enough to generate some diradicals that can initiate a radical chain polymerisation.

A complementary way of interpreting the results obtained, is the evaluation of the different chemical processes that can occur. An overview is given in Scheme 20.

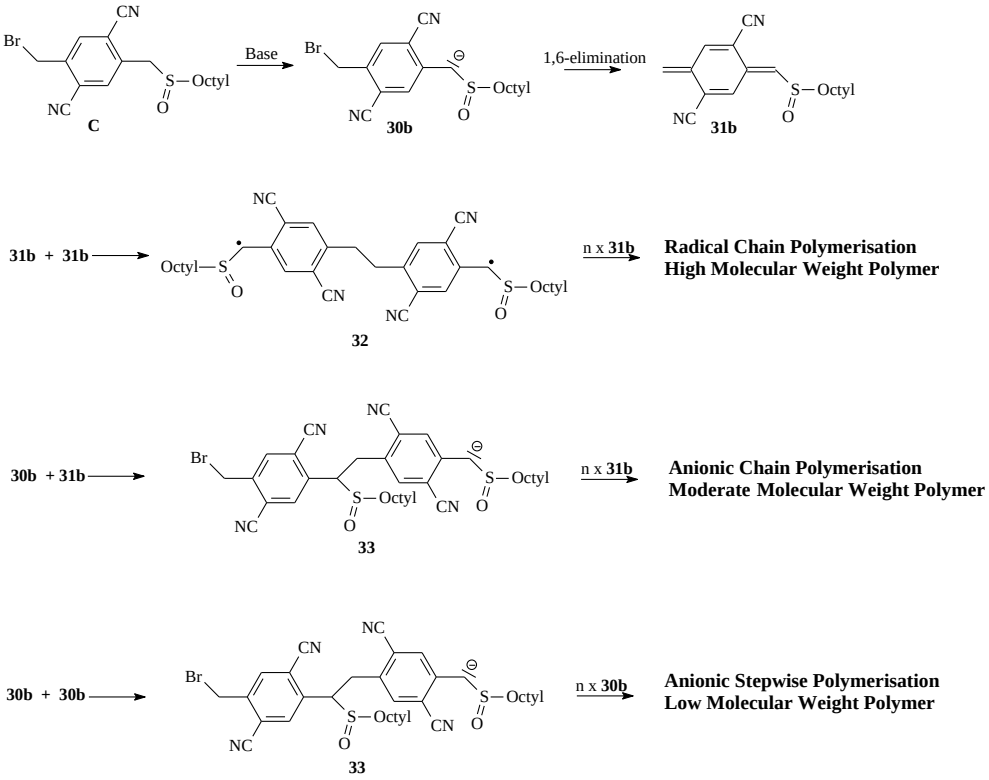

Scheme 20: Schematic overview of the different polymerisation pathways.

Because of the relatively high stability of the anion **30b** and assuming a high energy barrier that has to be overcome in order to form the quinoid structure **31b** three different processes can occur during the polymerisation reaction. In the end these different polymerisation processes account for the different signals observed in the GPC chromatogram. The chemical modifications on the monomer level (cyano groups) directly influence the formation of the actual monomer in polymerisation and its consecutive polymerisation.

1. In relatively non-polar solvents like dry THF and dry 1,4-dioxane the anion (**30b**) is not stabilised as well as for example in the more polar 2-BuOH. This little destabilisation

allows the formation of a critical amount of quinoid compounds necessary to initiate radical polymerisation. Once this initiating diradical is formed it can further propagate radically with successive additions of quinoid compounds **31b** to form high molecular weight precursor polymers. We should stress that the quinoid compound is probably formed in all solvents (although very slow) but only in dry THF, and even more so in dry 1,4-dioxane, a critical amount is formed fast enough to initiate a radical chain polymerisation. Even in these non-polar solvents the relative amount of high molecular weight polymer is very small. The majority of the precursor polymers obtained only have moderate molecular weights.

2. In all solvents tested the moderate molecular weight fraction proved to be the major fraction. Such lower molecular weight precursor polymers are obtained when the quinoid system is more electron deficient than compared to the plain sulphinyl PPV monomer. In the past a bimodal molecular weight distribution had already been observed during the polymerisation of the 2,5-xylene dichlorosulphinyl monomer and here it becomes even more important because the cyano groups are much stronger electron withdrawing groups. Because of the increased stability of anion **30b** and the relatively slow conversion to the quinoid structure (**31b**) a large amount of anion **30b** will be present during the polymerisation process. The presence of the anion is also suggested by the strong colour change upon addition of the base to the monomer solution. This colour change is not observed during the polymerisation of the classical sulphinyl PPV monomer. Such an anion **30b** may attack a quinoid compound **31b** in order to create compound **33** which can then propagate with successive attacks to quinoid compounds. This polymerisation mechanism is called an anionic chain polymerisation and because of the intrinsic nature of this process (e.g. sensitivity to water) and also because of the relatively low concentration of quinoid compounds the molecular weight of the precursor polymers formed in this way will only be moderate. Furthermore, the anion present during this polymerisation process can probably also be terminated by abstraction of an acidic proton from the precursor polymer. Again because of the presence of the cyano group the acidity of these protons is increased.

3. The third process that can occur is a simple anionic stepwise polymerisation of anion **30b**. In this way the very low molecular weight precursor polymer fraction is obtained.

The precursor polymers were characterised with NMR spectroscopic techniques. From the ^{1}H-NMR spectrum of the sulphinyl precursor polymer very little information can be obtained. (Figure 18) This spectrum is a typical proton spectrum of a sulphinyl precursor polymer and because of the relatively short T_2 (spin-spin relaxation time) signals are very broad. Because of the adjacent racemic centre (position 9), the protons H10 spit up and yield two broad signals around 3.6 and 2.7 ppm. The resonances below 2 ppm all belong to the proton in the octyl aliphatic chain.

The signals in the ^{13}C-NMR are less diffuse and can be assigned to the respective carbon atoms. (Figure 19) However, the aromatic region of this spectrum (150-110 ppm) shows rather broad signals and it is hard to determine the exact chemical shift of each carbon atom. By comparing this spectrum with that of the monomer all signals in the aromatic region can be assigned. Carbon C4 has the highest chemical shift (141 ppm). The signal around 135 ppm integrates for three carbon atoms and corresponds to C1, C2 and C5. The resonances of the carbon atoms of the cyano groups (C7 and C8) are situated around 117 ppm whereas these of the carbon atoms C3 and C6 show a resonance around 115 ppm. The carbon atoms of the ethylene bridge (C9 and C10) between the repeating units are at 60 and 35 ppm respectively. Cx (51 ppm) corresponds to the first carbon atom of the aliphatic chain, all other carbon atoms of the octyl chain can be observed between 32 and 14 ppm.

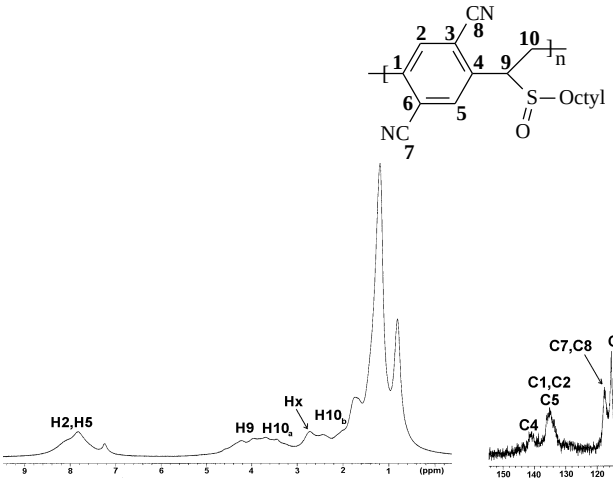

Figure 18: ^{1}H-NMR spectrum of the sulphinyl precursor polymer.

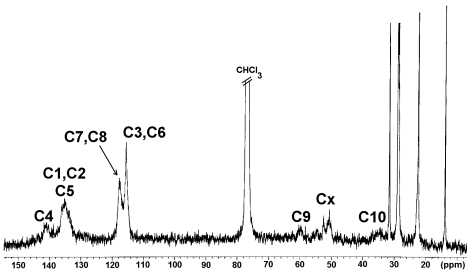

Figure 19: ^{13}C-NMR spectrum of the sulphinyl precursor polymer.

2.3.3 Conversion to the conjugated structure

The final step in the sulphinyl precursor route is the generation of the conjugated structure by a thermal elimination of the sulphinyl group. (Scheme 21)

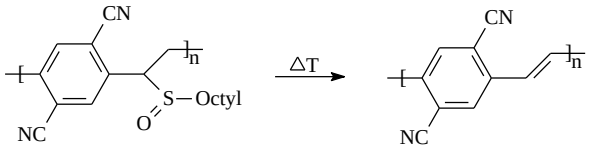

Scheme 21: Formation of the conjugated structure by a thermal elimination of the sulphinyl group.

As mentioned earlier, several techniques can be used to monitor the elimination process. The ones used here are *in situ* UV-Vis spectroscopy and *in situ* IR spectroscopy. Together, these complementary techniques give a very detailed picture about the elimination reaction. UV-Vis spectroscopy measurements were carried out on film, spin-coated on a quartz window. An experimental set-up was used which allowed *in situ* monitoring of the elimination process. For this purpose a specially designed oven which contained the precursor polymer spincoated on the quarts window was placed in the beam of the spectrometer. A dynamic heating program of 2°C/min up to 300°C, under a continuous flow of nitrogen, was used. Before heating the precursor polymer shows strong absorbencies below 250 nm. As the heating program progresses a new absorption band appears that gradually red shifts with increasing temperature. Finally the maximally conjugated poly(2,5-dicyano-1,4-phenylene vinylene) is obtained with an absorption maximum at 417 nm. (Figure 20) At higher temperatures some broadening of the absorption spectrum is noticed but no real decline in absorption can be observed. When the absorbance at this maximum wavelength (417 nm) is plotted versus temperature the thermal stability of the precursor and conjugated polymer becomes clear. (Figure 21) For this polymer, the conjugated structure starts to develop around 60°C. Notice that the majority of the conjugated segments have already been formed when the temperature reaches 110°C at a heating rate of 2°C/min. Starting from this temperature the increase in absorption at 417 nm slows down considerably but still slightly increases till about 160°C. Once the conjugated structure is fully formed no decline in absorption at 417 nm could be observed at higher temperatures. (Figure 21)

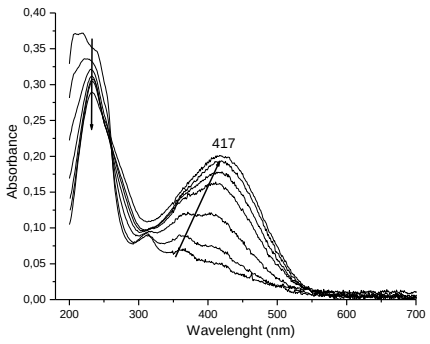

Figure 20. Gradual formation of the absorption spectrum of dicyano-PPV.

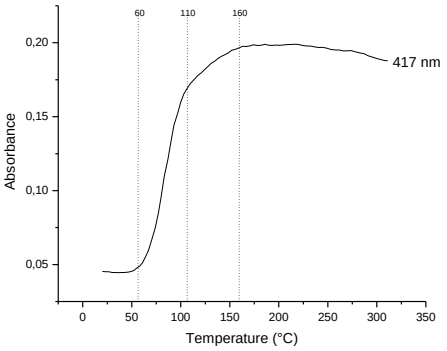

Figure 21: Absorbance at 417 nm versus temperature.

A second technique used to study the thermal elimination and stability with is *in situ* FT-IR spectroscopy. In these measurements an identical experimental set-up was used as during the *in situ* UV-Vis measurements. Because of the same experimental set-up the results derived from both techniques complement each other. *In situ* FT-IR measurements were performed on film, spincoated on KBr disks and a dynamic heating program of 2°C/min up to 300°C, under a continuous flow of nitrogen, was used. The most important and distinct absorption bands in the IR spectrum, which are changed during the elimination process, are those of the sulphoxide stretching at 1052 cm^{-1} and that of the *trans* vinylene double bond at 962 cm^{-1}. This polymer also shows the very characteristic absorption at 2230 cm^{-1} which originates from the CN stretching. As the temperature increases, the absorption at 1052 cm^{-1} decreases while that of the *trans* vinylene double bond at 962 cm^{-1} increases. The sulphinyl groups are eliminated to form the double bonds. When the intensity of these signals is plotted versus temperature the elimination process as well as the thermal stability of the conjugated structure becomes clear. (Figure 21) Between approximately 60 and 120°C the double bonds are formed, at 125°C the absorption for the *trans* vinylene double bond has reached its maximal value. However, the sulphinyl absorption at 1052 cm^{-1} still further decreases till the temperature has reached 200°C. This decrease in sulphinyl absorption without formation of additional double bonds is probably caused by the evaporation of some elimination products with interfering absorptions that stay in the polymer film till about 200°C. At temperatures above 125°C the vinylene absorption at 962 cm^{-1} steadily decreases again. Simultaneously, the absorption of the CN stretching (2230

cm^{-1}) also starts to decline. On the bases of the UV-Vis data and the similar thermal stability above 125°C, this decline in both absorption bands is probably caused by a thermochrome effect rather than the actual degradation of the structure. Moreover, the fact that the absorption bands of both signals (962 and 2230 cm^{-1}) are only weak signals will only intensify this effect.

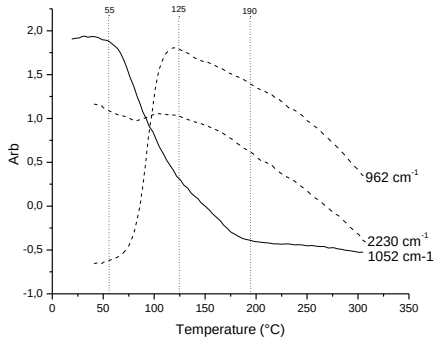

Figure 17: Absorbances at 2230, 1052 and 962 cm^{-1} versus temperature.

The combined results from both techniques allow to conclude that the elimination reaction for these dicyano precursor polymers starts around 60°C. The formation of the conjugated structure is a relatively fast process. From the FT-IR data it is concluded that elimination products stay in the film till about 200°C under nitrogen atmosphere. In order to evaporate all elimination products from the film at lower temperatures the pressure is best reduced.

2.4 Experimental Section

Materials. All chemicals were purchased from Aldrich or Acros and used without further purification unless otherwise stated. Tetrahydrofuran (THF) and 1,4-dioxane were always distilled over sodium/benzophenone prior to use.

Characterisation. NMR spectra were recorded, mostly in $CDCl_3$, on a Varian VXR300 spectrometer. Chemical shifts (δ) are given in ppm relative to the residual $CHCl_3$ absorption (7.24 ppm). The ^{13}C-NMR experiments were recorded at 100 MHz on the same spectrometer. Chemical shifts are determined relative to the ^{13}C resonance shift of $CHCl_3$ (77.0 ppm). Direct Insert Probe Mass Spectrometry (DIP-MS) analyses were carried out on a Finnigan TSQ 70, electron impact mode, mass range 35-550 and an interscan time of 2 s. The electron energy was 70 eV. Molecular weights and molecular weight distributions were determined relative to polystyrene standards (Polymer Labs) by Size Exclusion Chromatography (SEC). Chromatograms were recorded on a Spectra series P100 (Spectra Physics) equipped with two MIXED-B columns (10 μm, 2 x 30 cm, Polymer Labs) and a refractive index (RI) detector (Shodex) at 70 °C. A DMF solution of oxalic acid (1 mM) is used as the eluent at a flow rate of 1.0 ml/min. Toluene is used as flow rate marker.

Fourier transform-infrared spectroscopy (FT-IR) was performed on a Perkin Elmer Spectrum One FT-IR spectrometer (nominal resolution 4 cm^{-1}, summation of 16 scans). Samples for the FT-IR characterisation were prepared by spin-coating the precursor polymer from a chloroform solution (6 mg/ml) onto NaCl disks (diameter 25 mm and thickness 1 mm) at 500 rpm. The NaCl disks were heated in a Harrick oven high temperature cell (purchased from Safir), which was positioned in the beam of the FT-IR to allow *in situ* measurements. The temperature of the sample and the heating source were controlled by a Watlow temperature controller (serial number 999, dual channel). The heating source was in direct contact with the NaCl disk. Spectra were taken continuously and the heating rate was 2 °C/minute up to 450 °C. The atmosphere in the temperature cell could be varied from a continuous flow of nitrogen to vacuum (15 mmHg). Timebase software was used to investigate regions of interest.

Ultraviolet visible spectroscopy (UV-VIS) was performed on a CARY 500 UV-VIS-NIR spectrophotometer (interval: 1 nm, scan rate: 600 nm/min, continuous run from 200 to 700

nm). The precursor polymer was spin-coated from a chloroform solution (6 mg/ml) onto quartz glass (diameter 25 mm and thickness 3 mm) at 700 rpm. The quartz glass was heated in the same Harrick oven high temperature cell as was used in the FT-IR measurements. The cell was placed in the beam of the UV-Vis spectrophotometer and spectra were taken continuously. The heating rate was 2°C/minute up to 450°C. All measurements were performed under a continuous flow of nitrogen. Scanning kinetics software was used to investigate the regions of interest.

Direct insertion probe mass spectroscopy (DIP-MS) analysis was carried out on a Finnigan TSQ 70, in electron impact mode, mass range 35-650 and scan rate of 2 s. The electron energy was 70 eV. A chloroform solution the respective compound was placed on the heating element of the direct insertion probe. A heating rate of 10°C/min was used.

Synthesis of 1-(chloromethyl)-4-[(*n*-octylsulphanyl)methyl]benzene (11) and 1-(chloromethyl)-4-[(*n*-octylsulphinyl)methyl]benzene (13): These compounds were synthesised according to a procedure mentioned elsewhere.[31]

Synthesis of 1-(cyanomethyl)-4-[(*n*-octylsulphanyl)methyl]benzene (12): Sodiumcyanide (1g, 20.27 mmol) was added to 1 ml water and heated till the salt had completely dissolved. The clear solution was slowly added to a solution of **11**[31] (13.51 mmol) in 5 ml MeOH. This solution was heated at reflux over night. After cooling down, chloroform was added (10ml) and the aqueous layer was extracted. The combined organic layers were dried over $MgSO_4$ and the solvent was evaporated. A chromatographic separation (SiO_2, hexanes/ethylacetate (90/10)) yielded the pure product **12**. (62% yield) ^{1}H-NMR ($CDCl_3$, 300MHz): □ (ppm) 7.16 (2H, d, J=8.1 Hz), 7.08 (2H, d, J= 8.1 Hz), 3.69 (2H, s), 3.61 (2H, s), 2.31 (2H, t), 1.61 (2H, m), 1.4-1.05 (10H), 0.81 (3H, t). MS (EI, m/z, rel. int. (%)): 275 ($[M]^+$, 11), 145 ($[SC_8H_{17}]^+$, 66), 130 ($[M- SC_8H_{17}]^+$, 100), 104 ($[M-CNSC_8H_{17}]^+$, 8), 77 ($[C_6H_5]^+$, 6).

Synthesis of 1-(cyanomethyl)-4-[(*n*-octylsulphinyl)methyl]benzene (14): The pure compound **12** (1.5 g, 5.46 mmol) was dissolved in MeOH (40 ml), and tellurium dioxide (0.09 g, 0.014 mmol) was added. Hydrogen peroxide solution (30 wt% in water, 1.1 ml) was added drop wise. Thereafter, a few drops of concentrated hydrochloric acid were added and the reaction was monitored on TLC every half hour. When all starting product had reacted, the reaction was quenched by adding 50 ml of brine. The solution was extracted with chloroform and dried over magnesium sulphate. Column chromatography

(SiO2, hexane/ethyl acetate (73/30)) was used to purify the desired product. (83% yield) ^{1}H-NMR ($CDCl_3$, 300MHz): □ (ppm) 7.27 (2H, d, J= 9 Hz), 7.24 (2H, d, 9 Hz), 3.88 (2H, dd, J= 13.2 Hz), 3.69 (2H, s), 2.50 (2H, t), 1.66 (2H, m), 1.40-1.08 (10H), 0.79 (3H, t). MS (CI, m/z, rel. int. (%)): 582 ([dimmer+1]$^+$, 21), 292 ([M+1]$^+$, 100), 130 ([M- SC_8H_{17}]$^+$, 3).

Synthesis of 1-(chloromethyl)-4-[(*n*-octylsulphinyl)chloromethyl]benzene (monomer A) and 1-(cyanomethyl)-4-[(*n*-octylsulphinyl)chloromethyl] benzene (monomer B): The selective chlorination of the sulphoxides **13** and **14** proceeded as described in literature.[17] Monomer **A**: Compound **13** (3 g, 10 mmol) was dissolved in CH_2Cl_2 (30 ml). To this solution was added N-chlorosuccinimide (1.46 g, 11 mmol) as a solid and pyridine (1.68 ml, 20 mmol). This solution was stirred at room temperature over night. The solvent was evaporated and the reaction mixture was purified using a chromatographic separation (SiO_2, hexanes/chloroform (99/1)) and crystallisation from hexanes/chloroform. (69% yield) ^{1}H-NMR ($CDCl_3$, 300MHz): □ (ppm) 7.44 (4H, s), 5.51 (1H, s), 4.58 (2H, s), 2.55 (1H, m), 2.36 (1H, m), 1.65 (2H, m), 1.45-1.12 (10H), 0.85 (3H, t). MS (CI, m/z, rel. int. (%)): 335 ([M+1]$^+$, 100), 299 ([M-Cl+1]$^+$, 4), 190 ([M-$S(O)C_8H_{17}$+1]$^+$, 81). Monomer **B**: Compound **14** (0.5 g, 1.72 mmol) was dissolved in CH_2Cl_2 (10 ml). To this solution was added N-chlorosuccinimide (0.24 g, 1.81 mmol) as a solid and pyridine (0.28 ml, 3.44 mmol). This solution was stirred at room temperature over night. The solvent was evaporated and the reaction mixture was purified using a chromatographic separation (SiO_2, hexanes/ethyl acetate (60/40)) and crystallisation from hexanes/chloroform. (72% yield) ^{1}H-NMR ($CDCl_3$, 300MHz): □ (ppm) 7.47 (2H, d, J= 8.4 Hz), 7.39 (2H, d, 8.4 Hz), 5.53 (1H, s), 3.77 (2H, s), 2.58 (1H, m), 2.37 (1H, m), 1.63 (2H, m), 1.45-1.08 (10H), 0.82 (3H, t). MS (CI, m/z, rel. int. (%)): 327 ([M+1]$^+$, 100), 292 ([M-Cl+1]$^+$, 16), 182 ([M- $S(O)C_8H_{17}$+1]$^+$, 76), 147 ([M- $S(O)C_8H_{17}Cl$+1]$^+$, 86).

Polymerisation of monomers A and B. These monomers were polymerised according to the standard procedure. Solutions of monomer (5.8 ml, 0.14 M) and base (sodium *tert*-butoxide; 2.5 ml, 0.34 M) were prepared and degassed for 1 hour by a continuous flow of nitrogen. All polymerisations were performed at 30°C (except for the polymerisation of monomer **B** where AIBN was added, here the temperature was raised to 60°C). The base solution was added in one portion to the stirred monomer solution. During the reaction the temperature was maintained constant and the passing of nitrogen was continued. After 1 hour the reaction mixture was poured into well stirred ice water

whereupon the polymer precipitated. The water layer was extracted with chloroform to ensure that all polymer and residual fraction was collected, and the combined organic fractions were concentrated *in vacuo*. The precursor polymers were precipitated in a cold *n*-hexane/ethyl acetate mixture (volume ratio 50/50, 150 ml, 0°C), collected by filtration and dried *in vacuo*. The residual solvent fraction was concentrated *in vacuo*. Precursor polymer **21**: Polymerisation results are summarised in Table 1. ^{1}H-NMR ($CDCl_3$, 300 MHz): δ (ppm) 7.18, 6.83, 3.66, 2.55, 1.91, 1.60-1.05, 0.80. FT-IR (film, KBr): ν (cm^{-1}) 2956 (m), 2926 (s), 2854 (m), 1508 (w), 1464 (w), 1412 (w), 1068 (s), 974 (w), 890 (w), 832 (w). Precursor polymer **22**: Polymerisation results are summarised in Tables 3 and 4. ^{1}H-NMR ($CDCl_3$, 300 MHz): δ (ppm) 7.99-7.40, 4.06, 3.81, 3.72, 2.71, 2.0-1.65, 1.45-1.06, 0.82. FT-IR (film, KBr): ν (cm^{-1}) 2956 (m), 2928 (s), 2856 (s), 1650 (s), 1514 (w), 1460 (w), 1416 (w), 1050 (s), 916 (w), 832 (w).

Compound **26**: ^{1}H-NMR ($CDCl_3$, 300 MHz): δ (ppm) 7.53 (2H, s), 2.52 (6H, s). MS (EI, m/z, rel. int. (%)): 156 ($[M]^+$, 88), 141 ([M- CH_3]+, 100), 129 ([M- $CN]^+$, 21), 114 ([M- $CN(CH_3)_2]^+$, 17), 103 ([M- $C_2N_2]^+$, 13), 77 ($[C_6H_5]^+$, 6). FT-IR (KBr): ν (cm^{-1}) 3115 (w), 3038 (s), 2928 (w), 2225 (s), 1805 (m), 1495 (s), 1446 (m), 1391 (s), 1284 (s), 1271 (s), 1191 (w), 1037 (m), 982 (w) 906 (s), 465 (s).

Compound **27**: ^{1}H-NMR ($CDCl_3$, 300 MHz): δ (ppm) 7.84 (2H, s), 4.59 (4H, s). MS (EI, m/z, rel. int. (%)): 314 ($[M]^+$, 23), 234 ([M- $Br]^+$, 100), 154 ([M- $Br_2]^+$, 94), 127 ([M- $CBr_2N]^+$, 17), 100 ([M- $C_2Br_2N_2]^+$, 8), 76 ($[C_6H_4]^+$, 9). FT-IR (KBr): ν (cm^{-1}) 3107 (w), 3037 (m), 2974 (w), 2223 (m), 1825 (m), 1490 (m), 1437 (s), 1393 (m), 1291 (s), 1219 (s), 1194 (s), 1104 (m), 918 (s) 873 (s), 805 (s), 711 (s), 624 (s), 581 (s), 517 (s), 466 (s).

Monomer **C**: ^{1}H-NMR ($CDCl_3$, 300 MHz): δ (ppm) 7.89 (1H, s), 7.81 (1H, s), 4.60 (2H, s), 4.10 (2H, dd, J= 13.2 Hz), 2.74 (2H, m), 1.79 (2H, m), 1.51-1.21 (10H), 0.86 (3H, t). ^{13}C-NMR ($CDCl_3$, 75 MHz): δ (ppm) 142.57, 136.64, 136.01, 135.15, 118.62, 117.44, 116.29, 115.50, 55.34, 53.34, 32.36, 29.79, 29.64,, 29.44, 27.91, 23.32, 23.27, 14.76. MS (EI, m/z, rel. int. (%)): 395 ($[M]^+$, 4), 379 ([M- $O]^+$, 9), 234 ([M- $S(O)C_8H_{17}]^+$, 58), 154 ([M- $BrS(O)C_8H_{17}]^+$, 100), 128 ([M- $CNBrS(O)C_8H_{17}]^+$, 29), 102 ([M- $(CN)_2BrS(O)C_8H_{17}]^+$, 5), 76 ($[C_6H_4]^+$, 13). FT-IR (KBr): ν (cm^{-1}) 3028 (w), 2917 (s), 2850 (s), 2223 (m), 1765 (w),

1495 (m), 1468 (m), 1415 (m), 1295 (m), 1216 (w), 1186 (m), 1021 (s), 922 (m), 721 (w), 627 (w).

Monomer **D**: Monomer **C** (0.5 g, 1.27 mmol) was dissolved in aceton (30 ml) and NaI (0.38 g, 2.54 mmol) was addes in the solid state. This solution was stirred at room temperature for 2 hours and then the temperature was raised to 50°C and stirring was continued for another hour. During this period the reaction mixture became yellow. After cooling down, water was added (20 ml) and the aqueous layer was extracted with chloroform. The combined organic layers were washed with $NaHSO_3$, dried over $MgSO_4$ and the solvent was evaporated. Crystallisation from hexanes/chloroform yielded monomer D as a slightly off-white solid. (87% yield) ^{1}H-NMR ($CDCl_3$, 300 MHz): δ (ppm) 7.83 (1H, s), 7.75 (1H, s), 4.55 (2H, s), 4.10 (2H, dd, J= 13.2 Hz), 2.72 (2H, m), 1.76 (2H, m), 1.45-1.15 (10H), 0.83 (3H, t). MS (CI, m/z, rel. int. (%)): 443 ($[M+1]^+$, 100), 317 ($[M- I+1]^+$, 33), 289 ($[S_2(O)_2C_{16}H_{34}]^+$, 19), 155 ($[M- IS(O)C_8H_{17}+1]^+$, 26), 145 ($[S(O)C_8H_{17}]^+$, 39).

Monomer **E**: Monomer **C** (0.5g, 1.27 mmol) was dissolved in CH_2Cl_2 (40 ml) and the solution was cooled to 0°C. At this temperature *m*-CPBA (70 weight%, 0.33 g, 1.9 mmol) was added portion wise in such a way that the temperature did not rose above 5°C. After all the *m*-CPBA had been added the solution was allowed to come to room temperature and stirring was continued for another 2 hours. Then water (30 ml) was added and the aqueous layer was extracted with chloroform, dried over $MgSO_4$ and the solvent was evaporated. A chromatographic separation (SiO_2, hexanes/ethyl acetate (60/40)) yielded pure monomer **C** as white crystals. (89 % yield) ^{1}H-NMR ($CDCl_3$, 300 MHz): δ (ppm) 7.94 (1H, s), 7.91 (1H, s), 4.61 (2H, s), 4.44 (2H, s), 3.05 (2H, s), 1.90 (2H, m), 1.50-1.20 (10H), 0.86 (3H, t). MS (EI, m/z, rel. int. (%)): 411 ($[M]^+$, 6), 331 ($[M- Br]^+$, 58), 154 ($[M- BrS(O)_2C_8H_{17}]^+$, 100), 128 ($[M- CNBrS(O)_2C_8H_{17}]^+$, 19), 102 ($[M- (CN)_2BrS(O)_2C_8H_{17}]^+$, 6), 76 ($[C_6H_4]^+$, 13).

Monomer **F** was prepared from monomer **E** or monomer **D** according to the procedures just described. ^{1}H-NMR ($CDCl_3$, 300 MHz): δ (ppm) 7.88 (1H, s), 7.79 (1H, s), 4.60 (2H, s), 4.15 (2H, dd, J= 13.2 Hz), 2.77 (2H, m), 1.80 (2H, m), 1.48-1.20 (10H), 0.87 (3H, t). MS (EI, m/z, rel. int. (%)): 458 ($[M]^+$, 6), 331 ($[M- I]^+$, 26), 154 ($[M- IS(O)_2C_8H_{17}]^+$, 100), 145 ($[S(O)C_8H_{17}]^+$, 39).

Polymerisation of monomers C, D, E, F. These monomers were polymerised to the precursor polymers according to the standard polymerisation procedure. All polymerisation reactions were performed at 30°C under a continuous flow of nitrogen and the concentration (calculated on the total volume of solvent) was set at 0.1M. The base solution was added to the monomer solution in one shot and polymerisation time was 1 hour. Upon addition of the base the solution immediately changed colour from colourless to dark bleu-black. After extraction, the precursor polymers were precipitated in a mixture (60/40) of *n*-hexane/ethyl acetate, collected by filtration and dried under *vacuum*. The filtrate was also evaporated to yield the rest fraction. GPC measurements on all precursor polymers was performed versus PS standards and DMF was used as eluent. The polymerisation results for the various monomers are shown in Tables 6, 7 and 8. ^{1}H-NMR ($CDCl_3$, 300 MHz): δ (ppm) 7.83, 4.22, 3.94, 3.69, 3.45, 2.72, 2.44, 1.85-1.0, 0.83. ^{13}C-NMR ($CDCl_3$, 75 MHz): δ (ppm) 141.3, 135.08, 117.65, 115.47, 60.41, 59.32, 52.44, 50.60, 31.49, 28.95, 28.80, 28.59, 22.83, 22.41, 13.90. FT-IR (film, KBr): ν (cm^{-1}) 3021 (w), 2926 (s), 2855 (m), 2229 (m), 1721 (m), 1489 (w), 1460 (m), 1268 (m), 1129 (m), 1049 (s), 958 (m).

2.5 References

[1] Denton, F.R.; Sarker, A.; Lahti, P. M.; Garay, R. O.; Karasz, F. E. *J. Polym. Sci. Part A: Polym. Chem*. 30, **1992**, 2233.

[2] Sarker, A.; Lahti, P. M. *Polym. Prep*. 35(1), **1994**, 790.

[3] Van Der Borght, M. *Ph.D. Dissertation*, **1998**, Limburgs Universitair Centrum, Diepenbeek, Belgium.

[4] Greenham, N. C.; Moratti, S. C.; Bradley, D. D. C.; Friend, R. H.; Holmes, A. B. *Nature* 365, **1993**, 628.

[5]) Moratti, S. C.; Cervini, R.; Holmes, A. B.; Baigent, D. R.; Friend, R. H.; Greenham, N. C.; Grüner, J.; Hamer, P. J. *Synth. Met.* 71, **1995**, 2117. b) Samuel, I. D. W.; Rumbles, G.; Collison, C. J. *Phys. Rev. B* 52(16), **1995**, 573. c) Yu, Y.; Lee, H.; Vanlaeken, A.; Hsieh, B. R. *Macromolecules* 31, **1998**, 5553. d) Liu, M. S.; Jiang, X.; Liu, S.; Herguth, P.; Jen, A. *Macromolecules* 35, **2002**, 3532. e) Detert, H.; Sugiono, E. *Synth. Met.* 115, **2000**, 89.

[6] Morgan, P. W.; Kwolek, S. L.; Pletcher, T. C. *Macromolecules* 20,**1987**, 729.

[7] Olinga, T.; Inganas, O.; Andersson, M. *Macromolecules* 31, **1998**, 2676.

[8] a) Marsella, M. J.; Fu, D. K.; Swager, T. M. *Adv. Mater.* 7, **1995**, 145. b) Li, X.-C.; Cacialli, F.; Cervini, R.; Holmes, A. B.; Moratti, S. C.; Grimsdale, A. C.; Friend, R. H. *Synth. Met.* 84, **1997**, 159.

[9] Gillissen S. (Me); Jonforsen, M.; Kesters, E.; Johansson, T.; Theander, M.; Andersson, M. R.; Inganas, O.; Lutsen, L.; Vanderzande D. Macromolecules 34, 2001, 7294.

[10] Wasielewski, M. R.; Wang, B. *J. Am. Chem. Soc.* 119, **1997**, 12.

[11] Eichen, Y.; Nakhmanovich, G.; Gorelik, V.; Epshtein, O.; Poplawski, J. M.; Ehrenfreund, E. *J. Am. Chem. Soc.* 120, **1998**, 10463.

[12] Kanbara, T.; Kushida, T.; Saito, N.; Kuwajima, I.; Kubota, K.; Yamamoto, T. *Chem. Lett.* **1992**, 583.

[13] a) Stille, J. K. *Macromolecules* 14, **1981**, 870. b) Saito, N.; Kanbara, T.; Nakamura, Y.; Yamamoto, T.; Kubota, K. *Macromolecules* 27, **1994**, 756.

[14] Marsella, M. J.; Fu, D.-K.; Swager, T. M. *Adv. Mater.* 7, **1995**, 145.

[15] a) van Breemen, A.; Vanderzande, D.; Adriaensens, P.; Gelan, J. *J. Org. Chem.* 64, **1999**, 3106. b) van Breemen, A. *Ph.D. Dissertation*, **1999**, Limburgs Universitair Centrum, Diepenbeek, Belgium.

[16] Masaru, H.; Zen-ichi, Y. *J. Am. Chem. Soc.* 90, **1968**, 4496.

[17] Ogura, K.; Imaizumi, J.; Iida, H.; Tsuchihasshi, G.-I. *Chem. Lett.* **1980**, 1587.

[18] a) Williams, D. H.; Fleming, I. *Spectroscopic Methods in Organic Chemistry*, Fifth Edition, McGraw-Hill Publishing Company Europe, **1995**, p26 b) Cho, B. R.; Han, M. S.; Suh, Y. S.; Oh, K. J.; Jeon, S.J. *J. Chem. Soc., Chem. Commun.* **1993**, 564. c) Cho, B. R.; Kim, Y. K.; Han, M. S. *Macromolecules* 31, **1998**, 2098.

[19] a) Kingsbury, C. A.; Cram, D. J. *J. Am. Chem. Soc.* 82, **1960**, 1810. b) Shelton, J. R.; Davis, K. E. *Int. J. Sulphur Chem.* 8, **1973**, 205. c) Yoshimure, T.; Tsukurimichi, E.; Iizuka, Y.; Mizuno, H.; Isaji, H.; Shimasaki, C. *Bull. Chem. Soc. Jpn.* 62, **1989**, 1891.

[20] Van Den Berghe, D.; Hontis, L. *Internal Communication*, Limburgs Universitair Centrum, Diepenbeek, Belgium.

[21] a) Iwatsuki, S.; Itoh, T.; Horiuchi, K. *Macromolecules* 11, **1978**, 997. b) Iwatsuki, S.; Kamiya, H. *Macromolecules* 7, **1974**, 732.

[22] a) Iwatsuki, S.; Itoh, T.; Iwai, T.; Sawada, H. *Macromolecules* 18, **1985**, 2726. b) Iwatsuki, S.; Itoh, T.; Shimizu, Y. *Macromolecules* 16, **1983**, 532.

[23] Xiao, Y.; Yu, W.-L.; Pei, J.; Chen, Z.; Huang, W.; Heeger, A. J. *Synth. Met.* 106, **1999**, 165.

[24] a) Xiao, Y.; Yu, W.-L.;Chua, S.-J.; Huang, W. *Chem. Eur. J.* 6, **2000**, 1318. b) Pinto, M.R.; Hu, B.; Karasz, F. E.; Akcelrud, L. *Polymer* 41, **2000**, 8095.

[25] a) Friedman, L.; Shechter, H. *J. Org. Chem.* 26, **1961**, 2522. b) Ellis, G. P.; Romney-Alexander, T. M. *Chem. Rev.* 87, **1987**, 779.

[26] a) McCoy, R. K.; Karasz, F. E.; Sarker, A.; Lahti, P. M. *Chem. Mater.* 3, **1991**, 941. b) Cassidy, P. E.; Wallace, R. J.; Aminabhavi, T. M. *Polymer* 27, **1986**, 1131.

[27] Larock, R. C. in *Comprehensive Organic Transformations*, VCH Publishers Inc., NY, p313.

[28] Motmans, F. *Internal Communication*, Limburgs Universitair Centrum, Diepenbeek, Belgium.

[29] Van Der Borght, M. *Ph.D. Dissertation*, **1998**, Limburgs Universitair Centrum, Diepenbeek, Belgium.

[30] van Breemen, A. *Ph.D. Dissertation*, **1999**, Limburgs Universitair Centrum, Diepenbeek, Belgium.

Chapter 3

Hetero-aromatic poly(arylene vinylene) derivatives.

3.1 Poly(2,5-pyridylene vinylene)*

The first polymer that will be discussed in this chapter is the poly(2,5-pyridylene vinylene). (Scheme 1) This polymer differs from the plain PPV in this way that it has a pyridine aromatic moiety instead of the phenylene one in PPV. This will have certain consequences on the part of the monomer synthesis and also on the electronic and optical properties of the final conjugated polymer.

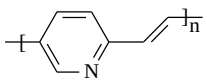

Scheme 1: Chemical structure of poly(2,5-pyridylene vinylene).

* Part of this paragraph was published in *Macromolecules* by Gillissen, S.; Jonforsen, M.; Kesters, E.; Johansson, T.; Theander, M.; Andersson, M.; Inganäs, O.; Lutsen, L.; Vanderzande, D. 32, **2001**, 7294-7299.

Because of the presence of the imine atom, the pyridine moiety is regarded upon as being electron accepting and thus polymers of this kind may posses high electron affinity. As mentioned earlier, this property could make this polymer useful in certain applications, for example in LEDs and photovoltaic cells. High electron affinity allows the fabrication of LEDs with good electron injection from stable cathodes like aluminium rather than the low work function metals required for more electron rich polymers.[1] Using an electron accepting pyridine ring is an elegant way to come to such electron accepting polymers. Other methodologies use electron-withdrawing groups to obtain these polymers like for example the highly electron deficient cyano groups in cyano-PPV (cyano groups attached to the phenylene ring) (Chapter 2) and in poly[2,5-bis(hexyloxy)-1,4-phenylene-(1-cyanovinylene)] (cyano groups attached to the double bond).[1]

Poly(2,5-pyridylene vinylene) was first synthesised by palladium catalysed cross-coupling reactions, which yielded relatively low molecular weight polymers.[2] The polymer obtained is insoluble in conventional organic solvents but dissolves in strong acids. It is also possible to methylate the nitrogen atom to induce solubility in polar organic solvents.[2] Another way to achieve a processable polymer is to synthesise a non-conjugated precursor polymer. After the processing step the final conjugated polymer can than be obtained by a thermal treatment. Three different poly(2,5-pyridylene vinylene) precursor polymers have been reported by Li *et al.*,[3] namely the sulfonium precursor, the chloro precursor and the methoxy precursor. The chloro precursor route was reported to give the best results, however it is not ideal. For example, the chloro precursor polymers are not soluble in conventional organic solvents which hampers device preparation. These precursor polymers are only soluble in strong acids like formic acid (protonation imine atom). Furthermore, high temperatures are needed to convert the precursor polymer to its conjugated form and from our experience the "Gilch" polymerisation reaction of this monomer is difficult to reproduce. All these limitations and difficulties give good reason to synthesise the poly(2,5-pyridylene vinylene) via the sulphinyl precursor route.

3.1.1 Monomer synthesis

The monomer synthesis (Scheme 2) started from the commercially available 2,5-lutidine which was chlorinated with N-chlorosuccinimide.[4] Freshly prepared benzoylperoxide was used as a radical initiator. Typically, this radical reaction yields a mixture of different

reaction products which had to be separated by column chromatography. Because of the low selectivity towards the desired dichloride (**2**), yields for such radical halogenation reactions seldom raise above 30 percent. Moreover, dichloride (**2**) proved to be highly unstable at room temperature and decomposed spontaneously to an unknown red substance, however it can be stored at –25°C for longer periods without degrading. Conversion of dichloride **2** into its bissulfonium salt derivative (**3**) was only possible in very low yield. The even higher instability of this compound caused immediate decomposition upon isolation of the salt. For this reason, the very selective approach for preparing the mono thioether via the bissulfonium salt could not be used. For this monomer, the thioether group had to be introduced in a less selective way. As outlined in Chapter one, the thioether group can also be introduced relatively selectively by using a two phase reaction mixture (water:toluene). In such a system a phase transfer reagent, Aliquat 336, is used to promote the migration of the base (OH^-) to the organic phase.[5,6] 1-octanethiol was used because the long aliphatic chain guarantees good solubility on both the monomer- and the precursor polymer stage. Due to the asymmetric position of the chloromethyl substituents on the pyridine ring a mixture of two isomers is obtained in this reaction. After oxidation of the crude product, to the sulphoxide, using the classical H_2O_2/TeO_2 system in 1,4-dioxane a chromatographic separation of the reaction products yielded the pure monomer as a white solid. The overall yield of this synthesis was determined at 13 percent. (Scheme 2)

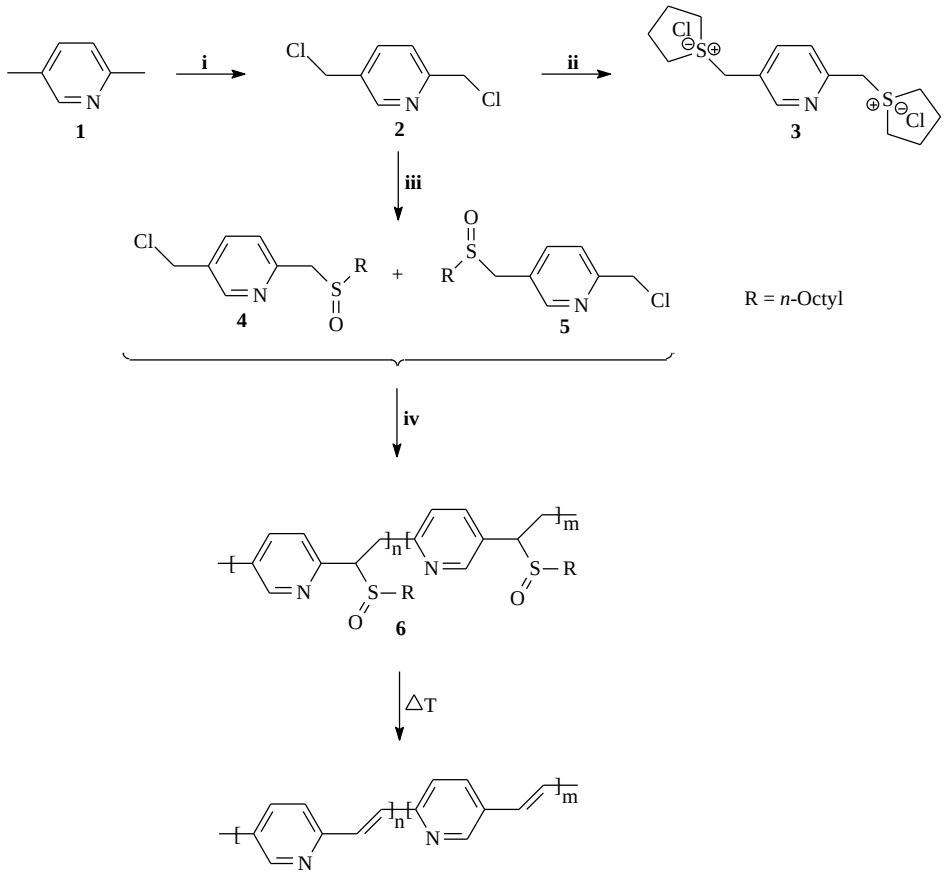

Scheme 2: Synthetic pathway toward the synthesis of poly(2,5-pyridylene vinylene). Reaction conditions: ***i****: NCS, CCl_4, DBP;* ***ii****: THT, MeOH;* ***iii****: a) H_2O, NaOH, toluene, HSOctyl, Aliquat 336 b) H_2O_2/TeO_2, 1,4-dioxane;* ***iv****: NatBuO, solvent.*

The monomer was mainly characterised with a number of NMR spectroscopic techniques. The complete assignment of all proton and carbon resonances on the monomer stage was accomplished by a combination of two dimensional HETCOR (heteronuclear chemical shift correlation) and one dimensional techniques like ^{1}H, ^{13}C-NMR and APT (attached proton test). These measurements also yield the exact ratio between the two isomers **4** and **5**, this ratio was found to be 1:2 in favour of the 5 substituted isomer (**5**). The 2D-HETCOR spectrum of the aromatic region of the isomer mixture is shown in Figure 1. From this measurement is it clear which hydrogen atom is coupled to which carbon atom. With this technique the quaternary carbon atoms do not give rise to a signal as they do not posses any

hydrogen atoms. These signals again become clear in the APT spectrum of the isomer mixture. (Figure 2) Here the quaternary carbon atoms are clearly recognised as they lead to a negative signal. The ^{1}H and ^{13}C-NMR chemical shifts of the aromatic resonances of isomers **4** and **5** are shown in Table 1.

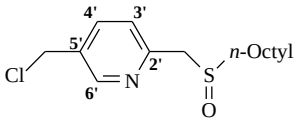

isomer 4

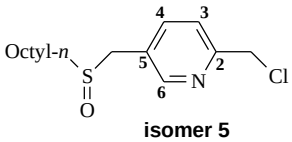

isomer 5

#	^{1}H shift	^{13}C shift	#	^{1}H shift	^{13}C shift
2'	-	151.51	**2**	-	157.11
3'	7.43	125.94	**3**	7.50	123.42
4'	7.81	137.75	**4**	7.73	139.42
5'	-	133.29	**5**	-	126.26
6'	8.60	149.99	**6**	8.47	150.81

*Table 1: ^{1}H and ^{13}C-NMR chemical shifts of the aromatic resonances of isomers **4** and **5**.*

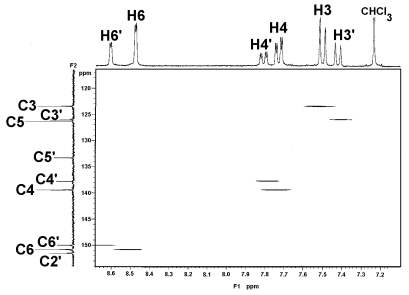

Figure 1: HETCOR of the isomer mixture.

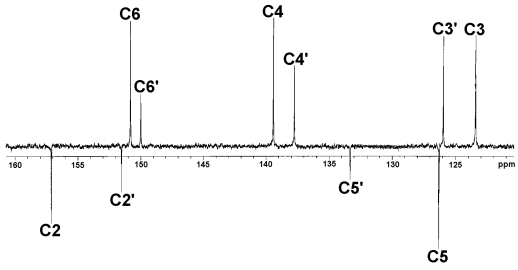

Figure 2: APT spectrum of the isomer mixture.

These two isomers were inseparable using simple chromatographic or crystallisation techniques. As a consequence, the mixture of isomers was used in all polymerisation reactions. The final monomer mixture was recrystallised from *n*-hexane:chloroform.

3.1.2 Polymerisation

All polymerisations were carried out under the same "standard" conditions (Experimental Section) in a range of solvents and solvent mixtures. (Table 2) Before bringing them together both the monomer and the base solution were degassed by passing nitrogen for one hour. The monomer concentration calculated on the total volume of solvent was set at 0.1M. Sodium *tert*-butoxide was used as base and was added in solution in a slight excess of 1.05 equivalents to correct for losses during addition. Polymerisation time was 1 hour during which the passing of nitrogen was continued. After precipitation into water the precursor polymer (**6**) was extracted with chloroform, concentrated and precipitated in diethylether. The precursor polymer was collected and both the precursor polymer and the residual fraction (filtrate) were analysed. The precursor polymers were soluble in organic solvents such as chloroform and THF as well as in formic acid.

Solvent	M_w ($x10^{-3}$)[c]	PD[c]	Yield (%)
2-butanol[a]	730	5.7	50
2-butanol[b]	47	3.3	27
2-butanol/1,4-dioxane (50/50)[a]	243	4.1	52
1,4-dioxane[a]	17	2.1	57
THF (dry)[a]	56	3.2	58
DMSO[a]	34	2.4	17

*Table 2: Polymerisation results for the precursor polymer (**6**) in different solvents. a: base = sodium tert-butoxide; b: base = sodium hydroxide; c: molecular weights and polydispersities of the precursor polymer according to GPC relative to polystyrene standards with chloroform as eluent.*

Precursor polymer was obtained in all tested solvents. (Table 2) The precursor polymers were analysed with GPC measurements relative to polystyrene standards and chloroform was used as eluent. The GPC curves of all precursor polymers were monomodal and the polymerisation process is a radical chain polymerisation as was confirmed by a control polymerisation experiment in 2-butanol where 0.5 equivalents of TEMPO (2,2,6,6-tetramethyl-1-piperidiniloxy) was added. TEMPO, a radical trap quenches the radical polymerisation and in this case no precursor polymer could be isolated.

The polymerisation yields were moderate in all solvents tested except when the polymerisation was performed in the polar non-protic solvent DMSO. In this solvent premature elimination of the sulphinyl group in the precursor polymer occurred. This resulted in an insoluble, strongly yellow coloured conjugated fraction, which could not be analysed. Nevertheless, a small fraction of soluble precursor polymer was formed but due to the side reaction the yield was rather low. The highest molecular weight was found in the protic "less polar" solvent 2-butanol. When the polymerisation was performed in a 50/50 (vol%) mixture of 2-butanol and 1,4-dioxane an intermediate molecular weight was obtained compared to the polymerisation in the respective pure solvent. This experiment shows that it is possible to control the molecular weight of the precursor polymer by adding an amount of 1,4-dioxane as a cosolvent. By doing so the molecular weight of the precursor polymer can be tuned between approximately 50000 and 700000. From Table 1 we also notice slightly higher polymerisation yields in 1,4-dioxane and THF than compared to the polymerisation in 2-butanol. A possible explanation to this was found when analysing the residual fraction with ^{1}H-NMR. The residual fraction from the polymerisation in the 50/50 mixture of 2-butanol and 1,4-dioxane contained a fraction of monomer that had been solvent substituted, i.e. 2-butoxide had replaced the chlorine group. In pure 2-butanol the residual fraction consisted only of solvent substituted monomers **7** and **8**, while with pure 1,4-dioxane or THF the residual fraction consisted only of unreacted monomer. This side reaction may account for the slightly lower polymerisation yield in 2-butanol.

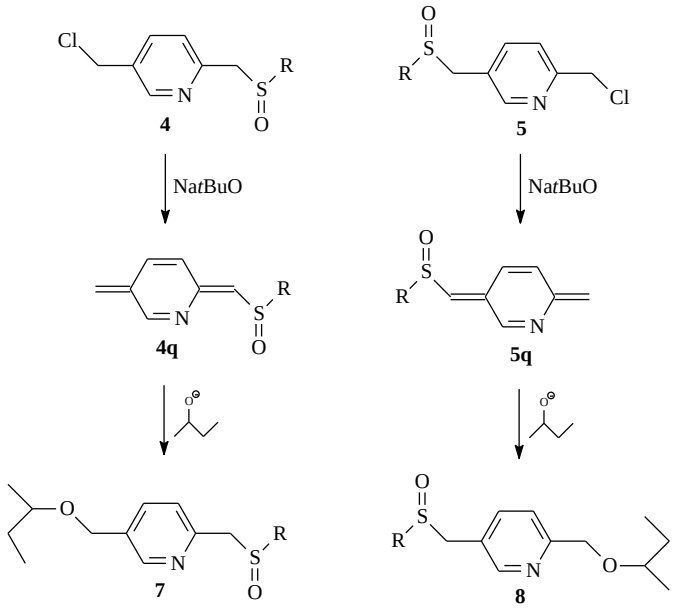

*Scheme 3: Formation of the solventsubstituted monomers **7** and **8***

Another observation worth mentioning, for the polymerisation performed in 2-butanol, is the fact that although the initial distribution between the two monomers was about 2 to 1 in favour of the 5 substituted monomer **5**, the restfraction after polymerisation shows exactly the opposite product distribution. Now, the ratio between the two solvent substituted monomers is about 2 to 1 in favour of compound **7** (which originates from isomer **4**) as was concluded from ^{1}H-NMR measurements. Apparently both monomers **4** and **5** have different reactivity towards solvent substitution. This difference can be caused by a different reactivity of the respective quinoid compounds (**4q** and **5q**) towards solvent substitution but more likely, this dissimilarity originates from the differences in formation rate of the respective quinoid compounds. In monomers **4** and **5** the different position of the nitrogen atom causes these monomers to have a different chemical reactivity. Firstly, in monomer **4** the proton that has to be abstracted in the first step of the polymerisation process is more acid than compared to that in monomer **5** because of the nitrogen atom in ortho position. Secondly, in monomer **4** the chlorine atom is a better leaving group than compared to that in monomer **5** because the nitrogen atom in meta position in the former. Both factors will lead to a faster formation rate of quinoid compound **4q** from monomer **4**. As already mentioned, the formation of the quinoid system is expected to be the rate determining step

in the overall polymerisation process. In the end, the quinoid compound (**4q**) is present at an earlier stage in the polymerisation process and therefore this compound is more likely to undergo solvent substitution especially in the very beginning of the polymerisation when the concentration of base is still high.

We have seen that, for PPV, solvent substitution in 2-butanol can be avoided by changing the base to sodium hydroxide without affecting the outcome of the polymerisation.[7] This is true for PPV but, in the case of PPyV, both polymerisation yield and molecular weight drop significantly yet solvent substitution is still observed.

From these results we can conclude that it is possible to perform this polymerisations in a range of solvents. Furthermore, by using the appropriate solvent or solvent mixture we have some control over the molecular weight of the precursor polymer.

The precursor polymer **6** was characterised with NMR spectroscopic techniques. Complete assignment of the proton and carbon resonances was possible by combining 2D-HETCOR (heteronuclear chemical shift correlation) experiments with one dimensional techniques like ^{1}H and ^{13}C-NMR. Figure 3 shows the aromatic region of the HETCOR spectrum of precursor polymer **6**. Due to the short T_2 (spin-spin relaxation time) the proton signals are broad. Six signals can clearly be observed in the ^{1}H-NMR spectrum, each of them originates from one proton on the pyridine ring. Because a mixture of two isomers (**4** and **5**) was polymerised, the precursor polymer in fact is a copolymer in which both monomers have been incorporated. Based on the ^{1}H-NMR spectrum the ratio between the two isomers in the polymer can roughly be estimated at 1 to 1, all six signals have approximately the same intensity. The correlation of each proton signal with the carbon atom it is attached to already affords the protonated aromatic carbon signals. (Figure 3) The quaternary carbon signals do not give rise to a signal as they do not posses any protons. In the ^{13}C spectrum the quaternary carbon atoms have lower intensities and these signals are broader than the protonated carbon atoms. H1 (which is the most down field) correlates with C1 and H1' with C1'. All other correlations can also be seen in Figure 3. Note that the signal for C4 and C4' in the ^{13}C spectrum are found at the same chemical shift. The quaternary carbon atoms are assigned by comparing this spectrum with the monomer spectrum as shown before. In this way all aromatic carbon and hydrogen atom absorptions are identified.

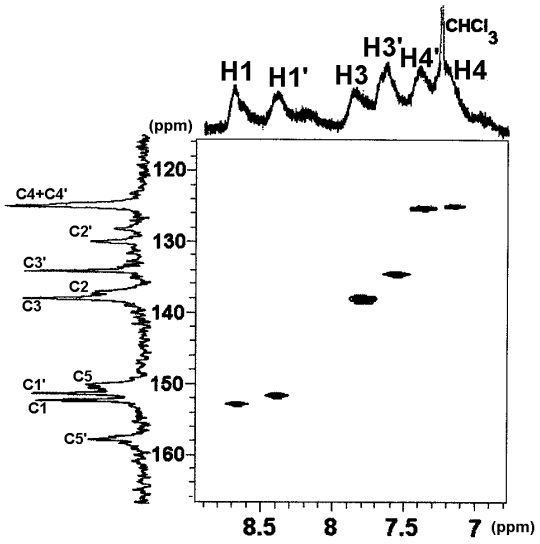

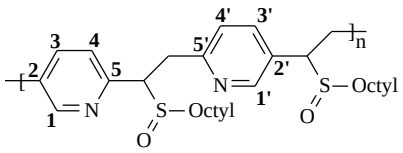

6

*Figure 3: Enlarged part of the HETCOR spectrum of precursor polymer **6**.*

3.1.3 Thermal conversion to the conjugated structure

In the following experiments the precursor polymer (**6**) synthesised in a 50/50 (vol%) mixture of 2-butanol and 1,4-dioxane is used. The elimination behaviour as well as the thermal stability of the conjugated structure proved to be independent of the polymer used, all precursor polymers showed an identical behaviour. The techniques used here are *in situ* FT-IR, *in situ* UV-Vis, TGA and DIP-MS.

In situ FT-IR spectroscopy measurements were carried out on film, spin-coated on NaCl disks. An experimental set-up was used (Experimental Part) which allowed *in situ* monitoring of the elimination process. A dynamic heating program of 2°C/min up to 450°C, under a continuous flow of nitrogen, was used. The most distinct absorption bands, which are changed during the elimination process, are the sulphoxide band at 1040 cm^{-1} and the *trans* vinylene band at 960 cm^{-1}. The elimination and the degradation process can be followed from the intensity of the vinylene signal at 960 cm^{-1}. Figure 4 shows an enlarged part of the IR spectrum at a few selected temperatures. The sulphoxide absorption declines as the double bond absorption appears. In Figure 5, the sulphoxide (1040 cm^{-1}) and double bond (960 cm^{-1}) absorption are plotted versus increasing temperature. In this way the relative trends in elimination and stability behaviour become clear. Both elimination and double bond formation start around 75°C, and when the temperature reaches 130°C the

processes slow down considerably, with hardly any change seen after 200ºC. When even higher temperatures are reached a decline in double bond signal is observed. This decomposition of double bonds starts at approximately 310°C and ends at 450°C when almost no double bond signal remains. (Figure 5)

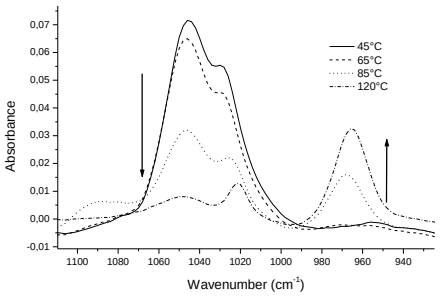

Figure 4: Enlarged part of the IR spectrum showing sulphoxide and vinylene absorption bands.

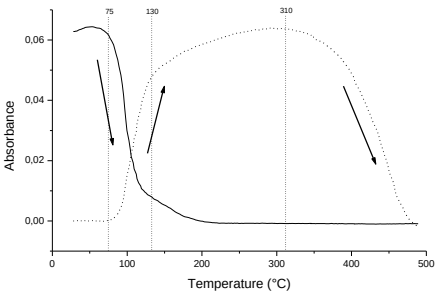

Figure 5: Sulphoxide (1040 cm^{-1}, solid line) and vinylene (960 cm^{-1}, dotted line) absorption versus temperature.

In situ UV-Vis spectroscopy measurements were carried out on film, spin-coated on quartz pellets. These pellets were placed in an oven which was placed in the beam of the UV-Vis spectrometer. This experimental set-up allows *in situ* monitoring of the elimination process. The heating set-up was identical as in the IR experiments and a dynamic heating program of 2°C/min up to 450°C under a continuous flow of nitrogen was used. Before heating, two absorption bands from the precursor polymer were present (maxima at 218 nm and 273 nm). As the heating program progressed, new absorption bands appeared that gradually redshifted with increasing temperature. When higher temperatures were reached the fine structure disappeared and the absorption band broadened to cover the various oligomer bands. When, at 130°C, the absorption was maximal, a conjugated polymer with an absorption maximum around 419 nm was obtained. The gradual formation of the conjugated structure is shown in Figure 6 (solid lines). At higher temperatures the absorbance declined very slowly until 310°C. The decay was very small and is probably due to thermochromism rather than degradation, which means that the polymer was stable up to 310ºC. At 310°C the absorbance at 419 nm started to decline faster. Together with this decline, a blue-shift in absorption maximum was noticed which may be explained by a

shortening of the conjugated segments. When 450ºC was reached, the absorbance was more than halved and a very broad signal remained. The gradual decomposition of the conjugated structure is also shown in Figure 6 (dashed lines). When the absorbance at 419 nm is plotted versus temperature (Figure 7) we conclude that the conjugated structure is formed between 75 and 130 °C and degradation occurs between 310 and 450 °C. This result is in accordance with the FT-IR results.

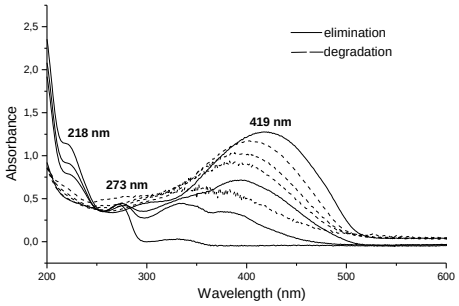

Figure 6: UV-Vis spectra of the formation (30, 98, 130 °C; solid lines) and degradation (340, 360, 390, 430 °C; dashed lines) of the conjugated structure.

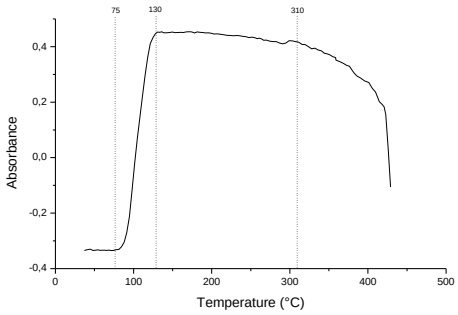

Figure 7: Absorption at 419 nm versus temperature.

The TGA experiment was performed at a heating rate of 10°C/min up to 600°C under a constant flow of nitrogen. In a TGA experiment the weight loss of the sample is recorded as a function of temperature. The thermogram shows two major steps of weight loss (Figure 8), the first one (120-310°C) is due to the elimination of the sulphoxide groups and evaporation of elimination products. The second period of weight loss (450-550°C) accounts for the degradation of the polymer backbone. After elimination, at 310ºC, an experimental residual weight of approximately 40% remains. This is in accordance with the theoretical residual value (39%). A typical thermogram is shown in Figure 8. The start temperatures observed with TGA were substantially higher to that observed with FT-IR and UV-VIS measurements. This difference is primarily caused by the fact that this technique monitors the evaporation of the elimination products and not the actual sulphinyl elimination/double bond formation process as is monitored in the IR and UV-Vis measurements. As proven earlier these two processes are kinetically separated.[8] The faster

heating in the TGA experiment also contributes to the rise in the observed elimination and degradation temperature.

The elimination was also studied by DIP-MS, to allow the analysis of the elimination products. In this technique the precursor polymer is placed directly on the heating element of the probe and heated at 10°C/min till 600°C. By plotting the total ion current versus temperature, the thermal stability of both precursor and conjugated polymer can be visualised. In accordance with the TGA measurements two signals were observed which can be assigned to an elimination step (80-110°C) and a degradation step (270-320°C), see Figure 8. The decrease in elimination and degradation temperature compared to TGA is caused by the high vacuum (10^{-6} mmHg) at the probe which makes the elimination products evaporate faster. In TGA a continuous nitrogen flow is used. The fragments analysed by MS correspond to the ones of the expected elimination products.

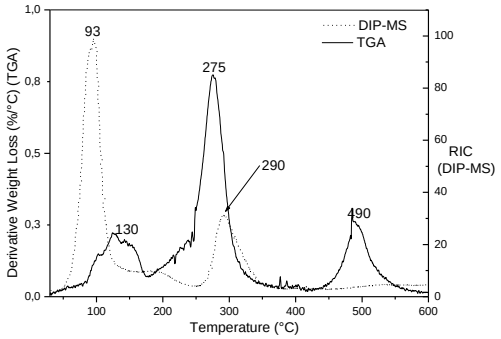

Figure 8: TGA-thermogram (solid line) and DIP-MS thermogram (dotted line) of the precursor polymer.

To conclude, the differences in elimination temperature observed with the different techniques suggests that, under nitrogen atmosphere, the elimination reaction can be performed starting from a temperature of 75°C. The elimination can also be performed at a higher temperature which will significantly raise the reaction rate.[36] By performing the conversion somewhere in the temperature domain between 75 and 130°C the conjugated structure is formed quickly and degradation does not yet occur. Furthermore it is advisable to apply a vacuum during the conversion to get good evaporation of the elimination products. Both the IR and the TGA measurement under nitrogen atmosphere showed that

elimination products stay in the film till approximately 250°C. When the pressure is reduced (DIP-MS) evaporation occurs simultaneously with the elimination process. Without reducing the pressure, heating up to 200-250°C is necessary to get complete elimination and evaporation of elimination products. The different spectroscopic data suggest that the conjugated polymer is stable up to at least 300°C.

3.1.4 Absorption and Photoluminescence

The photoluminescence (PL) and absorption spectra of a PPyV film which has been converted to its conjugated form by heating at 100°C in *vacuum* for 1 hour is shown in Figure 9.

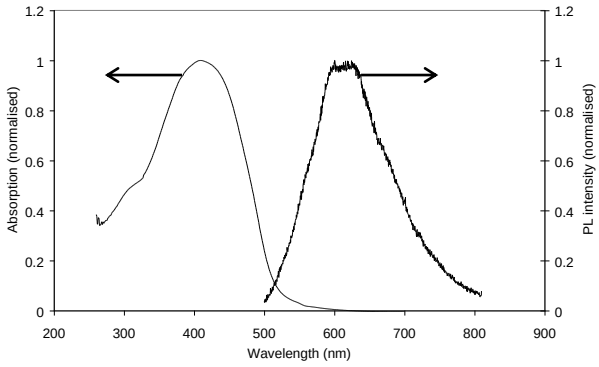

Figure 9: Absorption and PL spectra for PPyV.

The maximum photoluminescence intensity is at about 600 nm. The PL efficiency measured with an integrated sphere was 14%. This is a much higher value than those previously reported for PPyV (1.5-2%).[3,9] A probable explanation for the higher efficiency for our film is a different morphology. This can be caused by a difference in molecular weight, the long alkyl groups in our precursor polymer or spin-coating from chloroform rather than formic acid. The thermal conversion from precursor polymer to the conjugated form can also affect the morphology. Since our polymer has higher PL efficiency than both PPyV polymerised by step-wise polymerisation[9] and PPyV synthesised via the chloroprecursor[3] it is probably a combination of factors that cause the difference. More experiments are needed to test these hypotheses.

3.1.5 Electrochemical properties

Electrochemical measurements are valuable to determine the electron affinity and the ionisation potential of conjugated polymers. Cyclic voltammetry (CV) is such a technique in which the potential is varied cyclically while the current is measured.[10] In a CV measurement the conjugated polymer is brought on the working-electrode of an electrochemical cell. When a high enough potential is applied the conjugated polymer will be reduced or oxidised and a current can be measured. When the potential is reversed the polymer will be de-doped which also gives rise to a current. From the CV results it is possible to estimate the HOMO and LUMO levels of a conjugated polymer. In theory, these values can be calculated from the onset of the reduction and oxidation peaks respectively.[11] However, in practice, it is often hard to define where the reduction or oxidation exactly starts and the potential depends on the scan-rate (higher rates delay the reduction or oxidation, hence the potential is overestimated). Therefore the half-wave potential, which is the average between the reduction and re-oxidation (or oxidation and re-reduction peaks) is often used. The half-wave potential is easier to define and less sensitive to the scanning rate.

A cyclic voltammogram of a PPyV film (converted at 100°C for 1 hour in *vacuum*) on a Pt electrode is shown in Figure 10. For comparison also the curves for PPV (prepared via the sulphinyl precursor route and converted at 120°C for 1 hour in *vacuum*) and a cyano-MEH-PPV[12] polymer are shown. For PPyV no reduction is seen during the first cycle, probably because the film is very compact and has to be swelled first. In the second scan, a peak has started to form and in the third and fourth scans it is seen clearly, with the reduction peak at –1.74 V vs. Ag/AgCl. The corresponding oxidation (n-undoping) is at –1.54 V vs. Ag/AgCl. The reduction of the polymer is reversible but the oxidation of PPyV is irreversible with a peak at 1.2 V vs. Ag/AgCl (sweep rate 10 mV/s). The band-gap calculated from the formal reduction potential (estimated as the average of the reduction and re-oxidation peaks to be -1.64 V vs. Ag/AgCl) and the oxidation peak is 2.84 eV, which is in accordance with the band-gap as determined from the UV-Vis absorption spectrum (419 nm corresponds to about 2.9 eV). For comparison, PPV, synthesised via the sulphinyl precursor route and converted to the conjugated form at 120°C for 1 h at reduced pressure, and a cyano-MEH-PPV polymer, synthesised as described in literature,[12] were measured under the same conditions as PPyV. PPV had a formal potential of –2.03 V vs.

Ag/AgCl and the cyano-MEH-PPV polymer –1.30 V vs. Ag/AgCl, which is similar to previously reported values.[11] This means that PPyV synthesised via the sulphinyl precursor route has an electron affinity intermediate to that of the cyano-MEH-PPV polymer and PPV. Consequently the electron affinity of PPyV is higher than that of PPV but the nitrogen atom in PPyV only raises the electron affinity moderately. When stronger electron withdrawing groups are used, as for example in the cyano-MEH-PPV polymer the electron affinity is increased more significantly.

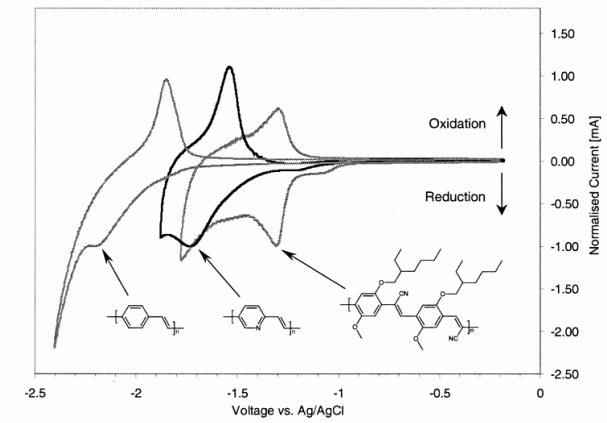

Figure 10: Cyclic voltammogram of PPV, PPyV and a cyano-MEH-PPV polymer.

3.1.6 Protonation or alkylation of poly(pyridynlene vinylene)

An additional feature of these nitrogen containing PPV derivatives is the possibility to protonate or alkylate these conjugated polymers. Recent papers motivate the synthesis of these charged polymers.[2,13,14] (Scheme 4) Poly(methylpyridinium vinylene) (PMPyV) (**10**) shows an iso-electronic analogy with PPV. Since reduction of PPV produces a negatively charged, highly conducting composition, the reduction of PMPyV, a positively charged polymer, produces an uncharged conducting material. Such a material may be considered to be an intrinsic conductor since it requires no dopant ion.[2] Charged PPV derivatives also provide the possibility to fabricate polymer films via the electrostatic deposition method.[14] It was also shown that protonation increases the interchain interactions significantly.[13]

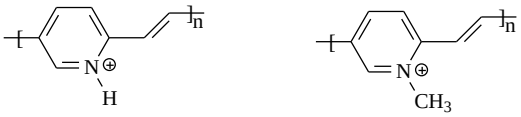

PHPyV (**9**) PMPyV (**10**)

*Scheme 4: Chemical structures of PHPyV (**9**) and PMPyV (**10**).*

PHPyV was prepared by solubilising a sample of PPyV in $HClO_4$. The conversion from the precursor stage to the conjugated form (PPyV) was performed by heating at 100°C for one hour under *vacuum*. Protonation of the nitrogen atom in PPyV by strong acids introduces solubility in these media. This procedure yielded a bright yellow solution and the absorption spectrum of PHPyV (in $HClO_4$) shows a maximum absorption at 438 nm. (Figure 11) Compared to the absorption maximum of PPyV (in film) the absorption maximum of PMPyV has red-shifted about 20 nm. This charged conjugated polymer (**9**) proved to be highly unstable when isolated.

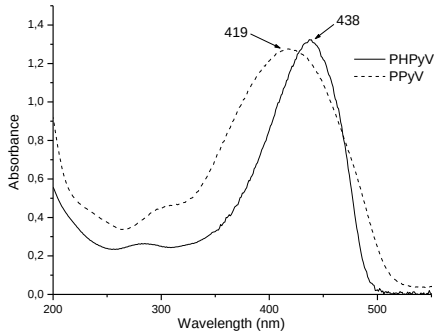

Figure 11: UV-Vis spectrum of PHPyV (solid line) and PPyV (dashed line).

Methylation of the conjugated PPyV sample was also tested using methyltriflate in dichloromethane. Due to the high molecular weight of the conjugated polymers synthesised via the sulphinyl precursor route the conjugated PPyV was completely insoluble in organic solvents and methylation could not be performed on this stage. In the references sited, methylation is possible because the PPyV used in these works only has a very low molecular weight thus allowing (partial) solubility. To solve this problem methylation was performed on the precursor stage using the same methodology. Unfortunately methylation

makes the polymers highly susceptible to nucleophilic reagents such as water. This high reactivity made the polymers degrade upon isolation and no further characterisation could be performed.

3.2 Poly(2,2'-bipyridylene vinylene)

A second material within the family of the hetero aromatic PPV derivatives discussed in this chapter is the poly(2,2'-bipyridylene vinylene). (Scheme 5)

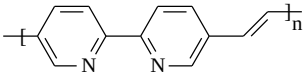

Scheme 5: Chemical structure of 2,2'-bipyridylene vinylene.

This conjugated polymer possess 2,2'-bipyridine units that are connected by vinylene bonds in the 5 position. The reasons for synthesising this polymer are similar as mentioned for the poly(pyridylene vinylene) in the previous paragraph. First, due to the electron accepting nature of the 2,2'-bipyridine moiety, this polymer may posses higher electron affinity compared to PPV which is required to fabricate more efficient polymer LEDs.[1] Second, the nitrogen atom may be protonated, alkylated or even oxidised to yield polymers with completely different optical and electronic properties.[14] Third, and this is a property which is absent in the pyridine PPV, the 2,2'-bipyridine unit possess superb ability to coordinate a large number of metal ions.[15] Such complexation will significantly alter the properties of the conjugated polymer since the electronic structure of the polymer backbone is modified upon complexation. This property will be discussed more into detail in Chapter 4 were the complexation behaviour of copolymers between the bipyridylene vinylene and OC_1C_{10} is handled. Here monomer- and homopolymer synthesis of the poly(2,2'-bipyridylene vinylene) will be discussed as well as the thermal conversion to the conjugated polymer.

3.2.1 Monomer synthesis

Monomer synthesis starts from the commercially available 5-methylpyridine (**11**). This compound was dimerised to form the 5,5'-dimethyl-2,2'-bipyridine (**12**) using a Raney Nickel catalyst.[16] The yield of this reaction was 27 percent which is rather low but not uncommon for this type of reactions.

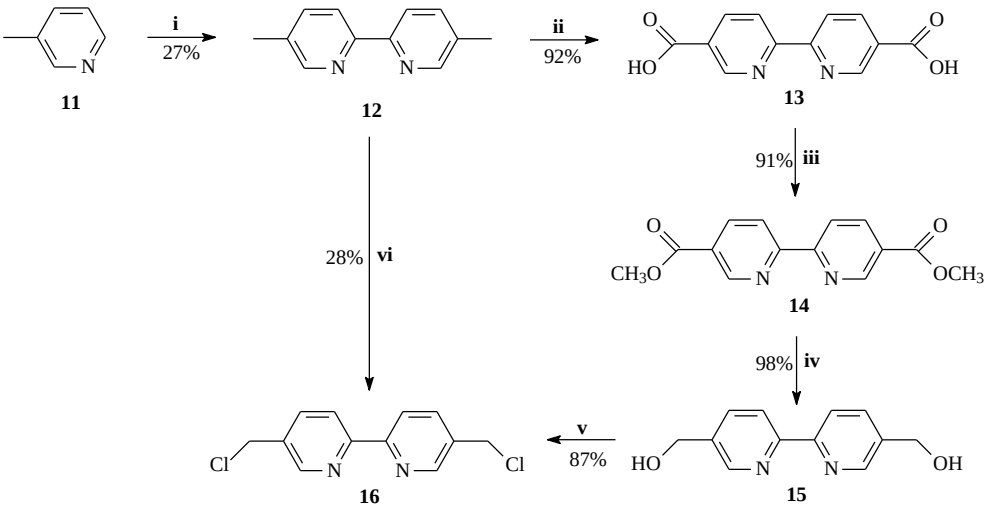

Scheme 6: Synthesis of 5,5'-di(chloromethyl)-2,2'-bipyridine. Reaction conditions: ***i****: RaneyNi;* ***ii****:* $K_2Cr_2O_7$, H_2SO_4; ***iii****:* $MeOH/H_2SO_4$; ***iv****:* $NaBH_4$; ***v****:* $SOCl_2$; ***vi****: NCS,* CCl_4.

Initially, compound (**12**) was halogenated using NCS or NBS in CCl_4. This resulted in a mixture of products which were difficult to isolate using conventional chromatographic techniques. Furthermore, the yield of such radical halogenation reactions only varies between 20 and 30 percent towards the desired dihalogenated product (**16**). These drawbacks obliged us to search for another synthetic pathway towards dichloride **16**. This synthetic method is outlined in Scheme 6. Here compound **12** is oxidised in high yield towards the diacid **13** using potassium dichromate in sulphuric acid (92 percent).[17] Consecutive esterification to the dimethyl ester derivative[17] (**14**) (91 percent) followed by reduction with $NaBH_4$ yielded diol **15** in excellent yield.[18,19] Normally $NaBH_4$ is not often used for the reduction of esters. Here however, reflux of diester **14** in ethanol with a large excess of $NaBH_4$ yielded pure compound **15** in a nearly quantitative way (98 percent). Transformation of diol **15** toward the desired dichloride **16** was achieved by using thionylchloride (87 percent).[19] These reactions are all relatively simple reactions that are commonly used in organic synthesis. More importantly, these reactions proceed in high yields thus allowing a very high overall yield (71 percent) for the synthesis of dichloride **16** from compound **12**. For this reason this more laborious approach is favoured over the radical halogenation of compound **12**.

Further conversion to the monomer is depicted in Scheme 7. The low yield (27%) for the synthesis of bissulfonium salt **17** together with the very slow formation of the quinoid compound from salt **17** inhibits the efficient synthesis of monosulfide **18** via this compound.[20] Instead, a two phase system (water:toluene) was used towards the synthesis of compound **18**. In this reaction a phase transfer catalyst (Aliquat 336) was used.[5,6] To avoid disubstitution, this reaction was carried out using a twofold excess of dichloride **16**. The *n*-octylsulfide was used to enhance solubility both on the monomer stage and on the precursor polymer stage. Oxidation of the monosulphide **18** toward the sulphoxide **19** was possible by using the TeO_2/H_2O_2 oxidising system in 1,4-dioxane. A flush chromatographic separation of the reaction mixture yielded the pure monomer **19** which was further purified by crystallisation from *n*-hexane/ethylacetate. Also, the large excess of dichloride **16** could be recuperated and could be recycled in the reaction sequence. The overall yield for these combined reactions was 73 percent, calculated from the *n*-octylthiolate.

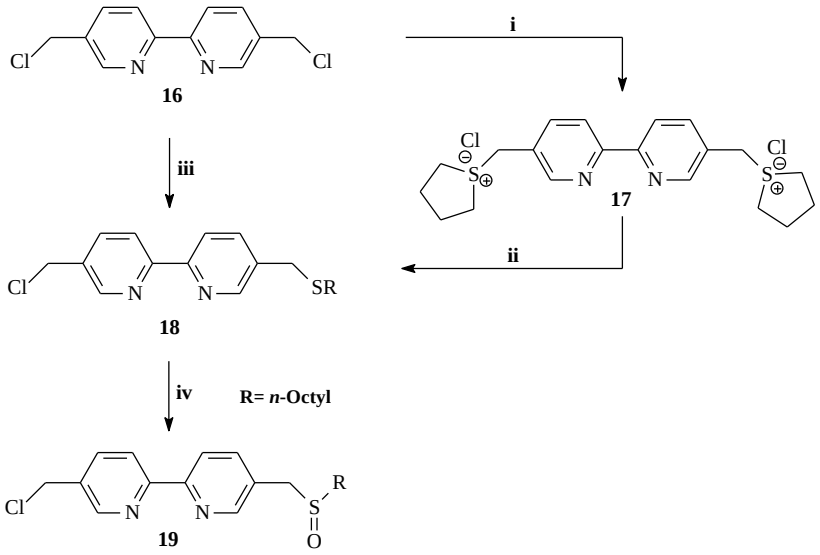

*Scheme 7: Monomer synthesis. Reaction conditions: **i**: THT/MeOH; **ii**: NaOtBu/HSR; **iii**: NaOH/HSR/Aliquat 336; **iv**: TeO_2/H_2O_2, 1,4-dioxane.*

Monomer **19** was characterised with NMR spectroscopic techniques. Combination of two dimensional (HETCOR) and one dimensional techniques (classical ^1H and ^{13}C-NMR) allowed the full assignment of all hydrogen and carbon atoms. Figure 12 shows the 2D-

HETCOR spectrum of the aromatic atoms of monomer **19** and Figure 13 illustrates that of the remaining atoms. By linking the different spectra to each other in a 2D spectrum it becomes clear which hydrogen atom is attaches to which carbon atom and assignment of all resonances is possible.

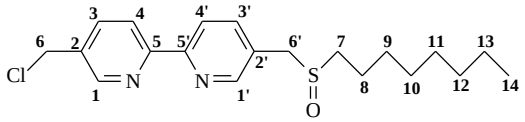

9

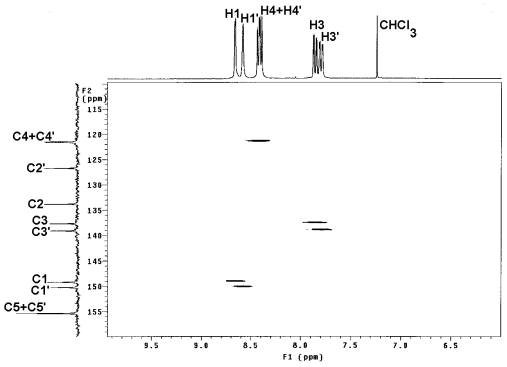

*Figure 12: 2D-HETCOR of the aromatic atoms in monomer **19**.*

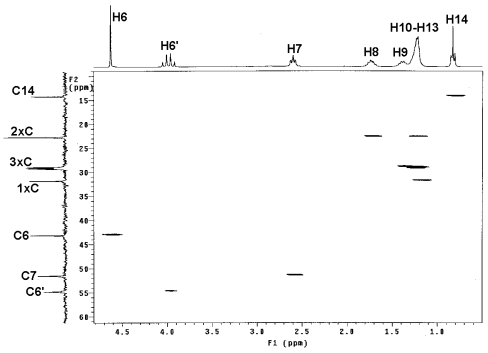

*Figure 13: 2D-HETCOR of the non-aromatic atoms in monomer **19**.*

Before commenting on the polymerisation results of monomer **19** we will first mention some small chemical modifications that were made on the monomer stage in order to enhance the polymerisation process. A UV-Vis study on the formation of the actual sulphinyl monomer – the *p*-quinodimethane system – of PPV has shown that this quinoid formation proceeds faster when the leaving group on the monomer stage is enhanced.[21] For this reason two slightly different monomers **20** and **21** were synthesised from monomer **19** via simple organic reactions that use LiBr and NaI respectively in refluxing aceton. In monomer **20** a bromine atom acts as leaving group, monomer **21** has the best leaving group (iodine atom). (Scheme 8)

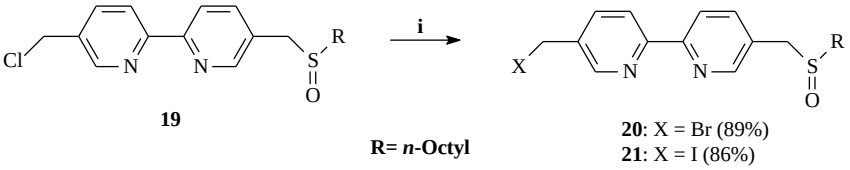

*Scheme 8: Substitution of the leaving group. Reaction conditions: **i**: X= Br: LiBr, aceton; X= I: NaI, aceton.*

3.2.2 Polymerisation

All polymerisations of monomers **19**, **20** and **21** were performed according to the "standard" procedure in different solvents. (Experimental Section) Before bringing them together the monomer and base solutions were degassed by passing nitrogen for one hour. Sodium-*tert*-butoxide was used as a base in a small excess of 1.05 equivalents to correct for losses during addition. This base solution was added to the monomer solution in one shot and reaction was allowed for one hour during which the passing of nitrogen was continued. Temperatures at which the different polymerisation reactions were conducted varied depending on the solubility of the monomer in the respective solvent. The reaction was terminated by pouring the reaction mixture in ice-water. Extraction and precipitation in *n*-hexane/ethylacetate yielded the precursor polymer. The filtrate was evaporated and analysed as restfraction. Molecular weights were determined using GPC versus polystyrene standards (eluent: DMF). (Table 3)

Monomer	Solvent	Temp. (°C)	M_w	PD	Yield (%)
19	1,4-dioxane	50	7300	1,38	21
19	DMSO	55	7000	1,21	26
19	CH_2Cl_2	30	6300	1,22	30
20	CH_2Cl_2	30	10300	1,49	37
21	CH_2Cl_2	30	12300	1,47	54

*Table 3:Polymerisation results for the homopolymerisation of 2,2'-bipyridine monomers **19**, **20** and **21**.*

As can be concluded from Table 3, the molecular weight of the precursor polymers obtained is relatively low. Due to the low solubility of monomer **19** in 1,4-dioxane and DMSO the temperature had to be raised to about 50°C. CH_2Cl_2 proved to be a better solvent to perform the polymerisation in but nevertheless, still very low molecular weight polymers were obtained. These results are in accordance with earlier work within our research group on the polymerisation of a similar monomer, i.e. the biphenyl sulphinyl monomer.[22] Polymerisation of this monomer proceeds only very difficult, even via the sulphinyl precursor route. Remember that Wessling polymerisation of the biphenyl derivative is impossible.[23] The limiting factor in the polymerisation process of monomers with extended aromatic systems like the biphenyl or bipyridine aromatic moiety, probably is the formation of the actual monomer in the polymerisation - the quinoid structure. In these two cases the aromaticity of two aromatic rings has to be broken in order to form the quinoid structure that can undergo polymerisation. UV-Vis measurements on monomers **19** to **21** did not show any quinoid formation even when a large excess of base was used. If formed at all, the quinoid structure of these monomers will be formed extremely slow, so slow that it is impossible to detect. This will cause the momentary concentration of quinoid compounds to be very low and dimerisation of two quinoid compounds is unlikely to occur to self-initiate a radical chain polymerisation. The precursor polymers formed are expected to be formed by an anion polymerisation process as is also indicated by the low molecular weights.

In order to ease quinoid formation and thus enhance the polymerisation process several options are at hand within the borders of the sulphinyl precursor route. First, as was shown by UV-Vis measurements, the quinoid formation of the plain sulphinyl PPV monomer may be enhanced by applying a better leaving group on the monomer stage.[21] In order to test this feature monomers **20** and **21** were prepared and polymerised in the same "standard" conditions. When comparing the molecular weight of the precursor polymers obtained for the polymerisations in CH_2Cl_2 a clear trend is noticed. When the leaving group capabilities are enhanced (in the series chlorine, bromine to iodine) both the molecular weight and the polymerisation yield increase significantly. For the polymerisation of monomer **21** in CH_2Cl_2 the polymerisation yield as well as the molecular weight of the precursor polymers almost doubled compared to the results obtained for the polymerisation of monomer **19** in identical conditions. This result again shows the versatility of the sulphinyl precursor route. The combined ^{1}H- and ^{13}C-NMR spectroscopic data of the precursor polymer confirm its

low molecular weight as the sulphinyl end groups can clearly be observed besides the sulphinyl groups in the internal part of the polymer chain.

Another path that was explored in order to obtain precursor polymers with higher molecular weight was the polymerisation of two complexed monomers. The 2,2'-bipyridine unit allows complexation with a large number of metal ions.[24] Based on the fact that the metal ion pulls the electrons away from the 2,2'-bipyridine unit thus lowering the aromaticity of the system we expect an easier quinoid formation for the complexed monomers. If this holds true, polymers with higher molecular weight should be accessible by polymerisation of the complexed monomers. The complexed monomer **22** (Scheme 5) was synthesised by mixing monomer **19** with $ZnCl_2$ in methanol at room temperature. The complex is isolated as its PF_6 salt, this to improve the solubility in organic solvents. According to literature data this complex coordinates three monomer units **19** around one Zn^{2+} ion.[15] (Scheme 9) Complex formation was confirmed by ^{1}H-NMR spectroscopy and by UV-Vis measurements in solution. Complexation leads to a ^{1}H-NMR spectrum which shows little differences from the original monomer spectrum, except the aromatic region has become more defuse. The absorption maximum (308 nm) in the UV-Vis spectrum of the Zn^{2+} complexed monomer **22** has red shifted compared to the maximum of the non-complexed monomer **9** (295 nm). Coordinating the monomer units around one Zn^{2+} ion apparently lowers the dihedral angle between the two pyridine planes thus improving the conjugation which results in a small red shift.[24] (Figure 14)

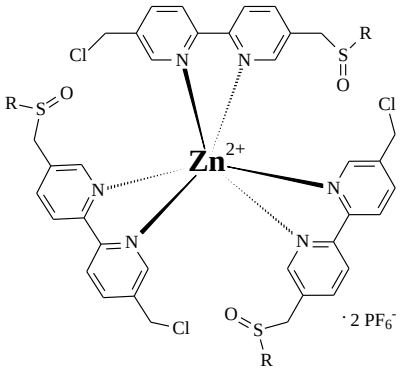

22

*Scheme 9: Chemical structure of monomer **22**.*

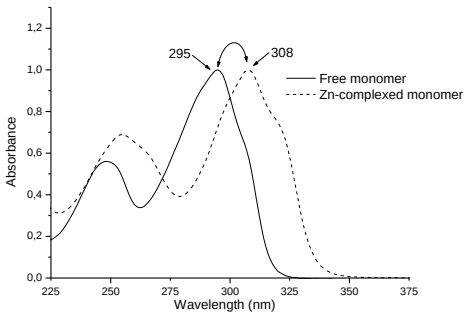

*Figure 14: UV-Vis spectrum of monomer **19** (solid line) and of the Zn-complexed monomer **22** (dashed line).*

An important requirement of this complex is its stability towards basic conditions since the polymerisation is performed in strong basic conditions. To test this, the absorption spectrum of the complexed monomer **22** was studied in basic conditions. Upon addition of a basic solution (Na*t*BuO) the absorption maximum of the complexed monomer **13** (308 nm) immediately shifted back to that of the non-complexed monomer (295 nm). Apparently, this complex is not stable in these basic conditions and spontaneously decomposes again to the free monomer units. This phenomenon is clearly visualised with UV-Vis spectroscopy. (Figure 14)

The ruthenium complexed monomer **23** (Scheme 10) was prepared by refluxing monomer **19** in ethanol with *cis*-Ru-$(bpy)_2Cl_2 \cdot 2H_2O$ for 24 hours. Precipitation in an aqueous PF_6 solution yielded monomer **23** as an orange salt. In this complex, only one monomer unit **19** is coordinated around the ruthenium ion next to two 2,2'-bipyridine ligands. This compound is orange on account of its MLCT (Metal to Ligand Charge Transfer) band in the absorption spectrum. Compounds which belong to the family of the diimines (2,2'-bipyridine, phenantroline, …) are commonly involved in MLCT transitions. Such transfer of charge from metal to ligand is observed in complexes with ligands that have π^* orbitals with low energy, especially aromatic ligands. If the metal has a low oxidation number, in which case its *d*-orbitals will be relatively high in energy, the transition will occur at low energy. The UV-Vis spectrum of monomer **23** shows several absorption maxima. (Figure

15) The maximum at 451 nm arises from the MLCT absorption. For comparison, also the spectra of the non-complexed monomer **19** as well as the *cis*-$Ru(bpy)_2Cl_2 \cdot 2H_2O$ are also shown. (Figure 15). For the latter compound, the absorption at 550 nm also corresponds to the MLCT transition. The absorption at 451 nm for the ruthenium-complexed monomer **23** is a very characteristic absorption that proves complexation.

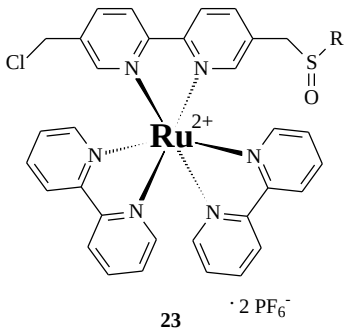

23

*Scheme 10: Chemical structure of monomer **23**.*

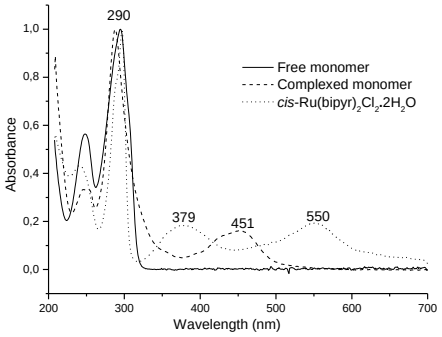

*Figure 15: UV-Vis spectrum of monomer **19** (dashed line), cis-Ru-$(bpy)_2Cl_2 \cdot 2H_2O$ (dotted line) and the Ru-complexed monomer **23** (solid line).*

The stability of the ruthenium-complexed monomer **23** towards basic conditions was also determined by UV-Vis measurements. Upon addition of a Na*t*BuO solution the absorption spectrum of the monomer **23** did not change, meaning that the complex does not dissociates in these conditions required to perform a polymerisation reaction.

Polymerisation of the complexed monomers **22** and **23** was performed in CH_2Cl_2 according to the "standard" method. Molecular weights and polydispersities were determined with GPC relative to PS standards. DMF was used as eluent. (Table 4)

Monomer	Solvent	Temp (°C)	M_w	PD	Yield (%)
22	CH_2Cl_2	30	5700	1.16	47
23	CH_2Cl_2	30	5900	1.06	63
23	CH_3CN	30	5800	1.08	89

*Table 4: Polymerisation results for the Zn(II) and Ru(II) complexed monomers **22** and **23**.*

In general the results shown in Table 4 do not differ a lot from those obtained during the polymerisation of the non-complexed monomers (Table 3). No high molecular weight polymers are formed. The molecular weight of these precursor polymers is similar to those mentioned earlier. The only thing that differs are the increased polymerisation yields which may indicate a more efficient quinoid formation.

In conclusion we can state that the molecular weight of the sulphinyl 2,2'-bipyridine precursor polymers can be increased substantially by improving the leaving group on the monomer stage. Simultaneously the polymerisation yield also increases. Complexation of the 2,2'-bipyridine unit prior to polymerisation did not lead to polymers with higher molecular weight although an increase of the polymerisation yield could be observed.

3.2.3 Thermal conversion to the conjugated structure

The thermal conversion to the conjugated structure as well as its stability was determined using techniques such as *in situ* FT-IR, *in situ* UV-Vis and DIP-MS. The thermal behaviour proved to be identical for all precursor polymers mentioned, so for simplicity reasons, only the graphs and data for the precursor polymer prepared from monomer **19** in CH_2Cl_2 will be shown.

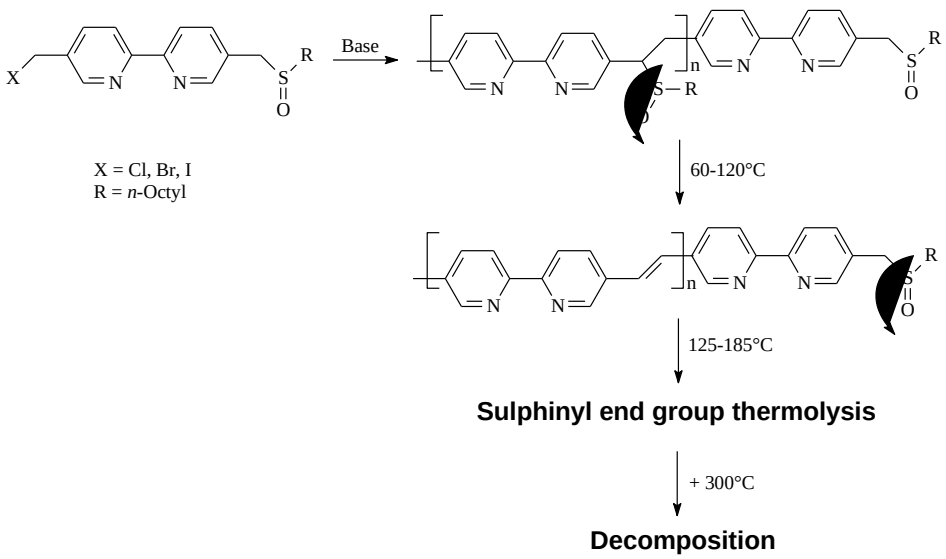

Scheme 11: Polymerisation, elimination, end group thermolysis and decomposition.

The first technique used to study the thermal stability with was DIP-MS, to allow the analysis of the elimination products. Three signals proved to be present in the thermogram. (Figure 16) The first signal (between 90 and 150°C) can be assigned to the elimination of the sulphinyl groups in the internal part of the oligomer chain. The fragments analysed correspond to the expected thiosulphonate and disulphide elimination products. (Table 5) The NMR spectroscopic data of the precursor polymers already proved that different sulphinyl groups exist in this low molecular weight precursor polymer. On the one hand there are the sulphinyl groups in the internal part of the oligomer chain that give rise to a double bond upon elimination. On the other hand, the sulphinyl groups at the end of the oligomer chain do not give rise to a double bond when thermally split off. The second signal in the DIP-MS thermogram (between 220 and 270°C), yields similar fragments as detected in the first signal which points to the evaporation of some sulphur containing compounds. Most likely, this signal corresponds to the thermolysis of the sulphinyl end groups. This measurement clearly shows the difference in temperature needed to bring about thermal elimination of the main chain sulphinyl groups and thermolysis of the sulphinyl end groups. Although similar fragments are observed, both processes must chemically proceed in totally different ways and a kinetic separation is present between them. Thermolysis of these benzylic sulphinyl end groups can occur at this low temperature because the C-S bond in these compounds is notable weak.[25] Furthermore, homolytic cleavage of this bond is further enhanced by the high stability of the radicals formed upon cleavage.[26] A similar phenomenon was also observed in the thermal elimination behaviour of other very low molecular weight sulphinyl precursor polymers. (Chapter 5) The exact nature of this phenomenon as well as a more in-depth explanation will be presented in Chapter 5. The third signal in the thermogram (between 400 and 500°C) accounts for the decomposition of the conjugated system.

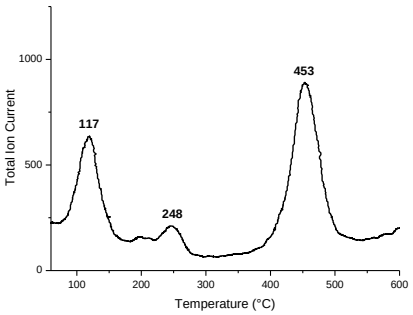

Figure 16: DIP-MS thermogram.

DIP-MS (117°C)		DIP-MS (248°C)	
Fragment	**m/z**	**Fragment**	**m/z**
$C_8H_{17}SSC_8H_{17}$	290	$C_8H_{17}S(O)_2SC_8H_{17}$	322
$SS(O)C_8H_{17}$	194	$HO_2SC8H17$	178
$S(O)C_8H_{17}$	161	SC_8H_{17}	145
SC_8H_{17}	145		

Table 5: Mass fragments of the elimination products.

In-situ FT-IR measurements were conducted on films of spincoated precursor polymer on KBr disks. A dynamic heating program of 2°C/min was used and all measurements were carried out under a continuous flow of nitrogen. Several absorption signals can be observed in the IR spectrum. The most distinct absorption bands at 1046 and 1026 cm^{-1} arise from the sulphoxide stretching. When the elimination progresses this signal decreases in intensity and the signal at 954 cm^{-1}, which represents the vinylene double bond, increases in intensity. (Figure 17) When the absorbance of these most important bands is plotted versus temperature the relative trends in elimination behaviour become clear. The sulphinyl groups (1046 and 1026 cm^{-1}) are eliminated to yield the double bonds (954 cm^{-1}). (Figure 18)

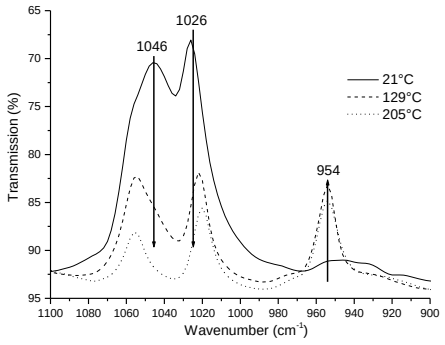

Figure 17: IR spectra at a few selected temperatures.

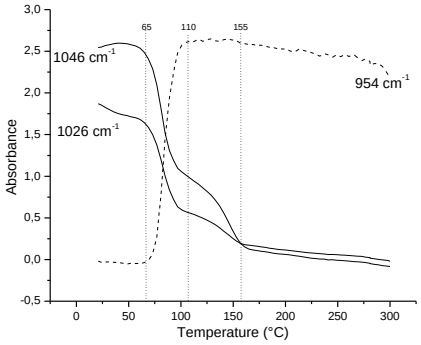

Figure 18: Absorbance at 1044 and 954 cm^{-1} versus temperature.

The sulphinyl groups start to eliminate at approximately 65°C at which temperature the first vinylene double bonds also start to form. At 110°C the vinylene absorption is maximal and during the further heat-up this signals remains constant which suggests the double bond is thermally stable till at least 300°C as no decline in absorption is noticed before this temperature. Moreover, from Figure 18 it becomes clear that the sulphinyl elimination is a two step process, this absorption decreases in two distinct steps. The first decrease (between 65 and 110°C) corresponds to the elimination of the sulphinyl groups in the internal part of the polymer chain which give rise to double bonds. At 110°C this elimination has finished as can be concluded from the vinylene absorption (954 cm^{-1}) which, at this temperature, has reached its maximal value. The second step in the sulphinyl decline (between 110 and 155°C) does not give rise to additional double bonds and must correspond to the thermolysis of the sulphinyl groups at the end of each polymer chain. Also with this technique the kinetic separation between the elimination and thermolysis of the different sulphinyl groups becomes clear. This different thermal behaviour of the two types of sulphinyl groups can only be noticed in rather low molecular weight sulphinyl precursor polymers. In high molecular weight polymers the thermal behaviour of the end groups will largely go unnoticed because of the low abundance of this group in the complete polymer chain. A similar phenomenon is also observed in the thermal behaviour of other sulphinyl oligomers and a full explanation of the issue will be handled there. (Chapter 5)

In situ UV-Vis experiments were performed on films of spincoated precursor polymer using an experimental set-up which was identical to the one used in the *in situ* FT-IR measurements. Before heating two absorption bands (253 and 301 nm) which originate from the precursor polymer are present. As the elimination progresses, a new absorption band gradually forms which reaches it maximal absorption at 385 nm when the conversion to the conjugated structure is maximal. The fully conjugated poly(2,2'-bipyridylene vinylene) has an absorption maximum at 385 nm. (Figure 19)

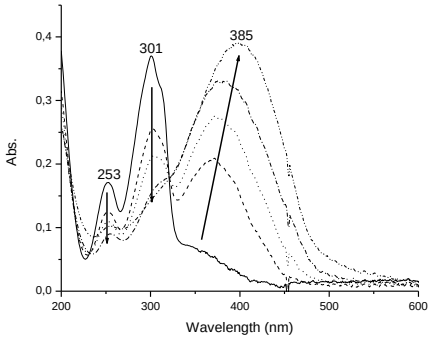

Figure 17: UV-Vis measurement showing the gradual formation of the conjugated structure.

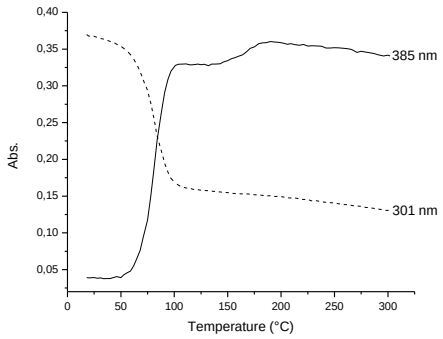

Figure 20: Absorbance at 301 and 385 nm versus temperature.

When the absorption at this maximum wavelength (385 nm) is plotted versus temperature, the trends in elimination behaviour again become clear. (Figure 20) The information obtained from this technique also suggests that the formation of the complete conjugated system is a two step process. The major part of the conjugated system is formed between 60 and 120°C. When the temperature has reached 130°C a conjugated polymer with an absorption maximum at 380 nm is already obtained. At higher temperatures (150-190°C) a second, small increase in maximum absorption wavelength is observed. This second increase coincides with a small red shift of the maximum absorption wavelength to 385 nm. (Figure 20) As will be explained later (Chapter 5) this second increase in "effective conjugation length" is caused by coupling of two polymer chains, probably in the temperature domain between 110 and 155°C, followed by consecutive oxidation above 150°C to yield an additional double bond which causes a red shift. The exact mechanism of these observations is clarified in Chapter 5 where the thermal behaviour of very low molecular weight sulphinyl precursor polymers is discussed more into detail. Extrapolation of these results will lead to an identical mechanism during the thermal elimination of the 2,2'-bipyridine sulphinyl precursor polymers.

The thermal behaviour of the metal complexed precursor polymers was also studied with *in situ* IR- and *in situ* UV-Vis spectroscopy. The precursor polymers prepared from the zinc-complexed monomer **22** show an identical thermal behaviour as the precursor polymers prepared from the non-complexed monomers. This was expected as the complexed

monomer **22** decomposes in the basic conditions used during the polymerisation reaction. In this aspect the precursor polymers prepared in this way do not differ from the ones prepared by polymerising the non-complexed monomers.

IR- and UV-Vis measurements on the ruthenium-complexed precursor polymers proved impossible since this precursor polymer shows very bad film forming properties and moreover, the dark colour of the "film" inhibits light to pass through it. These ruthenium-complexed precursor polymers could not be further characterised.

3.3 Poly(2,5-thienylene vinylene)

A third and last heterocyclic PPV derivative that will be discussed in this chapter is the poly(2,5-thienylene vinylene) or PTV. (Scheme 12) In contrast to the polymers discussed earlier in this chapter, the incorporation of the thiophene unit makes this polymer electron rich.

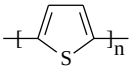

Poly(thiophene) (**PT**)

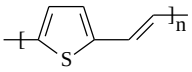

Poly(thienylenvinylene) (**PTV**)

Scheme 12: Chemical structures for PT and PTV.

Compared to poly(thiophene) (PT), the extra vinylene double bond in PTV further reduces the band gap (by about 0,4 eV) and makes a precursor synthesis accessible. Synthesis and characterisation of PTV and some alkyl-substituted PTVs has been reported by Elsenbuamer *et al.*[27] a long time ago, even before the discovery of the luminescent properties of PPV. Even at that time, the interesting properties of this material, arising from the low HOMO-LUMO energy gap were known. This allowed the synthesis of a so called "low band gap" polymer which proved useful in photovoltaic devices and plastic transistors. In the early days, PTV synthesis proceeded via the Wessling polymerisation method. However, for PTV, this synthetic method is far from ideal. Apart from the known drawbacks of the Wessling precursor route (Chapter 1) the relative high reactivity of this derivative seriously complicated both monomer and polymer synthesis. This high reactivity originates from the high electron density in the thiophene ring. In this aspect, PTV is a completely different materials than the other electron accepting polymers mentioned earlier in this chapter.

3.3.1 Monomer synthesis

A pivotal role in this monomer synthesis is played by the dichloride **4**. For this reason much effort was put into finding the most efficient synthesis of this compound. (Scheme 13)

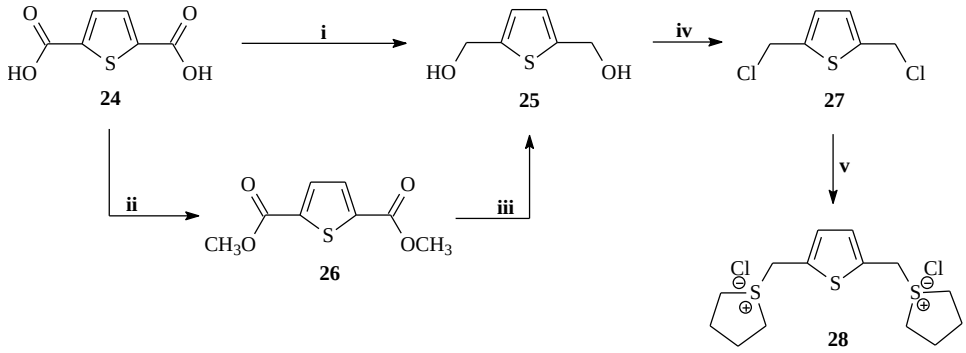

*Scheme 13: Synthesis of dichloride **4**. Reaction conditions: **i**: $LiAlH_4$ or BH_3:THF; **ii**: MeOH, H_2SO_4, ΔT; **iii**: $LiAlH_4$, THF; **iv**: $SOCl_2$, THF; **v**: THT, MeOH*

Initially the commercially available starting product, diacid **24**, was reduced to the diol **25** using $LiAlH_4$ in dry THF. The yield for this reaction was only moderate (63%). When this reduction was performed using BH_3:THF the diol **25** was obtained in comparable yield (56%). Note that in both cases a chromatographic purification was necessary to obtain the pure diol **25**. In order to attain higher yields and avoid an additional purification, diacid **24** was primarily converted to the diester **26** in nearly quantitative yield (97%). Subsequent reduction with $LiAlH_4$ in dry THF yielded pure diol (**25**) in high yield (91%). This reaction yielded the pure diol **25** without further purification. During this reduction a grey, sticky, concrete like substance was formed which became hard to mix. The formation of this substance could largely be suppressed by performing this reaction in very dilute conditions. Nonetheless, this two step synthetic sequence proved to be the most efficient way to synthesise diol **25**. Consecutive conversion to the dichloride **27** was accomplished in high yield (83%) using thionylchloride in THF. Compound **27** proved to be highly unstable when concentrated and spontaneously decomposed at room temperature to a black unknown solid. Probably, the chlorine atoms in this compound are such good leaving groups that isolation is very difficult without initiating degradation. Moreover, from the safety data sheet[28] it was clear that dichloride **27** is highly irritant and all contact should be avoided. An elegant way to circumvent isolation of dichloride **27** and avoid all direct contact is the *in situ* reaction to the less reactive bissulfonium salt **28**. This reaction was performed by mixing dichloride **27** in methanol with an excess of THT. Precipitation in CH_2Cl_2 yielded compound **28** which was more stable and could be stored in the freezer for longer periods of time without noticing degradation. (Scheme 13)

In the following sections, synthesis and polymerisation behaviour of three different thiophene based monomers (**A**, **B** and **C**) is discussed. (Scheme 14) Due to the high reactivity of several compounds certain chemical adaptations had to be made on the monomer stage in order to decrease the reactivity. The xanthate-group (-SC(S)OEt) proved very useful in this context.

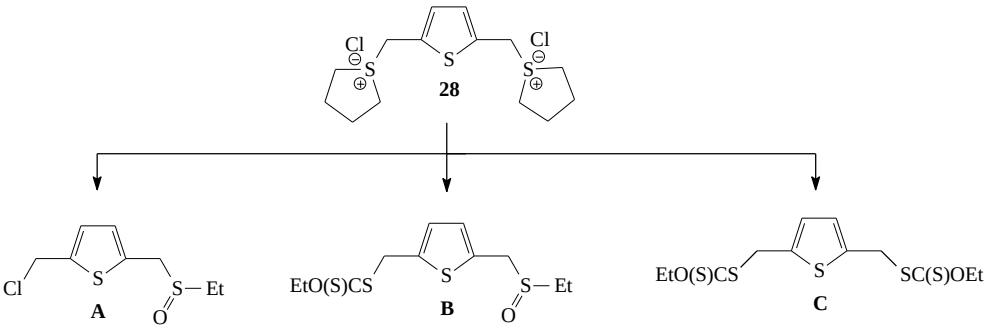

*Scheme 14: Chemical structures of the different monomers **A**, **B** and **C**.*

3.3.1.1 The chloro-sulphinyl monomer A

The first monomer synthesised was the classical asymmetrical chlorosulphinyl monomer **A**. An ethyl sulphinyl polarising group was used. This may be advantageous when eliminating the precursor polymer to the conjugated form. The boiling point of the elimination products formed during elimination will be sufficiently lower than those formed when eliminating an sulphinyl group with an octyl chain. This may reduce the temperatures needed to accomplish complete elimination and evaporation of all elimination products.

The synthesis of this monomer starts from the bissulfonium salt **28**. In the classical PPV monomer synthesis, such a bissulfonium salt is converted very selectively to the monosulphide in methanol.[20] This solvent could not be used in this synthesis because than solvent substitution predominantly occurred caused by the high reactivity of the chlorine atoms. The solvent in which this reaction was performed played a crucial role. When the reaction was performed in alcoholic solvents like methanol or *iso*-propanol only solvent substituted products (**29** and **30**) could be isolated. (Scheme 15)

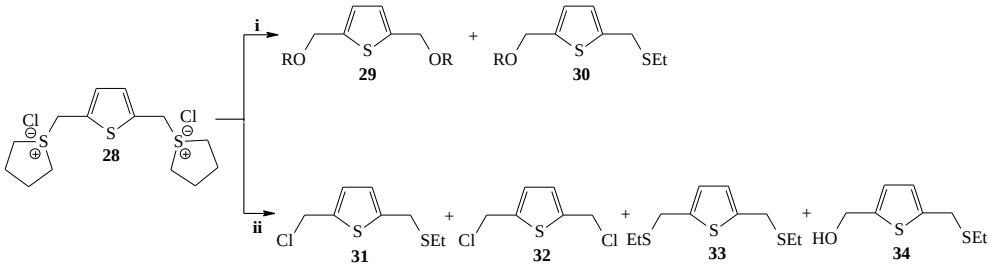

*Scheme 15: Product distribution when different solvents or solvent mixtures are used. Reaction conditions: **i**: ROH (R= Me or iso-prop), NatBuO, HSEt; **ii**: CH_3CN/H_2O, NatBuO, HSEt.*

Changing the solvent to acetonitril and water proved a successful way to avoid this side reaction and solvent substitution could largely be suppressed. The addition of water was necessary to keep the reagents soluble. Still, a mixture of different products (**31**-**34**) was obtained but by varying the amount of water the reaction could be tuned in such a way that the main product was the desired mono thioether **31**. As can be concluded from Table 6, a minimal amount of water is best applied in this reaction. Using 5 vol% of water resulted in a very selective formation of product **11**. When larger amounts of water were used the amount of undesired side products increased dramatically. The product distributions were calculated from ^{1}H-NMR measurements on the different crude reaction mixtures. (Table 6)

CH_3CN/H_2O (vol/vol)	**Product**	**31**	**32**	**33**	**34**
50/50		0	44	14	42
87/13		63	0	15	22
95/5		94	2	4	trace

Table 6: Product distribution when using different acetonitril:water ratios.

Compound **31** proved to be highly unstable when isolated and the consecutive oxidation to the sulphoxide (monomer **A**) was carried out *in situ* in order to minimise product degradation. Oxidation was impossible when using the classical H_2O_2/TeO_2 system in MeOH or 1,4-dioxane, in both cases hydroxy and/or methoxy solvent substitution mainly occurred which caused very low yields for the desired product. Using *m*-CPBA in dichloromethane resulted in overoxidation to the sulphon (**35**). When this oxidising system

was used it proved impossible to stop the reaction on the sulphoxide stage, even at lower temperatures. Selective oxidation to the sulphoxide (monomer **A**) was only possible when *t*-BuOOH in dichloromethane was used (5 mol% $Ti(OPr)_4$ as a catalyst).[29,30] (Scheme 16)

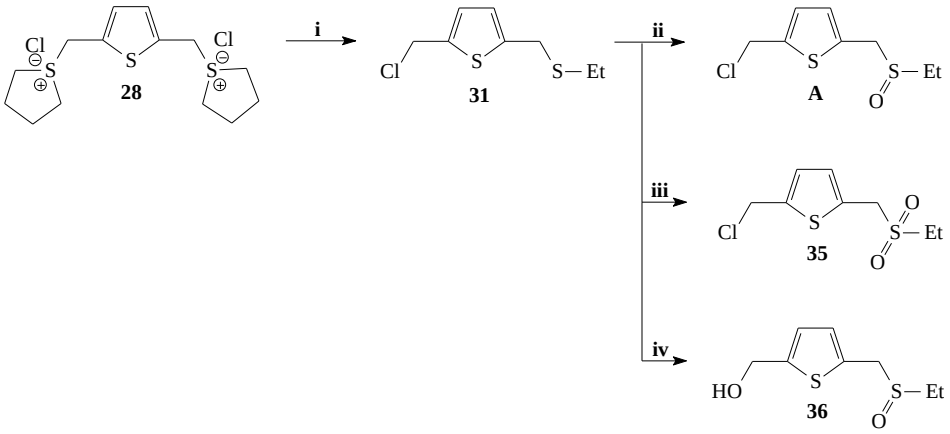

*Scheme 16: Selective synthesis of compound **31** followed by oxidation. Reaction conditions: **i**: CH_3CN/H_2O (5 vol%), NatBuO, HSEt; **ii**: t-BuOOH, CH_2Cl_2, $Ti(OPr)_4$; **iii**: m-CPBA, CH_2Cl_2; **iv**: H_2O_2/TeO_2, 1,4-dioxane.*

A lot of the problems we have come across in this synthesis arise from the high instability of the benzylic chlorine atoms. In this context it would be advantageous to alter the synthetic approach in such a way that the reactive benzylic chlorine atom is only introduced in the last step of the synthesis or is even replaced by another less reactive atom or group. In this way, monomer synthesis is simplified and the overall yield will increase since less degradation will occur.

A hydroxyl group is an example of a less reactive leaving group. In many of the reaction mentioned hydroxyl-substitution was an undesired side reaction. In this regard it should be possible to tune the reaction in such a way that mainly hydroxyl-substitution occurs. It proved possible to synthesise compound **36** in high selectivity by slightly altering the reaction conditions. If the synthesis of the mono thioether **34** was performed in pure water, only the desired product **34** together with a small amount of disubstituted products were obtained. Further selective oxidation to the sulphoxide **36** was accomplished using the H_2O_2/TeO_2 oxidising system in 1,4-dioxane. (Scheme 17) In this way compound **36** was accessible in high selectivity and degradation of the reaction products was restrained.

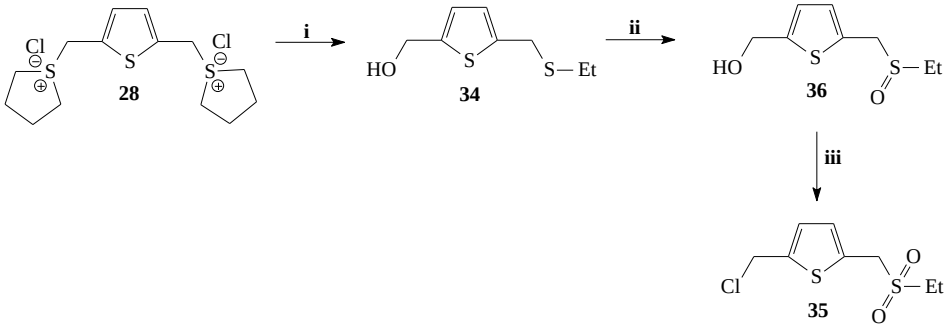

*Scheme 17: Selective synthesis of compound **36** and conversion to the sulphon **35**. Reaction conditions: **i**: H_2O, HSEt, NatBuO; **ii**: H_2O_2/TeO_2, 1,4-dioxane; **iii**: $SOCl_2$, THF.*

The final step in this synthesis towards monomer **A** is the substitution of the hydroxyl group in compound **36** by a chlorine atom. This replacement is necessary because the chlorine atom functions as a leaving group in the polymerisation process, the hydroxyl group is not suited for this purpose. Numerous reactions can be applied to convert a hydroxyl group to a chlorine atom.[31] However, we should keep in mind that this reaction should be performed in very mild reaction conditions. Basic conditions have to be avoided since then spontaneous polymerisation occurs. Furthermore, due to the high reactivity of the chlorine atom, nucleophilic solvents should be excluded in order to prevent solvent substitution and strong acid conditions will cause degradation. So in the end, only a small number of reactions are at hand to accomplish this conversion. Converting the hydroxyl group to a chlorine atom proved possible using $SOCl_2$ in THF in very dilute conditions but unfortunately simultaneous overoxidation to the sulphon occurred and only the undesired compound **35** resulted. (Scheme 17) Apparently it is difficult to convert the hydroxyl group to a suitable leaving group in conditions that are compatible with the sulphinyl group. Because of this drawback we opted for a different approach.

3.3.1.2 The xanthate-sulphinyl monomer B

A different way of reducing the reactivity is the conversion of the reactive benzylic chlorine atom in compound **31** to a xanthate group (-SC(S)OEt). The xanthate group is a less reactive leaving group and is easy to introduce. Introduction of the xanhate group immediately after the selective formation of thioether **31** yields the stable compound **37** in excellent yield. Subsequent oxidation to the xanthate-sulphinyl monomer **B** was possible

using the H_2O_2/TeO_2 oxidising system in methanol. No overoxidation to the sulphon or methoxy substitution occurred during this reaction. (Scheme 18)

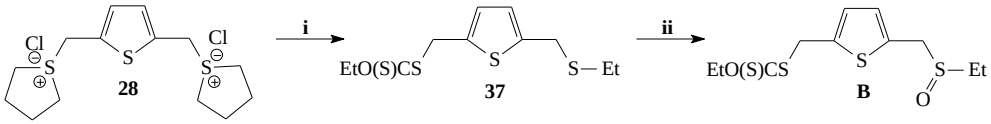

*Scheme 18: Synthesis of the xanthate-sulphinyl monomer **7**. Reaction conditions: **i**: 1) CH_3CN/H_2O (5 vol%), NatBuO, HSEt, 2) KSC(S)OEt; **ii**: H_2O_2/TeO_2, MeOH.*

3.3.1.3 The bisxanthate monomer C

A last monomer that was synthesised in this series was the bisxanthate monomer **C**. Undoubtedly the synthesis of this monomer was the simplest and monomer **C** could be synthesised in a high yield, single step reaction from bissulfonium salt **28**. (Scheme 19) Monomer **C** is crystalline and proved stable at room temperature.

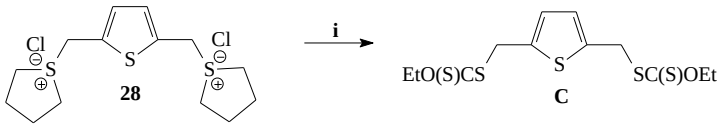

*Scheme 19: Synthesis of the bisxanthate monomer **C**. Reaction conditions: **i**: CH_3CN/H_2O (5 vol%), KSC(S)OEt.*

3.3.2 Precursor polymer synthesis and conversion to the conjugated structure

3.3.2.1 Precursor polymer synthesis

The different monomers (**A, B** and **C**) were polymerised in various conditions. Polymerisation of monomers **A** and **B** gave sulphinyl precursor polymers (**38**) while polymerisation of the bis-xanthate monomer **C** resulted in a xanthate precursor polymer (**39**). (Scheme 20) The thermal conversion to the conjugated structure as well as its stability were studied with different techniques such as *in situ* FT-IR, *in situ* UV-Vis and DIP-MS.

As will be mentioned further on, the elimination behaviour of both types of precursor polymers is quite different.

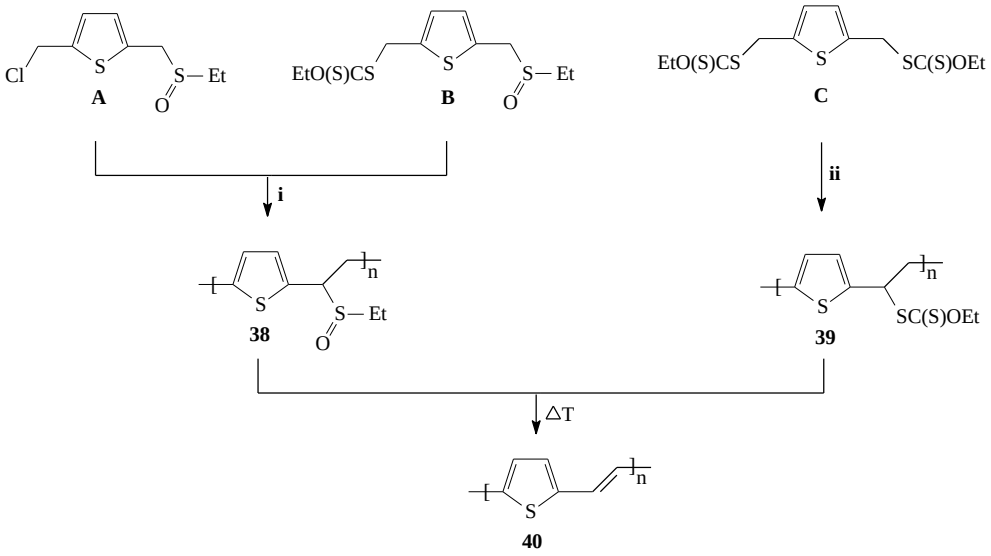

*Scheme 20: Schematic overview of the different polymers formed. Reaction conditions: **i**: NatBuO, various solvents; **ii**: LDA, THF.*

The polymerisation of monomer **A** as well as the thermal stability of the precursor polymers obtained is discussed elsewhere.[32]

Monomer **B** was polymerised under various conditions in different solvents or solvent mixtures. Solvents tested include 2-BuOH, CH_2Cl_2 and THF. Na*t*BuO was always used as a base. In neither of these solvents high molecular weight polymers were obtained in good yields. The precursor polymers were analysed with GPC versus PS standards, THF was used as eluent. Although the monomer had been consumed completely for the polymerisation in 2-BuOH, as was shown by ^{1}H-NMR measurements on the restfraction, both the molecular weight of the precursor polymer and the yield it was formed in were extremely low. When the polymerisation was performed in THF a very small fraction of high molecular weight precursor polymer was obtained in a yield of less than 10 percent. This result proved difficult to reproduce and both polymerisation yield and molecular weight fluctuated strongly. For this polymerisation the restfraction consisted purely of unreacted monomer. The same result was obtained when CH_2Cl_2 was used as a solvent.

UV-Vis measurements on monomer **B** in 2-BuOH showed the actual monomer in the polymerisation process - the quinoid structure (340 nm) - was actually formed (Figure 21) but for some reason polymerisation towards high molecular weight polymers was impossible. The absorption at 303 nm corresponds to the solvent substituted product (**41**) as was proven by mass spectroscopy. (Scheme 21) At 290 nm a clear isosbestic point is observed.

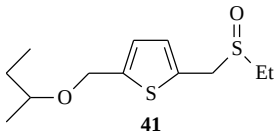

41

*Scheme 21: Chemical structure of the solvent substituted monomer **41**.*

As the absorbance at the most important absorption signals is plotted versus time the trends in the processes that occur become clear. (Figure 22) The absorbencies at 340 and 303 nm gradually increase while those at 277 and 255 nm decrease. The absorbance at the isosbestic point remains constant. Compared to other sulphinyl monomers (Chapter 2) the quinoid formation for this monomer is rather slow. Furthermore, the intensity of the signal at 303 nm increases at a faster rate compared to that of the quinoid formation at 340 nm. This indicates that the quinoid structures are consumed more rapidly than they are formed by the co-occurring and undesired solvent substitution. This difference in reactivity between the actual quinoid formation and its reacting away may lay at the basis of the poor polymerisation capabilities of this monomer in 2-BuOH. Note that a similar observation was made for the polymerisation of the phenylene analogue of this monomer, in this case also oligomer precursor fragments were obtained. The source for this behaviour is discussed in Chapter 5. Because of the requirement for high molecular weight polymers that should be accessible in good yields,[32] and the failure of this monomer **B** on the polymerisation stage, another monomer was synthesised and polymerised (Monomer **C**).

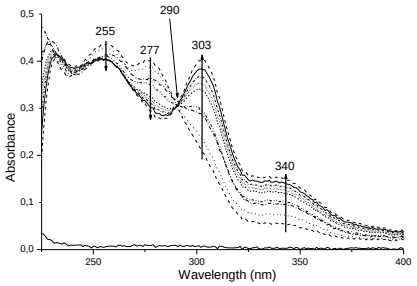

Figure 21: UV-Vis spectrum demonstrating quinoid formation.

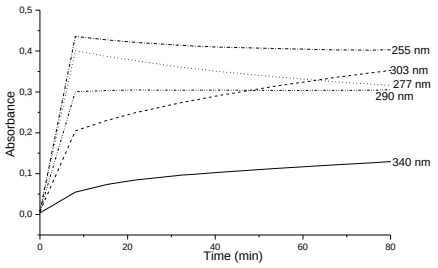

Figure 22: Absorbance plotted versus time for the most important absorptions.

The conditions that allow polymerisation of the bis-xanthate monomer **C** (the xanthate precursor route) are more strict than those needed in the sulphinyl precursor route. As can be concluded from literature data as well as from our own experience (Chapter 5) bis-xanthate monomers can only be polymerised in dried solvents (THF) at sufficiently low temperatures (mostly 0°C).[33,34] The precursor polymers were analysed by GPC measurements versus PS standards and THF was used as eluent. When the polymerisation was performed at 0°C with KO*t*Bu as the base precursor polymer was obtained in relatively low yield (18 %). The molecular weight of this precursor polymer is rather low and similar to that obtained in an identical polymerisation where LDA is used as the base. When LDA is used as a base in a polymerisation at 0°C, the polymerisation yield increased significantly compared to the polymerisation where KO*t*Bu was used. This increase is caused by the limited solubility of KO*t*Bu in THF, certainly at 0°C. Consequently, the polymerisation reactions at even lower temperatures were all performed with LDA as a base. When the base (LDA) was added at –78°C and the polymerisation mixture was allowed to gradually warm to 0°C (over a period of 2 hours) the molecular weight of the precursor polymers could be increased dramatically. The highest molecular weight was obtained when freshly prepared LDA was used. (Table 7) The yield for this polymerisation peaked when commercial LDA was used. All the precursor polymers synthesised proved to have very broad molecular weight distributions as can be concluded for the high PD values.

Base	Temperature (°C)	Yield	M_w x 10^{-3}	M_n	PD
KO*t*Bu	0	18	21.9	2300	9.4
LDA	0	47	24.6	2800	8.7
LDA	-78 → 0	47	78	4500	17.5
LDA*	-78 → 0	33	186	7800	23.8

*Table 7: Polymerisation results for monomer **C**. GPC was performed versus PS standards with THF being the eluent. *: Home made LDA.*

3.3.2.2 Thermal conversion to the conjugated structure

Like in the sulphinyl precursor route, the final step in the xanthate precursor route is a thermal elimination towards the conjugated polymer. This conversion as well as the stability of the conjugated polymer was studied with several techniques. *In situ* UV-Vis and *in situ* FT-IR measurements were performed in identical conditions in an oven that was especially designed to fit in both the UV and IR spectrometer. A dynamic heating rate of 2°C/min up to 300°C under a continuous flow of nitrogen was used. DIP-MS measurements were performed at a heating rate of 10°C/min in order to get a good idea of the elimination products that are liberated during the elimination process.

In Figure 23 the gradual formation of the conjugated structure as obtained from an *in situ* UV-Vis measurement is depicted. Before heating, the precursor polymer **20** shows a maximum absorption at 286 nm. When the heating program advances, a new absorption band is formed which progressively red shifts with increasing temperature. In the end, the fully conjugated polymer is obtained. The absorption peaks at 493 nm. PTV absorbs in nearly the complete visible spectrum which explains its black colour. Compared to PPV this conjugated polymer absorbs in a much broader wavelength domain. (Figure 23)

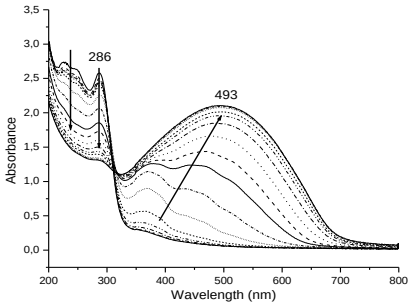

Figure 23: UV-Vis spectrum of the gradual formation of the conjugated system in PTV.

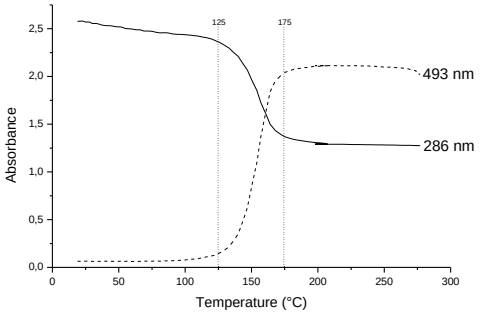

Figure 24: Absorbance at 286 and 493 nm versus temperature.

When the absorption at these two significant wavelengths (286 and 493 nm) is plotted versus temperature the relative trends in elimination behaviour become clear. (Figure 24) This measurement indicates that formation of the first conjugated segments commences at about 125°C and that the elimination process is complete at about 175°C. The fully conjugated PTV structure is thermally stable till at least 300°C since no decline in absorbance at 493 nm is noticed before this temperature.

A second technique that was applied to study the elimination was *in situ* FT-IR. In the precursor polymer **20**, most of the IR absorptions arise from stretchings within the xanthate group, i.e. the strong absorption bands at 1218 cm^{-1} and 1048 cm^{-1} both arise from the *O*-ethyl xanthate leaving group.[35] When the heating program progresses, these xanthate strechings decline in intensity as the xanthate group is eliminated. Simultaneously, a new absorption band appears at 928 cm^{-1} which is assigned to the *trans* vinylene double bond stretching. The IR spectra at a few selected temperatures are shown in Figure 25. When the most important absorptions (1218, 1046 and 928 cm^{-1}) are plotted versus temperature, the relative trends in elimination behaviour again become clear. (Figure 26) The xanthate group is thermally eliminated in the temperature domain between 125 and 150°C. Simultaneously the vinylene absorption at 928 cm^{-1} increases in intensity.

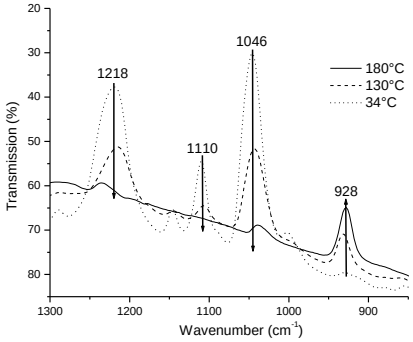

Figure 25: IR spectra at 34, 130 and 180°C.

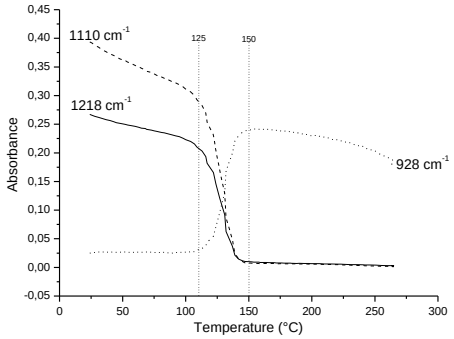

Figure 26: IR absorptions at 1218, 1046 and 928 cm^{-1} versus temperature.

A last technique used to study the thermal elimination and stability behaviour with was DIP-MS. In this way information about the elimination and degradation products is obtained. In this technique the precursor polymer is heated from ambient temperatures till 650°C under reduced pressure. The elimination products correspond well to the expected xanthate elimination products.[33,34] (Table 8) When the total ion current is plotted versus temperature, the thermal stability of both precursor and conjugated polymer can be visualised. (Figure 27) Two signals were observed, the first one (170-240°C), based on the fragments detected (Table 8), can be assigned to the elimination of the xanthate groups. The second one (350-450°C) is caused by the degradation of the conjugated polymer. The higher elimination temperature observed with this technique is probably caused by the differences in heating rate. Here a heating rate of 10°C/min is used while in the UV-Vis and IR measurements a slower heating rate of 2°C/min is used. As proven earlier the heating rate influences the observed elimination temperatures.[36]

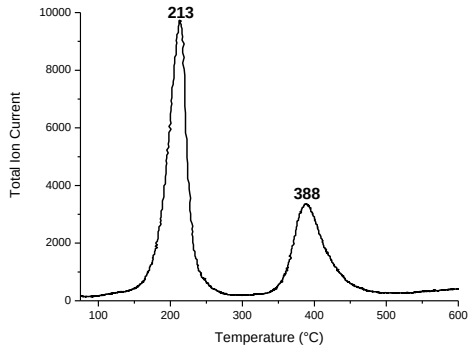

*Figure 27: DIP-MS thermogram of xanthate precursor polymer **39**.*

DIP-MS	
Fragment	**m/z**
EtO(S)CS	121
EtO(S)C	89
CS_2	76

Table 8: Mass fragments of the xanthate elimination products.

From these different measurements we conclude that the elimination of this xanthate precursor polymer can be performed starting from a temperature of 130°C. Furthermore the elimination reaction is a fast process and the fully conjugated structure is stable till at least 300°C.

3.3.3 Transistor behaviour of PTV

The transistor behaviour of PTV prepared via the xanthate precursor route was studied. The measurements were performed on a ring transistor (L= 10 μm; W= 2500 μm) under *vacuum* in dark. The precursor polymer samples used were converted to the conjugated form by heating in *vacuum* at 185°C for 40 minutes (including heating up). After conversion the samples were cooled to 25°C. The results are summarised in Table 9.

Mw (x 10^{-3})	186	78	24.6
Mobility (cm^2/Vs)	1.5 - 1.6 x 10^{-3}	2.4 x 10^{-4}	8.4 x 10^{-6}
Modulation	58000 - 240000	3680	492
Threshold Voltage (V)	-3.9 - -3.4	-6.7	-7.5

Table 9: Results for the transistor behaviour of PTV prepared via the xanthate precursor route.

From Table 9 it appears that the characteristics of the PTV samples are strongly related with the molecular weight of the polymer. Mobility , modulation and threshold voltage all

increase significantly when the molecular weight increases. The reason for this phenomenon is unclear and further experiments have to be carried out to reveal the exact relationship. The mobility for the highest molecular weight sample is very high. For comparison, the highest mobility measured for PTV prepared via the sulphinyl precursor route is 2.5 x 10^{-3} cm^2/Vs.[32] The relationship between the molecular weight and the mobility is shown in Figure 28.

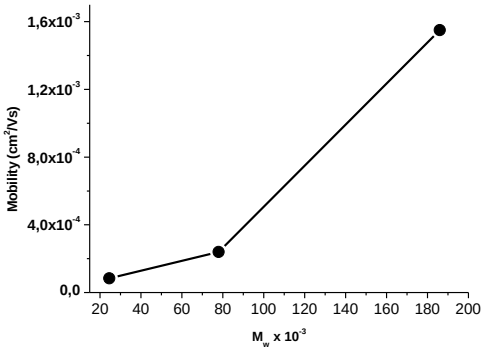

Figure 28: Mobility versus molecular weight.

Furthermore, life time measurements showed that the PTV prepared via the xanthate precursor route proved much more stable than compared to PTV prepared via the sulphinyl precursor route. This can probably be explained by the intrinsic nature of the elimination products. CS_2 and EtOH are liberated when eliminating a xanthate precursor polymer **39**. These products have low boiling points and evaporate fast in the given elimination conditions whereas the sulfenic acids, thiosulfonates and disulfides that are liberated upon elimination of a sulphinyl precursor polymers **38** have higher boiling points and for sure stay in the film for some percentage. The presence of these products may reduce the stability. Burn *et al.* already reported on the differences in lifetime of LEDs that use PPV prepared via different precursor routes.[33b] As it turns out, PPV prepared via the xanthate precursor route shows the highest stability due to the absence of harmful elimination products. This undoubtedly shows the importance of a controlled and complete elimination reaction when precursor polymers are used. For a more systematic and in dept study of the elimination process of precursor polymers we refer to the dissertation of Els Kesters.[36]

3.4 Experimental Section

Materials. All chemicals were purchased from Aldrich or Acros and used without further purification unless otherwise stated. Tetrahydrofuran (THF) and 1,4-dioxane were always distilled over sodium/benzophenone prior to use.

Characterisation. NMR spectra were recorded, mostly in $CDCl_3$, on a Varian VXR300 spectrometer. Chemical shifts (δ) are given in ppm relative to the residual $CHCl_3$ absorption (7.24 ppm). The ^{13}C-NMR experiments were recorded at 100 MHz on the same spectrometer. Chemical shifts are determined relative to the ^{13}C resonance shift of $CHCl_3$ (77.0 ppm). Direct Insert Probe Mass Spectrometry (DIP-MS) analyses were carried out on a Finnigan TSQ 70, electron impact mode, mass range 35-550 and an interscan time of 2 s. The electron energy was 70 eV. Molecular weights and molecular weight distributions were determined relative to polystyrene standards (Polymer Labs) by Size Exclusion Chromatography (SEC). Chromatograms were recorded on a Spectra series P100 (Spectra Physics) equipped with two MIXED-B columns (10 μm, 2 x 30 cm, Polymer Labs) and a refractive index (RI) detector (Shodex) at 70 °C. A DMF solution of oxalic acid (1 mM) is used as the eluent at a flow rate of 1.0 ml/min. Toluene is used as flow rate marker.

Fourier transform-infrared spectroscopy (FT-IR) was performed on a Perkin Elmer Spectrum One FT-IR spectrometer (nominal resolution 4 cm^{-1}, summation of 16 scans). Samples for the FT-IR characterisation were prepared by spin-coating the precursor polymer from a chloroform solution (6 mg/ml) onto NaCl disks (diameter 25 mm and thickness 1 mm) at 500 rpm. The NaCl disks were heated in a Harrick oven high temperature cell (purchased from Safir), which was positioned in the beam of the FT-IR to allow *in situ* measurements. The temperature of the sample and the heating source were controlled by a Watlow temperature controller (serial number 999, dual channel). The heating source was in direct contact with the NaCl disk. Spectra were taken continuously and the heating rate was 2 °C/minute up to 450 °C. The atmosphere in the temperature cell could be varied from a continuous flow of nitrogen to vacuum (15 mmHg). Timebase software was used to investigate regions of interest.

Ultraviolet visible spectroscopy (UV-VIS) was performed on a CARY 500 UV-VIS-NIR spectrophotometer (interval: 1 nm, scan rate: 600 nm/min, continuous run from 200 to 700 nm). The precursor polymer was spin-coated from a chloroform solution (6 mg/ml) onto quartz glass (diameter 25 mm and thickness 3 mm) at 700 rpm. The quartz glass was heated in the same Harrick oven high temperature cell as was used in the FT-IR measurements. The cell was placed in the beam of the UV-Vis spectrophotometer and spectra were taken continuously. The heating rate was 2°C/minute up to 450°C. All measurements were performed under a continuous flow of nitrogen. Scanning kinetics software was used to investigate the regions of interest.

Thermogravimetric analysis measurements (TGA) were performed on a TA Instrument 951 Thermogravimetric Analyser with a continuous nitrogen flow of 120 ml/min and a heating rate of 10°C/min. The precursor polymer was inserted in the solid state (15 mg) and heated from ambient temperature to 600°C.

Direct insertion probe mass spectroscopy (DIP-MS) analysis of the precursor polymers was carried out on a Finnigan TSQ 70, in electron impact mode, mass range 35-650 and scan rate of 2 s. The electron energy was 70 eV. A chloroform solution of precursor polymer was placed on the heating element of the direct insertion probe. A heating rate of 10 °C/min was used to ensure a good comparison with TGA data.

The photoluminescence (PL) spectrum of a film of the precursor polymer (**6**), polymerised in 50/50 vol% 2-butanol/1,4-dioxane, spin-coated from chloroform (10 mg/mL) and converted to the conjugated form by heating at 100^{o}C in vacuum for 1 hour, was measured by exciting the polymer sample with monochromatic light from a tungsten lamp. The emission was measured with an Oriel Intraspec IV diode matrix spectrometer. An integrated sphere made by Labsphere was used to measure the PL efficiency.

Electrochemical measurements of the precursor polymer (**6**) polymerised in 50/50 vol% 2-butanol/1,4-dioxane, adsorbed on a Pt wire from a chloroform solution and converted to the conjugated form by heating at 100^{o}C in vacuum for 1 hour, was measured in a single compartment electrochemical cell with a Pt counter electrode and a Ag/AgCl quasi reference electrode. Tetrabutylammonium perchlorate, 0.1 M, in acetonitrile (dried over molecular 3Å sieves) was used as the supporting electrolyte. The cell was purged with nitrogen before each measurement. Ferrocene (half-wave potential 0.326 V vs. Ag/AgCl)

was used for calibration of the reference electrode.[8] The sweep rate was 100 mV/s unless otherwise indicated.

Synthesis of 2,5-bis(chloromethyl)pyridine (2). 2,5-lutidine (**1**) (25 g, 0.23 mol) was refluxed in carbon tetrachloride (1000 mL) with *N*-chlorosuccinimide (63.7 g, 0.48 mol) and fresh benzoyl peroxide (1.0 g, 4.1 mmol) for 16 hours. The solution was filtered to remove succinimide and unreacted *N*-chlorosuccinimide, washed with 10% sodium sulphite solution and water, and dried over magnesium sulphate. Thereafter, column chromatography with chloroform was used to separate the product from monochlorinated and trichlorinated compounds. After recrystallisation from *n*-hexane, 9.4 g (yield 23%) white crystals were obtained. ^{1}H-NMR ($CDCl_3$, 300MHz): δ (ppm) 8.55 (1H, d, J_m=2.4 Hz); 7.77 (1H, dd, J_m=2.4 Hz, J_o=7.8 Hz); 7.47 (1H, d, J_o=8.1 Hz); 4.65 (2H, s); 4.57 (2H, s).

Synthesis of 2,5-bis(tetrahydrothiopheniomethyl)pyridine dichloride (3). A solution of **2** (2 g, 11.5 mmol) and tertrahydrothiophene (3.97 ml, 45 mmol) in MeOH (40ml) was stirred for 3 days at room temperature. The reaction mixture was precipitated in CH_2Cl_2 (150 ml) at 0°C. The precipitate was collected and immediately placed in de freezer to ovoid degradation, 0.76 g (yield 19%) of a white hygroscopic solid was obtained.

Synthesis of isomers 4 and 5: Dichloride (**2**) (4 g, 23 mmol) dissolved in toluene (76 ml) was mixed with an aqueous solution of sodium hydroxide (4.56 g, 1.5 M) and a phase transfer reagent, Aliquat 336 (0.188 g, 6.12 mM). 1-Octanethiol (1.94 g, 13 mmol) dissolved in toluene (22 ml) was added dropwise to the mixture over 3 hours. The reaction was stirred for another 17 hours at room temperature. The phases were separated and the organic layer washed with water and dried over magnesium sulphate. After evaporation of the solvent, the crude product was dissolved in 1,4-dioxane (140 ml), and tellurium dioxide (0.53 g, 3.2 mmol) was added. Hydrogen peroxide solution (30 wt% in water, 8.61 ml) was added dropwise over 4 hours. Thereafter, a few drops of concentrated hydrochloric acid were added and the reaction was stirred for another 9 hours. The reaction was quenched by adding 100 ml of brine. The solution was extracted with chloroform and dried over magnesium sulphate. Column chromatography with hexane/ethyl acetate (volume ratio 6/4) was used to separate the product from unreacted dichloride. When all dichloride had been collected, pure ethyl acetate was used to elute the product. 3.2 g (46% yield calculated from dichloride **2**) pure monomer was obtained. ^{1}H-NMR showed that the product consisted of

two isomers (**4** and **5**) in a ratio of 1:2 in favour of isomer **5**. HRMS: Calculated for $C_{15}H_{25}ClNOS$: 302.135. Found: 302.139. ^{1}H-NMR ($CDCl_3$, 300 MHz): Isomer **(4)**: δ (ppm) 8.60 (1H, d, J_m=2.1 Hz); 7.80 (1H, dd, J_o=8.1 Hz, J_m=2.1 Hz); 7.40 (1H, d, J_o=8.1 Hz); 4.59 (2H, s); 4.21 (1H, d, J_g=13.2 Hz); 4.08 (1H, d, J_g=13.2 Hz); 2.71 (1H, t, J=9 Hz); 2.67 (1H, t, J=9 Hz); 1.74 (2H, m); 1.40 (2H, m); 1.23 (8H, m); 0.85 (3H, t, J=7.2 Hz). Isomer **(5)**: δ (ppm) 8.48 (1H, d, J_m=2.1 Hz); 7.73 (1H, dd, J_o=8.1 Hz, J_m=2.2 Hz); 7.50 (1H, d, J_o=8.1 Hz); 4.67 (2H, s); 3.98 (1H, d, J_g=13.2 Hz); 3.86 (1H, d, J_g=13.2 Hz); 2.61 (1H, t, J=9 Hz); 2.59 (1H, t, J=9 Hz); 1.74 (2H, m); 1.40 (2H, m); 1.23 (8H, m); 0.85 (3H, t, J=7.2 Hz). ^{13}C-NMR ($CDCl_3$, 300 MHz): Isomer **(4)**: δ (ppm) 151.5; 149.9; 137.8; 133.3; 125.9; 59.5; 52.3; 43.3; 32.3; 29.7; 29.5; 29.4; 23.2; 23.2; 14.7. Isomer **(5)**: δ (ppm) 157.1; 150.8; 139.4; 126.3; 123.4; 54.8; 52.0; 46.8; 32.3; 29.7; 29.5; 29.4; 23.2; 23.2; 14.7. MS (EI, m/z, rel. int. (%)): 302 ($[M]^+$, 4), 188 ($[M- C_8H_{17}]^+$, 26), 158 ($[M- C_8C_{17}S]^+$, 44), 140 ($[M]^+$- $C_8H_{17}S(O)$, 100), 105 ($[M]^+$- $C_8H_{17}S(O)Cl$, 9), 77 ($[C_5H_3N]^+$, 13).

Synthesis of the precursor polymers. All polymers were synthesised according to the general procedure. Solutions of monomer (5.8 ml, 0.14 M) and base (sodium *tert*-butoxide or sodium hydroxide; 2.5 ml, 0.34 M) were prepared and degassed for 1 hour by a continuous flow of nitrogen at 30°C. The base solution was added in one portion to the stirred monomer solution. During the reaction the temperature was maintained at 30°C and the passing of nitrogen was continued. After 1 hour the reaction mixture was poured into well stirred ice water whereupon the polymer precipitated. The water layer was extracted with chloroform to ensure that all polymer and residual fraction was collected, and the combined organic fractions were concentrated *in vacuo*. The polymer was precipitated in cold ether (0°C), collected by filtration and dried *in vacuo*. The residual ether fraction was concentrated *in vacuo*. FT-IR (film, KBr): ν (cm^{-1}) 3435 (m); 2956/2926 (s); 2856 (s); 1596/1566 (m); 1464/1484 (m); 1046/1029 (s). ^{1}H-NMR ($CDCl_3$, 300 MHz): δ (ppm) 8.78; 8.46; 7.90; 7.68; 7.42; 7.22; 4.20; 3.74; 3.65; 2.32 (2H); 1.62 (2H); 1.20 (10H); 0.84 (3H). ^{13}C-NMR ($CDCl_3$, 300 MHz): δ (ppm) 157.2; 151.6; 150.6; 150.1; 137.3; 136.2; 133.4; 132.8; 124.3; 69.8; 66.4; 48.3; 31.6; 29.0; 28.8; 28.7; 22.5; 13.9

Synthesis of PHPyV (9) and PMPyV (10). PHPyV (**9**) was prepared by solubilising a sample of fully converted PPyV (conversion performed in film at 100°C under vacuum) in a strong acid. Mostly $HClO_4$ was used for this purpose. A bright yellow solution resulted and UV-Vis spectra of this sample were taken in $HClO_4$ (λ_{max}= 438 nm).

PMPyV (10) was prepared by mixing a sample of pyridine precursor polymer **6** (100mg, 0.38 mmol) in CH_2Cl_2 (5 ml) with methyltriflate (0.8 mmol). Shortly after bringing the reagens together a red precipitate was formed which degraded upon isolation.

Synthesis of 5,5'-dimethyl-2,2'-bipyridine (12). The synthesis of this compound is a two step procedure. First the Raney nickel catalyst will be synthesised and secondly this compound will be used to couple two 5-methyl pyridine moieties.

A. Synthesis of the Raney nickel catalyst. In a 2 l flask 600 ml of distilled water is brought and an stainless steel stirrer is used to allow very efficient mixing. The stirring is started and sodium hydroxide (160 g) is dissolved. Then the 1:1 aluminium-nickel alloy (125 g) is added in portions as rapidly as possible, but at such a rate that no material is lost by frothing with the mixer. When all the alloy has been added the stirring is slowed down and the catalyst is washed down from the sides with distilled water. As soon as the reaction has subsided the mixture is heated on a boiling water bath for 6 hours and slow mixing is continued so that the catalyst is well covered at all times (occasional additions of water were necessary to maintain the volume). After this time the mixture is allowed to stand at room temperature for 15 hours without stirring. It is then washed by decantation with ten 250 ml portions of distilled water and transferred to a 1 l, three-necked flaskby means of distilled water. The total volume of catalyst and water is adjusted to 300 ml and the flask is placed in a cold water bath containing a thermometer. One neck is fitted with a dropping funnel and the other two necks are each connected to a 3 l Büchner flask by rubber *vacuum* tubes. Both Büchner flasks are connected to a pump and to control the pressure inside the apparatus, a screw clamp is placed between each Büchner flask and pump. The pressure is then gradually reduced. After a few minutes the water bath is heated slowly until the water in the reaction flask starts to boil. The bath is kept at this temperature (maximum reduced pressure) until no more water is left in the flask. Then, the temperature of the water bath is raised to 10°C and kept t this temperature for 2 hours. After this time the catalyst is allowed to cool to 50-60°C, it is now ready to be used.

B. Coupling reaction. The dropping funnel is now loaded with 200 ml of 5-methyl pyridine under argon atmosphere and about 80 ml of this compound is added (slowly) to the catalyst. The screw clamps are completely closed during this addition. The flask is then shaken, and another 80 ml of 5-methyl pyridine is slowly added in the same way and shaken again. Finally the remaining 40 ml of 5-methyl pyridine is added and argon is allowed in the

system. The connections to the pumps and the dropping funnel are removed and a reflux condenser is fitted. The reaction mixture is then refluxed under argon atmosphere. After 48 hours the flask is allowed to cool and most of the liquid is decanted and filtered. Then 50 ml of toluene is added to the catalyst and the mixture is again heated to reflux for 10 minutes. The mixture is allowed to cool to about 60°C and the liquid is decanted and filtered as before. This procedure is repeated 2 times. The combined organic fractions are evaporated under reduced pressure and the reaction mixture is purified by a chromatographic separation (Al_2O_3, hexanes/$CHCl_3$ (volume ratio 90/10)) and crystallisation from hexanes (19 g, 27%). ^{1}H-NMR ($CDCl_3$, 400 MHz): δ (ppm) 8.45 (2H), 8.20 (2H, d, J_o= 8 Hz), 7.56 (2H, dd, J_o= 8 Hz, J_m= 1.6 Hz), 2.34 (6H). MS (EI, m/z, rel. int. (%)): 184 ($[M]^+$, 100), 169 ($[M- CH_3]^+$, 18), 156 ($[M- 2xCH_3]^+$, 18), 78 ($[C_5H_4N]^+$, 6).

Synthesis of 5,5'-dicarboxy-2,2'-bipyridine (13). To a stirred solution of sulphuric acid (98%, 125 ml) was added the 5,5'-dimethyl-2,2'-bipyridine (5g, 20.5 mmol). Potassium dichromate (24g, 81.5 mmol) was then added in small portions, such that the temperature remained between 70 and 80°C. Occasional cooling in a water bath was necessary during the addition of potassium dichromate. After the potassium dichromate had been added, the reaction was stirred at room temperature until the temperature fell below 40°C. The deep green reaction mixture was poured into 800 ml of ice water and filtered. The remaining solid was washed with water until the filtrate was colourless and allowed to dry. The resulting light yellow solid was then further purified (remove yellow impurity and traces of monomethyl acid) by refluxing in 170 ml of 50% nitric acid for 4 hours. This solution was poured in ice, diluted with 1 l of water and cooled to 5°C. The precipitate was filtered, washed with water (5 x 50 ml), acetone (2 x 50 ml) and allowed to dry. A white fine solid was obtained (5.6 g, 92%). ^{1}H-NMR (D_2O, 400 MHz): δ (ppm) 8.96 (2H, d, J_m= 1.6 Hz), 8.29 (2H, dd, J_m= 1.6 Hz, J_o= 8.4 Hz), 8.06 (2H, d, J_o= 8.4 Hz). MS (EI, m/z, rel. int. (%)): 244 ($[M]^+$, 100), 227 ($[M- OH]^+$, 16), 153 ($[M- C_2O_4H_2]^+$, 12), 78 ($[C_5H_4N]^+$, 6).

Synthesis of 5,5'-bis(methoxycarbonyl)-2,2'-bipyridine (14). To a stirred solution of MeOH (35 ml) and sulphuric acid (4.5 ml) was added the 5,5'-dicarboxy-2,2'-bipyridine (**13**) (2.25 g, 9.22 mmol). This solution was refluxed for 24 hours and after cooling down the reaction mixture was poured into ice water. The solution was brought to pH 8 by addition of the necessary amount of NaOH solution (25%). The desired compound (**14**) was extracted ($CHCl_3$), dried over $MgSO_4$ and the solvent was evaporated.

Crystallisation from toluene yielded the pure dimethoxy compound **14** as white crystals (2.28 g, 91%). ^{1}H-NMR ($CDCl_3$, 300 MHz): δ (ppm) 9.28 (2H, d, J_m= 1.8 Hz), 8.59 (2H, d, J_o= 8.4 Hz), 8.44 (2H, dd, J_m= 1.8 Hz, J_o= 8.4 Hz), 3.97 (6H). MS (EI, m/z, rel. int. (%)): 272 ($[M]^+$, 100), 241 ($[M- OCH]^+$, 43), 213 ($[M- CO_2CH_3]^+$, 26), 154 ($[M- 2xCO_2CH_3]^+$, 36), 78 ($[C_5H_4N]^+$, 6).

Synthesis of 5,5'-bis(hydroxymethyl)-2,2'-bipyridine (15). The diester 14 (1g, 3.68 mmol) was suspended in absolute ethanol (75 ml) and sodium borohydride (3 g, 79.25 mmol) was added in one portion. The reaction mixture was refluxed for 5 hours during which the solution colours orange. After cooling down a saturated ammonium chloride solution (75 ml) was added and the solution was stirred overnight. The ethanol was evaporated and the precipitated solids were dissolved by addition of the minimum necessary amount of water. The resulting solution was extracted 5 times with ethyl acetate and the combined organic layers were dried over MgSO4. The solvent was evaporated and a white powder was obtained (0.77 g, 98%). ^{1}H-NMR (CD_3OD, 300 MHz): δ (ppm) 8.59 (2H), 8.23 (2H, d, J_o= 8.4 Hz), 7.88 (2H, dd, J_o= 8.4 Hz, J_m= 2.4 Hz), 4.68 (4H). MS (EI, m/z, rel. int. (%)): 216 ($[M]^+$, 100), 200 ($[M- OH]^+$, 44), 185 ($[M- 2xOH]^+$, 40), 171 ($[M-CH_2(OH_2)]^+$, 28), 158 ($[M- 2xCH_2OH]^+$, 16), 78 ($[C_5H_4N]^+$, 6).

Synthesis of 5,5'-bis(chloromethyl)-2,2'-bipyridine (16). To compound **15** (10 g, 46.3 mmol) was added thionyl chloride (55 ml, 0.754 mol). This solution was refluxed (85°C) for 4 hours during which the solution becomes clear and brown coloured. After cooling down, the excess thionyl chloride was evaporated and the remainder was neutralised with a saturated sodium carbonate solution. This aqueous layer was extracted with $CHCl_3$ and the combined organic layers were dried over $MgSO_4$. The crude product was further purified by a chromatographic separation (SiO_2, eluent: hexanes/ethyl acetate (volume ratio 50/50)) which yielded the pure product **16** as white crystals (9.9 g, 87%). ^{1}H-NMR (CD_3OD, 300 MHz): δ (ppm) 8.65 (2H, d, J_m= 2.4 Hz), 8.40 (2H, d, J_o= 8.1 Hz), 7.85 (2H, dd, J_m= 2.4 Hz, J_o= 8.1 Hz), 4.64 (4H). MS (EI, m/z, rel. int. (%)): 253 ($[M]^+$, 21), 217 ($[M- Cl]^+$, 100), 182 ($[M- 2xCl]^+$, 63), 154 ($[M- 2xCH_2Cl]^+$, 29), 78 ($[C_5H_4N]^+$, 6).

Synthesis of 2,5-bis(tetrahydrothiopheniomethyl)-2,2'-bipyridine dichloride (17). A solution of **16** (2 g, 7.91 mmol) and tertrahydrothiophene (2.82 ml, 32 mmol) in MeOH (40ml) was stirred at room temperature for one week. The reaction mixture was precipitated in CH_2Cl_2 (150 ml) at 0°C and a slightly pink solid was obtained (0.91 g, 27%).

^{1}H-NMR (D_2O, 300 MHz): δ (ppm) 8.70 (s, 2H), 8.16 (2H, d, J_o= 8.4 Hz), 8.09 (2h, dd, J_o= 8.4 Hz, J_m= 1.8 Hz), 4.59 (s, 4H), 3.48 (m, 8H), 2.27 (m, 8H). UV-Vis (H_2O): λ_{max} at 292 and 244 nm.

Synthesis of 5-(chloromethyl)-5'-(*n*-octylsulphinyl)-2,2'-bipyridine (19). Dichloride (**16**) (7 g, 27.67 mmol) dissolved in toluene (450 ml) was mixed with an aqueous solution of sodium hydroxide (2.92 g, 0.2 M) and a phase transfer reagent, Aliquat 336 (0.188 g, 6.12 mM). 1-Octanethiol (2.02 g, 2.4 ml, 13.83 mmol) dissolved in toluene (15 ml) was added dropwise to the mixture over 30 minutes. The reaction was stirred for another 17 hours at room temperature. The phases were separated and the organic layer washed with water and dried over magnesium sulphate. After evaporation of the solvent, the crude product was dissolved in 1,4-dioxane (150 ml), and tellurium dioxide (0.54 g, 3.4 mmol) was added. Hydrogen peroxide solution (30 wt% in water, 9.16 ml) was added drop wise over 5 minutes. Thereafter, a few drops of concentrated hydrochloric acid were added and the reaction was monitored on TLC every half hour. After 6 hours all thioether (**18**) had been oxidised to the desired sulphoxide **19**. The reaction was quenched by adding 100 ml of brine. The solution was extracted with chloroform and dried over magnesium sulphate. Column chromatography with hexanes/ethyl acetate (volume ratio 60/40) was used to separate the product from unreacted dichloride. When all dichloride had been collected, pure ethyl acetate was used to elute the product. Crystallisation from hexanes/ethyl acetate yielded 3.82 g (73% yield calculated from *n*-octylthiolate) pure monomer as white needles. ^{1}H-NMR ($CDCl_3$, 300 MHz): δ (ppm) 8.66 (1H), 8.57 (1H), 8.41 (1H, d, J_o= 8.4 Hz), 8.38 (1H, d, J_o= 8.4 Hz), 7.85 (1H, dd, J_o= 8.4 Hz, J_m= 1.4 Hz), 7.78 (1H, dd, J_o= 8.4 Hz, J_m= 1.4 Hz), 4.63 (2H), 4.00 (2H, dd, J= 13.5 Hz), 2.61 (m, 2H), 1.75 (m, 2H), 1.48-1.19 (m, 10H), 0.84 (t, 3H). MS (EI, m/z, rel. int. (%)): 378 ($[M]^+$, 5), 217 ($[M- S(O)C_8H_{17}]^+$, 100), 182 ($[M- C_8H_{17}ClOS]^+$, 86), 154 ($[M- C_{10}H_{21}ClOS]^+$, 50). UV-Vis (THF): λ_{max} at 297 nm.

Synthesis of 5-(bromomethyl)-5'-(*n*-octylsulphinyl)-2,2'-bipyridine (20). This compound was prepared by refluxing a solution of the chloro monomer (**19**) (0.5 g, 1.32 mmol) in aceton (10 ml) together with lithium bromide (0.174 g, 2 mmol) for 2 hours. Then, water was added and the product was extracted ($CHCl_3$) and dried over $MgSO_4$. Evaporation of the solvent and consecutive crystallisation from hexanes/$CHCl_3$ yielded pure **20** as white needles (0.5 g, 89%). ^{1}H-NMR ($CDCl_3$, 300 MHz): δ (ppm) 8.65 (1H, s), 8.56 (1H, s), 8.38 (1H, d, J_o= 8.1 Hz), 8.33 (1H, d, J_o= 8.1 Hz), 7.83 (1H, dd, J_o= 8.2 Hz,

J_m= 1.4 Hz), 7.79 (1H, dd, J_o= 8.2 Hz, J_m= 1.4 Hz), 4.54 (s, 2H), 3.97 (2H, dd, J= 13.2 Hz), 2.60 (m, 2H), 1.75 (m, 2H), 1.48-1.19 (m, 10H), 0.84 (t, 3H).MS (EI, m/z, rel. int. (%)): 423 ($[M]^+$, 6), 263 ($[M- S(O)C_8H_{17}]^+$, 100), 182 ($[M- C_8H_{17}BrOS]^+$, 81), 154 ($[M- C_{10}H_{21}BrOS]^+$, 40).

Synthesis of 5-(iodomethyl)-5'-(*n*-octylsulphinyl)-2,2'-bipyridine (21). The iodo monomer **21** was synthesised from the chloro monomer **19** by refluxing this compound (0.3 g, 0.794 mmol) in aceton (50 ml) together with sodium iodine (0.18 g, 1.19 mmol) for 5 hours. After cooling down water was added and the desired product was extracted ($CHCl_3$). The combined organic layers were washed with a sodium thiosulfate solution ($Na_2S_2O_3$, 20%) to remove iodine remains and dried over $MgSO_4$. Evaporation yielded the pure monomer (0.31 g, 86%). ^{1}H-NMR ($CDCl_3$, 300 MHz): δ (ppm) 8.63 (1H, d, J_m= 2.1 Hz), 8.54 (1H, d, J_m= 2.1 Hz), 8.37 (1H, d, J_o= 8.1 Hz), 8.29 (1H, d, J_o= 8.1 Hz), 7.77 (2H, m, J_m= 2.1 Hz, J_o= 8.1 Hz), 4.44 (s, 2H), 3.95 (2H, dd, J= 13.2 Hz), 2.60 (m, 2H), 1.75 (m, 2H), 1.48-1.19 (m, 10H), 0.84 (t, 3H). MS (EI, m/z, rel. int. (%)): 423 ($[M]^+$, 6), 263 ($[M- S(O)C_8H_{17}]^+$, 100), 182 ($[M- C_8H_{17}BrOS]^+$, 81), 154 ($[M- C_{10}H_{21}BrOS]^+$, 40).

Synthesis of the monomer complexes 22 and 23.

A. The zinc complexed monomer **22** was prepared by mixing monomer **19** (0.4 g, 1.06 mmol) with zinc chloride (48.4 mg, 0.365 mmol) in MeOH (50 ml) under an argon atmosphere. After mixing for 3 hours at room temperature a saturated KPF_6 solution (20 ml) was added and the aqueous layer was extracted with $CHCl_3$ and dried over $MgSO_4$. After evaporation of the solvent a very sticky transparent substance remained (0.445 g, 88%). ^{1}H-NMR ($CDCl_3$, 300 MHz): δ (ppm) 8.68 (1H), 8.61 (1H), 8.2 (4H, m), 4.68 (2H), 4.12 (2H, dd, J= 13.2 Hz), 2.76 (2H, m), 1.73 (2H, m), 1.5-1.15 (10H, m), 0.85 (3h, t). UV-Vis (THF): λ_{max} at 309 nm.

B. The ruthenium complexed monomer **23** was prepared by heating a solution of monomer **19** (0.3 g, 0.79 mmol) and *cis*-Ru-$(bpy)_2Cl_2 \cdot 2H_2O$ (0.385 g, 0.79 mmol) in ethanol at reflux temperature for 24 hours. A clear purple solution resulted. The solution was allowed to cool and the ethanol was evaporated under reduced pressure. The remainder was solubilsed in water (50 ml) and KPF_6 (0.2 g, 1.09 mmol) was added as a solid to precipitate the complex as its PF_6 salt. The ruthenium complexed monomer **23** precipitated as a orange solid, was filtered off and dried under *vacuum* (0.82 g, 96%). ^{1}H-NMR ($CDCl_3$, 300 MHz): δ (ppm)

8.30 (6H, m), 8-7.4 (16H, m), 4.53 (2H), 4.11 (2H, m), 3.78 (2H, m), 1.7-1 (12H, m), 0.86 (3 H, t). UV-Vis (CH_3CN): λ_{max} at 451 and 288 nm.

Polymerisation of monomers 19, 20 and 21. These monomers were polymerised according to the standard procedure. Solutions of monomer (5.8 ml, 0.14 M) and base (sodium *tert*-butoxide; 2.5 ml, 0.34 M) were prepared and degassed for 1 hour by a continuous flow of nitrogen. The temperature at which the polymerisation was performed depended on the solubility of the monomer in the respective solvent. For the polymerisations in 1,4-dioxane and DMSO the temperature had to be raised to 50 and 55°C respectively in order to obtain a clear solution. The base solution was added in one portion to the stirred monomer solution. During the reaction the temperature was maintained constant and the passing of nitrogen was continued. After 1 hour the reaction mixture was poured into well stirred ice water whereupon the polymer precipitated. The water layer was extracted with chloroform to ensure that all polymer and residual fraction was collected, and the combined organic fractions were concentrated *in vacuo*. The precursor polymers were precipitated in a cold *n*-hexane/ethyl acetate mixture (volume ratio 50/50, 150 ml, 0°C), collected by filtration and dried *in vacuo*. The residual solvent fraction was concentrated *in vacuo*. Polymerisation results for these monomers are summarised in Table 2. ^{1}H-NMR ($CDCl_3$, 300 MHz): δ (ppm) 8.6-8.1, 7.89, 7.75, 7.614, 4.09, 3.65, 3.76, 3.45, 3.02, 2.57, 2.19, 2.02, 1.73, 1.58, 1.45-1.05, 0.9-0.7. FT-IR (film, KBr): ν (cm^{-1}) 2926 (s), 2854 (m), 1596 (w), 1550 (w), 1466 (s), 1385 (w), 1046 (m), 1026 (m), 844 (w), 750 (w). UV-Vis (film): λ_{max} at 301 and 253 nm.

Polymerisation of the complexed monomers 22 and 23. The polymerisation of monomer **22** was performed in CH_2Cl_2 according to the standard procedure just described. The amount of base was calculated on the total number of monomer units, each monomer complex **22** has 3. Analysis of this precursor polymer proved it is identical to the precursor polymers synthesised from the non-complexed monomers.

The polymerisation of the ruthenium-complexed monomer **23** was performed in acetonitril according to the standard procedure just described. In this case each monomer complex only possess 1 monomer unit. After allowing the polymerisation reaction to proceed for 2 hours the reaction mixture was poured into ice-water whereupon the precursor polymer precipitated as a black sticky solid. The water was decanted and the black sticky solid was collected. ^{1}H-NMR (DMSO-D6, 300 MHz): δ (ppm) 8.82, 8.17, 7.65, 4.75, 4.15, 3.95,

3.39, 2.07, 1.5-1.18, 0.86. FT-IR (film, KBr): ν (cm^{-1}) 2928 (m), 1604 (w), 1466 (m), 1446 (m), 1244 (w), 1038 (m), 840 (s), 764 (m). UV-Vis (CH_3CN): λ_{max} at 453 and 288 nm.
The polymerisation results for the complexed monomers are summarised in Table 3.

Synthesis of 2,5-bis(methoxycarbonyl)thiophene (26). To a stirred solution of MeOH (140 ml) and sulphuric acid (2 ml) was added the 2,5-dicarboxythiophene (**24**) (10 g, 58.14 mmol). This solution was heated at reflux temperature for 24 hours. After cooling down the desired compound **16** precipitated and was filtered off. The residue was solubilised in $CHCl_3$ and this organic layer was washed with a K_2CO_3 solution (20%). The organic layer was dried over $MgSO_4$ and the solvent was evaporated. Crystallisation from methanol yielded the pure dimethoxy compound **26** as white crystals (11.3 g, 97%). ^{1}H-NMR ($CDCl_3$, 300 MHz): δ (ppm) 7.71 (2H), 3.89 (6H). MS (EI, m/z, rel. int. (%)): 200 ($[M]^+$, 100), 141 ($[M- COOCH_3]^+$, 47), 82 ($[M- 2x\ COOCH_3]^+$, 74).

Synthesis of 2,5-bis(hydroxymethyl)thiophene (25). In a 100 ml round-bottomed flask was added $LiAlH_4$ (0.38 g, 10 mmol) to dry THF (50 ml, dried over sodium) under argon atmosphere. This slurry was cooled to 0°C and the diester (**26**) (1 g, 5 mmol) was added portion wise in such a way that the reaction did not proceed too vigorously. When the addition is complete a reflux condenser was fitted and the slurry was heated at reflux temperature for 2 hours. During this time a grey, concrete-like substance was formed that was hard to stir. After cooling down air was allowed in the system and the reaction mixture was placed in an ice bath. Then a minimal amount of saturated ammonium chloride solution was added until no more gas development could be detected. This solution was stirred over night and filtered. The residue was washed 5 times with boiling CH_2Cl_2. The combined organic layers were dried over $MgSO_4$ and the solvent was evaporated under reduced pressure. The diol **25** was obtained as a light yellow oil (0.65 g, 91%). ^{1}H-NMR ($CDCl_3$, 300 MHz): δ (ppm) 6.73 (2H), 4.62 (4H), 3.57 (2H). MS (EI, m/z, rel. int. (%)): 144 ($[M]^+$, 78), 113 ($[M- CH_2OH]^+$, 100), 82 ($[M- 2x\ CH_2OH]^+$, 74).

Synthesis of 2,5-bis(chloromethyl)thiophene (27). To a cooled (0°C), stirred solution of diol **25** (0.9 g, 5 mmol) in THF (20 ml) was slowly added a solution of $SOCl_2$ (0.9 ml, 1.49 g, 12.5 mmol) in THF (5 ml). The reaction mixture was allowed to come to room temperature and stirring was continued for 1 hour. Then the mixture is cooled again at 0°C and a saturated sodium carbonate solution was added drop wise until the solution was neutral. The layers were separated and the aqueous layer was extracted with CH_2Cl_2 and

dried over $MgSO_4$. The solvent was evaporated and the highly reactive dichloride **27** was obtained as a yellow oil (0.78 g, 83%). ^{1}H-NMR ($CDCl_3$, 300 MHz): δ (ppm) 6.75 (2H), 4.58 (4H). MS (EI, m/z, rel. int. (%)): 181 ($[M]^+$, 29), 146 ($[M- Cl]^+$, 100), 110 ($[M- 2x Cl]^+$, 47).

Synthesis of 2,5-bis(tetrahydrothiopheniomethyl)thiophene dichloride (28). A solution of **27** (2 g, 11.05 mmol) and tertrahydrothiophene (4.3 ml, 48.62 mmol) in MeOH (40ml) was stirred at room temperature for 3 days. The reaction mixture was precipitated in CH_2Cl_2 (150 ml) at -10°C and a white solid was obtained (3.39 g, 86%). ^{1}H-NMR (D_2O, 300 MHz): δ (ppm) 7.22 (2H), 4.72 (4H), 3.52-3.35 (8H), 2.16 (8H).

Synthesis of 2-(ethylsulphinyl)-5-(chloromethyl)thiophene (Monomer A). A acetonitril/water solution (8 ml) (5 vol% water) of bissulfonium salt **28** (0.5 g, 1.2 mmol) was neutralised using a 0.25 M K_2CO_3 solution. To this solution was added a mixture of Na*t*BuO (0.115 g, 1.2 mmol) and ethane thiol (88.7 µl, 1.2 mmol) in acetonitril/water (2 ml) (5 vol% water) that had been stirred for 0.5 hours at room temperature. This clear solution was added in one portion and reaction was allowed for one hour at room temperature. Then the organic layer was washed with water (20 ml) and dried over $MgSO_4$. The solvent was nearly evaporated to dryness and then *n*-octane (15 ml) was added and the solution was concentrated again to remove tetrahydrothiophene. This sequence was repeated three times. A yellow oil was obtained that already contained some dark particles (degradation products). ^{1}H-NMR proved that the soluble part of this oil consisted for 94 percent of the desired mono thioether **31**. Results are summarised in Table 6. Compound **31**: ^{1}H-NMR ($CDCl_3$, 300 MHz): δ (ppm) 6.86 (1H, d, J= 3.3 Hz), 6.74 (1H, d, J= 3.3 Hz), 4.72 (2H), 3.85 (2H), 2.50 (2H, q), 1.23 (3H, t). MS (EI, m/z, rel. int. (%)): 207 ($[M]^+$, 42), 171 ($[M- Cl]^+$, 31), 145 ($[M- C_2H_5S]^+$, 100), 110 ($[M- C_2H_5SCl]^+$, 76). Compound **33**: ^{1}H-NMR ($CDCl_3$, 300 MHz): δ (ppm) 6.71 (2H), 3.86 (4H), 2.51 (4H, q), 1.22 (6H, t). MS (EI, m/z, rel. int. (%)): 232 ($[M]^+$, 33), 171 ($[M- C_2H_5S]^+$, 100), 110 ($[M- C_4H_{10}S_2]^+$, 66). Compound **34**: ^{1}H-NMR ($CDCl_3$, 300 MHz): δ (ppm) 6.80 (1H, d, J= 2.7 Hz), 6.77 (1H, d, J= 2.7 Hz), 4.76 (2H), 3.88 (2H), 2.69 (2H, q), 2.2 (1H, bs), 1.22 (3H, t). MS (EI, m/z, rel. int. (%)): 189 ($[M]^+$, 21), 127 ($[M- C_2H_5S]^+$, 100), 110 ($[M- C_2H_6SO]^+$, 9).

Oxidation of the thioether 31.

A. An aqueous (35 wt.%) solution of H_2O_2 (0.24 g, 2.47 mmol) was added drop wise to a solution of the crude thioether (1.2 mmol) reaction mixture obtained in the previous

reaction in 1,4-dioxane. TeO_2 (0.02 g, 5 mol%) was added as a catalyst and the oxidation was monitored on TLC. After 5 hours all the starting mono thioether had been consumed and the reaction was quenched by adding brine (40 ml). The reaction mixture was extracted ($CHCl_3$) and the combined organic layers were dried over $MgSO_4$ and concentrated. Only compound **36** was obtained. ^{1}H-NMR ($CDCl_3$, 300 MHz): δ (ppm) 6.89 (2H, dd, J= 3.6 Hz), 4.77 (2H), 4.10 (2H, dd, J= 13.8 Hz), 3.18 (1H, bs), 2.62 (2H, m), 1.31 (3H, t). MS (CI, m/z, rel. int. (%)): 409 (dimer), 205 ($[MH]^+$, 100), 187 ($[M- H_2O]^+$, 16), 127 ($[M-C_2H_5SO]^+$, 40).

B. The oxidation towards monomer A was also performed by adding *m*-CPBA (70 mol%, 0.17 g, 1 mmol) to a cooled solution (-10°C) of the crude thioether in CH_2Cl_2 (15 ml). When all the *m*-CPBA had been added the reaction was allowed to come to room temperature and after 15 minutes a dilute NaOH (20 ml, 0.2 M) was added. The reaction mixture was extracted ($CHCl_3$) and the combined organic layers were dried over $MgSO_4$ and concentrated. This reaction only yielded the sulphon compound **35**. ^{1}H-NMR ($CDCl_3$, 300 MHz): δ (ppm) 6.99 (2H, s), 4.73 (2H,s), 4.36 (2H,s), 2.93 (2H, q), 1.37 (3H, t). MS (CI, m/z, rel. int. (%)): 239 ($[MH]^+$, 8), 203 ($[MH- Cl]^+$, 57), 145 ($[MH- C_2H_5SO_2]^+$, 100), 111 ($[MH- C_2H_5ClSO_2]^+$, 4).

C. The oxidation of this compound towards the sulphoxide (Monomer A) was performed at TNO within the framework of the Plastronix project.

Synthesis of 2-(ethylsulphinyl)-5-(hydroxymethyl)thiophene (36). The synthesis towards this compound was performed in such a way that hydroxy substitution was promoted as much as possible. Therefore, the introduction of the thioether was performed in water and the consecutive oxidation to the sulphoxide was performed in 1,4-dioxane using the classical H_2O_2/TeO_2 system. These reaction were performed in the same way as the ones just described keeping in mind these adjustments.

Synthesis of 2-(ethylsulphinyl)-5-[ethoxy(thiocarbonyl)thiomethyl]thiophene (Monomer B). A acetonitril/water solution (8 ml) (5 vol% water) of bissulfonium salt **28** (0.5 g, 1.2 mmol) was neutralised using a 0.25 M K_2CO_3 solution. To this solution was added a mixture of Na*t*BuO (0.115 g, 1.2 mmol) and ethane thiol (88.7 µl, 1.2 mmol) in acetonitril/water (2 ml) (5 vol% water) that had been stirred for 0.5 hours at room temperature. This clear solution was added in one portion and reaction was allowed for one hour at room temperature. At this point potassium *O*-ethyl xanthate (0.23 g, 1.44 mmol)was

added as a solid an stirring was continued for 30 minutes after which water (30 ml) was added. The reaction mixture was extracted ($CHCl_3$) and the combined organic layers were dried over $MgSO_4$ and concentrated. A chromatographic separation (SiO_2, $CHCl_3$) yielded the pure monomer **B** (0.27 g, 73%). ^{1}H-NMR ($CDCl_3$, 300 MHz): δ (ppm) 6.91 (1H, d, J= 3.6 Hz), 6.83 (1H, d, J= 3.6 Hz), 4.73 (2H,s), 4.63 (2H,q), 4.51 (2H, s), 4.06 (2H, dd, J= 13.2 Hz), 2.61 (2H, m), 1.41 (3H, t), 1.29 (3H, t). MS (CI, m/z, rel. int. (%)): 309 ($[MH]^+$, 4), 232 ($[MH- C_2H_5SO]^+$, 100), 188 ($[MH- SC(S)OC_2H_5]^+$, 16), 111 ($[MH- C_5H_{10}O_2S_3]^+$, 4).

Synthesis of 2,5-bis[ethoxy(thiocarbonyl)thiomethyl]thiophene (Monomer C). A acetonitril/water solution (8 ml) (5 vol% water) of bissulfonium salt **28** (0.5 g, 1.2 mmol) was neutralised using a 0.25 M K_2CO_3 solution. To this solution was added potassium *O*-ethyl xanthate salt (1.06 g, 3 mmol) as a solid and this solution was stirred overnight. Water (30 ml) was added and the desired bis-xanthate monomer **C** was extracted ($CHCl_3$) and dried over $MgSO_4$. Evaporation of the solvent yielded the pure product (0.38 g, 89%). ^{1}H-NMR ($CDCl_3$, 300 MHz): δ (ppm) 6.79 (2H, s), 4.64 (4H,q), 4.48 (4H, s), 1.41 (6H, t). MS (EI, m/z, rel. int. (%)): 352 ($[M]^+$, 9), 263 ($[M- C(S)OC_2H_5]^+$, 5), 231 ($[M- SC(S)OC_2H_5]^+$, 100), 143 ($[M- C_6H_{10}O_2S_3]^+$, 38), 110 ($[M- C_6H_{10}O_2S_4]^+$, 52).

Polymerisation of monomer A. The polymerisation of this monomer is discussed elsewhere.[32]

Polymerisation of monomer B. Monomer **B** was polymerised in 2-BuOH, THF and CH_2Cl_2 according to the "standard" procedure. Monomer **B** (0.15 g, 0.487 mmol) and Na*t*BuO (0.048 g, 0.487 mmol) were both separately dissolved in the respective solvent (3.85 ml and 1 ml, concentration= 0.1M) and degassed by passing nitrogen for one hour. Then the base was added to the monomer solution in one shot whereupon the solution turned red. The polymerisation was allowed to proceed for one hour at 30°C and the passing of nitrogen was continued. The reaction was terminated by pouring the mixture in ice water (50ml). The polymer was extracted with chloroform, the solvent was evaporated and the precursor polymer was precipitated in ether (100 ml, 0°C). Sometimes a small fraction of precursor polymer precipitated and sometimes it did not. The polymerisation of this monomer proved very irreproducible. GPC analysis of the precursor polymers fluctuated between very low (10^2) and high (10^5).

Polymerisation of monomer C. The home made LDA was prepared by mixing diisopropylamine (DPA, 0.103 ml, 0.74 mmol) with butyllithium (1.6 M in hexanes, 0.444

ml, 0.71 mmol) at room temperature in a pre-dried flask under argon atmosphere. After mixing for 1 hour this solution was cooled to –78°C and transferred (in one shot) to a solution that contained the monomer (0.25 g, 0.71 mmol in 5 ml dry THF) at –78°C. Upon addition of the base the solution turned yellow. Reaction was allowed at –78°C for 1.5 hours under a constant argon flow after which the polymerisation mixture was allowed to come to 0°C over 1 hour. The reaction mixture was then poured into ice water whereupon the precursor polymer precipitated. The polymer was extracted from the aqueous layer with chloroform and the solvent of the combined organic layers was evaporated under reduced pressure. Precipitation in a hexanes/ether mixture (50/50, 100ml, 0°C) yielded the precursor polymer **39** as a light yellow solid. The procedure for the polymerisation reactions with KO*t*Bu or commercial LDA are identical to that just described with this difference that the temperature at which the polymerisation is performed may be different (Table 7). GPC on the precursor polymers was performed versus PS standards and THF was used as eluent. Polymerisation results are shown in Table 7. ^{1}H-NMR ($CDCl_3$, 300 MHz): δ (ppm) 6.65 (1H), 6.48 (1H), 5.06 (1H), 4.57 (2H), 3.50 (1H), 3.32 (1H), 1.37 (3H). FT-IR (film, KBr): ν (cm^{-1}) 2986 (w), 1643 (m), 1439 (w) 1219 (s), 1146 (w), 1110 (m), 1046 (s), 806 (w), 755 (m).

3.5 References

[1] Greenham, N. C.; Moratti, S. C.; Bradley, D. D. C.; Friend, R. H.; Holmes, A. B. *Nature* 365, **1993**, 628.

[2] Marsella, M. J.; Fu, D.-K.; Swager, T. M. *Adv. Mater.* 7, **1995**, 145.

[3] Li, X.-C.; Cacialli, F.; Cervini, R.; Holmes, A. B.; Moratti, S. C.; Grimsdale, A. C.; Friend, R. H. *Synth. Met.* 84, **1997**, 159.

[4] Klemm, L. H.; Johnson, W. O.; White, D. V. *J. Mater. Chem.* 9, **1972**, 843.

[5] Herriott, A. W.; Picker, D. *Synthesis* **1975**, 447.

[6] Issaris, A.; Vanderzande, D.; Adriaensens, P.; Gelan, J. *Macromolecules* 31, **1998**, 4426.

[7] van Breemen, A.; Issaris, A. C. J.; de Kok, M. M.; Van der Borght, M.; Adriaensens, P. J.; Gelan, J.; Vanderzande, D. J. M. *Macromolecules* 32, **1999**, 5728.

[8] de Kok M.; van Breemen A.; Carleer R.; Adriaenssens P.; Vanderzande D. *Acta Polym. 50*, **1999**, 28.

[9] Blatchford, J. W.; Jessen, S. W.; Lin, L. B.; Gustafson, T. L.; Fu, D. K.; Wang, H. L.; Swager, T. M.; MacDiarmid, A. G., *et al. Phys. Rev. B-Condens Matter* 54, **1996**, 9180.

[10] Sundaresan, N. S. in *Electrical and Optical Polymer Systems*; Wise, D. L.; Wnek, G. E.; Trantolo, D. J.; *et al*. Eds. M. Dekker, Inc.: NY, **1998**, 97-136.

[11] Li, Y.; Cao, Y.; Gao, J.; Wang, D.; Yu, G.; Heeger, A. J. *Synth. Met.* 99, **1999**, 243.

[12] Kraft, A.; Grimsdale, A. C.; Holmes, A. B. *Angew. Chem. Int. Ed.* 37, **1998**, 402.

[13] Eichen, Y.; Nakhmanovich, G.; Gorelik, V.; Epshtein, O.; Poplawski, J. M.; Ehrenfreund, E. *J. Am. Chem. Soc.* 120, **1998**, 10463.

[14] Tian, J.; Wu, C.-C.; Thompson, M. E.; Sturm, J. C.; Register, R. A. *Chem. Mater.* 7, **1995**, 2190.

[15] Wasielewski, M. R.; Wang, B. *J. Am. Chem. Soc.* 119, **1997**, 12.

[16] a) Sasse, W. H. F. *J. Chem. Soc.* **1959**, 3046. b) Badger, G. M.; Sasse, W. H. F. *J. Chem. Soc.* **1956**, 616. c) Sasse, W. H. F.; Whittle, C. P. *J. Chem. Soc.* **1961**, 1347.

[17] Oki, A. R.; Morgan, R. J. *Synth. Comm.* **1995**, 4093.

[18] Ciana, L. D.; Dressick, W. J.; von Zelewsky, A. *J. Heterocyclic Chem.* 27, **1990**, 163.

[19] Norrby, T.; Börje, A.; Zhang, L.; Akermark, B. *Acta Chemica Scandinavica* 52, **1998**, 77.

[20] a) van Breemen, A.; Vanderzande, D.; Adriaensens, P.; Gelan, J. *J. Org. Chem.* 64, **1999**, 3106. b) van Breemen, A. *Ph.D. Dissertation*, **1999**, Limburgs Universitair Centrum, Diepenbeek, Belgium.

[21] Motmans, F. *internal communication* **2001**.

[22] Van Der Borght, M. *Ph.D. Dissertation*, **1998**, Limburgs Universitair Centrum, Diepenbeek, Belgium.

[23] Garay, R.; Lenz, R. W. *Makromol. Chem. Suppl.* 15, **1989**, 1.

[24] Kaes, C.; Katz, A.; Hosseini, M. W. *Chem. Rev.* 100, **2000**, 3553.

[25] Miller E. G.; Rayner D. R.; Thomas H. T.; Mislow K. *J. Amer. Chem. Soc.* **1968**, *90*, 4861.

[26] Mislow K.; Axelrod M.; Rayner D. R.; Gotthardt H.; Coyne L. M.; Hammond G. S. *J. Amer. Chem. Soc.* **1965**, *87*, 4958.

[27] Elsenbaumer, R. L. *Mol. Cryst. Liq. Cryst.* 186, **1990**, 211.

[28] Safety Data Sheets for compounds **24** to **27** are available at Covion, Manchester, UK.

[29] a) Drabowicz, J.; Kielbasinski, P.; Mikolajczyk, M. in: *The Chemistry of Sulfones and Sulfoxides* Patai, S; Rappoport, Z.; Stirling, C. John Wiley & Sons Ltd., Chichester, UK, **1988**, 233-378. b) Drabowicz, J.; Kielbasinski, P.; Mikolajczyk, M. in: *The Chemistry of Sulfones, Sulfoxides and Cyclic Sulphides* Patai, S; Rappoport, Z. John Wiley & Sons Ltd., Chichester, UK, **1994**, 255-388.

[30] This oxidising system was successfully used within the framework of the PLASTRONIX project.

[31] Larock, R. C. in *Comprehensive Organic Transformations*, VCH Publishers Inc., NY, p353.

[32] Results within the framework of the PLASTRONIX project.

[33] a) Son S.; Dodabalapur A.; Lovinger A. J.; Galvin M. E. *Science* **1995**, *269*, 376. b) Lo S-C.; Palsson L-O.; Kilitziraki M.; Burn P. L.; Samuel I. D. W. *J. Mat. Chem*. **2001**, *11*, 2228.

[34] Kesters, E.; Gillissen, S.; Motmans, F.; Lutsen, L.; Vanderzande, D. *Accepted for publication in Macromolecules*.

[35] Lo S-C.; Sheridan A.; Samuel I. D. W.; Burn P. L. *J. Mat. Chem*. 9, **1999**, 2165.

[36] Kesters, E. *Ph.D. Dissertation*, **2002**, Limburgs Universitair Centrum, Diepenbeek, Belgium.

Chapter 4

Copolymers.

4.1 Introduction

An interesting approach to tune the physical and chemical properties of conjugated polymers is the synthesis of copolymers. Various parameters can be manipulated in this way and polymers with intermediate and/or improved properties often arise. Emission maxima, solubility, film forming and redox properties can all be changed significantly as was demonstrated in various papers. [1,2]

Gilch copolymerisation of a PEO-PPV type monomer (ethylene oxide chains on the phenylene unit) and an alkylsilyl-PPV type monomer resulted in statistical copolymers (**1**). (Scheme 1) The PEO-PPV moiety allows ion coordination which makes ion motion possible under an applied electrical field. The alkylsilyl-PPV is incorporated to compensate for the poor luminescence properties of PEO-PPV thus making these copolymers suitable to be used in LECs (Light-emitting electrochemical cell).[3,4] These devices use an electroluminescent polymer blended with an ion transporting polymer such as poly(ethylene oxide) (PEO).[5]

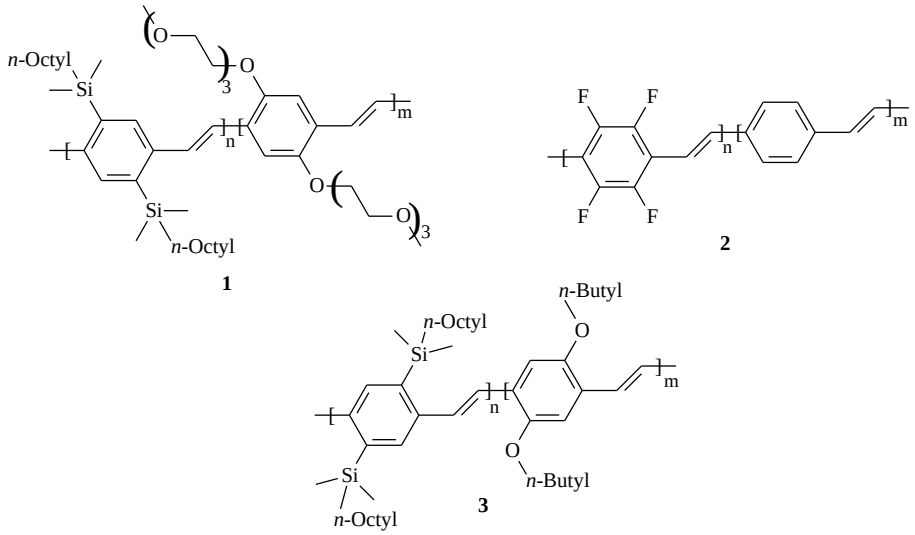

Scheme 1: Chemical structure of some PPV copolymers.

Most PPV copolymers synthesised to date were designed with the idea to improve a specific property of the conjugated material by the merger of properties of the respective homopolymers. In this way devices, mainly LEDs, with increased stability and/or higher quantum efficiencies were accessible.

Benjamin *et al*. reported on the Wessling copolymerisation of PPV and a fluorinated PPV analogue (**2**).[6] By incorporation of the fluoro-PPV derivative they wanted to increase the durability of LEDs by increasing the chemical stabilisation of PPV toward degradation by incorporation of fluorinated segments.

Statistical copolymers between 2,3-dialkoxy-substituted PPV and an alkylsilyl-substituted PPV (**3**) combine the intrinsically high EL efficiency present in the homo alkylsilyl-substituted PPV with the considerably reduced turn-on voltage of 2,3-dialkoxy-substituted PPV which makes these copolymers suitable to be used in LEDs.[1,7]

As mentioned earlier, one of the key factors determining the efficiency of a LED is played by the imbalance of charge carriers with opposite signs. In a single MEH-PPV chain, the mobility of electrons is higher than that of holes by one order of magnitude.[8] However, due to the presence of electron traps in the bulk polymer film a dramatic decrease in electron mobility is observed which leads to a reversal of the order of the mobilities.[9] So, on the whole, for most PPV materials, hole mobilities are larger than electron mobilities by approximately 1 order of magnitude.[10] Furthermore, charge injection is generally easier for

holes than for electrons. These factors shift the recombination zone of hole and electron toward the region near the polymer/cathode interface and therefore result in a lowering of the device efficiency due to quenching of excitons by the metal cathode. Several solutions have been proposed to solve these problems. Inserting an additional electron transport layer (ETL) between the emissive layer and the cathode or using a blend of emissive polymer with charge transport material as active layer have proven successful to increase quantum efficiency.[11] Derivatives of 1,3,4-oxadiazoles were among the most frequently used ETL materials.[12] However, spincoating the ETL layer is tricky and a multilayer device always results in an unfavourable increase in turn-on voltage. A second solution to improve device performance is the use of a low work function metal such as calcium or magnesium.[13] Due to the better matching of cathode workfunction with the LUMO of PPV the quantum efficiency slightly improves but devices using these low work function metals have to be hermetically encapsulated because of their sensitivity to air and moisture.

A third and more attractive way for chemists and materials scientists to achieve high efficiency in LEDs is by developing new conjugated polymers with intrinsically balanced injection of electrons and holes. To do so, a close match between the cathode workfunction and corresponding LUMO of the polymer is required on the one hand and also the anode workfunction has to coincide with the HOMO of the polymer. In this regard, electron withdrawing substituents have shown to increase both electron affinity and ionisation potential, allowing for easier electron injection from stable cathodes such as Al thus generating devices with much higher efficiency.[14,15] For example, CN-PPV has been shown to be a good electron acceptor and allowed the fabrication of a very efficient two layered devices with Al cathodes and a PPV layer between the ITO and the luminescent CN-PPV (**4** + **5**).[14] (Scheme 2) It is generally accepted that this efficiency increase results from both the enhanced electron injection at the cathode and the reduction of the hole current, caused by the presence of an energy barrier for hole injection into CN-PPV at the interface with PPV. Importantly, this carrier effect also increases the distance between the cathode and the recombination zone, thereby reducing luminescence quenching by the cathode. Cyano groups have been introduced on the double bond[14,16] or on the phenylene ring[17,18] of PPV. Synthesis of these compounds always proceeded via a Wittig/Knoevenagel or Heck type reaction and in fact these polymerisations were copolymerisations between a cyano containing monomer and an alkoxy-substituted PPV monomer. The latter was always

incorporated to keep the final conjugated polymer soluble in organic solvents to allow efficient device fabrication.

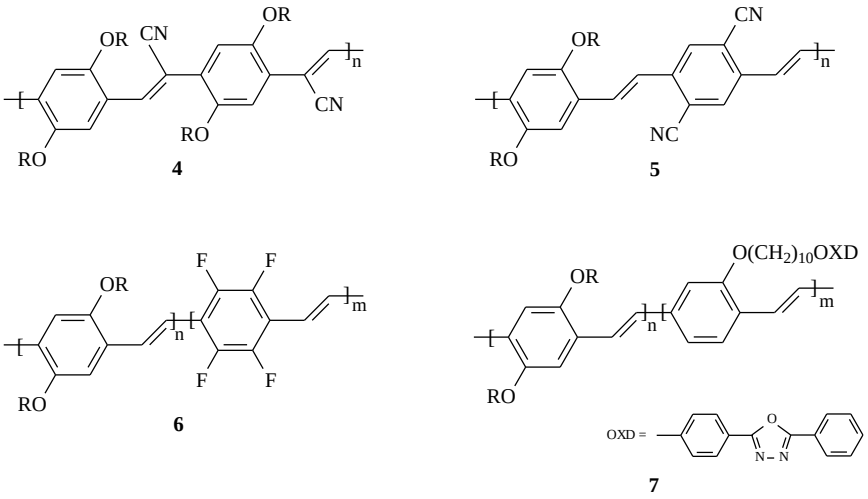

*Scheme 2: Chemical structures of copolymers **4** – **7**.*

Other interesting examples of copolymers that pursuit a balanced electron- and hole transport include Gilch polymerisation of a fluorine- and alkoxy-substituted PPV. In this case random copolymers (**6**) were obtained and up to 26% of the fluorine comonomer was incorporated in the polymer structure.[19] Also the Gilch copolymerisation between MEH-PPV and an 1,3,4-oxadiazole containing PPV derivative is reported (**7**).[2] (Scheme 2) This design is based on the consideration that the PPV backbone is a good hole transporting electroluminescent material and the alkoxy side chains provide solubility and prevent crystallisation. The 1,3,4-oxadiazole unit is attached to the polymer backbone through a non conjugated spacer and improved the electron transport. In this way incorporation of the 1,3,4-oxadiazole unit at the full composition range is possible and random copolymers were obtained. LEDs prepared with these copolymers show significantly improved quantum yields and the turn-on voltage is reduced for the devices with a Ca or Al cathode.[2]

All copolymers mentioned above were synthesised via the Wessling or Gilch precursor route on the one hand or by a direct synthetic approach, i.e. Wittig/Knoevenagel or Heck type reaction, on the other hand. All conjugated copolymers (except for **2**) were soluble in common organic solvents. This proved to be a necessity for efficient device engineering. In the precursor routes mentioned, HCl is liberated during conversion to the conjugated

structure and it has been shown that this reacts with the ITO anode thus seriously lowering the device efficiency.[20,21] In order to prevent this, elimination is best performed in solution and alkoxy side chain substitution is necessary to obtain soluble conjugated polymers that can be processed. Note that we refer to the Wessling and Gilch routes as being precursor routes but in this concept the conjugated system is generated immediately after polymerisation without isolation of the precursor polymer. This is only possible because the alkoxy substitution allows the fully conjugated copolymer to be soluble in organic solvents. In this context, one can question the exact terminology for "precursor route" used.

4.2 Synthesis

In the following paragraphs, results will be presented about the copolymerisation of several sulphinyl monomers via the sulphinyl precursor route. The idea behind this study was twofold. Firstly, we would like to come to new materials with intermediate properties with respect to the respective homopolymers. Secondly, and even more importantly, we would like to understand why a certain comonomer feed leads to a specific copolymer composition. This aspect was never addressed in any of the references mentioned above, but in order to come to a well defined procedure for the synthesis of conjugated copolymers a clear understanding of the factors that influence the copolymer composition is indispensable. The copolymer composition was determined on the precursor stage using NMR spectroscopic techniques. In order to comprehend the results derived from these measurements a UV-Vis study was set up to relate the initial comonomer feed to the final copolymer composition. As will be shown, an important parameter that predominantly determines the copolymer composition is the rate of quinoid (the actual monomer) formation during the polymerisation. This study led to new insights in the formation of the actual monomer - the *p*-quinodimethane system - and made it possible to roughly predict the copolymer composition once the reactivity of the different monomers was know from UV-Vis spectroscopy.

The copolymers discussed in this work are those between PPV, PPyV and OC_1C_{10}. (Scheme 3) Once these copolymers have been discussed two other copolymers between OC_1C_{10} and PBPyV on the one hand and between OC_1C_{10} and cyano-PPV on the other

hand will also be handled. Each of the respective homopolymers shows interesting properties and by combining these into one copolymer intermediate properties may result. Poly(1,4-phenylene vinylene) (PPV) was selected because of it relative simplicity and the existing knowledge on monomer and polymer synthesis within our research group. Poly[2-(3',7'-dimethyloctyloxy)-5-methoxy-1,4-phenylene vinylene] a MEH-PPV variant and from now on referred to as OC_1C_{10} was chosen because its long alkoxy side chains guarantee good solubility, even in the conjugated form. Poly(2,5-pyridylene vinylene) (PPyV) and poly(2,5-dicyano-1,4-phenylene vinylene) (cyano-PPV) were used because these structures are electron deficient and hence polymers with higher electron affinities result. As explained earlier, this is desired for example in light emitting diodes (LEDs), allowing an improved electron injection from stable cathodes like aluminium rather than the low work function metals required for more electron rich polymers.[14] The poly(2,2'-bipyridylene vinylene) (PBPyV) was copolymerised with OC_1C_{10} in order to obtain soluble conjugated polymers that allow complexation with a variety of metal ions. As mentioned earlier (Chapter 3), the 2,2'-bipyridine unit possess superb ability to coordinate a large number of metal ions.[22]

4.2.1 PPV-OC_1C_{10}, PPV-PPyV and PPyV-OC_1C_{10} copolymers

The copolymers discussed in this paragraph were all synthesised in exactly the same "standard" conditions in 1,4-dioxane. (Experimental Section) This solvent was chosen because in 1,4-dioxane all monomers can be polymerised in relatively good yields to high molecular weight polymers.[23,24] Furthermore, in 1,4-dioxane the unwanted solvent substitution on the quinoid stage is avoided. This side reaction considerately reduced the polymerisation yield when polymerising the pyridine monomer **3** in 2-butanol.[24]

To a solution of the comonomer mixture (0.1 M in total) in 1,4-dioxane was added the base, sodium-*tert*-butoxide, in a slight excess of 1.05 equivalents to correct for losses during addition. The base solution was added in one shot and reaction was allowed to proceed for 1 hour at 30°C after which the polymerisation mixture was poured into ice water. Extraction (chloroform) of the aqueous layer, evaporation of the solvent and precipitation of the polymer in a non-solvent yielded the precursor polymer. In each set of experiments five (co)polymerisations were conducted and the comonomer ratios were 100/0, 75/25,

50/50, 25/75 and 0/100. All precursor polymers and the residual fractions were analysed. The precursor polymers were soluble in organic solvents such as chloroform and THF.

Note that monomers for OC_1C_{10} and PPyV are mixtures of two isomers. In the latter, isomers arise due to the position of the nitrogen atom with respect to the methylene substituents on the pyridine ring whereas in OC_1C_{10} the different alkoxy substituents give rise to a mixture of isomers during monomer synthesis. The mixtures of monomers were used in all copolymerisation reactions. (Scheme 3)

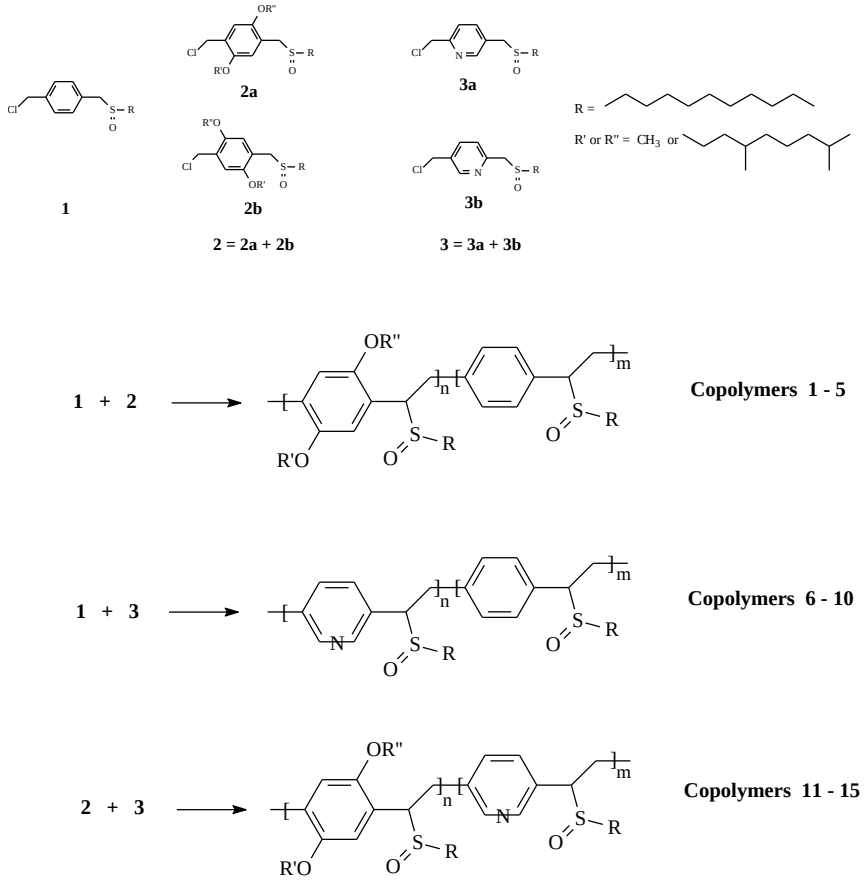

Scheme 3: Chemical structure of the monomers and precursor polymers.

The exact chemical composition of all copolymers was determined with quantitative ^{13}C-NMR spectroscopy. Earlier, all homopolymers had been characterised with ^{13}C-NMR spectroscopy and combination of the different spectra made it possible to understand the

spectra of the copolymers. These measurements allowed a high precision determination of the comonomer distribution in the copolymer. The residual fraction was analysed with ^{1}H-NMR spectroscopy to define the ratio between the low molecular weight products .
The final step in the sulphinyl precursor route is a thermal elimination of the sulphinyl group to yield the double bond. Here *in situ* UV-Vis spectroscopy is applied successfully to monitor the sulphinyl elimination process. This technique gives good indications on elimination and degradation temperatures and also affords the absorption maximum of the conjugated polymer.

4.2.1.1 PPV-OC_1C_{10} Copolymers

Copolymerisations were performed according to the "standard" procedure and copolymerisation results are shown in Table 1. GPC measurements were performed in THF versus PS standards. Although there is no clear trend noticeable between the different molecular weights, high molecular weight precursor polymers are obtained in all (co)polymerisation reactions. The polymerisation yield systematically increases when the amount of PPV monomer in the comonomer feed was raised. Quantitative ^{13}C-NMR analysis revealed the exact copolymer composition. In all copolymers relatively more PPV is incorporated than OC_1C_{10} compared to the initial comonomer feed ratios. Apparently, the PPV comonomer is incorporated much more efficiently into the copolymer than its OC_1C_{10} counterpart. Even when the initial comonomer feed only contains 25 percent of PPV monomer still more of this monomer is build in into the copolymer. Analysis of the restfraction showed the opposite trend, relatively more OC_1C_{10} monomer remained compared to the initial amount.

Entry	Polymerisation					Copolymer			Restfraction	
	PPV[a]	OC_1C_{10}[a]	yield (%)	M_w ($x10^{-3}$)	PD	PPV[b]	OC_1C_{10}[b]	λ_{max}[c] (nm)	PPV[d]	OC_1C_{10}[d]
1	100	0	71	150	3.80	100	0	410	100	0
2	75	25	63	158	4.98	86	14	422	53	47
3	50	50	48	131	3.98	68	32	434	26	74
4	25	75	41	162	3.27	57	43	453	8	92
5	0	100	35	111	2.69	0	100	472	0	100

[a]: initial mol percentage monomer, [b]: percentage monomer in the copolymer as determined with ^{13}C-NMR, [c]: absorption maximum in film, [d]: mol percentage monomer in restfraction as was determined with ^{1}H-NMR.

*Table 1: Copolymerisation results of monomer **1** and **2**.*

In situ UV-Vis spectroscopy measurements were carried out on precursor polymer films, spin-coated on a quartz window. A dynamic heating program of 2°C/min up to 300°C, under a continuous flow of nitrogen, was used. This measurement afforded a clear picture of the thermal elimination and stabilisation behaviour of the copolymers and yielded the absorption maximum of the fully conjugated copolymer. The gradual formation of the conjugated system obtained from copolymer **3** (50/50 comonomer feed) is shown in Figure 1. Before heating, an absorption band from the precursor polymer is present below 260 nm. At 304 nm a small absorption band is noticeable which results from a few premature formed double bonds. As the heating program progresses, new absorption bands appear that gradually red-shift with increasing temperature. At 250 nm a clean isosbestic point is observed. At 120°C, the absorption is maximal and a conjugated polymer with an absorption maximum around 433 nm is obtained. (Figure 1) When the absorbance at this maximum wavelength (433nm) is plotted versus temperature the thermal elimination and stability behaviour of copolymer **3** becomes clear. (Figure 2) The fully conjugated structure is formed between 70 and 120°C and is stable up to at least 250°C since there is no significant decline in the maximal absorbance before this temperature.

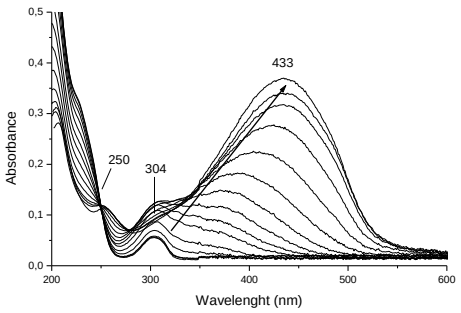

*Figure 1: Gradual formation of the conjugated structure of copolymer **3**.*

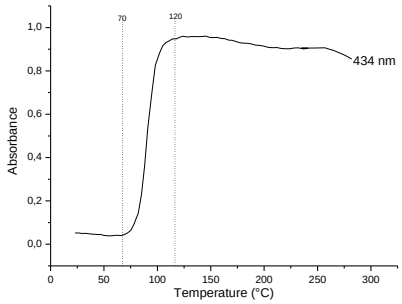

*Figure 2: Absorbency at 433 nm versus temperature of copolymer **3**.*

In Figure 3 the normalised absorption spectra at maximal conversion for the homopolymers (**1** and **5**) and all copolymers (**2**, **3** and **4**) are plotted simultaneously. The position of the absorption maximum clearly shifts depending on the copolymer composition. The PPV homopolymer has an absorption maximum at 410 nm. When OC_1C_{10} is incorporated into the copolymer, the maximum absorption gradually shifts towards the absorption maximum of OC_1C_{10} (472 nm). In this way copolymers with intermediate and tuneable absorption maxima are accessible. When the absorption at the maximum wavelength for each (co)polymer (**2**-**5**) is plotted as a function of temperature the thermal stability of the (co)polymers becomes clear. (Figure 4) The temperature domain (70-115°C) in which the conjugated structure is formed is identical for all (co)polymers but the thermal stability behaviour at higher temperature is quite different. It is known that, once formed, the fully conjugated OC_1C_{10} structure thermally is not very stable and the maximal absorption (at 473 nm) quickly declines at temperatures above 200°C. PPV on the contrary shows no significant decrease in maximal absorption below 250°C. The thermal behaviour of copolymers **2** and **3** proved identical to that of PPV, apparently the incorporation of about 30 percent of OC_1C_{10} is possible without affecting the thermal stability of the copolymer. It is only when larger amounts of OC_1C_{10} are build in into the copolymer that the thermal stability starts to decrease. Copolymer **4** (43 percent OC_1C_{10} incorporated) shows an intermediate stability behaviour and the decline in maximum absorption starts at around 200°C. (Figure 4)

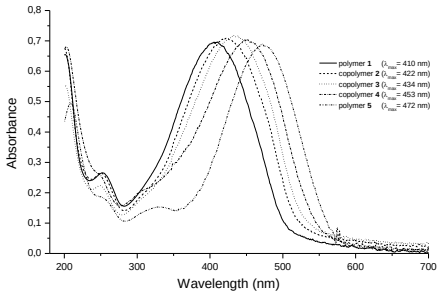

*Figure 3: Normalised absorption spectra for (co)polymers **1** to **5**.*

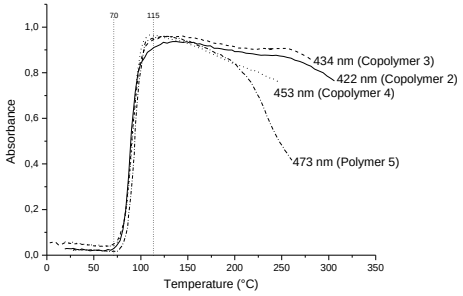

*Figure 4:Absorbance at the maximum absorption wavelength versus temperature for (co)polymers **2**-**5**.*

In Figure 5 the mol% OC_1C_{10} in the copolymer is plotted versus the maximum absorption wavelength. Although this figure only affords a very rough estimation of this relationship, a trend can be observed between the maximum absorption and the mol% OC_1C_{10} incorporated in the copolymer. As more OC_1C_{10} is build in into the copolymer the absorption maximum gradually red-shifts. Figure 4 also shows the relation between the (co)polymerisation yield and the amount of OC_1C_{10} incorporated. As the quantity of OC_1C_{10} in the initial comonomer feed increases the (co)polymerisation yield systematically drops.

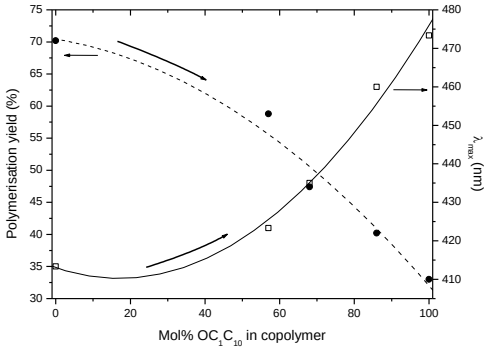

Figure 5: Polymerisation yield and λ_{max} as a function of mol% OC_1C_{10} in the copolymer.

The precursor copolymers **3** and **4** were also converted to the respective conjugated copolymer by reflux in toluene to examine their solubility properties in the fully conjugated form. During the conversion both copolymers largely precipitated and they both proved to be insoluble in organic solvents even under reflux conditions. Only a very small percentage of the conjugated copolymer (probably with high OC_1C_{10} content) proved soluble. An OC_1C_{10} content of 32 and 43 percent respectively is not sufficient to dissolve the fully conjugated copolymers **3** and **4**. For this purpose longer alkoxy side chains or a higher OC_1C_{10} content are probably needed.

In conclusion, the PPV-OC_1C_{10} copolymers (**2**-**4**) contain relatively more PPV than OC_1C_{10} compared to the initial comonomer feed ratio as was confirmed by the quantitative ^{13}C-NMR measurements. Different monomer ratios lead to different copolymer compositions which on their turn result in variable absorption maxima of the fully conjugated copolymer. Thus, tuning of the optical properties of the PPV-OC_1C_{10} copolymer is possible by varying the comonomer feed. The thermal stability of the copolymers also increases when more PPV is incorporated.

4.2.1.2 PPV-PPyV Copolymerisation

A second series of copolymerisations between monomers **1** and **3** were also performed in 1,4-dioxane according to the "standard" procedure. The precursor (co)polymers were precipitated in an ether/*n*-hexane mixture. Molecular weights were determined with GPC versus PS standards using DMF as the eluent. (Table 2) A systematic trend can be observed in the molecular weight of the different precursor copolymers. As the amount of PPyV monomer in the initial comonomer feed is increased the molecular weight of the copolymer systematically decreases. Another point worth mentioning is the fact that the polydispersity of the copolymers are higher than those of the homopolymers.

Entry	Polymerisation			Copolymer					Restfraction	
	PPV[a]	PPyV[a]	yield (%)	M_w ($x10^{-3}$)	PD	PPV[b]	PPyV[b]	λ_{max} (nm)	PPV[c]	PPyV[c]
6	100	0	71	150	3.80	100	0	410	100	0
7	75	25	63	130	4.71	71	29	422	100	0
8	50	50	42	98	4.33	41	59	425	92	8
9	25	75	41	51	3.71	13	87	416	68	32
10	0	100	57	17*	2.10*	0	100	419	0	100

[a]: initial mol percentage monomer, [b]: percentage monomer in the copolymer as determined with ^{13}C-NMR, [c]: mol percentage monomer in restfraction as determined by ^{1}H-NMR. (*GPC performed in chloroform)

*Table 2: Copolymerisation results of monomer **1** and **3**.*

The copolymer composition was determined using quantitative ^{13}C-NMR spectroscopy and showed that the copolymers contain relatively more PPyV than PPV compared to the initial comonomer distribution in the feed. Although the difference is rather small it could be visualised clearly by quantitative ^{13}C-NMR spectroscopy. An enlarged part of the aromatic region of the ^{13}C-NMR spectra of the (co)polymers **7** to **10** is shown in Figure 7. The bottom spectrum shows the aromatic carbon atoms of the homo PPyV. For this homo polymer, complete assignment of all carbon resonances was demonstrated in Chapter 3. The PPV had been characterised in former work within our research group.[23] As more PPV monomer is incorporated into the copolymer the intensities for the PPyV resonances gradually decrease while the ones for PPV become increasingly important. (Figure 7) The protonated carbon atoms of the aromatic PPV unit give rise to two signals at 128.4 and 129.6 ppm. The quaternary atoms have a higher chemical shift at 132.4 and 138.1 respectively (top spectrum). The top spectrum shows the carbon atoms of the copolymer that contained the least pyridine monomer (29 percent). By comparing the different carbon resonances of the different repeating units the composition can be determined. (Table 2)

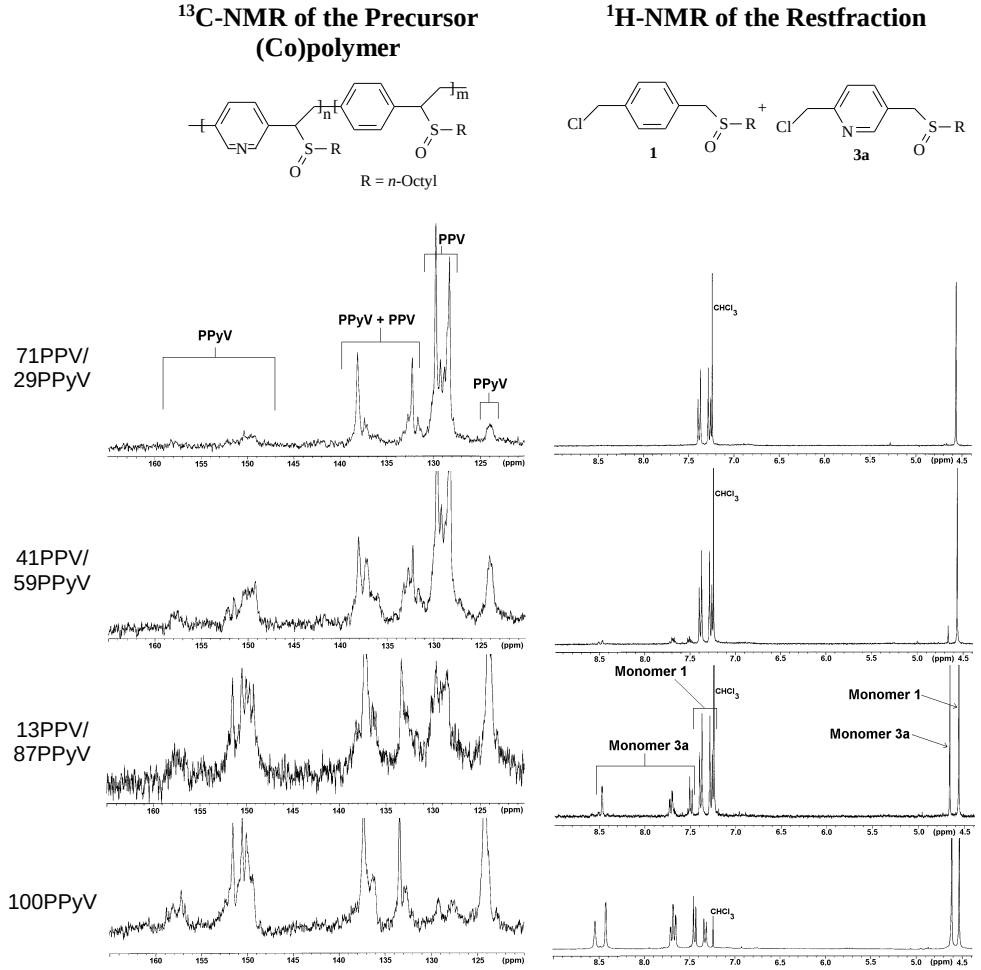

*Figure 7: Enlarged part of the aromatic region of the ^{13}C-NMR spectrum of the precursor (co)polymers **7-10** (left) and enlarged part of the ^{1}H-NMR spectrum of the respective restfraction (right).*

Initially the pyridine monomer **3** consists of a mixture of two equal distributed isomers (**3a** and **3b**). (Scheme 4) These isomers originate from the non-symmetric position of the methyl substituents on the pyridine ring in relation to the pyridine atom. As a consequence a mixture of two isomers, inseparable using simple chromatographic or crystallisation techniques, was obtained during the monomer synthesis. The ratio between the two isomers was determined by ^{1}H-NMR experiments and found to be 1:1. Note that during the synthesis of another batch of this monomer (Chapter 3) a different isomer ratio was

obtained, apparently the isomer distribution is batch dependant. The 1:1 mixture of isomers, obtained in this case, was used in all copolymerisation reactions.

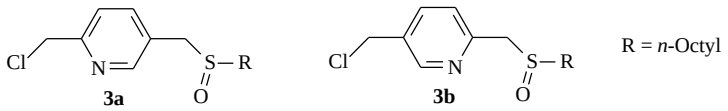

*Scheme 4: Two isomers (**3a** and **3b**) of the pyridine monomer.*

The restfraction of each copolymerisation was analysed with ^{1}H-NMR spectroscopy. (Figure 7) The selected region of the spectra show the aromatic hydrogen atoms of the monomers (**1** and **3a**) (7.25-8.6 ppm) and the benzylic protons adjacent to the chlorine atom (4.5-4.6 ppm). The bottom spectrum shows these hydrogen atoms for the initial pyridine monomer mixture. This analysis of the restfraction showed that, an excess of PPV monomer **1** always remained, even in copolymerisation **9** were the initial comonomer feed consisted for only 25 percent of PPV monomer **1**. In the restfraction of copolymerisation **7** no pyridine monomer **3** remained. When, in copolymerisations **8** and **9**, some pyridine monomer remained, only one of the isomers (**3a**) proved to be present in the restfraction. (Figure 7, Table 2) Note that the bottom spectrum of the isomer mixture (**3a** and **3b**) before polymerisation also shows a resonance at 4.55 ppm which originates from the benzylic protons adjacent to the chlorine atom in isomer **3b**. In the other spectra only isomer **3a** remained so the resonance at 4.55 stems from the similar protons in the PPV monomer **1**. Not surprisingly there seems to be a difference in reactivity between isomers **3a** and **3b**. In isomer **3b** the proton that has to be abstracted in the first step of the polymerisation process is more acid than that in isomer **3a**. Moreover, the chlorine atom in isomer **3b** is a better leaving group than that in isomer **3a**. Both factors arise from the position of the nitrogen atom and probably result in a faster formation of the *p*-quinodimethane system from monomer **3b**. So on the whole, isomer **3b** is available for polymerisation faster than isomer **3a** and this reflects in both copolymer and restfraction composition. It is also possible that differences in the reactivity of the respective quinoid compounds, although both very reactive, may contribute to the different polymerisation degree of isomers **3a** and **3b**, however the difference in quinoid formation rate probably is the dominating effect.

Figure 6 shows the relation between the copolymer composition and the molecular weight of the precursor (co)polymers. As the mol% of PPV in the copolymer increases the molecular weight of the copolymers systematically increases. (Figure 6)

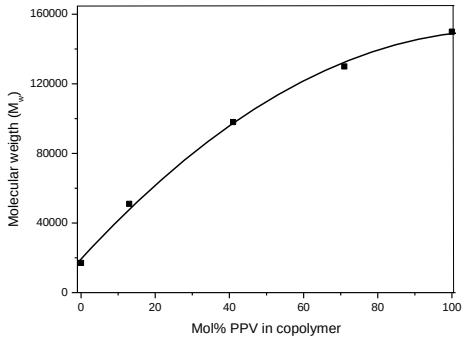

*Figure 6: Molecular weight of copolymers **6** to **10** versus the mol% PPV in the copolymer.*

The elimination process as well as the stability of the conjugated (co)polymers **6**-**10** was examined with *in situ* UV-Vis spectroscopy. In these measurements a dynamic heating program of 2°C/min up to 300°C, under a continuous flow of nitrogen, was used. Figure 7 shows the absorbance at the maximum wavelength versus temperature for copolymers **7** to **9**. All copolymers have a thermal elimination and stability behaviour similar to that of the PPV and PPyV homopolymers. For all copolymers (and homopolymers, not shown in Figure 7) the conjugated structure is formed between 75 and 115°C and copolymers **7** to **9** are stable till at least 300°C as no significant decline or blue shift in maximal absorption is noticed.

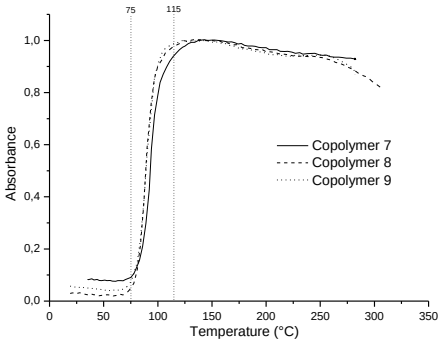

*Figure 7: Absorbance versus temperature for copolymers **7** to **9**.*

In this set of copolymerisations, a different copolymer composition does not give rise to copolymers with different absorption maxima, because the absorption maxima of the PPV and PPyV homopolymer are both situated around 418 nm. (Table 2)

4.2.2.3 OC_1C_{10}-PPyV Copolymerisation

In these experiments monomers **2** and **3** were copolymerised in 1,4-dioxane according to the "standard" conditions. Polymerisation results are summarised in Table 3. In the previous sections the precursor copolymers were precipitated completely in a specific solvent system. In this series, selective precipitation of the different precursor copolymers obtained from one copolymerisation reaction is possible. After work up, the precursor copolymers were first precipitated in ether. In this solvent the copolymer with high pyridine content will precipitate as the homo PPyV precursor polymers are also precipitated in ether.[23] In (co)polymerisations **11**, **12** and **13** the copolymer with high pyridine content precipitates in ether while the copolymers with high OC_1C_{10} content remain soluble. In copolymerisation **14** there is no precipitation in ether. When the precipitated polymers are collected, the filtrate is evaporated and the remainder is precipitated in methanol. Methanol is used to precipitate homo OC_1C_{10} precursor polymers and thus the precursor copolymers with high OC_1C_{10} content will precipitate in this solvent. After these precursor copolymers had been collected the methanol was evaporated and the remainder was used as restfraction. Molecular weights and polydispersities were determined with GPC in THF versus polystyrene standards. (Table 3) Also the maximum absorption wavelength for each

copolymer in film is shown as determined by UV-Vis spectroscopy. The yield of these copolymerisations could not be determined precisely because the copolymers were nearly homopolymers and this seriously complicated the exact determination of the copolymer composition with ^{13}C-NMR measurements.

Entry	Polymerisation		**Copolymer**			
			Precip. in ether		Precip. in methanol	
	PPyV[a]	OC_1C_{10}[a]	M_w (x10^{-3})	λ_{max} (nm)	M_w (x10^{-3})	λ_{max} (nm)
11	100	0	17* (2.1)*	419	-	-
12	75	25	49 (4.3)	421	-	-
13 a + b	50	50	50 (5.7)	408 a	70 (2.0)	463 b
14	25	75	-	-	130 (4.1)	460
15	0	100	-	-	137 (2.7)	473

Polydispersity in brackets. *: GPC performoed in chloroform, [a]: initial mol percentage monomer, **a**: maximum wavelength of copolymer **13a**, **b**: maximum wavelength of copolymer **13b**.

*Table 3: Copolymerisation results of monomer **2** and **3**.*

Quantitative ^{13}C-NMR analysis revealed copolymers **12**, **13a** and **13b** to be nearly homopolymers. Only a very small percentage of OC_1C_{10} was incorporated in the copolymers **12** and **13a** with high pyridine content and vice versa for copolymer **13b** with high OC_1C_{10} content. These observations were further supported by *in situ* UV-Vis measurements in film. The absorption maxima of the copolymers nearly coincide with those of the respective homopolymers meaning that very little comonomer of the other kind is incorporated in the (co)polymer. Note that the absorption maximum for copolymer **13a** with high pyridine content is situated around 408 nm. This is at lower wavelength than the homo PPyV polymer (419 nm). The reason for this phenomenon is unclear. ^{13}C-NMR spectroscopy on copolymer **14** showed that it consists for about 20 percent of PPyV and 80 percent of OC_1C_{10}. UV-Vis spectroscopy showed that this polymer has an absorption maximum at 460 nm which is close to the absorption maximum of the homo OC_1C_{10} polymer (473 nm).

^{1}H-NMR analysis on the restfractions showed they consist of pure unreacted OC_1C_{10} monomer **2**. In copolymerisation **12** with an initial feed of 75% pyridine monomer **3** only a trace of pyridine monomer could be observed in the ^{1}H-NMR spectrum of the restfraction.
These observations all point to the fact that it is very difficult to copolymerise PPyV and OC_1C_{10} efficiently in 1,4-dioxane via the sulphinyl precursor route. In the best case approximately 20 percent of pyridine monomer **3** can be incorporated (copolymerisation **14**) which results in a copolymer with an absorption maximum at 460 nm. When larger amounts of pyridine monomer are used in the initial comonomer feed, both monomers tend to homopolymerise rather than to copolymerise effectively.
The thermal behaviour of the copolymers **12**-**14** was examined with UV-Vis spectroscopy and proved to be identical to that of the respective homopolymers even for copolymer **14**. The very low percentages of comonomer incorporate in the copolymers did not effect the elimination nor the stability behaviour.

4.2.2.4 UV-Vis study of the different monomers

In the previous paragraph, different copolymers with diverse composition were synthesised. In this section, we will try to formulate a rationalisation how a certain initial comonomer feed gives rise to a specific copolymer composition. When looking for an explanation for a specific composition one has to evaluate the process by which the actual monomer in the polymerisation – the *p*-quinodimethane system – is formed. As explained earlier, the formation of the actual monomer is best monitored by UV-Vis spectroscopy since the quinoid structure shows a very distinct and characteristic absorption.

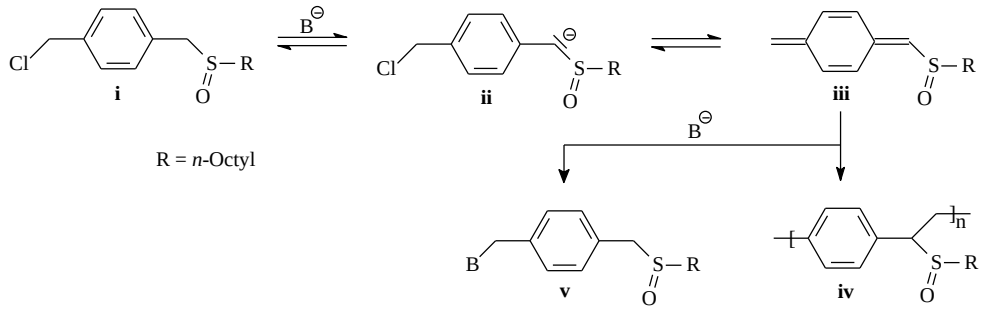

Scheme 5: General pathway for the formation and polymerisation of the p-quinodimethane via the sulphinyl precursor route.

The first step in the polymerisation process is a base-induced formation of the *p*-quinodimethane intermediate (**iii**). This reaction is assumed to proceed via the monomer anion (**ii**) which expels a leaving group to yield the actual monomer (**iii**) in the polymerisation. In our case it is not yet clear whether this elimination proceeds via a reversible or an irreversible E_{1cb} elimination mechanism.

The second step in the polymerisation process is the actual polymerisation of the highly reactive *p*-quinodimethane intermediate via either a radical or an anionic pathway, to yield the precursor polymer (**iv**). Independent of the exact mechanism, polymerisation is assumed to proceed via the *p*-xylylene or *p*-quinodimethane intermediate (**iii**). In Scheme 5 the general formation and polymerisation of the *p*-quinodimethane system via the sulphinyl precursor route is depicted. This figure generalises the polymerisation process for all sulphinyl monomers used in this study. We assume that the quinoid structures formed are highly reactive and will be consumed immediately in the polymerisation process. When this assumption is made the copolymer composition can directly be linked to the differences in formation rate of the various actual monomers. The *p*-quinodimethane intermediates of monomers **1**-**3** have strong absorbencies in the UV-Vis around 310-350 nm and the formation can be clearly monitored by this technique. A stop-flow apparatus was used as experimental set up to allow very fast measurements. Monomer and base solutions were injected simultaneously and all measurements were performed in threefold to insure good reproducibility. All UV-Vis measurements were performed in 1,4-dioxane. Monomer concentrations (10^{-4} M) were too low to initiate polymerisation and a fivefold excess of base ($5x10^{-4}$ M; Na*t*BuO) was used to guarantee fast and complete formation of the *p*-quinodimethane system. These conditions are not those used in a real polymerisation reaction but the results obtained give good indications about the formation of the actual monomer. Besides, using identical conditions as in a real polymerisation is impossible since polymerisation will result in a cloudy solution which will prevent light from passing through the sample and measuring will become impossible.

When monomer and base solutions are combined in the measuring cell, a new absorption band appears that originates from the *p*-quinodimethane system. In Figure 8 the formation of the *p*-quinodimethane (λ_{max} = 311 nm) from the PPV monomer **1** is shown. After 14 minutes the maximum absorption intensity is reached and the signal starts to decline again. This is clearly visualised in Figure 9 where the absorption at maximum wavelength (311

nm) is plotted versus time. The decline in absorption can not be caused by solvent substitution since the measurements are performed in the non nucleofilic solvent 1,4-dioxane. Because of the large base excess used, the decrease in *p*-quinodimethane absorption only occurs by base substitution on the quinoid structure to yield the base substituted monomer (**v**). This was proven with mass spectroscopy.

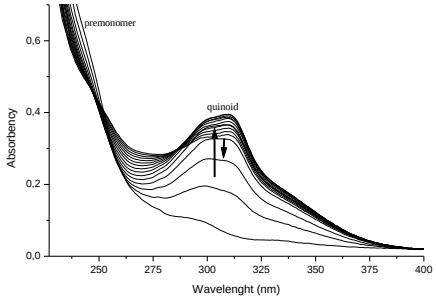

Figure 8: Periodically scanned spectra of quinoid formation and degradation..

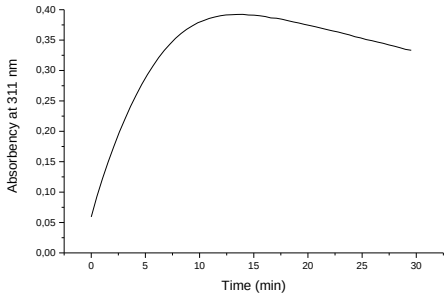

Figure 9: Profile of PPV p-quinodimethane absorbance at 311 nm versus time.

The three different monomers (**1**, **2** and **3**) used in this study were treated to exactly the same conditions (Experimental Part) and formation of the respective *p*-quinodimethane systems was examined. For each monomer, the maximum absorbency is reached after a different time. The quinoid structure from the PPyV monomer **3** reaches its maximum absorbency after 7 minutes whereas the ones from the PPV and OC_1C_{10} monomer (**1** and **2**) reach their maximum absorbencies after 14 and 33 minutes respectively. The maximal absorbencies of the three different monomers versus time are plotted in Figure 10.

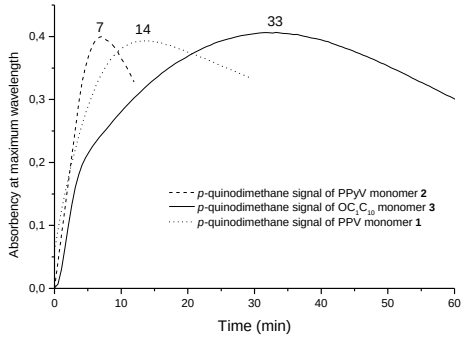

Figure 9: Profiles of the different p-quinodimethane absorbencies at maximum wavelength versus time.

The chemical differentiations on the monomer stage clearly affect the formation rate of the actual monomer and these differences on their turn will significantly influence the copolymer composition. When the results obtained from this UV-Vis study are compared with the ^{13}C-NMR composition analysis of the actual precursor copolymers, the relationship between the quinoid formation rate and the copolymer composition becomes clear. The copolymer systematically contains more repeating units of the monomer that reaches its maximum absorbency first. For example, in copolymerisation **3** (50/50 initial comonomer feed PPV/OC_1C_{10}) the copolymer consists for 68 percent out of PPV units and only 32 percent OC_1C_{10} units. This copolymer composition can directly be correlated to the differences in formation rate between the actual monomers in this polymerisation process as was demonstrated by UV-Vis spectroscopy measurements on the various monomers. This trend is general and can be found in each copolymer composition. In the copolymerisation series between the PPV monomer **1** and the PPyV monomer **3** the differences between the initial comonomer feed and the actual copolymer composition are rather small but the trend remains visible due to the accurate composition determination by quantitative ^{13}C-NMR spectroscopy. When the OC_1C_{10} monomer **2** is copolymerised with the PPyV monomer **3**, copolymers with large content on one monomer were obtained. For these monomers, the UV-Vis study revealed that the reactivity towards quinoid formation is very different and probably too diverse to allow an efficient copolymerisation in 1,4-dioxane via the sulphinyl precursor route. In 1,4-dioxane about 20 percent of PPyV can be incorporated at most. It might be possible to copolymerise these monomers in another

solvent since the quinoid formation rate can be altered significantly by changing the solvent. This will be a topic of further research.

These differences in quinoid formation rate can be linked to the chemical structure of the monomer and one of the important factors is the acidity of the benzylic proton adjacent to the sulphinyl group. This proton has to be abstracted in the first step of the polymerisation process to yield the monomer anion (**ii**). In the next step the leaving group is eliminated and the *p*-quinodimethane intermediate (**iii**) is formed. From the UV-Vis measurements it can be concluded that, the more acid the benzylic proton, the faster the quinoid formation will occur. Faster quinoid formation further leads to a larger amount of the respective repeating unit incorporated in the copolymer. In total the quinoid formation rate is influenced by a lot of factors.[25,26] It is beyond the scope of this work to explain all the aspects involved, for a detailed description we refer to the references sited.

Finally, for this set of copolymerisation reactions, we can conclude that the copolymer composition is determined by the initial comonomer feed and the reactivity of each monomer towards quinoid formation. The relationship between copolymer composition and actual monomer formation has been showed repeatedly. In the end it is possible to more of less predict the copolymer composition in advance if the formation rate of the respective quinoid structures is known from UV-Vis spectroscopic measurements.

4.2.2 OC_1C_{10}-bipyridylene vinylene copolymers

Another interesting copolymer that was investigated is the copolymer between OC_1C_{10} and poly(2,2'-bipyridylene vinylene) (PBPyV).

Monomer- and homopolymer synthesis of poly(2,2'-bipyridylene vinylene) (PBPyV) was discussed in Chapter 3. Incorporation of 2,2'-bipyridine units in the conjugated backbone may result in new copolymers with interesting properties. First, the 2,2'-bipyridine unit is an electron withdrawing heterocycle and hence conjugated polymers with increased electron affinity may result. As mentioned earlier, such polymers may show intrinsically balanced injection/mobility capabilities for both holes and electrons from the opposite electrodes when incorporated in polymer LEDs.[27] Secondly, in these polymers the conjugated backbone plays a dual role as transporting channel for the charge carriers and as a macroligand to chelate with a transition metal complex. The 2,2'-bipyridine unit proves to be highly sensitive towards complexation with a broad range of metal ions.[22,28] In recent years, numerous efforts have been devoted to the design of chemosensory systems that are capable of detecting metal ions in both real-time and reversible fashion.[22] Other possibilities make use of the unique characteristics of particular metal ions, which may be employed to fine-tune the electronic properties of the conjugated polymer in order to perform a desired function. Thirdly, the 2,2'-bipyridine unit may be protonated or alkylated. It has been shown that the optoelectronic properties of conjugated polymers containing bipyridine units can be tuned in this way.[29]

4.2.2.1 Copolymer synthesis

In literature different papers report on the synthesis and characterisation of copolymers between an alkoxy-substituted PPV derivative and poly(2,2'-bipyridylene vinylene) (PBPyV). A Wittig reaction is always used in the polymer synthesis which inherently results in very low molecular weight polymers (M_w below 10000).[22,27] In this work two different copolymers between OC_1C_{10} and poly(2,2'-bipyridylene vinylene) (PBPyV) have been synthesised via the sulphinyl precursor route. (Scheme 6) The idea behind this synthesis was to obtain conjugated polymers that were soluble in organic solvents and that were more electron accepting compared to plain OC_1C_{10}. Moreover, complexation of the

2,2'-bipyridine unit with various metal ligands proved possible. The copolymers were synthesised in CH_2Cl_2 according to the "standard" procedure. (Scheme 6) Note that the OC_1C_{10} monomer **2** is a mixture of equally distributed isomers.

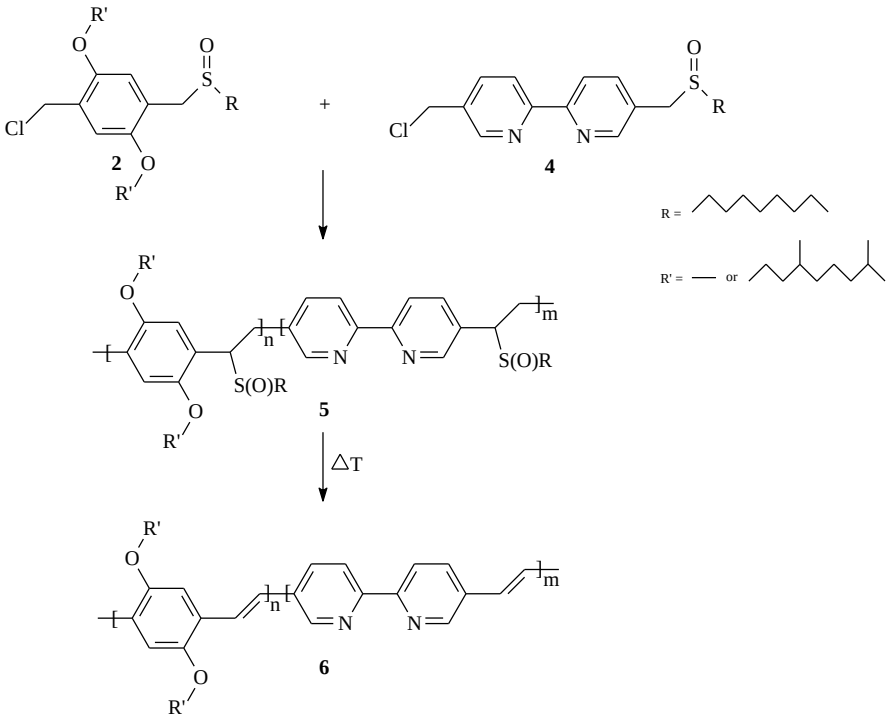

*Scheme 6: Schematical overview of the OC_1C_{10}-poly(2,2'-bipyridylene vinylene) copolymer (**6**) synthesis.*

The initial comonomer ratios were 80/20 and 50/50 OC_1C_{10} monomer **2**/bipyridine monomer **4**. After synthesis and isolation a part of the precursor copolymer (**5**) was converted to the conjugated form by reflux in toluene for 7 hours to yield the soluble conjugated polymers **6**. GPC on the precursor polymers **5** was performed in THF versus PS standards. The exact copolymer composition (OC_1C_{10}/PBPyV) was determined on the precursor stage using ^{1}H- and ^{13}C-NMR spectroscopic techniques. The restfraction of each copolymerisation was analysed using ^{1}H-NMR spectroscopy. Copolymerisation results are summarised in Table 4.

Polymerisation				Copolymer			Restfraction	
Mon **2**[a]	Mon **4**[a]	Yield (%)	M_w (x 10^{-3})	OC_1C_{10}	PBPyV	λ_{max}(nm)[b]	Mon **2**	Mon **4**
80	20	53	94 (2.6)	94	6	477	42	58
50	50	42	72 (6.9)	73	27	449	84	16

[a]: initial mol percentage monomer, [b]: absorption maximum in film, polydispersity in brackets

*Table 4: Copolymerisation results of monomer **2** and **4**.*

Both copolymerisation reactions proceed in moderate yield, increasing the initial amount of bipyridine monomer **4** reduces the polymerisation yield as the polymerisation of this monomer is less effective than that of OC_1C_{10} in CH_2Cl_2. Simultaneously the molecular weight of the polymers drops, nevertheless relatively high molecular weight polymers are obtained in both copolymerisation reactions. In the 50/50 copolymerisation 27 percent of bipyridine monomer **4** is incorporated in the copolymer. When only 20 percent of monomer **4** is present in the initial comonomer feed the amount of bipyridine monomer **4** incorporated in the copolymer falls to about 6 percent. The absorption maximum of this copolymer (477 nm), measured in film, does not differ from the absorption maximum of OC_1C_{10} (478 nm). Incorporation of this small amount of 2,2'-bipyridine monomer **4** does not influence the optical absorption properties of the fully conjugated polymer. It is only when larger amounts of bipyridine monomer are incorporated that the absorption maximum shifts towards the absorption maximum of the homo PBPyV (385 nm). For the 73/27 copolymer (prepared in the 50/50 copolymerisation) the absorption maximum is situated around 449 nm. For this copolymer the "effective conjugation length" is disturbed by the 2,2'-bipyridine repeating units which causes a bleu shifts of about 30 nm.

4.2.2.2 Conversion to the conjugated structure

For these two copolymers, the conversion to the conjugated structure as well as its thermal stability was studied with UV-Vis spectroscopic and DIP-MS measurements.

UV-Vis measurements were performed on films of spincoated precursor polymer **5** at a heating rate of 2°C/min till 300°C. All measurements were performed under a continuous flow of nitrogen. As higher temperatures are reached a new absorption band appears that gradually increases in intensity. The gradual formation of the conjugated structure for the 73/27 copolymer (prepared in the 50/50 copolymerisation) is shown in Figure 11 (solid

lines). At higher temperatures the absorption starts to decline again and simultaneously the absorption maximum bleu shifts which corresponds to a degradation of the conjugated structure (dashed lines). For both copolymers the maximum absorbance intensity is reached at around 110°C and this results in copolymers with absorption maxima at 477 nm (6 percent PBPyV) and at 449 nm (27 percent PBPyV). (Table 4) Incorporation of 27 percent of PBPyV significantly bleu shifts the absorption maximum. When the absorption at the maximum wavelength (477 and 449 nm) is plotted versus temperature the trends in elimination and stability behaviour become clear. (Figure 12) For comparison, comparable curves for the homo OC_1C_{10} and PBPyV polymers are also shown. The conjugated structure of all (co)polymers is formed in approximately the same temperature domain between 65 and 110°C. However the thermal stability of the polymers is quite different. As already shown, OC_1C_{10} is not very stable at elevated temperatures and the maximum absorption quickly starts to decline above 200°C. For PBPyV the absorbance does not decrease at temperatures below 300°C, remember that the small increase in absorbance around 175°C is caused by coupling of two polymer chain thus resulting in an extension of the conjugated system. (Chapter 3 and Chapter 5) The two OC_1C_{10}-PBPyV copolymers show a thermal stability that is intermediate to that of the respective homopolymers. As more bipyridine repeating units are incorporated the thermal stability of the copolymers increases. (Figure 12)

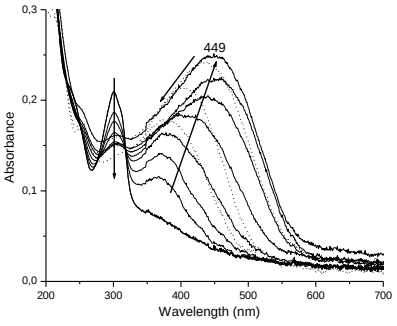

Figure 11: Gradual formation of the conjugated structure for the 73/27 copolymer.

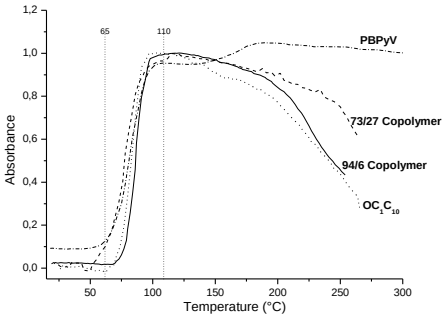

Figure 12: Absorption at the maximum absorption versus temperature.

The thermal elimination and stability behaviour of the copolymers was also studied by DIP-MS measurements. During these measurements a sample of precursor copolymer is heated at 10°C/min from ambient temperature till 650°C under *vacuum*. Both copolymers show a nearly identical thermal behaviour. (Figure 13) The first signal in the thermogram (between 75 and 125°C) corresponds to the formation of the conjugated structure and the second (between 340 and 450°C) relates to its degradation. In the thermogram, the peak maxima for the degradation signals are at slightly different temperatures. The degradation peak maximum (371°C) for the 73/27 copolymer (prepared in the 50/50 copolymerisation) is slightly shifted towards higher temperatures compared to that of the 94/6 copolymer (prepared in the 80/20 copolymerisation). Note that the degradation signal for the homo PBPyV polymer, obtained in an identical measurement, peaks at 453°C. This small variation in degradation temperature is caused by the different chemical composition of the (co)polymers. Like in the UV-Vis measurements, the different thermal stability behaviour of both copolymers is again observed with this technique. In DIP-MS the difference in thermal stability is only small because of the faster heating rate used.

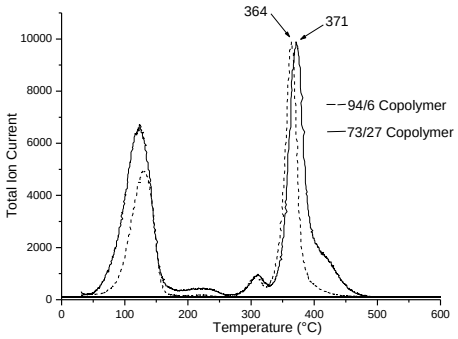

Figure 13: DIP-MS thermogram of the OC_1C_{10}-bipyridine copolymers.

4.2.2.3 Complexating properties

Nowadays, the sensory properties of a variety of materials are under investigation. Among them, the vast majority are either crown ether derivatives or conjugated polymers.[30,31] The appeal of polymers containing molecular recognition sites is that they make use of the high sensitivity of conjugated polymers to external structural perturbations and to electron

density changes within the polymer backbone, when they interact with metal ions. In this work two soluble conjugated copolymers between OC_1C_{10} and poly(2,2'-bipyridylene vinylene) were synthesised. The reasons for selecting the 2,2'-bipyridine unit as a building block is based on the following considerations. It is well-known that 2,2'-bipyridine and its derivatives possess superb ability to coordinate a large number of metal ions.[28] As such, the scope of metal ion sensors could be extended towards new ion-sensitive ensembles. A second reason for selecting the 2,2'-bipyridine unit is the fact that there is approximately a 20° dihedral angle between the two pyridine planes in a 2,2'-bipyridine moiety when it is in its transoid-like conformation. Polymers incorporating these units are therefore not fully conjugated, before complexation they are in a so called "pseudoconjugated form" (**1**). Upon chelating with a metal ion, however, the coordination between the metal ion and bipyridine would force the twisted conformation into a planar one, thus converting the polymer to a fully or nearly fully conjugated entity (**2**). (Scheme 7) Such conjugation enhancement, along with the simultaneous electron density changes caused by incorporating metal ions should generate corresponding changes in optical- and electronic properties of the polymer. In addition, incorporation of a recognition unit in the polymer backbone is expected to give rise to a more sensitive response upon metal ion binding compared to binding sites that are situated outside the polymer backbone.

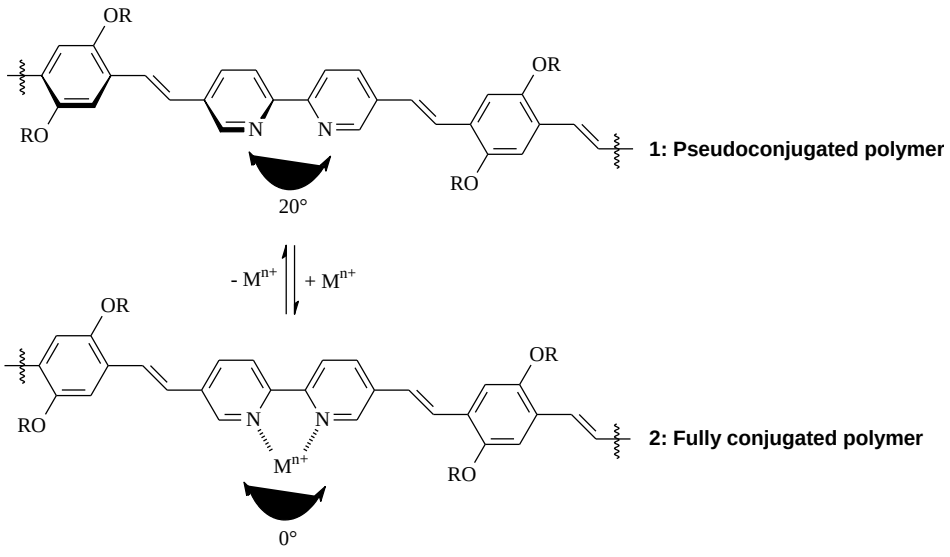

Scheme 7: Conformational changes in the copolymer upon complexation with a metal ion.

The most apparent ionochromic effect of these two copolymers is their *instant* colour change upon the addition of metal salts to the polymer solution. Even the copolymer with very little bipyridine units incorporated still visibly changed colour immediately. In all cases the colour changed from deep red to purple. This illustrates the high sensitivity of these polymers towards complexation. The complexing properties of the copolymers were investigated using UV-Vis measurements in chloroform to which methanolic solutions of various metal salts were added. Upon addition of the metal ion the absorption maximum clearly shifts to higher wavelengths (red-shift), which means the "effective conjugation length" is effectively enhanced. (Figure 14) The ion-free conjugated 73/27 copolymer (prepared in the 50/50 copolymerisation) in chloroform absorbs at a maximum wavelength of 469 nm. The extent of the shift after complexation depends on the nature of the metal ion, different metal ions give rise to different red-shifts. By complexing the copolymer with Cu^{2+} ions a maximum red-shift of 35 nm could be achieved.

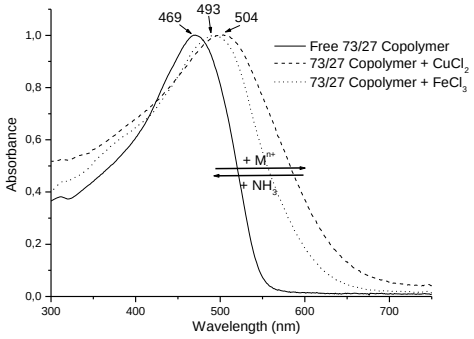

Figure 13: Absorption spectra of the (complexed) 73/27 copolymer (in chloroform).

Identical experiments were also performed on the copolymer prepared in the 80/20 copolymerisation but due to the very low 2,2'-bipyridine content in this copolymer the maximal red-shift that could be observed was 4 nm. The fluorescence emission spectra of the ion-free and the metal ion complexed copolymers were also taken in chloroform. Upon complexation the emission maximum did not change at all but a strong quenching of the emission signal was observed. Even when very low concentrations of metal ions were used, the emission signal was largely quenched. The absorption and emission maxima of the different ion-free and complexes copolymers are summarised in Table 5.

	94/6 Copolymer		73/27 Copolymer	
	Absorption (nm)	Emission (nm)	Absorption (nm)	Emission (nm)
Ion-free	491	546	469	542
Cu^{2+}	494	q	504	q
Fe^{3+}	494	q	493	q
Zn^{2+}	493	q	501	q
Ag^{+}	495	q	497	q

Table 5: Absorption and emission maxima of the various (un)complexed copolymers. q = quenched.

From a practical point of view it is interesting to see whether the metal-ion-induced responsive properties also hold true in the solid state. It is conceivable that conformational changes for a polymer may not occur as readily in the solid state as in solution. To this end the metal ion responsive properties were tested on copolymer films. A solution of the converted copolymer were spincoated on a quarts window that was placed in the UV-Vis spectrometer. The ion-free 73/27 copolymer (prepared in the 50/50 copolymerisation and converted in solution) shows an absorption maximum at 476 nm. As was the case in the solution experiments, a quick colour change, but over a period of a few seconds, was noticed when the polymer film was immersed in methanolic solutions of metal salts. Dipping the polymer film in a $CuCl_2$ solution red-shifts the absorption maximum to 513 nm. (Figure 15)

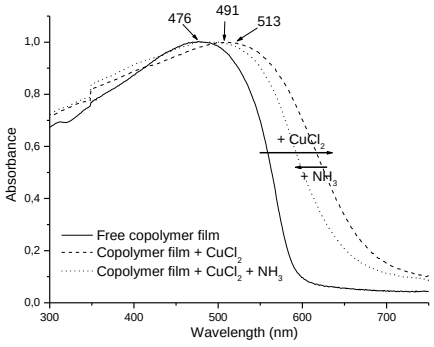

Figure 15: Absorption spectra of the (complexed) 73/27 copolymer (in film).

Also in film a significant shift in maximum absorption wavelength can be seen before and after exposure to the metal ions. Note that the spectra are noticeable broader for the measurements in film.

One important design criterion for a practical chemosensory material is its reversibility. In other words, such a material should be able to produce a measurable signal in the presence of metal ions, but also produce no signal in the absence of such ions. In light of this requirement, conditions were explored in which the metal ions could be removed from the conjugated polymer chain. The strategy behind this is simply to add a competitive ligand, such as ammonia. In fact, this turns out to be a very effective way to convert the metal-ion-chelated polymers to their ion-free states. For example, in the solution experiments the colour of the Cu^{2+} complexed polymers (504 nm) instantly changed from pink to the original red (469 nm) for the non complexed state when a methanolic ammonia solution was added. (Figure 14) In solution complete decomplexation could be achieved instantly upon addition of a competitive ligand. This observation proved also true for the polymer film and here as well a (partial) regeneration to the initial uncomplexed polymer is noticed upon dipping in an ammonia solution. (Figure 15) In film the decomplexation is only partial probably because of the restrictions in conformational changes in the solid state.

4.2.3 OC_1C_{10}-2,5-dicyanophenylene vinylene copolymer

A last copolymer that will be discussed in this chapter is that between OC_1C_{10} and 2,5-dicyanophenylene vinylene. By incorporation of the latter, the electron affinity of the conjugated copolymer will increase significantly when compared to plain OC_1C_{10}. Moreover, when relatively small amounts of dicyano monomer are incorporated the final conjugated copolymer will still be soluble in common organic solvents which will allow an efficient device preparation. Copolymers between an alkoxy-PPV derivative and a cyano containing PPV derivative have been used extensively as soluble high electron affinity copolymers in numerous applications.[14,32,33] The reasons for synthesising high electron affinity polymers have been cited repeatedly throughout this work.

The polymerisation of monomers **2** and **7** was performed in dry 1,4-dioxane according to the "standard" procedure at 30°C. An initial comonomer ratio of 75/25 OC_1C_{10} monomer **2**/dicyano monomer **7** was polymerised and Na*t*BuO was used as a base. Note that monomer **2** is a mixture of two equally distributed isomers.

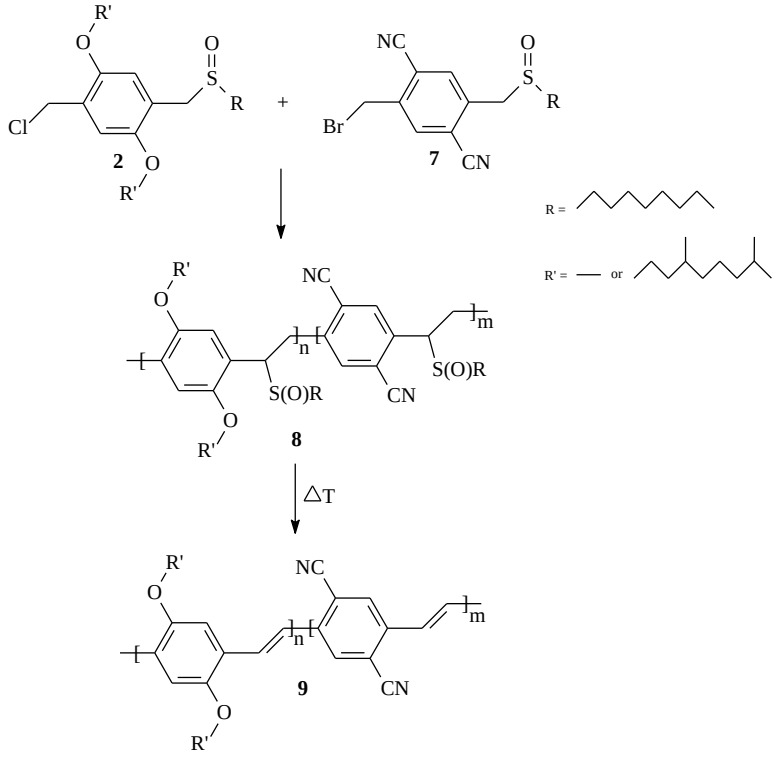

Scheme 8: Schematic overview of the OC_1C_{10}-poly(2,5-dicyanophenylene vinylene) copolymer synthesis.

The precursor polymer **8** was precipitated in MeOH, the filtrate was evaporated and the restfraction was analysed with ^{1}H-NMR spectroscopy. GPC on the precursor polymer was performed in THF versus PS standards. The exact copolymer composition was determined by quantitative ^{13}C-NMR spectroscopic measurements. (Table 6) The high molecular weight copolymer proved to contain 18 percent of dicyano units.

Polymerisation			*Copolymer*				**Restfraction**	
Mon **2**[a]	Mon **7**[a]	Yield (%)	M_w x 10^{-3}	PD	OC_1C_{10}	dicyano	Mon **2**	Mon **7**
75	25	39	100	3.52	82	18	88	12

*Table 6: Analysis of precursor copolymer **8**. [a]: initial mol percentage monomer.*

For this copolymer, the thermal conversion towards the conjugated structure as well as its stability was studied with UV-Vis spectroscopy and DIP-MS measurements.

UV-Vis measurements are performed on films of spincoated precursor copolymer. The quartz window, containing the polymer, is placed in an oven that is placed in the beam of the UV-Vis spectrometer. A dynamic heating program of 2°C/min till 300°C was applied and all measurements were performed under a flow of nitrogen. Even before heating, a small absorption band is already present. (Figure 16) This absorption originates from a few double bonds in the precursor copolymer that are formed prematurely by basic elimination during the polymerisation process. This premature elimination is probably triggered by the presence of the cyano groups on the phenylene ring. These electron withdrawing groups increase the acidity of the proton that has to be abstracted in order to cause basic elimination of the sulphinyl group. As the heating program progresses this absorption signal gradually increases in intensity and the maximum absorption shift towards higher wavelengths. Finally a conjugated copolymer with an absorption maximum around 450 nm is obtained. (Figure 16) When the absorption at this maximum wavelength (450 nm) is plotted versus temperature the trends in elimination and stability behaviour for this copolymer become clear. (Figure 17) For comparison also a similar curve for the homo OC_1C_{10} polymer (473 nm) is plotted as obtained in identical conditions. As can be concluded from this graph, the conjugated structure of both polymers is formed in the same temperature domain between 75 and 110°C. Moreover, the thermal stability of OC_1C_{10} is significantly increased by incorporation of some 2,5-dicyano phenylene vinylene repeating units. For the copolymer the absorption at 450 nm does not start to decline till approximately 250°C whereas the plain OC_1C_{10} is only stable till about 200°C.

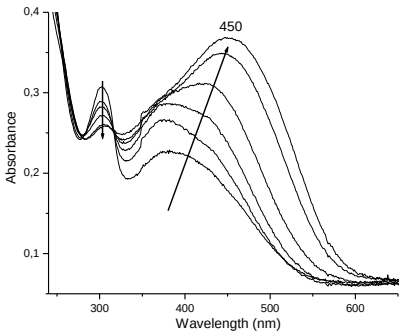

Figure 16: Gradual formation of the conjugated structure.

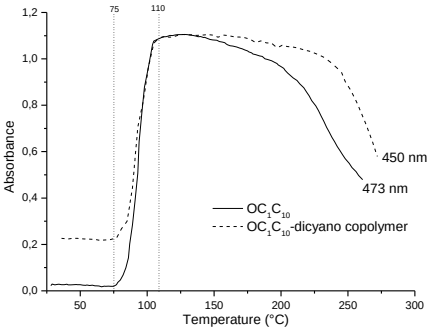

Figure 17: Absorption versus temperature.

The thermal elimination and stability behaviour was also studied with DIP-MS. In these measurements the precursor polymer is heated at 10°C/min till 650°C under *vacuum*. In the DIP-MS thermogram several signals can be observed. (Figure 18) The first one (between 100 and 170°C), based on the fragments detected, corresponds to the elimination of the sulphinyl groups from the precursor polymer to form the double bonds. The second signal (between 340 and 440°C) is caused by the degradation of the conjugated structure and peaks at 375°C.

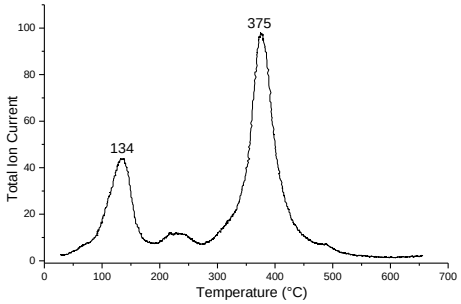

*Figure 18: DIP-MS thermogram of the precursor copolymer **8**.*

4.3 Experimental Section

Materials. All chemicals were purchased from Aldrich or Acros and used without further purification. 1,4-Dioxane was distilled over sodium prior to use.

Characterisation. ^{1}H-NMR spectra were recorded in $CDCl_3$ at 300MHz on a Varian Inova Spectrometer using a 5 mm probe. Chemical shifts (δ) in ppm were determined relative to the residual $CHCl_3$ absorption (7.24 ppm). The ^{13}C-NMR experiments were recorded in $CDCl_3$ at 75 MHz on a Varian VXR 300 spectrometer using a 5 mm broadband probe. Chemical shifts were defined relative to the ^{13}C-resonance shift of $CDCl_3$ (77.0 ppm). Preparative delay time was 60 seconds. Molecular weights and molecular weight distributions were determined relative to polystyrene standards (Polymer Labs) with a narrow polydispersity by Size Exclusion Chromatography (SEC). Separation to hydrodynamic volume was obtained using a Spectra series P100 (Spectra Physics) equipped with a pre-column (5 μm, 50 mm*7.5 mm, guard, Polymer Labs) and two mixed-B columns (10 μm, 2x300 mm*7.5 mm, Polymer Labs) and a Refractive Index (RI) detector (Shodex) at 40°C. SEC samples are filtered through a 0.45 μm filter. HPLC grade THF or DMF (p.a.) is used as the eluent at a constant flow rate of 1.0 ml/min. Toluene is used as flow rate marker.

Direct Insert Probe Mass Spectroscopy analysis was carried out on a Finnigan TSQ 70, electron impact mode, mass range of 35-500. Electron energy is 70 eV. A $CHCl_3$ solution of precursor (co)polymer is applied on the heating element of the direct insert probe. A heating rate of 10°C/min from room temperature till 650°C was used.

In-situ UV-Vis measurements were performed on a Cary 500 UV-Vis-NIR spectrophotometer, specially adopted to contain the Harrick high temperature cell (scan rate 600 nm/ min, continuous run from 200 to 600 nm). Precursor (co)polymer was spincoated from a $CHCl_3$ solution (6 mg/ ml) on a quartz glass (diameter 25 mm, thickness 3mm) at 700 rpm. The quartz glass was heated in the Harrick oven high temperature cell. The cell was positioned in the beam of the UV-Vis-NIR-spectrophotometer (Varian Cary 500 spectrophotometer; interval: 1 nm; scan rate: 600 nm/min; continuous run from 200 to 700 nm) and spectra were taken continuously. The heating rate was 2°C/min up to 300°C. All

measurements were performed under a continuous flow of nitrogen. "Scanning Kinetics software" supplied by Varian is used to investigate regions of interest.

UV-Vis study of the *p*-quinodimethane system. UV-Vis measurements on the *p*-quinodimethane system were carried out in 1,4-dioxane, dried over sodium. Spectra from 200 nm to 400 nm are recorded continuously (interval: 1 nm, scan rate: 600 nm/min) on a Varian Cary 500 spectrophotometer equipped with a stop-flow module. Monomer solution (10^{-4} M) and base solution (Na*t*BuO, 5.4 x 10^{-4} M), prepared in 100 ml flasks dried prior to use, are injected simultaneously. Scanning kinetics software was used to investigate the regions of interest. The maximum absorbency for the *p*-quinoid lays at 311 nm for PPV monomer **1**, at 316 nm for OC_1C_{10} monomer **2** and at 319 nm for PPyV monomer **3**.

Synthesis. Monomer and homopolymer synthesis were reported elsewhere in this dissertation. (Chapter 2 and 3)

PPV-OC_1C_{10}, PPV-PPyV and PPyV-OC_1C_{10} copolymers

All precursor copolymers were synthesised according to a general procedure. The molar monomer feed ratios of the copolymerisations were 75/25; 50/50; 25/75. Solutions of the monomers (5.8 ml, 0.14 M) and base (Na*t*BuO, 2.5 ml, 0.34 M) were prepared and degassed for 1 hour by a continuous flow of nitrogen at 30 °C. The base solution was added in one portion to the stirred monomer solution. During the reaction the temperature was maintained at 30 °C and the passing of nitrogen was continued. After 1 hour the reaction mixture was poured into well stirred ice water whereupon the polymer precipitated. The water layer was extracted with chloroform to ensure that all polymer and residual fraction was collected, and the combined organic fractions were concentrated *in vacuo*. The polymer was precipitated in ether, ether/hexanes or methanol, depending on the copolymer composition, collected by filtration and dried *in vacuo*. The residual fraction was concentrated *in vacuo*. Polymerisation results are summarised in Tables 1-3.

Copolymers 2-4 (PPV/OC_1C_{10}): The precursor polymers were precipitated in hexanes/ether (50/50; 0 °C) and GPC was performed with THF as the eluent. ^{1}H-NMR ($CDCl_3$,300 MHz): δ (ppm) 7.1; 4.1; 3.6; 3.1; 2.1; 1.5; 1.2; 0.8.^{13}C-NMR ($CDCl_3$, 75 MHz): δ (ppm) 152, 139, 133, 130.6, 130.1, 129.8, 129.2, 128, 116, 112, 70.6, 67.8, 57.0, 50.5, 39.9, 38.1, 37.1, 32.4, 30.7, 29.6, 28.7, 25.4, 23.1, 23.3, 23.7, 20.4, 9.9. The exact

copolymer composition was determined with quantitative ^{13}C-NMR spectroscopy. The signal at 150-152.5 ppm arises from the aromatic C-O carbon atoms in OC_1C_{10}. The signals at 139 (1C), 133 (1C) and 129.2-130.6 (4C) ppm originate from the aromatic PPV carbon atoms. The ratios between these signals and the one from the OC_1C_{10} carbon atoms is made and the average of these three results is taken to determine the copolymer composition. The restfraction was analysed with ^{1}H-NMR spectroscopy. ^{1}H-NMR ($CDCl_3$,300 MHz): δ (ppm) 7.32 (4H, dd); 6.91 (2H, d); 6.89 (2H, d); 4.65 (4H, d); 4.56 (2H); 4.1-3.9 (10H, m); 3.8 (9H); 2.6; 1.8-1; 1-0.8. The ratio between the integration of aromatic protons (7.3 ppm versus 6.91 and 6.89 ppm) and the benzylic protons (4.65 ppm versus 4.56 ppm) of the OC_1C_{10} and PPV monomers were calculated to determine the composition of the restfraction. The copolymerisation results are shown in Table 1.

Copolymers 7-9 (PPV/PPyV): The precursor polymers were precipitated in hexanes/ether (50/50; 0 °C) and GPC was performed with DMF as eluent. ^{1}H-NMR ($CDCl_3$,300 MHz): δ (ppm) 8.8; 8.6; 7.9-7.1; 4.1; 3.8; 3.6; 3.1; 2.5-2.1; 1.8-1.6; 1.4-1.0; 0.8. ^{13}C-NMR ($CDCl_3$, 75 MHz): δ (ppm) 150, 138.1, 137.3, 132.7, 132.2, 129.7, 129.2, 128.7, 128.3, 124.1, 69.7, 66.4, 49.7, 36.2, 31.5, 28.9, 28.7, 28.6 , 22.8, 22.4, 13.9. The exact copolymer composition was determined by integrating the carbon signal at 124 ppm that originates from the carbon atom meta to the nitrogen atom in the pyridine ring. The ratio between this integration and the integration of the carbon atoms of the phenylene ring (129-128 ppm) yields the copolymer composition after averaging. The restfraction was analysed with ^{1}H-NMR spectroscopy. ^{1}H-NMR ($CDCl_3$,300 MHz): δ (ppm) 8.47 (1H, d, Jm= 1.8Hz); 7.71 (1H, dd, Jm= 1.8 HZ, Jo= 8.1 Hz); 7.49 (1H, d, Jo= 8.1 Hz), 7.38 (2H, d, Jo= 8.1 Hz), 7.27 (2H, d, Jo= 8.1 Hz); 4.66 (2H); 4.57 (2H); 4.0-3.82 (4H, m); 2.55 (4H, m); 1.8-1.5 (4H, m); 1.4-1.1 (20H); 0.85 (6H, t). The ratio between the two monomers was determined by comparing the integration of all aromatic protons (PPyV monomer **3**: 8.47, 7.71, 7.49 ppm versus PPV monomer **1**: 7.38, 7.27 ppm). Also the ratio between the integration of the benzylic protons for the PPyV monomer (4.66 ppm) and PPV monomer (4.57 ppm) was determined and eventually averaging all these values yielded the composition of the restfraction. The copolymerisation results are shown in Table 2.

Copolymers 12-14 (PPyV/OC_1C_{10}): As shown in Table 3 the precursor polymers were precipitated in different solvents depending on their composition. Determining the exact copolymer composition proved difficult because one of the comonomers was only

incorporated in a very low percentage and ^{13}C-NMR signals only rose slightly above the noise. The ^{13}C-NMR spectra looked just like those of the respective homopolymers. A UV-Vis spectrum of the final conjugated polymer suggested more or less the copolymer composition on the bases of the absorption maximum. The restfraction was analysed with ^{1}H-NMR spectroscopy and in all copolymerisations the restfraction consists purely of OC_1C_{10} monomer **2**. Only when 75 % of PPyV monomer **3** was used in the initial comonomer feed a trace of PPyV monomer remained in the restfraction. The copolymerisation results are shown in Table 3.

OC_1C_{10}-bipyridylene vinylene copolymers: This copolymerisation was performed according to the standard procedure starting from two initial comonomer feeds (mol ratios 80/20 and 50/50) between the OC_1C_{10} monomer **1** and the BPPyV monomer **4**. The polymerisation was performed in dichloromethane at 30°C. The precursor polymers were precipitated in methanol and their molecular weight and polidispersit were determined with GPC versus PS standards. The exact copolymer composition was determined on the precursor copolymer stage using ^{13}C-NMR spectroscopy. ^{1}H-NMR ($CDCl_3$,300 MHz): δ (ppm) 9.1-8.5, 8.1, 7.0, 6.7, 4.1, 4.0-3.4, 2.6, 1.8-1.1, 0.8. ^{13}C-NMR ($CDCl_3$, 75 MHz): δ (ppm) 156.2, 155.6, 152.2, 151.6, 149.8, 149.3, 136.9, 136.3, 130.5, 129.6, 121.3, 69.6, 66.8, 49.3, 36.1, 31.3, 28.8, 28.7, 28.6, 22.6, 22.4, 14.2. The exact copolymer composition was determined by calculating the integration of the different signals in the ^{13}C-NMR spectrum, mainly those of the aromatic carbon atoms and comparing one with the other. The ratio between the signals at 156.2 and 155.6 ppm or that at 121.3 ppm (which belong to the bipyridine unit) and the signals at 130.5 and 129.6 ppm (which belong to the OC_1C_{10} unit) yields the exact copolymer composition. The restfraction of each copolymerisation was analysed with ^{1}H-NMR spectroscopy. ^{1}H-NMR ($CDCl_3$,300 MHz): δ (ppm) 8.85; 8.21; 6.90; 4.66; 4.56; 4.1; 3.92; 3.77; 3.65; 2.6; 1.8-1.1; 0.88. The ratio between the two monomers was determined by comparing the integration of all aromatic protons (BPPyV monomer **4**: 8.85 and 8.21 ppm versus OC_1C_{10} monomer **2**: 6.9 ppm). Also the ratio between the integration of the benzylic protons for the BPPyV monomer (4.66 ppm) and OC_1C_{10} monomer (4.56 ppm) was determined and eventually averaging all these values yielded the composition of the restfraction. Polymerisation results for these two copolymers are summarised in Table 4.

Polymer-Metal complex formation: The precursor copolymers were converted to the conjugated form by reflux in toluene for 7 hours under argon atmosphere. After cooling down the fully converted copolymer was precipitated in cold methanol (0°C) and collected. The polymer-metal complex solutions used for the optical measurements were prepared from a polymer solution (13.8 mg conjugated copolymer in 2 ml chloroform) and a metal salt solution (10^{-3} Min methanol). From the copolymer solution was always taken 10 µl (syringe) and this was further diluted in a cuvette by addition of 2.4 ml chloroform. To this solution was added (drop wise) the methanolic metal solution and the absorption spectrum was taken till the maximum stayed at a constant wavelength. Decomplexation was accomplished by addition of one drop of a methanolic ammonia solution which resulted in regeneration of the original deer red colour. The polymer films were made by spin-coating solutions of the copolymer on a quartz window.

OC_1C_{10}-2,5-dicyanophenylenevinylene copolymer: This copolymer was synthesised in dry 1,4-dioxane according to the "standard" procedure. The initial mol ratio between the comonomers was 75/25 (OC_1C_{10} monomer **2**/cyano monomer **7**). Na*t*BuO was used as the base and the temperature was set at 30°C. After work-up the precursor copolymer was precipitated in methanol, collected and dried *in vacuo*. FT-IR (KBr, film): ν (cm^{-1}) 2954, 2902 (aliphatic stretchings), 2224 (CN stretching), 1629, 1505, 1463, 1410, 1214, 1040 (SO stretching). ^{1}H-NMR ($CDCl_3$,300 MHz): δ (ppm) 7.9, 7.0, 6.7, 4.1, 4.0-3.4, 2.6, 1.8-1.1, 0.8. ^{13}C-NMR ($CDCl_3$, 75 MHz): δ (ppm) 152.1, 151.5, 143.2, 136.9, 136.3, 136.1, 130.5, 129.6, 118.2, 117.4, 116.3, 115.5, 69.5, 66.6, 49.1, 36.1, 31.2, 28.7, 28.6, 28.5, 22.6, 22.4, 14.5. The exact copolymer composition was determined by calculating the integration of the different signals in the ^{13}C-NMR spectrum, mainly those of the aromatic carbon atoms and comparing one with the other. The ratio between the signals at 143.2 and 136 ppm or that at 118.2 and 117.4 ppm (which belong to the dicyano phenylene unit) and the signals at 130.5, 129.6 ppm and 152.1, 151.5 ppm (which belong to the OC_1C_{10} unit) yields the exact copolymer composition. The restfraction of the copolymerisation was analysed with ^{1}H-NMR spectroscopy. ^{1}H-NMR ($CDCl_3$,300 MHz): δ (ppm) 8.89; 8.81; 6.90; 4.60; 4.56; 4.1; 3.92; 3.77; 3.65; 2.6; 1.8-1.1; 0.85. The ratio between the two monomers was determined by comparing the integration of all aromatic protons (cyano monomer **7**: 8.89 and 8.81 ppm versus OC_1C_{10} monomer **2**: 6.9 ppm). Also the ratio between the integration of the benzylic protons for the cyano monomer (4.60 ppm) and

OC_1C_{10} monomer (4.56 ppm) was determined and eventually averaging all these values yielded the composition of the restfraction. Polymerisation results for this copolymer are summarised in Table 5.

4.4 References

[1] Martin, R. E.; Geneste, F.; Chuah, B. S.; Fischmeister, C.; Ma, Y; Holmes, A. B.; Riehn, R.; Cacialli, F.; Friend, R. H. *Synth. Met.* 122, **2001**, 1.

[2] Lee, Y.-Z.; Chen, X.; Chen, S.-A.; Wei, P.-K; Fann, W.-S. *J. Am. Soc. Chem.* 123, **2001**, 2296.

[3] Morgado, J.; Cacialli, F.; Friend, R. H.; Chuah, B. S.; Rost, H.; Holmes, A. B. *Macromolecules* 34, **2001**, 3094.

[4] Morgado, J.; Cacialli, F.; Friend, R. H.; Chuah, B. S.; Rost, H.; Moratti, S. C.; Holmes, A. B. *Synth. Met.* 119, **2001**, 595.

[5] a) Pei, Q.; Yu, G.; Zhang, C.; Yang, Y.; Heeger, A. J. *Science* 269, **1995**, 1086 b) Pei, Q.; Yu, G.; Zhang, C.; Yang, Y.; Heeger, A. J. *J. Am. Chem. Soc.* 118, **1996**, 3922.

[6] Benjamin, I.; Faraggi, E. Z.; Avny, Y.; Davidov, D.; Neumann, R. *Chem. Mater.* 8, **1996**, 352.

[7] Martin, R. E.; Geneste, F.; Riehn, R.; Chuah, B. S.; Cacialli, F.; Holmes, A. B.; Friend, R. H. *Synth. Met.* 119, **2001**, 43.

[8] Hoofman, R. J. O. M.; de Hass, M. P.; Siebbeles, L. D. A.; Warman, J. M. *Nature* 392, **1998**, 54.

[9] a) Blom, P. W. M.; de John, M. J. M.; Vleggaar, J. J. M. *Appl. Phys. Lett.* 68, **1996**, 3308. b) Martens, H. C. F.; Huiberts, J. N.; Blom, P. W. M. *Appl. Phys. Lett.* 77, **2000**, 1852.

[10] Blom, P. W. M.; Vissenberg, M. C. J. M. *Phys. Rev. Lett.* 80, **1998**, 3819.

[11] a) Uchida, M.; Ohmori, Y.; Noguchi, T.; Ohnishi, T.; Yoshino, K. *Jpn. J. Appl. Phys.* 32, **1993**, L921. b) Zhang, C.; Höger, S.; Pakbaz, K.; Wudl, F.; Heeger, A. J. *J. Electron. Mater.* 23, **1994**, 543. c) Cimrova, V.; Neher, D.; Remmers, M.; Kminek, I. *Adv. Mater.* 10, **1998**, 676.

[12] a) Brown, A. R.; Bradley, D. D. C.; Burroughes, J. H.; Friend, R. H.; Greenham, N. C. *Appl. Phys. Lett.* 61, **1992**, 2793. b) Berggren, M.; Gustafsson, G.; Inganäs, O.; Andersson, M. R.; Hjertberg, T.; Wennerström, O. J. *Appl. Phys.* 76, **1994**, 7530.

[13] a) Braun, D.; Heeger, A. J. *Thin Solid Films* 216, **1992**, 96. b) Parker, I. D. *J. Appl. Phys.* 75, **1994**, 1656.

[14] Greenham, N. C.; Moratti, S. C.; Bradley, D. D. C.; Friend, R. H.; Holmes, A. B. *Nature* 365, **1993**, 628.

[15] Strukelj, M.; Papadimitrakopoulos, F.; Miller, T. M.; Rothberg, L. J. *Science* 267, **1995**, 1969.

[16] Peng, Z.; Galvin, M. E. *Chem. Mater*. 10, **1998**, 1785.

[17] Xiao, Y.; Yu, W.-L.; Pei, J.; Chen, Z.; Huang, W.; Heeger, A. J. *Synth. Met.* 106, **1999**, 165.

[18] a) Xiao, Y.; Yu, W.-L.;Chua, S.-J.; Huang, W. *Chem. Eur. J.* 6, **2000**, 1318. b) Pinto, M.R.; Hu, B.; Karasz, F. E.; Akcelrud, L. *Polymer* 41, **2000**, 8095.

[19] Riehn, R.; Morgado, J.; Iqbal, R.; Moratti, S. C.; Holmes, A. B.; Volta, S.; Cacialli, F. *Macromolecules* 33, **2000**, 3337.

[20] Lo S-C.; Palsson L-O.; Kilitziraki M.; Burn P. L.; Samuel I. D. W. *J. Mat. Chem*. 11, **2001**, 2228.

[21] a) Brütting W.; Meier M.; Herold M.; Karg S.; Schwoerer M. *Synth. Met*. 91, **1997**, 163. b) Andersson A.; Kugler T.; Logdlund M.; Holmes A. B.; Li X.; Salaneck W. R. *Synth. Met.*, **1999**, *106*, 13.

[22] Wasielewski, M. R.; Wang, B. *J. Am. Chem. Soc.* 119, **1997**, 12.

[23] van Breemen, A. *Ph.D. Dissertation*, **1999**, Limburgs Universitair Centrum, Diepenbeek, Belgium.

[24] Gillissen S. (Me); Jonforsen, M.; Kesters, E.; Johansson, T.; Theander, M.; Andersson, M. R.; Inganas, O.; Lutsen, L.; Vanderzande D. *Macromolecules* 34, **2001**, 7294.

[25] a) Cho, B. R.; Kim, Y. K.; Han, M. S. *Macromolecules* 31, **1998**, 2098. b) Cho, B. R.; Kim, T. H.; Kim, Y. K.; Kim, N. S. *Macromolecules* 32, **1999**, 3583. c) Cho, B. R.; Kim, T. H.; Son, K. H.; Kim, Y. K.; Lee, Y. K.; Jeon, S.-J. *Macromolecules* 33, **2000**, 8167.

[26] Cho, B. R. *Prog. Polym. Sci.* 27, **2002**, 307.

[27] a) Wang, L.-H.; Kang, E.-T.; Huang, W. *Polymer* 42, **2001**, 3949. b) Wang, L.-H.;Chen, Z.-K.; Xiao, Y.; Kang, E.-T.; Huang, W. *Macromol. Rapid Commun.* 21, **2000**, 897.

[28] Kaes, C.; Katz, A.; Hosseini, M. W. *Chem. Rev.* 100, **2000**, 3553.

[29] Eichen, Y.; Nakhmanovich, G.; Gorelik, V.; Epshtein, O.; Poplawski, J. M.; Ehrenfreund, E. *J. Am. Chem. Soc.* 120, **1998**, 10463.

[30] Gerard, M.; Chaubey, A.; Malhotra, B. D. *Biosensors & Bioelectronics* 17, **2002**, 345.

[31] a) Heeger, P. S.; Heeger, A. J. *PNAS* 96, **1999**, 12219. b) Chen, L.; McBranch, D. W.; Wang, H.-L.; Helgeson, R.; Wudl, F.; Whitten, D. G. *PNAS* 96, **1999**, 12287.

[32] a) Moratti, S. C.; Cervini, R.; Holmes, A. B.; Baigent, D. R.; Friend, R. H.; Greenham, N. C.; Grüner, J.; Hamer, P. J. *Synth. Met.* 71, **1995**, 2117. b) Samuel, I. D. W.; Rumbles, G.; Collison, C. J. *Phys. Rev. B* 52(16), **1995**, 573. c) Yu, Y.; Lee, H.; Vanlaeken, A.; Hsieh, B. R. *Macromolecules* 31, **1998**, 5553. d) Liu, M. S.; Jiang, X.; Liu, S.; Herguth, P.; Jen, A. *Macromolecules* 35, **2002**, 3532. e) Detert, H.; Sugiono, E. *Synth. Met.* 115, **2000**, 89.

[33] a) Xiao, Y.; Yu, W.-L.; Pei, J.; Chen, Z.; Huang, W.; Heeger, A. J. *Synth. Met.* 106, **1999**, 165. b) Xiao, Y.; Yu, W.-L.;Chua, S.-J.; Huang, W. *Chem. Eur. J.* 6, **2000**, 1318. c) Pinto, M.R.; Hu, B.; Karasz, F. E.; Akcelrud, L. *Polymer* 41, **2000**, 8095.

Chapter 5

Xanthates.*

5.1 The xanthate precursor route

As already outlined in the introduction, several precursor routes exist towards the synthesis of PPV. The precursor route to which the least attention was devoted to till now is the xanthate precursor route.[1,2] Nevertheless, the xanthate precursor route shows interesting prospects. In this precursor route a xanthate group (-SC(S)OEt) is used as thermally eliminable group to yield the double bound. The xanthate precursor polymers are soluble in organic solvents which makes them processable. Son *et al*. reported higher external quantum efficiencies for xanthate prepared PPV compared to Wessling PPV.[1] They explained this increase by the presence of more *cis*-linkages in the conjugated polymer which causes shorter "effective conjugation lengths" and makes the material more amorphous. However, a recent publication by Burn *et al.* questions this explanation, they contribute the higher efficiencies to the absence of harmful interactions between elimination products and ITO in a LED where xanthate prepared PPV is used as active material.[2] It has been shown that hydrogen chloride which is produced during the elimination step in the Wessling and Gilch route reacts with ITO and thus reduces PL.[2,3,4] This clearly shows the potential of the xanthate group in the synthesis of PPV and the importance of a controlled elimination reaction in a device structure. Very recently some papers have appeared that use the xanthate group in the synthesis of some new PPV derivatives.[5,6,7]

---

* Part of this chapter was published in *Macromolecules* by Kesters, E.; Gillissen, S.; Motmans, F.; Lutsen, L.; Vanderzande, D. 35 (21), **2002**, 7902-7910.

Of interest to us is an evaluation of the possibilities the xanthate group offers in the synthesis of PPV and some derivatives that are hard or impossible to realize via the sulphinyl precursor route. To serve this purpose, three different monomers, combining sulphinyl and xanthate properties (Scheme 1) were synthesised and polymerised. Once the precursor polymers were formed, the thermal conversion to the conjugated structure was studied with *in-situ* FT-IR, *in-situ* UV-Vis-spectroscopy, TGA and DIP-MS.

5.1.1 Monomer synthesis and polymerisation reactions

In literature, monomers used in the xanthate precursor route are synthesised from a dihalogenide in a single step reaction.[5,7] Usually the *O*-ethyl xanthatic group (-SC(S)OEt) is used. A drawback of the xanthate precursor route is the rather strict way in which the polymerisation has to be carried out. Dry THF is needed as a solvent and the polymerisation temperature must be sufficiently low to get good polymerisation yields and high molecular weight polymers. In the sulphinyl precursor route, the polymerisation conditions are less strict and polymerisations can proceed in a wide range of solvents at different temperatures.[9] Another advantage of the sulphinyl precursor route is the broad scope of PPV derivatives that can be synthesised whereas for the xanthate precursor route, so far, only a few PPV derivatives have been reported.[1,2,5,6,7] Another point worth mentioning is the fact that a sulphinyl group generally eliminates at lower temperatures compared to the xanthate group.

Despite the shortcomings of the xanthate precursor route, we have an interest in exploring a combination of both xanthate and sulphinyl precursor routes towards the synthesis of PPV in order to acquire a better understanding of the influence of the eliminable group on the properties of the final conjugated polymer. For this purpose, three different monomers (**3**, **4** and **5**) were synthesised. All monomers consist of a classical 1,4-xylene unit to which different groups (xanthate, chlorine or sulphinyl) are attached. In the traditional symmetrical bisxanthate monomer **3** there is no chemical differentiation between polariser and leaving group. In monomer **4** one xanthate group is replaced by a chlorine atom and in monomer **5** a sulphinyl group is introduced. These chemical modifications on the monomer stage allow to evaluate the outcome of the polymerisation in relation to the chemical structure of the monomer.

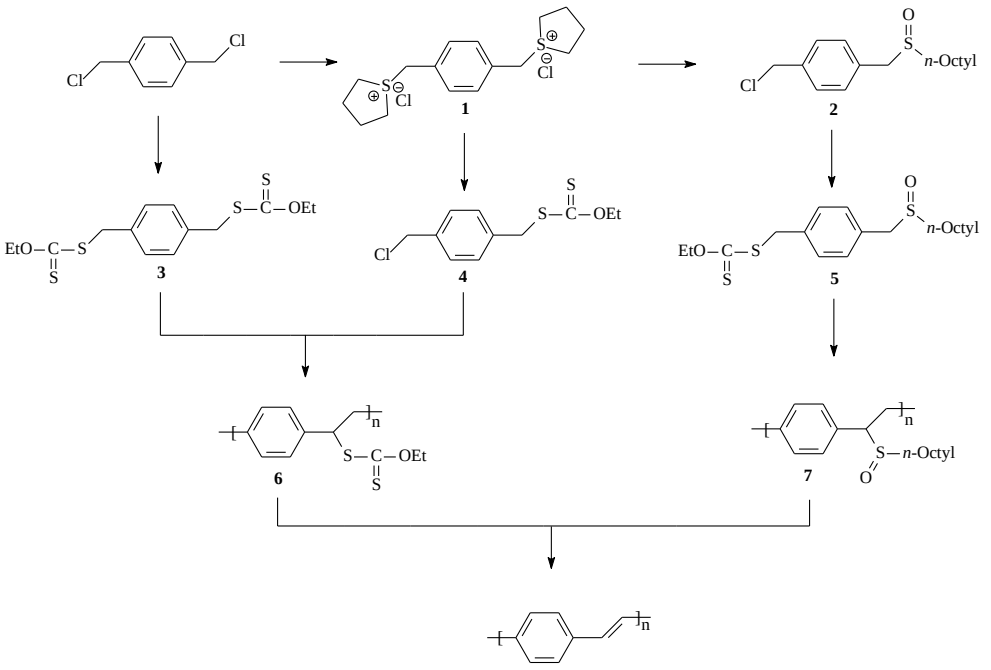

Scheme 1: Different synthetic pathways towards PPV.

The different synthetic pathways to PPV are shown in Scheme 1. The bisxanthate monomer **3** was synthesised from its dichloro analogue whereas the monoxanthate monomer **4** was synthesised departing from the bissulfonium salt **1**. This approach is similar to the one used in the very selective synthesis of the classical PPV sulphinyl monomer (**2**).[13] The one thing that differs is that no additional base had to be used during this reaction. In the classical monomer synthesis N*a*t*B*uO is needed to transform the thiol to the thiolate before being brought together with the bissulfonium salt **1**. In the synthesis of monomer **4** however, the potassium *O*-ethyl xanthatic salt already is in its deprotonated form and can abstract a proton from the bissulfonium salt **1** to form the quinoid structure. In this way the mono xanthate monomer **4** could be synthesised in 78 percent selectivity. Attempts to make compound **4** directly from the dichloride were less selective and a difficult chromatographic separation had to be carried out to separate the different products formed in this reaction. The sulphinyl-xanthate monomer **5** was synthesised by reacting the classical sulphinyl monomer **2** with and excess of potassium *O*-ethyl xanthic acid salt in THF.

These three monomers (**3**, **4** and **5**) were all polymerised in the same "standard" conditions. (Experimental Section) Each monomer was polymerised at three different temperatures and

dry THF was used as a solvent in all polymerisation reactions. Potassium *tert*-butoxide was used as a base and was added in solution in a slight excess of 1.05 equivalents. Polymerisation time was 1 hour, after which the reaction mixture was poured into ice water. The polymer was extracted with chloroform, concentrated and precipitated in diethylether/hexanes. The precursor polymers were soluble in organic solvents such as chloroform and THF.

Molecular weights and polydispersities were determined by GPC versus PS standards (eluent THF). Monomers **3** and **4** were polymerised to the xanthate precursor polymer **6** at –20, 0 and 30°C. The spectral data for these xanthate precursor polymers are consistent with those in literature.[1,2] Monomer **3** could only be polymerised to high molecular weight polymer at temperatures equal or lower than 0°C whereas in the case of monomer **4** high molecular weight polymers were obtained at all temperatures tested. (Table 1) Polymerisation yields vary from rather low to good but no clear trend can be observed. Note that the polydispersities of the precursor polymers obtained from monomer **4** are significantly higher then those obtained for the polymerisation of monomer **3**. From Table 1 we observe an inverse relationship between the molecular weight and the temperature at which the polymerisation is performed. Decreasing the temperature in both cases leads to higher molecular weight precursor polymers. This observation is in accordance with our experience in the polymerisation of monomer **2** via the sulphinyl precursor route. On the other hand, within a certain temperature domain (0-60°C), the polymerisation yield for the classical sulphinyl monomer **2** is relatively independent of temperature.[8] This is in contrast with the data obtained for the polymerisation of the bisxanthate monomer **3**.

	Temp (°C)	Yield (%)	M_w (x10^{-3})	PD
	-20	35	313	3.5
6 from 3	0	34	300	2.6
	30	15	25	2.0
	-20	55	472	5.1
6 from 4	0	26	272	5.5
	30	35	202	5.6
	0	23	1.6	1.3
7 from 5	30	35	1.6	1.2
	50	65	1.6	1.3

*Table 1: Polymerisation results of the monomers **3**, **4** and **5**. M_w and PD were determined by GPC versus PS standards using THF as eluent.*

Monomer **5** was polymerised at 0, 20 and 50°C. For this monomer higher polymerisation temperatures were needed to keep the reagents soluble. To our surprise all polymerisations of monomer **5** only yielded oligomer fragments of the sulphinyl precursor **7**. GPC showed these oligomers all had very similar molecular weights. Increasing the polymerisation temperature left the molecular weight unchanged but the polymerisation yield increased significantly. (Table 1) ^{1}H and ^{13}C NMR spectroscopy on oligomer **7** clearly showed different signals for the sulphinyl groups in the main chain compared to those situated at the end of the oligomer chain. In Figure 1 an enlarged part of the ^{13}C-NMR spectrum for oligomer **7** is shown. Chemical shifts of the carbon atoms 1 and 2 (51.0 and 57.5 ppm respectively) are identical to the ones observed for the respective atoms in monomer **5** and are thus assigned to the sulphinyl end groups. The signals 3, 4 and 5 belong to carbon atoms situated in the internal part of the oligomer chain as was concluded by comparing the chemical shifts to those of a high molecular weight sulphinyl precursor polymer. The signal for carbon atom 5 (49.5 ppm) is shifted upfield compared to the reciprocal signal of carbon 1. Signals 3 (36.0 ppm) and 4 (70.1 and 65.5) originate from the carbon atoms in the ethylene bridge that connects the different repeating units. Because of the asymmetric carbon 4 together with the asymmetric sulphinyl group, four different diastereomers per monomeric unit are formed during the polymerisation. This phenomenon causes the two

different signals observed for carbon atom 4. Furthermore, the integration of both types of sulphinyl groups proved to be nearly identical which suggests that the different sulphinyl groups exist for approximately an equal amount.

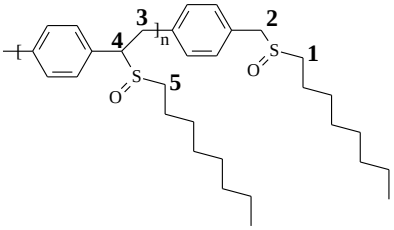

*Scheme 2: Chemical structure of oligomer **7**, showing both types of sulphinyl groups.*

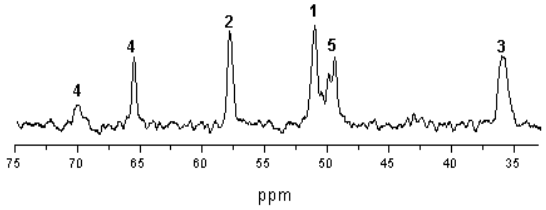

*Figure 1: Part of the ^{13}C-NMR spectrum of oligomer **7**.*

Combination of a xanthate group (leaving group) and a sulphinyl group (polariser) in the same monomer apparently limits the polymerisation capabilities. A similar phenomenon was observed in the polymerisation of the xanthate-sulphinyl thienylene monomer. (Chapter 3) For this monomer towards PTV, UV-Vis measurements in solution had shown that the quinoid structure is actually formed but this reactive species is readily consumed by the co-occurring and undesired solvent substitution reaction. UV-Vis measurements on monomer **5** did not show any quinoid formation. If formed at all, the actual monomer concentration (quinoid structures) will constantly be very low and it is unlikely that a radical chain polymerisation will propagate towards high molecular weight polymers. That quinoid formation can be observed in the case of the xanthate-sulphinyl thienylene monomer, whilst it is apparently impossible to detect in the case of monomer **5**, can be explained by the differences in resonance energy of the aromatic moieties. It is well know that hetero aromatic rings (such as thiophene, furan, pyridine…) can be transformed to their respective quinoid structures much easier than the phenylene counterpart.[9] Due to the presence of the hetero atom, the former have lower resonance energies compared to phenylene and consequently the aromaticity is easier broken to form the quinoid structure. For monomer **5** the actual quinoid formation is to be expected the limiting step in the complete polymerisation process. Further research is needed on this topic to reveal the exact polymerisation mechanism.

5.1.2 Thermal conversion of the xanthate precursor polymer (6)

The final step in both the sulphinyl and xanthate precursor route is a thermal elimination reaction to form the double bond. In the latter the xanthate group is eliminated by a modified Chugaev reaction to yield the double bond. The xanthate group is attached to the polymer backbone via the sulphur atom instead of the oxygen atom in a normal Chugaev reaction. This effectively lowers the elimination temperature and also simplifies the monomer synthesis.[1] The elimination products that are liberated during elimination are unstable and further react to form ethanol and carbondisulphide on the one hand and ethanethiol and carbonoxysulphide on the other hand.[10,11] The conversion to the conjugated structure, as well as its thermal stability, was studied by different techniques. The ones used here are *in-situ* FT-IR, *in-situ* UV-Vis-spectroscopy, TGA and DIP-MS.

The elimination behaviour of all xanthate precursor polymers **6** proved to be identical, independent of the monomer (**3** or **4**) or temperature used during polymerisation. For a more detailed description of the elimination behaviour of this sort of precursor polymers we refer to the dissertation of Els Kesters.[12]

The *in situ* FT-IR and UV-Vis experiments were performed on films of spin-coated precursor polymer **6**. The combined measurements confirm the presence of *cis* double bonds in the conjugated structure as was reported earlier.[1] Furthermore, our measurements showed that at higher temperatures, an isomerisation process of the *cis*-double bonds into the thermodynamically more favourable *trans*-double bonds occurs. (Scheme 3)

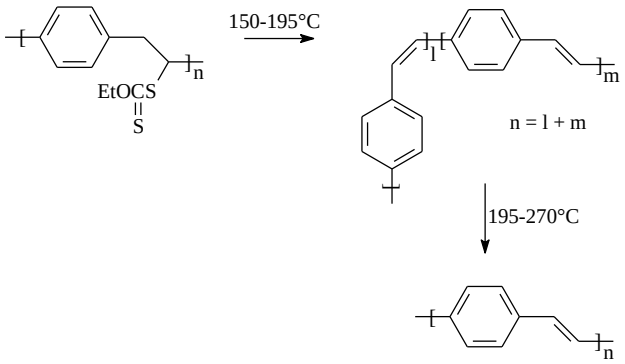

*Scheme 3: Schematical overview of the elimination reaction and isomerisation of a xanthate precursor polymer **6** to PPV.*

In Figure 2 the evolution of the most distinct IR signals versus temperature is shown. Both the thermal xanthate elimination (1218 cm^{-1}) and the *cis* and *trans*-double bond formation start around 150°C. Between approximately 195 and 270°C the signal of the *cis*-vinylene double bond at 858 cm^{-1} decreases again while the signal of the *trans*-vinylene double bond (956 cm^{-1}) still slightly increases in this temperature domain. In this temperature interval the xanthate groups (1218 cm^{-1}) have already been eliminated completely and the slight increase in *trans*-vinylene double bond signal can not be caused by the elimination of additional xanthate groups. This phenomenon is interpreted as an isomerisation process of the *cis*-double bonds into the thermodynamically more favourable *trans*-double bonds. The signal of the *p*-phenylene C-H out-of-plane deformation at 834 cm^{-1} also increases during the elimination process.[10]

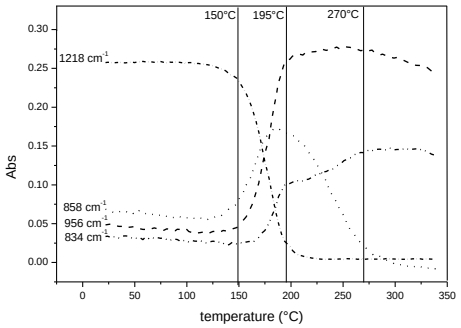

*Figure 2: Evolution of the most distinct IR signals of xanthate precursor polymer **6** versus temperature.*

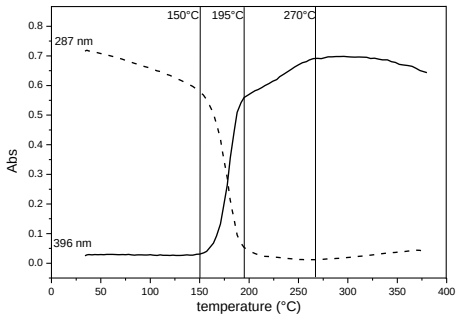

Figure 3: UV absorptions at 287 and 396 nm versus temperature.

Figure 3 shows the UV-Vis absorptions at 287 and 396 nm versus temperature as obtained from the *in situ* UV-Vis measurements. It is clear that the absorption spectrum develops in two distinct steps, a first step between 150°C and 195°C (fast) leading to a λ_{max} value of 386 nm and a second step between 195°C and 270°C (slower) which results in the maximal conjugated PPV structure with a λ_{max} at 396 nm. The first step coincides with the decrease in IR of the xanthate signal, and this indicates that on elimination of the xanthate group the "effective conjugation length" is limited by the simultaneous formation of *trans* and *cis* double bonds in the backbone of the conjugated system. The second step leads to an increase of "effective conjugation length" as demonstrated by the red shift of λ_{max}. This

second increase coincides with the decrease of the signal in IR of the *cis* double bonds (858 cm^{-1}) and is again attributed to the *cis-trans* isomerisation.
Combination of these different data clearly demonstrates the *cis-trans* isomerisation process in the temperature domain between 195 and 270°C. It is also concluded that when the elimination of the xanthate precursor polymer **6** towards a PPV is performed below 195°C a mixed *cis-trans* configuration will be obtained. To obtain an all *trans* PPV structure the conversion should be performed above 200°C.

5.1.3 Thermal conversion of the sulphinyl precursor polymer (7)

The study of the thermal elimination and stability of precursor polymer **7** shows quite different results because here a sulphinyl group is eliminated to yield the double bond. In general much lower temperatures are needed to convert a sulphinyl precursor polymer to the conjugated structure compared to the xanthate precursor polymer.[13] As mentioned earlier, GPC showed that precursor polymer **7** is an oligomer and the elimination and stability behaviour of oligomers is somewhat different from that of the corresponding high molecular weight polymers.[18] Indeed in oligomer **7** a relatively large percentage of the sulphinyl groups act as end groups which allows to study the thermal stability behaviour of such sulphinyl end groups separately from to the sulphinyl groups in the internal part of the oligomer backbone.
The first techniques used to study the thermal behaviour of oligomer **7** were DIP-MS and TGA. Surprisingly, both techniques show three signals in the thermogram which could be assigned based on the fragments detected in MS. The first signal (80-150°C), based on the fragments detected, corresponds to the elimination of the sulphinyl groups in the internal part of the polymer chain and the formation of the double bonds. Again on the bases of the fragments detected, the second signal (200-300°C) can be assigned to the splitting off of the sulphinyl end groups. This phenomenon will from now on be referred to as sulphinyl end group thermolysis. Chemically this process proceeds in a totally different way compared to the elimination process of the sulphinyl groups in the internal part of the oligomer chain. As becomes clear from these measurements, both processes are kinetically separated. The third signal (400-550°C) in the thermogram relates to the degradation of the conjugated structure.

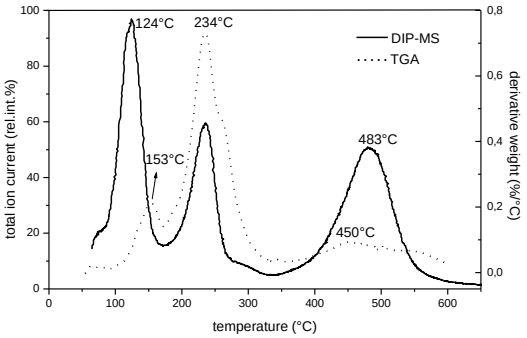

*Figure 7: TGA (dashed line) and DIP-MS (solid line) thermogram of sulphinyl precursor oligomer **7**.*

The thermal stability of oligomer **7** was also studied with *in-situ* FT-IR and *in situ* UV-Vis spectroscopy. Experiments were carried out on films of spin-coated precursor oligomer **7** and a non-isothermal heating rate of 2°C/min up to 275°C under a continuous flow of nitrogen was used. In Figure 8 the IR spectra at 4 different temperatures (60, 100, 175 and 250°C) are shown. At 60°C the main absorptions arise from the sulphinyl stretching (1043 cm^{-1}) and from stretchings in the aliphatic region (2750-3000 cm^{-1}). When higher temperatures are reached both these absorptions decrease strongly and a new absorption at 963 cm^{-1} appears which can be assigned to the *trans*-vinylene double bond. In this case, as in high molecular weight sulphinyl precursor polymers, no *cis*-double bonds could be observed.[14] At 175°C the sulphinyl absorption has disappeared completely and a new signal has appeared at 1696 cm^{-1} which may correspond to the formation of aromatic aldehydes.[15]

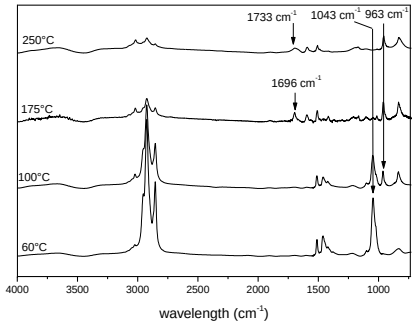

*Figure 8: FT-IR spectra of the oligomer **7** at 60°C, 100°C, 175°C and 250°C.*

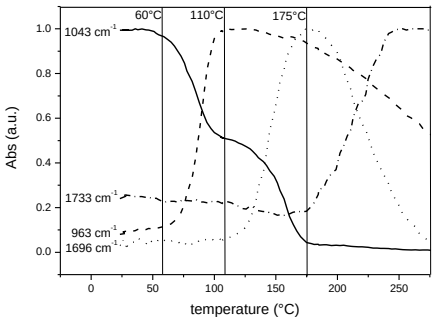

Figure 9: Absorptions at 963, 1043, 1696 and 1733 cm^{-1} versus temperature.

When these absorptions are plotted versus increasing temperature (Figure 9), the trends in elimination behaviour of oligomer **7** become clear. The sulphinyl absorption (1043 cm^{-1}, solid line) decreases in two distinct steps. The first decrease takes place in a temperature domain between 60 and 110°C and is caused by the elimination of the sulphinyl groups in the oligomer main chain as it coincides with the increase of the *trans*-vinylene double bond signal at 963 cm^{-1}, between 60 and 110°C. The second step in the decrease of the sulphinyl absorption occurs between 130 and 175°C. This second decline does not give rise to additional double bonds and thus has to originate from the thermolysis of the sulphinyl end groups. Note that the main chain sulphinyl groups and the sulphinyl end groups have similar intensities which again suggests both sulphinyl groups are present for approximately an equal amount. As mentioned earlier, this was also confirmed on the precursor stage by ^{13}C-NMR spectroscopic measurements. Furthermore, between 130 and 175°C the absorption for the carbonyl stretching (1696 cm^{-1}) increases. This observation may indicate that an unidentified number of sulphinyl end groups is converted to a carbonyl functionality. At even higher temperatures (+175°C) the absorption at 1696 cm^{-1} again decreases and a new absorption band at 1733 cm^{-1} emerges (Figure 9) which partially overlaps the signal at 1696 cm^{-1} and probably corresponds to the higher oxidised products.

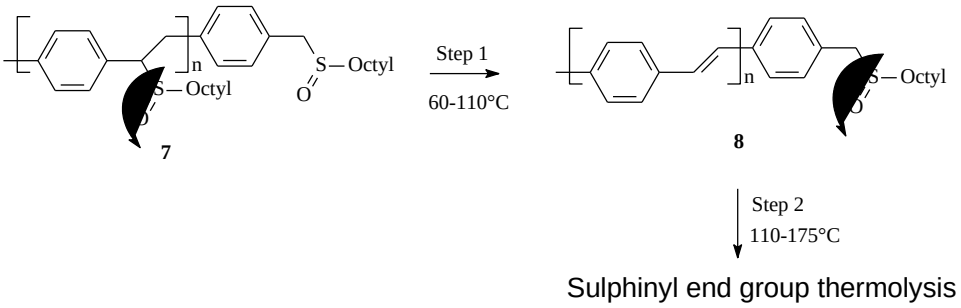

Scheme 3: The elimination of the sulphinyl eliminable groups to a trans-double bond and the thermolysis of the sulphinyl end groups.

Before commenting on the origin and the mechanism of formation of these carbonyl functionalities, we will discuss the results of the same experiment performed with in-situ UV-Vis spectroscopy. Before heating, an absorption band at 324 nm is present from the precursor oligomer. After heating till 270°C a conjugated oligomer with an absorption maximum at 351 nm is obtained. When the absorption at this maximum wavelength is plotted versus temperature two steps can be visualised in the elimination process (Figure 10). The major part of the conjugated structure is formed between 60 and 110°C. This result is perfectly in accordance with the results obtained from the FT-IR measurements that already confirmed the sulphinyl groups in the oligomer main chain are eliminated in this temperature domain. At 110°C a conjugated oligomer with an absorption maximum at 339 nm has been formed. Around 175°C, a second small increase in absorption can be observed and in the end a conjugated oligomer with an absorption maximum at 351 nm is obtained.

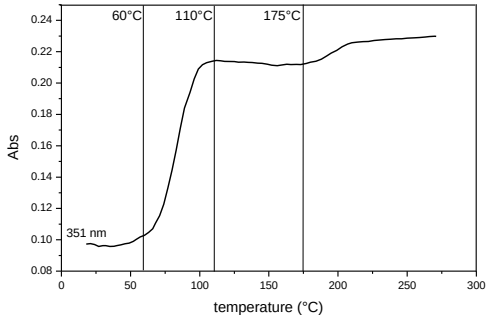

Figure 9: Absorption at 351 nm versus temperature.

Remember that it was clear from the previous FT-IR experiment that both the sulphinyl main chain as well as the sulphinyl end groups had been eliminated completely at 175°C. The second increase of the "effective conjugation length" observed in UV-Vis can therefore only be explained by a new process that is initiated by the thermolysis of the sulphinyl end groups. Explaining this phenomenon observed during the thermolysis of the sulphinyl end groups, was possible by combining literature data on the thermal and/or photochemical conversion of sulphinyl functionalities in general[16],[17] and what is know on the dimerisation and disproportionation behaviour of sulphenic acids.[14] Mislow et al. suggested the benzylic C-S bond to be notable weak in benzyl sulphinyl compounds.[16a,18] At elevated temperatures this may result in homolytic cleavage and formation of a radical pair. The same cleavage was also observed in photochemical experiments on benzyl sulphinyl compounds.[17] These papers also report the presence of benzaldehyde upon thermolysis or photolysis of benzyl sulphinyl compounds. This explains the formation of aldehyde functionalities as observed in the FT-IR experiment in the temperature domain between 110 to 175°C. In order to clarify the second small increase in "effective conjugation length" observed in UV-Vis, an additional experiment was set up in which we mimicked the thermal behaviour of the sulphinyl end groups. To do so a model compound **9** was heated at 200°C for 15 hours and the resulting reaction mixture was analysed by GC-MS. A complex reaction mixture resulted and products **18** to **26** all proved to be present. (Scheme 4) Once the weak C-S bond is broken the radicals formed (**10**, **11**) can recombine again to yield several reaction products. Product **18** clearly arises from radical coupling of two benzyl radicals. Combination of two sulphinyl radicals (**12** and **13**) results in the formation of the unstable product **14** which further disproportionates to form products **15** and **16**. Understanding the formation of benzaldehyde was possible by combining products **10** and **13** to from the sulfenic ester **20**. Thermal decomposition of this compound can yield benzaldehyde **21** and thiol **22**. The other products in the reaction mixture also arise from radical coupling of the respective radicals. (Scheme 4) The observed stilbene (**19**) is presumed to be formed by oxidation of dibenzyl **18**. Probably radical **13** acts as an oxidising agent in this reaction yielding a sulphenic acid and consequently also **25** and **26**. Extrapolation of this result towards the thermal behaviour of the oligomer **7** would lead to coupling of two oligomer chains followed by oxidation and thus an extension of the "effective conjugated system"

which can account for the observed red shift in UV-Vis spectroscopy at temperatures above 175°C.

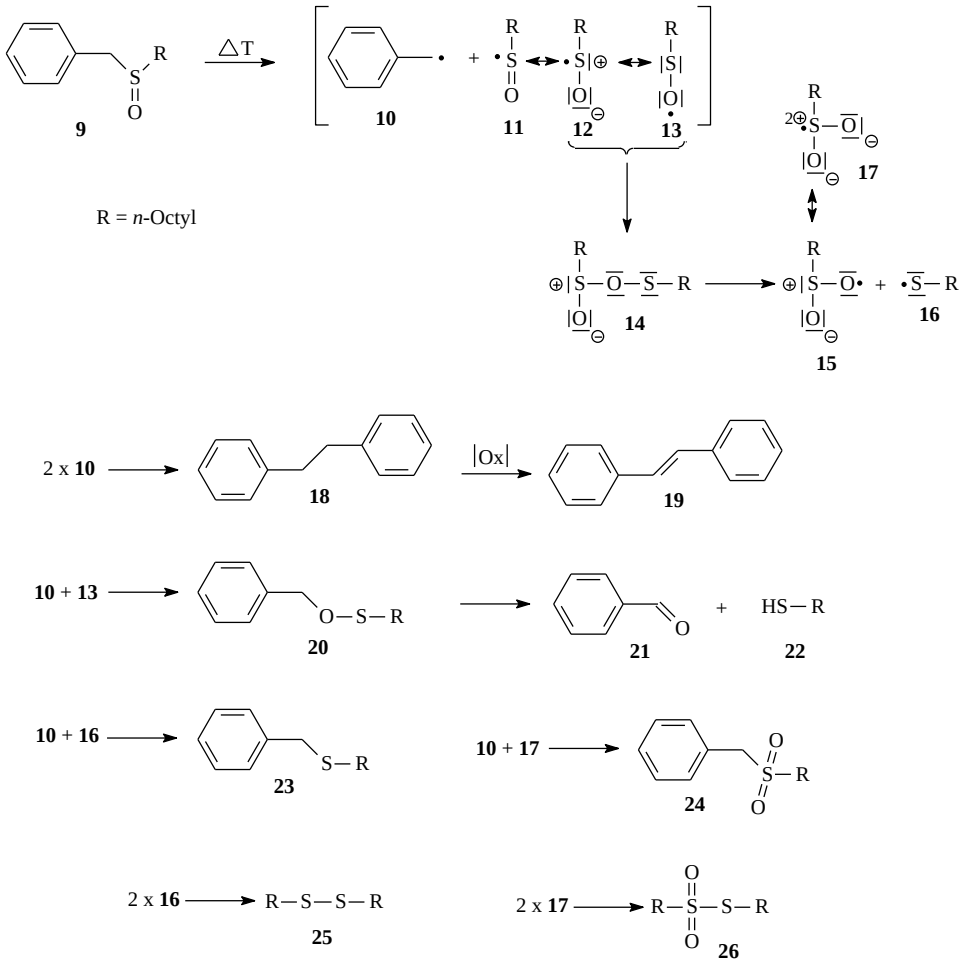

*Scheme 4: Schematic overview of the formation of products **18** to **26** upon homolytic cleavage of the C-S bond in compound **9**.*

In order to demonstrate the kinetic separation in the elimination processes of the different sulphinyl groups present in oligomer **7** an experiment was set up which should allow the sulphinyl groups, that give rise to double bonds, to be eliminated selectively whereas the sulphinyl end groups are left unchanged. *In-situ* FT-IR spectroscopy was used to monitor the elimination process. In this experiment the sample was heated at 2°C/min till 100°C, kept at this temperature for 3 hours and then heated further till 300°C at 2°C/min. In Figure

11 this temperature program is shown next to the intensity profiles (absorbance versus temperature) for the signal of the *trans*-double bond (956 cm^{-1}, dashed line) and the sulphinyl groups (1043 cm^{-1}, solid line). At 100°C all sulphinyl groups which give rise to double bonds have been eliminated and the intensity of the *trans*-vinylene double bond signal has reached its maximal absorption. During the isothermal stay at 100°C neither of these signals change. In the third part of the heating program (100 till 300°C), the sulphinyl signal further declines. This second decrease in sulphinyl signal progressed without formation of additional double bonds and thus has to originate from the elimination of the sulphinyl end groups. At 175°C both the main chain sulphinyl groups and the sulphinyl end groups have been eliminated completely from the oligomer. (Figure 11)

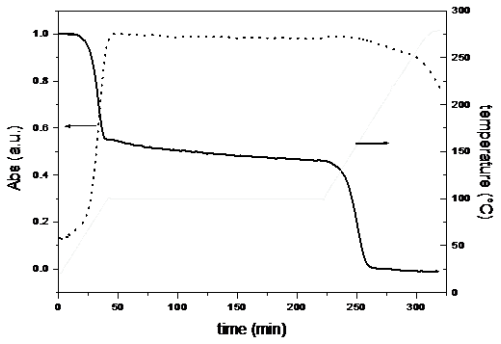

Figure 11: The absorbance of the signal at 956 cm^{-1} (dotted line) and the signal at 1043 cm^{-1} (solid line) in function of time and temperature.

The selective elimination was further investigated on a sample of precursor oligomer **7** which was converted to the conjugated oligomer **8** by heating a thick precursor film for 3 hours at 100°C under *vacuum*. The resulting conjugated oligomer **8** still proved to be soluble in common organic solvents. The UV spectrum (in toluene) of this conjugated oligomer shows several maxima at different wavelengths (Figure 12).

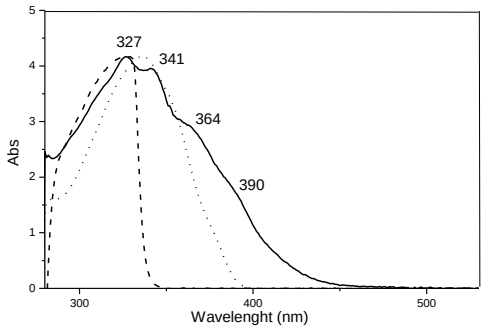

*Figure 12: UV spectrum in toluene of the conjugated oligomer **8** (solid line), trans-stilbene (dashed line), 1,4-bis-(2-phenylvinylene)benzene (dotted line).*

These maxima probably arise from a distribution in conjugated chain lengths. The first maximum in the UV spectrum of the oligomer at 327 nm corresponds to that of *trans*-stilbene (328 nm). The other maxima at 341, 363 and 390 nm probably correspond to the larger conjugated systems were n is 2, 3 and 4 respectively. (Figure 12) These wavelengths are in the line of expectation when compared with the wavelengths of PPV oligomers synthesised previously.[19]

The selective elimination was also confirmed by ^{13}C-NMR spectroscopy. In the ^{13}C spectrum of the precursor oligomer **7** chemical shifts of several carbon atoms of the main chain sulphinyl groups slightly differ from those of the sulphinyl end groups. In Figure 13 an enlarged part of the ^{13}C spectrum for both the precursor and the conjugated oligomer are shown. On the precursor stage different signals are observed that can be assigned to C1 to C5.[20] (Figure 13) When the precursor oligomer has been eliminated to the conjugated structure only the two signals for the sulphinyl end groups C1 and C2 remain. All sulphinyl groups in the main chain have been eliminated and this results in the formation of a new ^{13}C signal at 127 ppm which is attributed to the carbon atoms of the double bond (not shown).

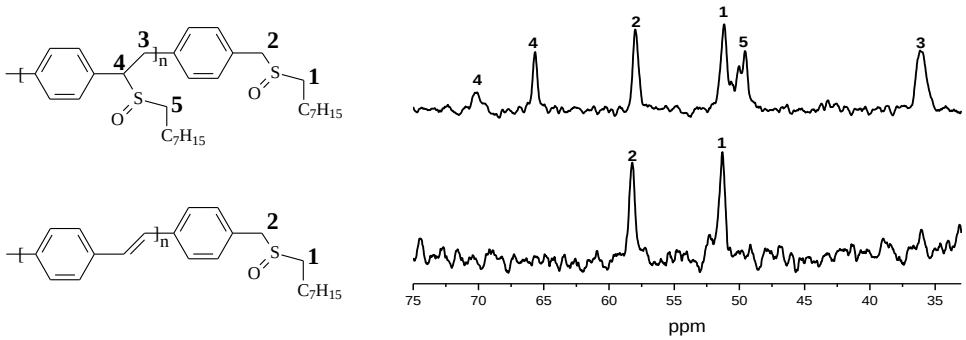

*Figure 13: Enlarged part of the ^{13}C-NMR spectrum of the precursor oligomer **7** (upper) and the conjugated oligomer **8** (lower)*

These experiments clearly demonstrate that it is kinetically possible to separate elimination of the main chain sulphinyl groups and thermolysis of the sulphinyl end groups in the oligomer chain. At lower temperatures the sulphinyl groups from the main chain are eliminated and the double bonds are formed. At higher temperatures thermolysis of the sulphinyl end groups occurs. Furthermore, above 175°C, we found indications that these sulphinyl end groups were partially converted to carbonyl functionalities or that two oligomer chains may couple, which after oxidation, leads to an extension of "effective conjugation length".

5.2 Experimental Section

Materials. All chemicals were purchased from Aldrich or Acros and used without further purification unless otherwise stated. Tetrahydrofuran (THF) was distilled over sodium/benzophenone.

Characterisation. ^{1}H-NMR spectra were recorded in $CDCl_3$ at 300MHz on a Varian Inova Spectrometer using a 5 mm probe. Chemical shifts (δ) in ppm were determined relative to the residual $CHCl_3$ absorption (7.24 ppm). The ^{13}C-NMR experiments were recorded at 75 MHz on the same spectrometer using a 5 mm broadband probe. Chemical shifts were defined relative to the ^{13}C resonance shift of $CHCl_3$ (77.0 ppm). Molecular weights and molecular weight distributions were determined relative to polystyrene standards (Polymer Labs) with a narrow polydispersity by Size Exclusion Chromatography (SEC). Separation to hydrodynamic volume was obtained using a Spectra series P100 (Spectra Physics) equipped with a pre-column (5 μm, 50 mm*7.5 mm, guard, Polymer Labs) and two mixed-B columns (10 μm, 2x300 mm*7.5 mm, Polymer Labs) and a Refractive Index (RI) detector (Shodex) at 40°C. SEC samples are filtered through a 0.45 μm filter. HPLC grade THF (p.a.) is used as the eluent at a constant flow rate of 1.0 ml/min. Toluene is used as flow rate marker. The molecular weight of the sulphinyl precursor oligomers 7 was also measured on a low-molecular weight column (5 μm, 300 mm*7.5 mm, 100Å, Polymer Labs). The results obtained from these measurements are nearly identical to those obtained on the high molecular weight column.

TGA measurements are performed on a TA instrument 951 thermogravimetric analyser with a continuous nitrogen flow of 80 ml/min and a heating rate of 10°C/min. Samples of precursor polymer (10 mg) are inserted in the solid state.

Direct Insert Probe Mass Spectroscopy analysis is carried out on a Finnigan TSQ 70, electron impact mode, mass range of 35-500. Electron energy is 70 eV. A $CHCl_3$ solution of precursor polymer is applied on the heating element of the direct insert probe. A similar heating rate of 10°C/min was used to ensure a good comparison with TGA data.

The *in-situ* elimination reactions were performed in a Harrick High Temperature Oven (purchased from Safir), which is positioned in the beam of a Perkin Elmer spectrum one FT-IR spectrometer (nominal resolution 4 cm^{-1}, summation of 16 scans). The temperature

of the sample is controlled by a Watlow (sereal number 999, dual channel) temperature controller. The precursor polymer was spincoated from a $CHCl_3$ solution (6 mg/ ml) on a KBr pellet at 500 rpm. The spincoated KBr pellet (diameter 25 mm, thickness 1 mm) is in direct contact with the heating element. All experiments were performed at 2°C/min under a continuous flow of nitrogen. "Timebase software" supplied by Perkin Elmer is used to investigate regions of interest.

In-situ UV-Vis measurements were performed on a Cary 500 UV-Vis-NIR spectrophotometer, specially adopted to contain the Harrick high temperature cell (scan rate 600 nm/ min, continuous run from 200 to 600 nm). Precursor polymer (**6** or **7**) was spincoated from a $CHCl_3$ solution (6 mg/ ml) on a quartz glass (diameter 25 mm, thickness 3mm) at 700 rpm. The quartz glass was heated in the same Harrick oven high temperature cell as was used in the FT-IR measurements. The cell was positioned in the beam of the UV-Vis-NIR-spectrophotometer and spectra were taken continuously. The heating rate was 2°C/min up to 300°C. All measurements were performed under a continuous flow of nitrogen. "Scanning Kinetics software" supplied by Varian is used to investigate regions of interest.

Synthesis of 1,4-bis(tetrahydrothiopheniomethyl)xylene dichloride (1) and 1-(chloromethyl)-4-[(*n*-octylsulphinyl)methyl]benzene (2): These products were synthesised according to a procedure described elsewhere.[21]

Synthesis of 1,4-bis[ethoxy(thiocarbonyl)thiomethyl]benzene (3): This monomer was prepared by stirring a solution of 1,4-bis(chloromethyl)benzene (2.5 g, 0.0143 mol) and *O*-ethoxyxanthic acid potassium salt (5 g, 0.03125 mol) in methanol (50 ml) for 2 hours at room temperature. The reaction mixture was poured into water and the aqueous solution was extracted with chloroform and dried over magnesium sulphate. The filtrate was concentrated *in vacuo* and recrystallised from chloroform/hexane (10/90) and yielded product **3** as white needles. (4.7 g, yield: 95%). ^{1}H-NMR ($CDCl_3$,300 MHz): δ (ppm) 7.27 (4H, s); 4.63 (4H, q, *J* =7.2 Hz); 4.32 (4H, s); 1.40 (6H, t, *J* =7.2 Hz) .^{13}C-NMR ($CDCl_3$, 75 MHz): δ (ppm) 135.36; 129.53; 70.35; 40.22; 14.01. UV-VIS (λ_{max}, CH_2Cl_2): 356 nm, m.p.: 57.2°C-58°C, FT-IR (KBr, cm^{-1}): 2980 (ν_{C-H} aliph.), 1510-1397 (ν_{C-H} CH_3,CH_2), 1251 (*p*-phenylene CH out of plane bend), 1217-1107-1048 ($\nu_{SC(S)OCH2CH3}$) ,688 (ν_{C-S}).

Synthesis of [1-ethoxy(thiocarbonyl)thiomethyl-4-(chloromethyl)]benzene (4): A clear solution of *O*-ethoxyxanthic acid potassium salt (2.96 g, 19 mmol) in methanol (40 ml) was added in one portion to a stirred solution of 1,4-bis(tetrahydrothiopheniomethyl)xylene dichloride (**1**) (10 g, 19 mmol) in methanol (100ml). After one hour the reaction mixture was concentrated *in vacuo*. The crude product was diluted with chloroform (200 ml) and the precipitate was filtered off. The filtrate was concentrated and *n*-octane (75 ml) was added. The *n*-octane was concentrated *in vacuo* to remove tetrahydrothiophene. This sequence was repeated three times. The reaction mixture was purified using column chromatography (SiO_2,eluent: $CHCl_3$/hexane 50/50). (yield: 74%). ^{1}H-NMR ($CDCl_3$, 300 MHz): δ (ppm) 7.32 (2H, s); 7.27 (2H, s); 4.60-4.67 (2H, q, *J* = 7.2 Hz); 4.55 (2H, s); 4.34 (2H, s); 1.38-1.42 (3H, t, *J* =7.2 Hz). ^{13}C-NMR ($CDCl_3$, 75MHz): δ (ppm) 137.87 (1C); 135.37 (1C); 129.53 (2C); 129.16 (2C); 70.39 (1C); 45.91 (1C); 40.18 (1C); 14.00 (1C). UV-VIS (λ_{max}, CH_2Cl_2): 353 nm, m.p.: 114.7°C-116°C, FT-IR (KBr, cm^{-1}): 2980 (ν_{C-H} aliph.), 1510-1397 (ν_{C-H} CH_3,CH_2), 1251 (*p*-phenylene CH out of plane bend), 1217-1107-1048 ($\nu_{SC(S)OCH2CH3}$) ,688 (ν_{C-S}).

Synthesis of 1-((*n*-octylsulphinyl)methyl)-4-(ethoxy(thiocarbonyl)thiomethyl) benzene (5): *O*-ethoxyxanthic acid potassium salt (1.5 eq) was added portion wise to a solution of 1-(chloromethyl)-4-[(*n*-octylsulphinyl)methyl]benzene (prepared as reported earlier)[21] (2 g, 6.6 mmol) in methanol (50 ml). The mixture was stirred for 12 hours at room temperature. The reaction mixture was poured into water and extracted three times with chloroform. The organic layer was dried over magnesium sulphate and concentrated in vacuo to yield the pure product (**4**). (2.42 g, yield: 95%). ^{1}H-NMR ($CDCl_3$, 300 MHz): δ (ppm) 7.32 (2H, d, *J* = 8.4 Hz); 7.20 (2H, d, *J* = 8.4 Hz); 4.61 (2H, q, *J* = 7.2 Hz); 4.32 (2H, s); 3.90 (2H, dd, *J* = 13.2 Hz); 2.52 (2H, t, *J* = 7.8 Hz); 1.70 (2H, m); 1.38 (3H, t, *J* = 7.2 Hz); 1.22 (10H, s(br)); 0.83 (3H, t, *J* = 6.9 Hz). ^{13}C-NMR ($CDCl_3$, 75MHz): δ (ppm) 136.28 (1C); 130.46 (1C); 129.85 (2C); 129.51 (2C); 70.42 (1C); 58.02 (1C); 51.26 (1C); 40.16 (1C); 31.92 (1C); 29.37 (1C); 29.21 (1C); 29.04 (1C); 22.82 (1C); 22.68 (1C); 14.30 (1C); 14.01 (1C). UV-VIS (λ_{max}, CH_2Cl_2): 355 nm. m.p.: 81.4°C-82.8°C, FT-IR (KBr, cm^{-1}): 2957-2918-2849 (ν_{C-H} aliph.), 1511-1486-1419 (ν_{C-H} CH_3,CH_2), 1211-1117-1071 ($\nu_{SC(S)OCH2CH3}$), 1056-1025 (ν_{S-O}), 849 (1,4-subst.arom.).

Synthesis of the precursor polymer (6 and 7): All polymerisations were carried out under the same conditions in dry tetrahydrophuran (THF, dried over sodium with

benzophenon) at different temperatures (Table 1). Solutions of monomer (1 mmol in 6.5 ml THF) and base (potassium-*tert*-butoxide; 1.05 mmol in 3.5 ml THF) were prepared and degassed for 1 hour by a continuous flow of nitrogen. The base solution was added in one portion to the stirred monomer solution. During the reaction the temperature was kept constant and the passing of nitrogen was continued. After 1 hour the reaction mixture was poured into well stirred ice water whereupon the polymer precipitated. The water layer was extracted with chloroform to ensure that all polymer and residual fraction was collected, and the combined organic fractions were concentrated *in vacuum*. The polymer was precipitated in cold diethylether/hexane (1/1; 100 ml; 0 °C), collected by filtration and dried *in vacuum*. The residual diethylether/hexane fraction was concentrated *in vacuum*. GPC was performed in THF versus polystyrene standards. Polymerisation results are summarised in Table 1. The restfractions only contain monomer residues.

Precursor polymer **6**: ^{1}H-NMR ($CDCl_3$, 300 MHz): δ (ppm) 6.90-6.99 (4H); 4.79 (1H); 4.51 (2H); 3.27 (1H); 3.05 (1H); 1.29 (3H).^{13}C-NMR ($CDCl_3$, 75 MHz): δ (ppm) 213.97 (1C); 137.68-137.35 (2C); 129.27 (2C); 127.88 (2C); 69.78 (1C); 55.28 (1C); 41.97 (1C); 13.67 (1C). FT-IR (KBr, cm^{-1}): 2980, 1510, 1397, 1251, 1217, 1107, 1048, 688.

Precursor oligomer **7**: ^{1}H-NMR ($CDCl_3$, 300 MHz): δ (ppm) 6.80-7.50 (4H); 3.25-3.99 (2H); 2.39-2.78 (1H); 1.95-2.23 (2H); 1.45-1.75 (2H); 1.11-1.42 (10H); 0.75-0.9 (3H). ^{13}C-NMR ($CDCl_3$, 75 MHz): δ (ppm) 137.87; 130.10; 129.66; 129.30; 128.88; 128.58; 126.48; 70.02; 65.32; 57.67; 50.89; 49.65; 49.27; 36.02; 31.51; 28.97; 28.80; 28.69; 22.84; 22.40; 13.92. FT-IR (KBr, cm^{-1}): 2957, 2918, 2849, 1511, 1486, 1419, 1056, 1025.

Conjugated oligomer **8**: This compound was made from the precursor oligomer **7** by heating a film of **7** (30 mg in 2 ml $CHCl_3$ and allow the $CHCl_3$ to evaporate) at 100°C for 3 hours under *vacuum*. ^{13}C-NMR ($CDCl_3$, 75 MHz): δ (ppm) 137.45; 130.42; 129.08; 127.01; 57.99, 50.92; 31.76; 29.21; 29.04; 28.87; 22.65; 22.46; 14.14. FT-IR (KBr, cm^{-1}): 3025, 1511, 956, 858, 834. UV-Vis spectra of the conjugated oligomer **8** were taken in toluene at room temperature (λ_{max} at 327, 341, 364 and 390 nm). For comparison the spectrum of *trans*-stilbene (purchased from Aldrich and used as received) was also taken in the same conditions (λ_{max}= 328 nm).

5.3 References

[1] Son S.; Dodabalapur A.; Lovinger A. J.; Galvin M. E. *Science* 269, **1995**, 376.

[2] Lo S-C.; Palsson L-O.; Kilitziraki M.; Burn P. L.; Samuel I. D. W. *J. Mat. Chem*. 11, **2001**, 2228.

[3] Brütting W.; Meier M.; Herold M.; Karg S.; Schwoerer M. *Synth. Met*. 91, **1997**, 163.

[4] Andersson A.; Kugler T.; Logdlund M.; Holmes A. B.; Li X.; Salaneck W. R. *Synth. Met.* 106, **1999**, 13.

[5] Lo S-C.; Sheridan A.; Samuel I. D. W.; Burn P. L. *J. Mat. Chem*. 9, **1999**, 2165.

[6] Lo S-C.; Sheridan A.; Samuel I. D. W.; Burn P. L. *J. Mat. Chem. 10*, **2000**, 275.

[7] Mitchell, W. J.; Pena, C.; Burn, P. L. *J. Mater. Chem.* 12, **2002**, 200.

[8] Van den Berghe, D. *internal communication* LUC, **2000**.

[9] Cho, B. R. *Prog. Polym. Sci.* 27, **2002**, 307.

[10] Keil G. A.; Liszewski Y.; Peng Y.; Hsieh B. *Polymer Preprints* 41, **2000**, 826.

[11] Keil G. A.; Liszewski Y.; Wilking J.; Hsieh B. *Polymer Preprints* 42, **2001**, 306.

[12] Kesters, E. *Ph.D. Dissertation*, **2002**, Limburgs Universitair Centrum, Diepenbeek, Belgium.

[13] a) de Kok M.; van Breemen A.; Carleer R.; Adriaenssens P.; Vanderzande D. *Acta Polym.* 50, **1999**, 28. b) Kesters E.; Lutsen L.; Vanderzande D.; Gelan J. *Synthetic Metals* 119, **2001**, 311.

[14] de Kok M.; van Breemen A.; Carleer R.; Adriaenssens P.; Vanderzande D. *Acta Polym.* 50, **1999**, 28.

[15] Colthup N. B.; Daly L. H.; Wiberley S. E. *Introduction to Infrared and Raman Spectroscopy*, 3rd ed.; Academic, San Diego, **1990**, p 289.

[16] a) Miller E. G.; Rayner D. R.; Thomas H. T.; Mislow K. *J. Amer. Chem. Soc.* 90, **1968**, 4861. b) Barnard-Smith D. G.; Ford J. F. *Chem. Commun* **1965**, 120.

[17] Guo Y.; Jenks W. S. *J. Org. Chem* 60, **1995**, 5480.

[18] Mislow K.; Axelrod M.; Rayner D. R.; Gotthardt H.; Coyne L. M.; Hammond G. S. *J. Amer. Chem. Soc.* 87, **1965**, 4958.

[19] Müllen K.; Wagner G. in *Electronic Materials: The Oligomer Approach*; Wiley-VCH: Weinheim, Germany, **1998**, p 58.

[20] van Breemen A.; de Kok M.; Adriaenssens P.; Vanderzande D.; Gelan J. *Macromolec. Chem. Phys.* 2, **2001**, 202.

[21] van Breemen A.; Vanderzande D.; Adriaensens P.; Gelan J. *J. Org. Chem*. 64, **1999**, 3106.

Summary

This thesis deals with the synthesis and characterisation of some new conductive polymers. Within this large family of polymers the poly(arylene vinylene) derivatives were selected. In this work these derivatives are synthesised via the sulphinyl precursor route. The results presented unambiguously demonstrate that this synthetic pathway currently is the most versatile way to synthesise these derivatives. Ever since electroluminescence was first discovered in PPV (anno 1989), the search for the most effective synthetic pathway was on and a lot of new derivatives have seen the daylight. More recently, conductive polymers have also been used in other applications and in time these compounds may posses substantional commercial value.

Chapter one provides a general introduction on the subject and focuses on the different synthetic pathways towards PPV and its derivatives. The sulphinyl precursor route is discussed in detail and derivatives that have been synthesised in the past are presented. Chapter one also deals with some applications that conductive polymers can be used in. Polymer light emitting diodes (LEDs), photovoltaic cells and thin film transistors can all use conductive polymers as an active material.

In *chapter two* the synthesis and characterisation of some PPV derivatives with an increased electron affinity is discussed. The reasons for synthesising these polymers are manifold. Most of the conjugated polymers, synthesised to date, have low electron affinity (p-type), which makes them highly susceptible to oxidation. Conjugated polymers with high electron affinity (n-type) are less sensitive to oxidation and are desired in certain applications. The first and most obvious choice for the design of high electron affinity PPV derivatives would be the attachment of one or more electron withdrawing side-group to the aromatic moiety or the vinylene double bond. A halogen atom, a cyano- or nitro-group are common examples of such groups. These PPV derivatives are almost impossible to synthesise via the other known precursor routes (Wessling and Gilch precursor route). As proven by the results these derivatives are more easily accessible via the sulphinyl precursor route. The electron withdrawing groups used here are a chlorine atom and a

cyano group. These groups are introduced on the double bond or on the aromatic ring and the presence of these atoms or groups affects the polymerisation capabilities of the different monomers.

Chapter 3 copes with the synthesis and characterisation of some hetero-aromatic poly(arylene vinylene) derivatives. A second way to obtain PPV derivatives with increased electron affinity is to introduce more electronegative atoms, such as an imine nitrogen, in the polymeric backbone. Poly(pyridylene vinylene) and poly(bipyridylene vinylene) will be discussed. In the case of the bipyridine derivatives complexation with a large number of different metal ions is possible thus yielding a set of conductive polymers with completely different properties. A third heterocyclic PPV derivative that will be discussed in chapter 3 is the poly(2,5-thienylene vinylene) or PTV. In contrast with the polymers discussed earlier, the incorporation of the thiophene unit makes this polymer electron rich. This allowed the synthesis of a so-called "low band gap" polymer, which proved useful in photovoltaic devices and plastic transistors.

Chapter 4 deals with another interesting approach to tune the physical and chemical properties of conductive polymers, i.e. the synthesis of copolymers. Various parameters can be manipulated in this way and polymers with intermediate and/or improved properties often arise. Emission maxima, solubility, film forming and redox properties can all be changed significantly as was demonstrated in various papers. In chapter 4 results will be presented about the copolymerisation of several sulphinyl monomers via the sulphinyl precursor route. The copolymers discussed are those between PPV, PPyV and OC_1C_{10}. Also, two other copolymers between OC_1C_{10} and PBPyV on the one hand and between OC_1C_{10} and cyano-PPV on the other hand will also be handled. Each of the respective homopolymers shows interesting properties and by combining these into one copolymer intermediate properties result. Complexation of the bipyridine unit in the copolymers again proved a successful approach to alter the copolymer characteristics.

Finally, *chapter 5* explores the possibilities the less used xanthate precursor route offers in the synthesis of PPV. The potential of this synthetic pathway was suggested by some recent publications and of interest to us is an evaluation of the possibilities the xanthate group offers in the synthesis of PPV and some derivatives that are hard or impossible to realize via the sulphinyl precursor route. To serve this purpose, three different monomers, combining sulphinyl and xanthate properties were synthesised and polymerised. Once the

precursor polymers were formed, the thermal conversion to the conjugated structure was studied with *in-situ* FT-IR, *in-situ* UV-Vis-spectroscopy, TGA and DIP-MS. Combination of a xanthate group and a sulphinyl group in the same monomer in the end proved a useful way to obtain very short PPV oligomers.

Samenvatting

Deze thesis handelt over de synthese en karakterisatie van enkele nieuwe, geleidende polymeren. Binnen de familie van deze polymeren werden de poly(aryleen vinyleen) derivaten geselecteerd en de synthese van deze derivaten gebeurde via the sulphinyl precursor route. De resultaten die worden gepresenteerd tonen onomstotelijk aan dat deze route momenteel de meest veelzijdige route is om PPV en zijn derivaten te synthetiseren. Vanaf het moment dat de elektronluminescentie van PPV was vastgesteld (anno 1989) heeft het onderzoek naar PPV en zijn derivaten, en naar geleidende polymeren in het algemeen, een enorme vlucht gekend. Dergelijke geconjugeerde polymeren kunnen gebruikt worden als actief materiaal in verschillende toepassingen en met de tijd zouden deze polymeren wel eens een aanzienlijk commercieel potentieel kunnen hebben.

Hoofdstuk 1 geeft een algemene inleiding and spits zich toe op de verschillende routes die heden ten dage bestaan om PPV en zijn derivaten te synthetiseren. The sulphinyl precursor route wordt in detail behandeld en derivaten in het verleden gesynthetiseerd worden belicht. Hoofdstuk 1 geeft ook de verschillende toepassingen weer van geleidende polymeren. Polymeer licht emitterende diodes (LEDs), polymere zonnecellen en dunne film transistoren kunnen geleidende polymeren allen gebruiken als actief materiaal.

De synthese en karakterisatie van 3 PPV derivaten met verhoogde elektron affiniteit wordt behandeld in hoofdstuk 2. Dergelijke materialen zijn in tal van opzichten interessant. De meeste geleidende polymeren tot op heden gemaakt hebben allen een lage elektron affiniteit wat hen heel gevoelig maakt voor oxidatie. Geleidende polymeren met een hogere elektron affiniteit zijn dit minder en daarom gewenst in verschillende toepassingen. Dergelijke geleidende polymeren met een verhoogde elektron affiniteit ontstaan door één of meerdere elektronen zuigende atomen/groepen op de polymeer keten in te planten. Een halogeen atoom, een nitro groep en een cyano groep behoren tot de mogelijkheden en worden in het algemeen veel gebruikt als elektron zuigende groep in de organische synthese. De polymerisatie van monomeren die dergelijke elektron zuigende groepen bevatten gaat moeilijk en soms zelfs helemaal niet via de bestaande precursor routes (Wessling en Gilch

precursor route). In dit werk worden een chloor atoom en een cyano groep als elektron zuigende entiteit gebruikt. Deze groep wordt op het monomeer stadium ingeplant en de polymerisatie mogelijkheden van dergelijke monomeren werd onderzocht. Zoals de resultaten bewijzen zijn dergelijke derivaten makkelijker toegankelijk als gewerkt wordt via de sulphinyl precursor route.

Hoofdstuk 3 belicht de synthese en karakterisatie van 3 hetero cyclische PPV derivaten. Een alternatieve aanpak in de synthese van elektron accepterende PPV derivaten is de implementatie van een elektronen accepterend atoom in de polymeer backbone. Een stikstof atoom is een voorbeeld hiervan. Poly(pyridileen vinyleen) en poly(bipyridileen vinyleen) werden beiden gesynthetiseerd en zijn meer elektronen accepterend dan het klassieke PPV door de aanwezigheid van het stikstof atoom in de polymeer keten. Een derde hetero cyclisch derivaat dat wordt behandeld in dit hoofdstuk is het poly(2,5-thienylene vinylene) of PTV. In contrast tot de twee polymeren eerder vernoemd in dit hoofdstuk is PTV eerder elektron rijk. Dit maakt dat PTV behoort tot de klasse van de zg. "low band gap" geleidende polymeren. Dergelijke polymeren zijn bijzonder nuttig gebleken in zonnecellen en transistoren.

Hoofdstuk 4 handelt over een andere interessante manier om de fysische en chemische eigenschappen van geleidende polymeren te sturen, nl. de synthese van enkele copolymeren. Op deze manier kunnen verschillende parameters (emissie maxima, oplosbaarheid, redox eigenschappen etc.) aangepast worden. De copolymeren zijn deze tussen PPV, poly(pyridileen vinyleen) of PPyV en OC_1C_{10} enerzijds en deze tussen OC_1C_{10} en poly(bipyridileen vinyleen) en OC_1C_{10} en dicyano-PPV anderzijds. Elk van de respectievelijke homopolymeren bezit interessante eigenschappen en door de verschillende homopolymeren te combineren in een copolymeer ontstaan polymeren met intermediaire eigenschappen.

Hoofdstuk 5 uiteindelijk verkent de mogelijkheden van de minder gebruikte xanthaat precursor route. Het potentieel van deze precursor route werd gesuggereerd in een aantal recente publicaties. Interessant voor ons was de evaluatie van de mogelijkheden de xanthaat groep bezit in de synthese van PPV en enkele derivaten waar de sulphinyl groep minder geschikt is. Om dit te testen werden een aantal verschillende monomeren gesynthetiseerd en gepolymeriseerd. De gevormde precursor polymeren werden gekarakteriseerd met verschillende technieken zoals *in-situ* FT-IR, *in-situ* UV-Vis spectroscopie, TGA en DIP-

MS. Uiteindelijk bleek dat de combinatie van een xanthaat groep en een sulphinyl groep in hetzelfde monomeer resulteerde in heel laag moleculaire fragmenten op het precursor polymeer stadium. Dergelijke methodiek kan bijgevolg worden aangewend wanneer oligomer fragmenten vereist zijn.